

University of Nottingham
UK | CHINA | MALAYSIA

Macrocyclic Peptides as Inhibitors of Protein-Protein Interactions

Frances Smith

Thesis submitted to the University of Nottingham for the degree of Doctor of Philosophy

September 2019

Supervisors: Prof Christopher J Moody

Prof Mark Searle

i Abstract

Inhibition of the Keap1-Nrf2 protein-protein interaction (PPI) is thought to have therapeutic potential in several diseases including neurodegenerative conditions such as Alzheimer's and Parkinson's, as well as cardiovascular diseases and cancer. Cyclic peptides provide interesting scaffolds that not only display enhanced metabolic stability, but also induce conformational rigidity that may maximise interaction with the target. This project aims to develop peptidomimetic inhibitors of the Keap1-Nrf2 PPI using a portion of the natural binding sequence of a ligand of Keap1 and cyclising with a non-peptide linker.

Chapter 2 discusses the solution phase synthesis of the linear tripeptide Pro-Glu-Thr and coupling to three alkyl chain linkers of differing lengths. The orthogonal protecting group strategy used Boc and Bn groups on the *N*-terminus and side chains respectively. The *C*-terminal protecting group first used was the phenacyl group, however, due to difficulties in its removal, this was changed to the trimethylsilyl group. Following preparation of the linear peptide, its cyclisation was performed using a variety of conditions, though challenges with racemisation were encountered.

Chapter 3 details the solid phase synthesis of the linear peptides Pro-Glu-Thr-alkyl chain. This was first attempted with a linker between the resin and the peptide which was then activated to the labile linker benzotriazole, resulting in cyclisation under basic conditions. However, as this method failed to yield any cyclic peptide, the peptide was synthesised on resin and cyclised in solution. Once again this resulted in the formation of multiple products. Addition of glycine to the *C*-terminal of the peptide gave Pro-Glu-Thr-Gly-linker. This peptide was successfully cyclised, along with two analogues, and brief molecular modelling and NMR spectroscopy studies were performed on these compounds.

Chapter 4 discusses the cyclisation of the linear peptide by formation of a variety of heterocycles. These procedures were all based upon literature precedent and included the preparation of 1,2,3-triazoles *via* click chemistry, oxidative diyne coupling, formation of a 1,3,4-oxadiazole, and 1,3-dipolar cycloaddition to give pyrazoles.

Chapter 5 details a catalyst-free 1,3-dipolar cycloaddition of alkynes and stabilised diazo compounds to give pyrazoles. The oxidising reagent TsNIK was used to prepare a variety of α-diazophosphonates and were used to generate pyrazoles in both intra- and intermolecular cycloadditions, as well as strain-promoted cycloadditions.

ii. Acknowledgements

Firstly, I would like to express my great thanks to my supervisors Chris Moody and Mark Searle for their help and guidance over the past four years.

Thank you to both the BBSRC and University of Nottingham for funding, without which I would not have been able to complete my PhD.

Thank you to all the Moody group members who have made my PhD so much more enjoyable. Coffee break chats and lunches provided the encouragement and support that got me through this work.

A big thank you to Nick Mitchell and Rhys Griffiths for all their advice on the project, both practical and theoretical. Thank you also to Huw Williams, who has helped me continuously over my PhD. Thank you to all three for always being more than willing to help.

The greatest thank you goes to my parents who always been there for me, lending an ear and giving helpful advice. Without their love and support I would not be where I am today.

Finally, to Paul, who has lived through this experience with me and has been a constant support through every bad day, silly question, and frustrated rant. Thank you for always making me smile.

Contents

i Abstract ii

ii. Acknowledgements iii

iii. Abbreviations vii

1. Introduction 1

1.1 Proteins and Their Interactions 1

1.2 Targeting Protein-Protein Interactions 2

1.3 Identification of PPI Inhibitors 2

1.3.1 High-Throughput Screening (HTS) 3

1.3.2 Fragment Based Drug Design (FBDD) 3

1.3.3 Computational Approaches 5

1.3.4 Rational Design 5

1.4 The Keap1-Nrf2 Signalling System 6

1.4.1 Regulation of Nrf2 7

1.4.2 Crystal Structure of the Binding Site 7

1.5 Disrupting the Nrf2-Keap1 Interaction 10

1.5.1 Small Molecule Inhibitors 11

1.5.2 Peptide Inhibitors of Keap1 11

1.6 Chemical Synthesis of Peptides 15

1.6.1 Peptide Coupling Reagents 16

1.6.1.1 Carbodiimides as Coupling Reagents 16

1.6.1.2 Phosphonium and Aminium/Uronium Salts 18

1.6.1.3 Organophosphorus Reagents 20

1.6.1.4 Triazine Coupling Reagents 21

1.7 Solid Phase Peptide Synthesis 23

1.8 Cyclic Peptides 27

1.8.1 Diketopiperazines 28

1.8.2 Macrocyclisation of Peptides 30

1.8.3 Ring Closing Metathesis (RCM) 32
1.8.4 Alkyne-Azide Cycloaddition 34
1.9 Conclusion to Introduction 36
1.10 Project Aims and Objectives 37
2. Solution Phase Peptide Synthesis 38
2.1 Cyclisation by Ring Closing Metathesis 38
2.2 Peptide Protecting Groups 42
2.3 Removal of the Pac Protecting Group 46
2.4 New Protecting Group Strategy 49
2.5 Synthesis of Analogues 52
2.5.1 Investigation of Cyclisation Conditions 53
2.5.2 Reverse Coupling 58
2.5.3 Deprotection of the Benzyl Side Chain Protecting Groups 61
2.6 Conclusion 65
3. Solid Phase Peptide Synthesis 67
3.1 Synthesis Using Labile Linkers 67
3.2 Solid Phase Synthesis of Cyclic Peptides Using Solution Phase Cyclisation 79
3.3 NMR Spectroscopy and Molecular Modelling Studies 85
3.3.1 Molecular Modelling 85
3.3.2 NMR Spectroscopy 94
3.4 Conclusion 102
4. Macrocyclic Peptides with Heterocyclic Linkers 103
4.1 Triazole Linkers 103
4.2 Cyclisation Through Formation of a Diyne 110
4.3 Cyclisation Through Formation of an Oxadiazole 117
4.4 Pyrazole Linkers 123
4.5 Conclusion 128

5. Synthesis of Pyrazoles Through Catalyst-Free Cycloaddition of Diazo Compounds to Alkynes 130
5.1 Introduction 130
5.1.1 Classical Methods for the Synthesis of Pyrazoles 131
5.1.1.1 Cyclocondensation of Hydrazine with Carbonyl Compounds 131
5.1.1.2 Multicomponent Reactions 133
5.1.1.3 1,3-Dipolar Cycloadditions 135
5.1.2 Diazo Compounds 137
5.2 Previous Work Completed in the Group 140
5.3 Synthesis of Pyrazoles 142
5.3.1 Intermolecular Synthesis of Pyrazoles 143
5.3.2 Strain-Promoted Synthesis of Pyrazoles 147
5.4 Conclusion 150
6. Overall Conclusions and Future Work 152
7. Experimental Procedures 155
7.1 General Experimental 155
7.2 Experimental Procedures 155
8. PIPS Reflective Statement 226
9. References 228
10. Appendix 235

iii. Abbreviations

AMBER	Assisted model building with energy refinement
BCN	Bicyclo[6.1.0]nonyne
Boc	*tert*-Butyloxycarbonyl
BOP	Benzotriazol-1-yloxytris(dimethylamino)phosphonium hexafluorophosphate
BTB	Bric-a-brac
Bzl	Benzoyl
CBP	CREB-binding protein
CDI	1,1'-Carbonyldiimidazole
CDMT	2-Chloro-4,6-dimethoxy-1,3,5-triazine
CTR	*C*-Terminal region
CuAAC	Copper-catalysed azide-alkyne cycloaddition
DBU	1,8-Diazabicyclo[5.4.0]undec-7-ene
DCC	*N*,*N*'-Dicyclohexylcarbodiimide
DCU	Dicyclohexylurea
DEPC	Diethyl pyrocarbonate
DGR	Double glycine repeat
DIBO	Debenzylated cyclooctynes
DIC	*N*,*N*'-Diisopropylcarbodiimide
DIFO	Difluoronated cyclooctynes
DIPEA	*N*,*N*-Diisopropylethylamine
DKP	Diketopiperazine
DMAP	4-Dimethylaminopyridine

Dmb	Dimethoxybenzyl ester
DMTM	4-(4,6-Dimethoxy-1,3,5-triazin-2-yl) morpholine
DMTMM	4-(4,6-Dimethoxy-1,3,5-triazin-2-yl)-4-methyl morpholinium chloride
DNA	Deoxyribonucleic acid
DPPA	Diphenylphosphoryl azide
DVB	Divinylbenzene
EDCI	1-Ethyl-3-(3-dimethylaminopropyl)carbodiimide hydrochloride
FBDD	Fragment-based drug discovery
GAFF	General AMBER force field
HATU	1-[Bis(dimethylamino)methylene]-1H-1,2,3-triazolo[4,5-b]pyridinium 3-oxide hexafluorophosphate
HBTU	2-(1*H*-benzotriazol-1-yl)-1,1,3,3-tetramethyluronium hexafluorophosphate
HFIP	Hexafluoroisopropanol
HMPA	Hexamethylphosphoramide
HOAt	1-Hydroxy-7-azabenzotriazole
HOBt	Hydroxybenzotriazole
HOMO	Highest occupied molecular orbital
HPLC	High-performance liquid chromatography
HTS	High throughput screening
ITC	Isothermal titration calorimetry
IVR	Intervening region
Keap1	Kelch-like ECH-associated protein 1
KIR	Keap1-interacting region
LUMO	Lowest unoccupied molecular orbital

MBHA	4-Methylbenzhydrylamine hydrochloride
MCR	Multi-component reaction
MDM2	Mouse double minute 2 homolog
MEM	2-Methoxyethoxymethyl chloride
MOM	Methoxymethyl
MPTA	α-Methoxy-α-trifluoromethylphenylacetic acid
MPTO	3-Dimethylphosphinothioyl-2(3H)-oxazolone
NMM	*N*-Methylmorpholine
NMP	*N*-Methylpyrrolidinone
NMR	Nuclear magnetic resonance
Oxyma	Ethyl cyanohydroxyiminoacetate
Pbf	2,2,4,6,7-Pentamethyldihydrobenzofuran-5-sulfonyl
PDB	Protein data bank
PPI	Protein-protein interaction
PyBOP	Benzotriazol-1-yl-oxytripyrrolidinophosphonium hexafluorophosphate
RCM	Ring-closing metathesis
RuAAC	Ruthenium-catalysed azide-alkyne cycloaddition
SPAAC	Strain-promoted azide-alkyne cycloaddition
SPR	Surface plasmon resonance
STFI	Sunflower trypsin-inhibitor 1
TASF	Tris(dimethylamino)sulfonium difluorotrimethylsilicate
TBAF	Tetra-*n*-butylammonium fluoride
TBAT	Tetrabutylammonium difluorotriphenylsilicate

TFA	Trifluoroacetic acid
TMEDA	Tetramethylethylenediamine
TMSE	(Trimethylsilyl)ethyl

1. Introduction

1.1 Proteins and Their Interactions

Proteins rarely act alone, and their complexes are essential for processes such as DNA replication, DNA transcription, translation, signal transduction, ubiquitination, responding to stimuli, and transportation of molecules. Consequently protein-protein interactions (PPIs) are essential to cellular function.[1] Due to the importance of these interactions, many studies have been conducted that investigate the structural aspects of these surfaces.[2] PPIs can be classed as either obligate or non-obligate (Figure 1). Obligate or permanent complexes are tightly bound, with fewer water molecules between the two surfaces, for example RNA polymerase and haemoglobin.[3] Non-obligate or transient PPIs associate and dissociate *in vivo* and therefore their lifetime is dependent on physiological conditions and modulators such as cofactors.[4] Non-obligate interactions may be transient or permanent, whereas obligate PPIs are always permanent and are not found as stable structures on their own *in vivo*.

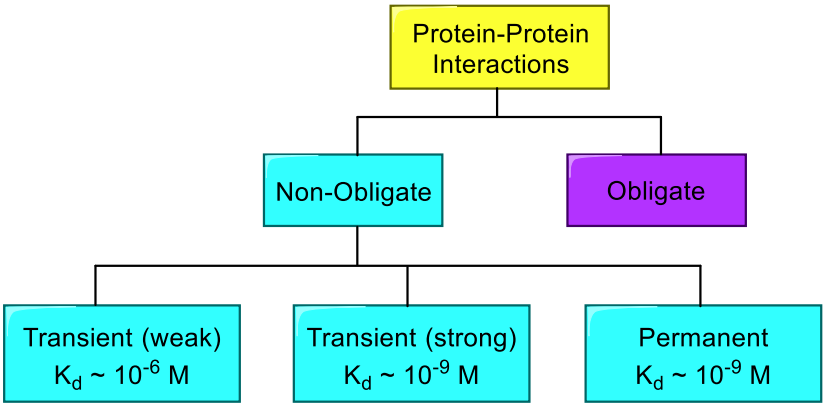


Figure 1. Transient and permanent protein-protein interactions[2]

Studies have shown that the binding interface between proteins is large, typically 1500-3000 Å^2, compared to the interactions between small molecules and protein targets that are in the range of 300-1000 Å^2.[5] However, interactions that are important for the binding of two proteins are not evenly distributed across the protein surface, instead specific residues or regions deemed 'hot spots' are responsible.[6] Alanine scanning is a process through which these hot spots can be investigated. By sequentially mutating the individual amino acids in a protein to alanine, or alanine to glycine, the effect on the binding affinity can be investigated, thereby experimentally indicating the key binding residues.[7,8] This may result in specific key residues or a cluster of residues termed a 'hot region'. The three most

common amino acids to appear in hot spots are tryptophan, arginine and tyrosine.[8] Analysis by Tsai *et al.* found that tryptophan and tyrosine were found equally both internally and on the surface of proteins, and are found more frequently in protein interfaces.[9] This may be due to the ability of these proteins to form multiple interactions. For example, tyrosine can participate in π-stacking interactions, hydrophobic interactions, and hydrogen bonding through the 4-hydroxy group. Arginine can also form multiple interactions including a salt bridge with its positive charge, a number of hydrogen bonds, and the delocalised guanidinium motif can participate in hydrophobic interactions.[10] Aspartic acid also appears in hot spots, twice as often as glutamic acid, due to differences in side chain entropy.[10]

1.2 Targeting Protein-Protein Interactions

As protein-protein interactions play such an essential role in normal physiology, it follows that disruption of these interactions may lead to the development of diseases, including cancers and neurodegenerative conditions.[11] Consequently, PPIs have become an alternative drug target to enzymes, ion channels and transporters.[12] However, protein-protein interactions are notoriously difficult to target. The complexity and incomplete structural knowledge of interactions makes the design of small molecules to inhibit this large surface area challenging, compounded with the lack of binding pockets or grooves within the surface.[13] PPIs are also highly interconnected; participating in a large number of interactions, including hub proteins that may have over 100 binding partners.[14] This along with the lack of naturally occurring small-molecule binding partners results in a lack of natural starting points for the design of potential modulators.[15] Despite this, a number of inhibitors of PPIs have recently been reported.[16–19]

1.3 Identification of PPI Inhibitors

In 1996, Lipinski *et al*. reported the 'rule of five' which predicts that molecules with a molecular weight greater than 500, more than five hydrogen bond donors, 10 hydrogen bond acceptors and a calculated logP greater than 5 would have poor permeability and absorption.[20] Compared to this, the suitability of small molecule inhibitors for PPIs is an ongoing debate. Analysis by Hyvönen *et al.* of small molecules that bind to PPIs showed a broad range in molecular weight of 241-974 Da, a logP of 1.6-10.5, a range between one and six hydrogen bond acceptors and up to three hydrogen bond donors.[21] The diversity of these properties indicates that the effectiveness of a modulator of a PPI depends heavily on the

target and the mode of action. Due to this complexity there are a wide variety of strategies to identify PPI modulators.

1.3.1 High-Throughput Screening (HTS)

Since the early 1990's, high-throughput screening (HTS) has allowed for the rapid identification of small molecule modulators of traditional drug targets. However, it is often difficult to identify modulators of protein-protein interactions in this way as the chemical space of PPIs may not be significantly covered by these libraries, although is still a useful technique for identifying starting points. HTS hits for PPIs are typically active in the low- to sub-micromolar concentrations and are large, complex structures that lack the potential for optimisation. Nevertheless, HTS has been successful in the identification of PPI inhibitors with the discovery of nutlins as MDM2-p53 inhibitors, which led to the development of the nutlin derivative RG7112, **1**, (Figure 2) as a clinical candidate for the treatment of leukaemia.[22–24]

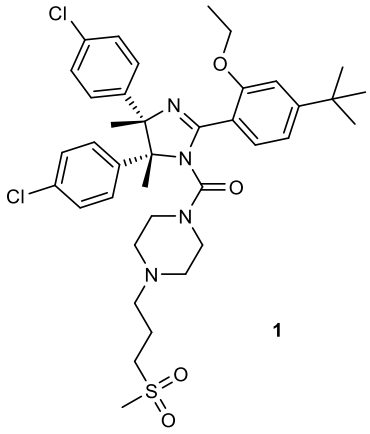


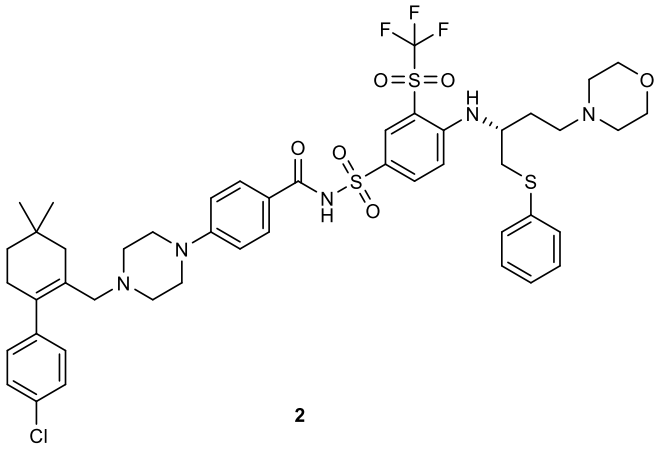
Figure 2. Structure of the nutlin derivative RG7112, **1**[18,23,24]

By expanding screening libraries to include molecules of more complexity may help to improve the hit rates of HTS for PPIs. Majmudar *et al.* investigated both commercial compound libraries and natural product libraries to identify a coactivator of CBP/p300 inhibitors. There were no hits obtained from the 5000 commercial library, however, three were identified from the natural product library.[25]

1.3.2 Fragment Based Drug Design (FBDD)

Fragment screening had been shown to be an effective against targets such as PPIs that were previously thought of as 'undruggable' and it has been illustrated that there is correlation

between the hot-spots of a protein and fragment binding sites.[26,27] By screening low molecular weight fragments the likelihood of finding a hit is increased compared to larger and more complex molecules.[28] As FBDD produces moderate to weak binders, typically 5 mM to 1 µM, a number of highly sensitive techniques have been developed to detect any weak hits. Nuclear magnetic resonance (NMR), mass spectrometry, X-ray crystallography, surface plasmon resonance (SPR) and isothermal calorimetry (ITC) have been used to successfully validate fragment hits.[29–32] FBDD has several advantages over HTS, including a higher hit rate, but also because fragments can be used to bind to multiple different hot spots and then linked together to form complete molecules. However, using FBDD to target PPIs does have some challenges. A relatively large amount of pure, soluble protein is required, and the screening involves expensive equipment. Fragment optimisation often begins with the experimental determination of the binding mode and so it is difficult to apply to PPIs where the structure has not been elucidated, limiting the scope of the technique.[33] It has also been shown experimentally that proteins may undergo conformational changes upon binding of a fragment. Rees *et al.* investigated the maximal protein movement from 25 fragment screens. A maximal protein movement of greater than 5 Å was observed for more than half the fragments screened, emphasising that fragments are capable of causing an induced fit in proteins.[34] Optimisation of a fragment from a hit to a lead compound may also cause deviations in the key binding interactions and so developing suitable linkers is still an area that needs to be investigated.[35] Despite these limitations FBDD remains one of the most promising approaches to targets such as PPIs; one of the most successful applications of FBDD to PPIs was the discovery of navitoclax, **2**, (Figure 3), a potent inhibitor of Bcl-2 family proteins in phase II clinical trials for the treatment of cancer.[36]



2

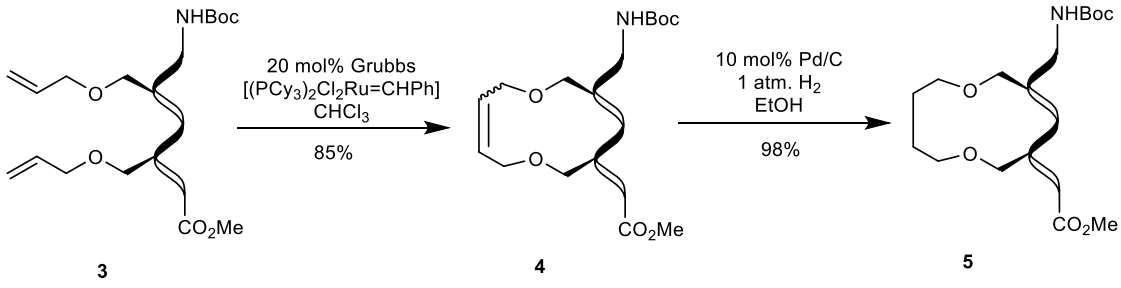
Figure 3. Structure of Navitoclax, **2**[36]

1.3.3 Computational Approaches

Computational screening methods are a high throughput and cost-effective way of identifying initial hits for druggable targets. Databases are freely available for purchase, with suitable properties such as good stability and aqueous solubility, absence of toxic or unwanted groups, and can also be focussed on compounds with the desirable functional groups for interaction with a target. Virtual screening can be divided into two main groups, ligand-based screening and receptor-based screening.[37] Ligand-based screening uses 2D or 3D structures that are known active ligands of a target protein to select other compounds of interest by common substructure or pharmacophore for lead identification and optimisation. Receptor-based screening docks a library of compounds into the binding site of a target to predict protein-ligand interaction geometries and binding affinity.

1.3.4 Rational Design

Due to the problematic nature of small molecules binding to such a large interaction surface, it follows that medium size inhibitors of molecular weight between 1000-2000 Da could be more effective in targeting PPIs. Of the compounds of this size, peptides are the most widely studied. Designing scaffolds that mimic the recognition motifs of peptides, such as α-helices, β-sheets and reverse turns, has been the subject of much research.[38] α-Helices are the largest class of secondary structures of proteins and have a significant role in PPIs. The binding energy for the interactions of α-helices is largely due to hydrophobic residues of the side chains on one face of an α-helix, however, once removed from the protein a peptide rarely retains its biologically relevant conformation.[39] A number of approaches exist to stabilise or mimic an α-helix, including helix stabilisation by including hydrogen or electrostatic bonds at select positions, introduction of α,α-disubstituted amino acids, or covalent approaches such as introducing lactam or disulfide bridges.[40–43] Another strategy to retain helical conformation is peptide stapling. In 1998, Grubbs published his olefin metathesis catalyst that allowed cross-linkages between *O*-allyl serine residues, introducing a carbon-carbon constraint into the peptide (Scheme 1). Diene **3** was reacted with Grubbs catalyst in chloroform to yield the 21-membered macrocycle **4** as a mixture of isomers in 85% yield. Hydrogenation of compound **4** using 10% Pd/C then gave the saturated macrocycle **5** in excellent yield.[44]



Scheme 1. Grubbs synthesis of peptide macrocycles

Grubbs failed to show evidence of improving helical stability through this method. Verdine *et al*. published the ruthenium-catalysed ring closing metathesis (RCM) of olefin containing non-natural amino acids across both one and two α-helical turns.[45] By screening multiple configurations of crosslinks which differ in length, point of attachment and stereochemistry they were able to determine which configurations were stabilising and those which destabilise the helix. This linking of non-natural amino acids can lead to changes in peptide cellular penetration and affinity.[46]

Mimics of β-strands are less common as they typically participate in hydrophilic amide-backbone hydrogen bonding interactions that characteristically bind to flat protein surfaces and are often used to link two hydrophobic hot spots together. These structures also have high flexibility and so efforts have been put into increasing rigidity by conformational restraint.

1.4 The Keap1-Nrf2 Signalling System

The PPI targeted in the project is the Keap1-Nrf2 interaction. The Keap1-Nrf2 signalling pathway is considered one of the most important ways a cell combats oxidative stress through the negative regulation of the transcription factor known as nuclear factor erythroid 2-related factor-2 (Nrf2).[47] Nrf2, often referred to as the master regulator of intracellular antioxidant responses, controls the expression of multiple detoxification enzymes including those involved with glutathione production, regeneration and utilisation as well as NADPH production.[48] Upon exposure to oxidative stress, Nrf2 translocates to the nucleus where it can bind to an antioxidant response element (ARE) which leads to the expression of enzymes involved in the antioxidant response. Under resting conditions, the intracellular levels of Nrf2 are controlled by the protein Keap1 that constitutively degrades it until reactive oxygen species (ROS) interfere with this pathway, resulting in the accumulation of intracellular Nrf2.

1.4.1 Regulation of Nrf2

Keap1, also known as Kelch-like ECH-associated protein 1, acts as an adaptor for the proteasomal degradation of Nrf2 by the E3 ligase Cul3 that catalyses the formation of a bond between Nrf2, and ubiquitin, therefore signalling for its degradation (Figure 4).[49,50]

x

Figure 4. Scheme representing the structure of Keap1 (far left), how it dimerises through its BTB domain and binds to Cul3. The binding of Nrf2 is also represented through its high and low affinity domains. Image used with permission.[51]

For Keap1 to sequester Nrf2 it must bind to Cul3 as a dimer *via* its BTB domain.[52] Although the full structure of the Keap1 protein is yet to be elucidated, the structure can be divided into five main domains: an N-terminal domain (NTD), a Broad complex, Tramtrack and Bric-a-Brac (BTB) domain, an intervening region (IVR), a double glycine repeat and Kelch domain (DGR), and a C-terminal region (CTR).[53] Whilst the BTB region is involved in the interaction with Cul3, it is the Kelch domain that binds Nrf2 non-covalently through two subunits with differing affinities.[54] The 'high-affinity' region of Nrf2 contains the amino acid sequence Glu-Thr-Gly-Glu (ETGE) and the 'low affinity' region contains Asp-Leu-Gly (DLG) and these two portions are separated by an α-helical region containing seven lysine residues (Figure 4).[55] It is these lysine residues that ubiquitin binds to in order to signal for degradation of Nrf2.

The presence of two regions in Nrf2 with different binding affinities has been termed the 'hinge and latch model' whereby the high affinity ETGE sequence acts as a hinge and anchors the Nrf2 protein to Keap1 and the low affinity DTG sequence acts as a latch.[56] This mechanism demonstrates that although both sites need to bind for ubiquitination of Nrf2 to occur, inhibitors that block binding of the DLG domain are effective enough to prevent degradation of Nrf2 whilst the ETGE domain remains bound.[51] This allows newly synthesised Nrf2 to accumulate within the cell.

1.4.2 Crystal Structure of the Binding Site

The crystal structure of the binding site of Keap1 to Nrf2 has been elucidated.[57] This domain, known as the Kelch domain, forms a cylindrical structure comprised of six distinct areas of antiparallel β-sheets forming a β-propeller structure (Figure 5).[57] Each propeller is comprised

of four twisted anti-parallel β-strands, with the *C*- and *N*-terminal ends closing the ring structure through hydrogen bonding with the neighbouring propeller (Figure 5). Overall the Kelch domain has a negative charge but the surface and the binding domain at the bottom of Keap1 is made up of mostly positive charges.[58]

x

Figure 5. Crystal structure of the Kelch domain of Keap1 which has a cylindrical structure made up of six domains (labelled I-VI) comprising of four β-sheets (labelled A-D on blade V). The *N*- and *C*-terminal ends close the structure through hydrogen bonds (labelled N and C respectively). Ligands for Keap1 bind to the bottom portion of the Kelch domain (PDB 1U6D). Image used with permission.[58]

Nrf2 binds to the Keap1 through its Neh2 domain which adopts a β-hairpin conformation that is stabilised by intramolecular hydrogen bonds. This region is made up of the sequence Asp-77, Glu-78, Glu-79, Thr-80, Gly-81 and Glu-82 with three hydrogen bonds that are between the amino group of Gly-81 and the carbonyl of Asp-77, the amino of Glu-79 and the carboxyl group of Asp-77, and the amino group of Glu-82 and the hydroxyl group of Thr-80.[57]

Binding of Nrf2 to Keap1 is preserved through a network of hydrogen bonds between the ETGE and DLG domains of the Nrf2 sequence and the Kelch domain. The key amino acids within the Kelch domain are Asn-382, Arg-380, Ser-363, Ser-602, Ser-508, Arg-483, Arg-415, Gln-530, Tyr-334 and Ser-555 which form 13 hydrogen bonds with the Neh2 fragment peptide ETGE domain (Figure 6), whilst the DLG motif forms nine (Figure 7).[57] Additionally, from the crystal structure it can be seen that the ETGE peptide is further embedded into the binding site than the DLG motif, with Glu-79 of ETGE sitting much further into the pocket, therefore resulting in the stronger binding of the ETGE 'hinge' region.[59] Mutagenesis studies have shown the two glutamate residues, Glu-79 and Glu-82 of ETGE, to be essential to binding to the Kelch domain.[60] The side chains of these residues form electrostatic interactions with multiple residues in the binding site including three key arginine residues. The remainder of interactions of ETGE with the binding domain are from the backbone carbonyl and amino groups.

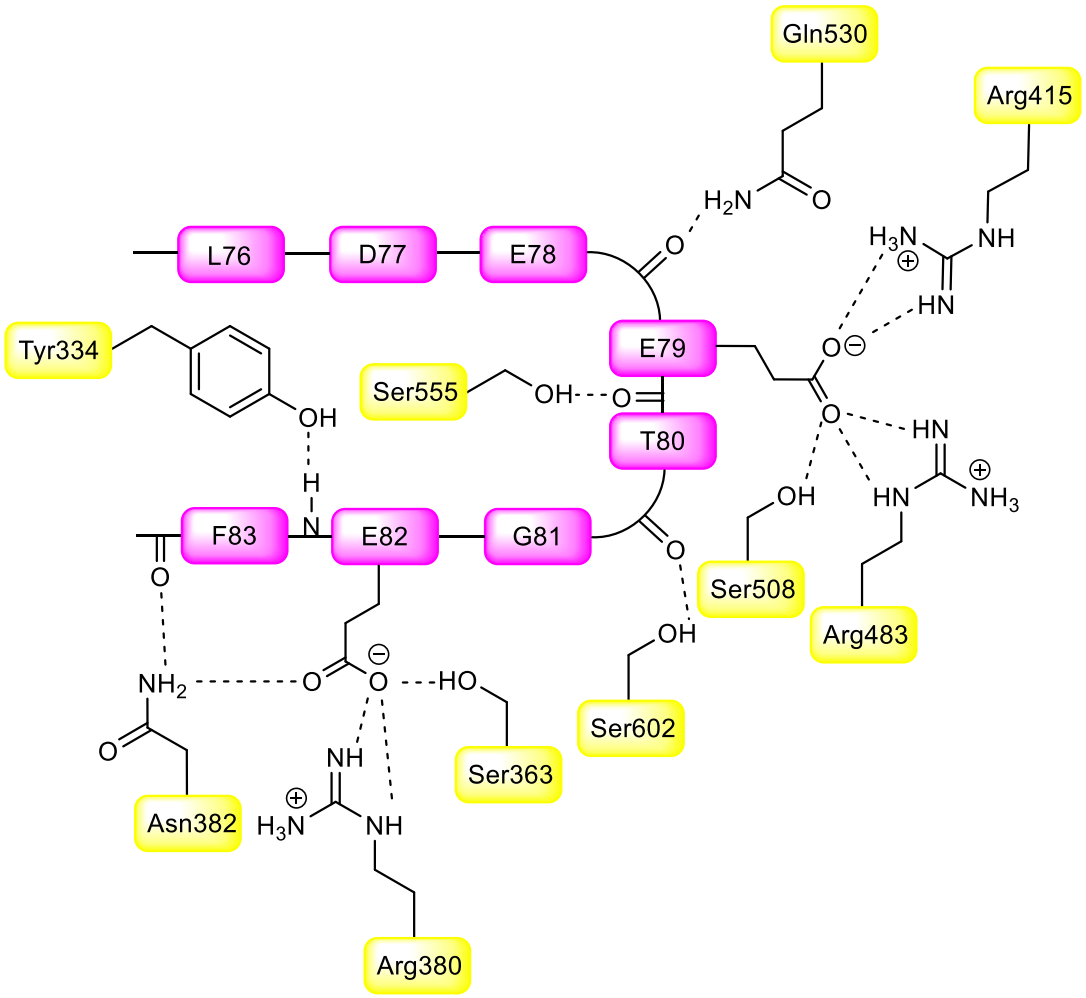


Figure 6. Backbone and side chain hydrogen bonds (dashed lines) from the ETGE region of the Nrf2 peptide (pink) to Kelch domain residues of Keap1 (yellow).[57]

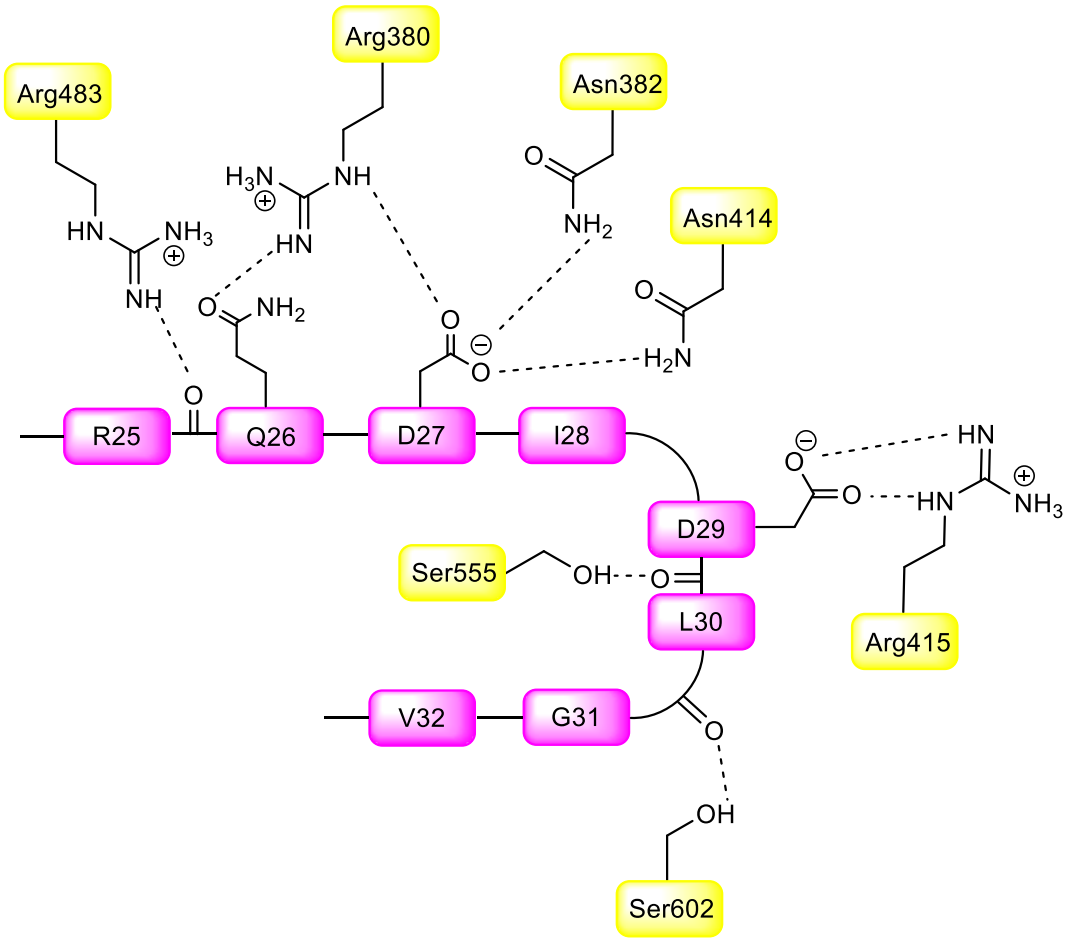


Figure 7. Backbone and side chain hydrogen bonds (dashed lines) from the DLG region of the Nrf2 peptide (pink) to Kelch domain residues of Keap1 (yellow).[57]

1.5 Disrupting the Nrf2-Keap1 Interaction

Numerous natural and synthetic small molecules have been studied for their effect on Nrf2 activation. However, these compounds act indirectly, inhibiting Keap1 by reacting with cysteine residues away from the binding site, resulting in a covalent modification of Keap1. The development of direct inhibitors of the protein-protein interaction of Keap1 and Nrf2 that circumvent the toxic off-target effects of these indirect inhibitors has progressed rapidly, with *in vitro* potencies of lead small molecules showing promising activities for the progression into *in vivo* studies.[61] However, the development of drug-like PPI inhibitors remains challenging, making it ever more critical to explore new techniques to improve therapeutic potential.

1.5.1 Small Molecule Inhibitors

By using the data obtained from the crystal structure of the Kelch domain, virtual libraries can be employed to screen large numbers of compounds before medicinal chemistry analysis of any 'hits' begins.[62] The number of compounds screened can be reduced by the production of a focus library that uses information collected from the Keap1 crystal structure, such as using a species that has the capacity to become negatively charged due to the nature of the binding site existing as largely positive. Binding of any hits may then be analysed using assays that have been developed and structure-activity relationship studies may be performed.

Several compounds have come from this method of high-throughput screening (Figure 8). One example is LH601A **6** which had an initial IC_{50} of 3.0 µM.[63] Experiments were also carried out using glutathione to mimic the cysteine residues of Keap1. During these experiments there was no decomposition or reaction of the thiol present showing that compound LH601A was the first small molecule to directly inhibit the Keap1-Nrf2 binding interaction.[63]

Also generated from assay screening of libraries, compounds **7** and **8** (Figure 8) were found to have IC_{50} of 118 µM and 2.7 µM respectively.[64] These molecules were confirmed to bind to the central cavity of the Kelch domain through a protein-protein interaction by labelling nitrogen atoms of the key arginine residues, Arg-415, Arg-483 and Arg-380, and monitoring changes in their resonance frequency due to a change in their electronic environment.[64]

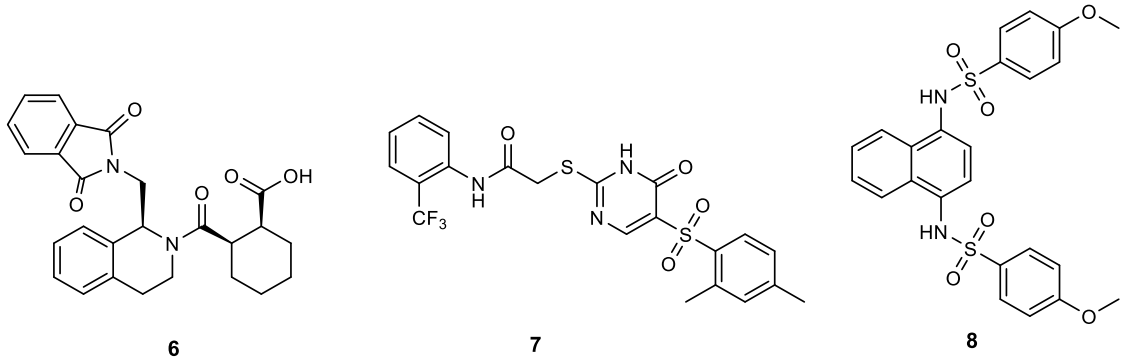


Figure 8. Structures of some small molecule inhibitors of Keap1 to come from screening of libraries of lead compounds.[63–65]

1.5.2 Peptide Inhibitors of Keap1

Nrf2 binds to Keap1 through two domains known as ETGE and DLG. It has been demonstrated that peptides that mimic these sequences can bind to these domains and inhibit the action of Keap1.[60] Peptide sequences that mimic the DLG domain are found to bind with low affinity

and will therefore dissociate easily and are ineffective at inhibiting Keap1. Peptides that mimic the ETGE domain have been found to bind Keap1 with higher affinity within the range of an IC_{50} of 0.257-5.38 μM.[66]

In 2012, Wells *et al*. screened a series of peptides based upon proteins that are known to also bind to Keap1.[60] Besides Nrf2, Keap1 can also interact with other intracellular proteins such as sequestosome-1 or p62, and prothymosin-α. Prothymosin-α and p62 bind to Keap1 through a single binding site, and in the case of p62 through its Keap1-interacting region (KIR) which resembles the ETGE motif of Nrf2. Isothermal calorimetry and luciferase reporter assays showed that sequences derived from p62 may compete *in vivo* with the Nrf2 DLG motif. A partial peptide sequence of the KIR of p62, Ac-DPSTGEL-OH (residues 347-353) was shown to have an IC_{50} of 34.4, which is comparable to that of the DLG motif of Nrf2 (Table 1, Entry 1). Modification of this sequence to become more 'ETGE-like', by replacing the serine residue with glutamic acid, significantly improved the binding affinity by 300-fold, giving an IC_{50} of 0.115 μM (Table 1, Entry 2). Peptides that also showed improved binding from the original sequence were the phosphoserine derivative (Table 1, Entry 5), and two peptides that had replaced leucine for more branched side chain amino acids (Table 1, Entry 3 and 4). However, these peptides were still less active than the glutamic acid derivative (Table 1, Entry 2).

Entry	Sequence	IC_{50} ± SE (μmol/L)
1	Ac-DPSTGEL-OH	34.4 ± 9.4
2	Ac-DPETGEL-OH	0.115 ± 0.013
3	Ac-DPETGEI-OH	0.144 ± 0.018
4	Ac-DPETGEV-OH	0.236 ± 0.024
5	Ac-DPS(p)TGEL-OH	3.97 ± 0.47

Table 1. IC_{50} values for the binding of p62 derived peptides to the Kelch protein.[60]
SE = standard error

This work was continued in 2013 with the development of peptide inhibitors of Keap1 with modified *C*- and *N*-termini to reduce the overall charge and increase the lipophilicity of the molecule.[66] Modifications of the original sequence, Ac-DPSTGEL-OH, included replacement of *N*-terminal aspartic acid to asparagine, and replacing the *C*-terminal α-carboxylate with a carboxamide, as well as replacement of the *C*-terminal glutamic acid with glutamine (Table 2). The binding of these peptides was studied by fluorescence polarisation (FP) assays where

the peptides compete with a fluorescein labelled peptide. Changing the *C*-terminal carboxylate to a carboxamide (Table 2, Entry 2) lowered the binding affinity of the peptide, and the same occurred upon replacement of the *N*-terminal aspartic acid to asparagine (Table 2, Entry 3). Combining both modifications into the peptide reduced the binding affinity by a further order of magnitude (Table 2, Entry 4). Replacement of the *C*-terminal glutamic acid, which forms fewer interactions with Keap1, with glutamine also resulted in poor binding to the Kelch domain (Table 2, Entry 5). Substituting the *N*-terminal acetyl group with benzoyl and stearoyl groups introduced more lipophilicity into the molecule (Figure 9). Addition of the benzoyl group (Table 2, Entry 6) resulted in retention of activity, and introduction of steric acid resulted in 5-fold greater activity than the original peptide (Table 2, Entry 7). Performing the same alterations to the steric acid conjugates decreased the activity of the peptides when compared to the equivalent acetyl peptides (Table 2, Entries 8 and 9). The steric acid conjugated peptides were also able to show micromolar and nanomolar activity in cell-based assays and therefore may be used as lead-like molecules for the development of peptidomimetic inhibitors of Keap1 (Table 2, Entries 7-9).

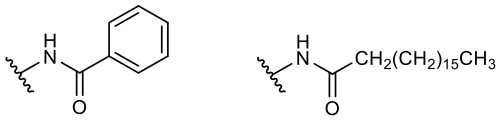


Figure 9. Structures of the benzoyl (left) and stearoyl (right) *N*-terminal groups

Entry	Sequence	FP IC_{50} ± SE (μM/L)
1	Ac-DPETGEL-OH	0.115 ± 0.013
2	Ac-DPETGEL-NH_2	0.634 ± 0.064
3	Ac-NPETGEL-OH	0.875 ± 0.082
4	Ac-NPETGEL-NH_2	8.33 ± 1.12
5	Ac-NPETGQL-OH	68.9 ± 15.2
6	Bz-DPETGEL-OH	0.159 ± 0.017
7	St-DPETGEL-OH	0.022 ± 0.003
8	St-NPETGEL-OH	0.272 ± 0.029
9	St-NPETGEL-NH_2	3.71 ± 1.14

Table 2. IC_{50} values for the binding of p62 derived peptides to the Kelch protein using an FP assay.[66]
SE = standard error, St = steroyl group, Bz = benzoyl group

Lu *et al*. have studied the effect of head-to-tail cyclisation, using the optimised template peptide Ac-LDPETGEFL-OH.[67] A molecular dynamics (MD) simulation was first performed in

order to direct the synthesis of peptides. From these studies it was shown that this peptide adopted a conserved binding pattern similar to those of other ETGE-containing peptides. However, direct head-to-tail cyclisation of this peptide would have resulted in affected the conformation of the key binding residues and so additional residues were required. As the *N*-terminal of the peptide was much shorter than the *C*-terminal, residues were added to ensure a consistent length of the two antiparallel β-strands. A glutamine residue was added, allowing for the introduction of glycine as a flexible linker, resulting in the cyclic peptide (c[GQLDPETGEFL]). MD studies of this peptide showed it interacted with Keap1 in a similar manner to the Ac-LDPETGEFL-OH peptide (Figure 10). The potency of these peptides, along with the linear Ac-GQLDPETGEFL-OH peptide, were then tested in an FP assay. The head-to-tail cyclic peptide gave in IC_{50} of 18.31 nM, which was more potent than its linear equivalent that gave an IC_{50} of 63.15 nM. Cellular activation of Nrf2 was tested using the Nrf2/ARE-luciferase reporter assay, with the linear peptide showing only weak binding even at the highest concentration (10 μM). In contrast, the cyclic peptide showed a notable concentration-dependent increase in luciferase activity upon treatment with the peptide, suggesting that the peptide substantially enhanced the activation of the Nrf2-ARE system in the cellular level.

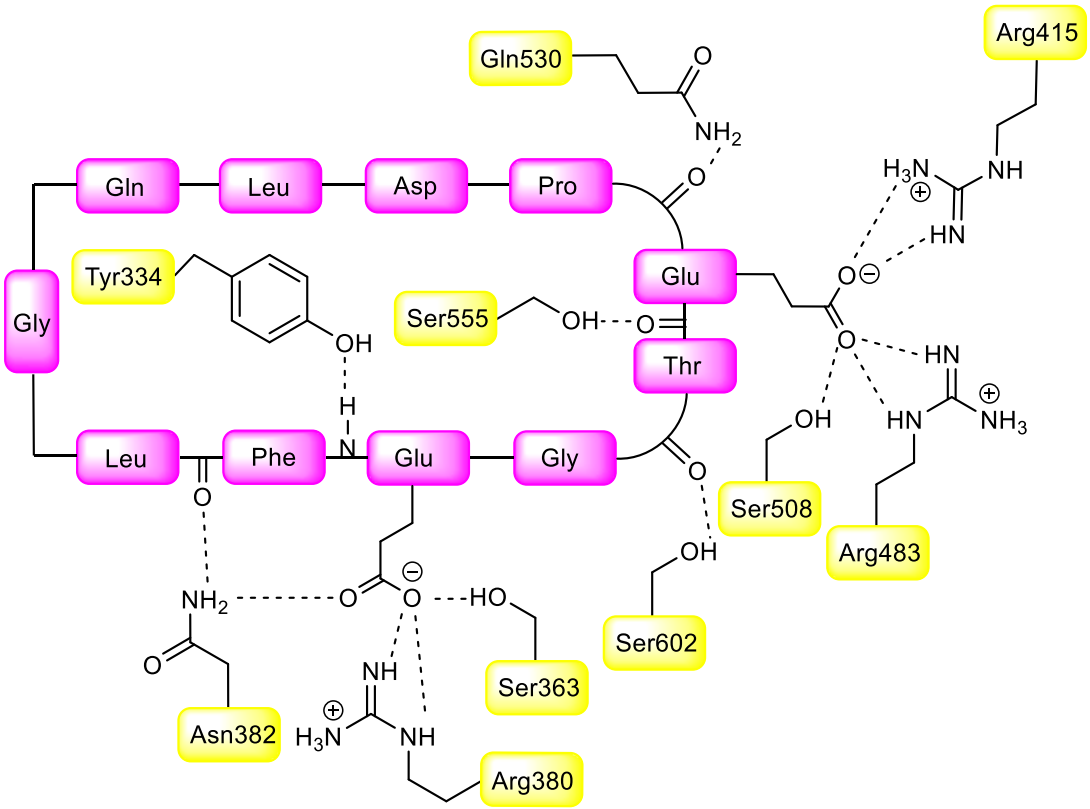


Figure 10. Interaction model of the cyclic peptide (c[GQLDPETGEFL]) (pink) with Keap1 (yellow) showing it binds in a similar manner to the native Nrf2.[67]

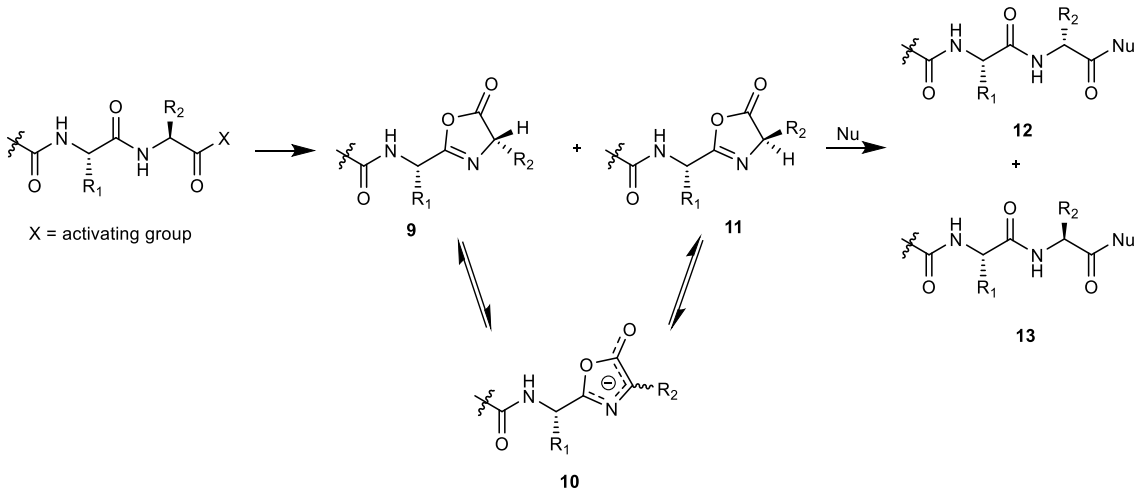
In order for these peptides to be tested for their inhibitory effect on the Keap1-Nrf2 PPI, they first needed to be synthesised. In this project, both solution phase and solid phase methods were used for peptide synthesis, along with a number of different macrocyclisation techniques. Herein, these synthetic procedures are briefly discussed.

1.6 Chemical Synthesis of Peptides

Amino acids combine *via* a condensation reaction to form peptides and proteins. Peptide coupling reactions involve the attack of an amino group of one entity to a carbonyl group of another. In chemical peptide synthesis this most commonly occurs from the *C*-terminal end of the peptide and proceeds towards the *N*-terminal end. However, in living organisms this occurs in the opposite direction. The formation of a peptide bond involves two steps, activation of the carboxyl group of one residue followed by nucleophilic attack of the amino group of another residue. The activated form of the acid may be stable, such as an active ester, have intermediate stability, such as an acyl halide, azide or anhydride, or be a transient intermediate, that immediately reacts with a nucleophile originating from the other

reactants. The amide bond is formed when the amino group of the amine reacts with the activated acid.

To activate a carboxylic acid, coupling reagents are used. The choice of coupling reagent is often critical to the outcome of the reaction, as amides with a wide range of chemical groups and reactivities are formed, for example, when building a library for medicinal chemistry. Another important feature of a coupling reagent needs to be the minimisation of racemisation during the reaction. This epimerisation usually occurs when the terminal acid is activated, leading to the formation of an oxazolone **9** that under basic conditions forms the conjugated anionic intermediate **10** (Scheme 2). The resulting oxazolone then reacts with a nucleophile leading to the racemisation of the chiral centre. Therefore, peptides are usually synthesised from the *N*-terminus and mild activation conditions are needed.



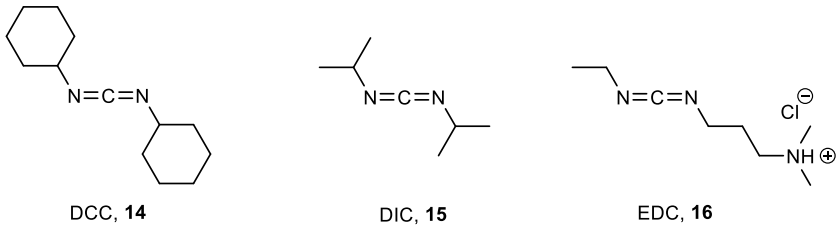
Scheme 2. Racemisation during amide coupling

1.6.1 Peptide Coupling Reagents

1.6.1.1 Carbodiimides as Coupling Reagents

Among the most widely used coupling reagents for amide bond formation are carbodiimides. Carbodiimides have the core structure of R-N=C=N-R and were the first coupling reagents to be synthesised. Dicyclohexylcarbodiimide **14** (DCC, Figure 11) has been used since 1955 and is still widely used for amide and ester formation.[68] The synthesis of an amide using carbodiimides is relatively simple, however, several side reactions are possible. The first step involves the formation of *O*-acylurea from the reaction of DCC and the carboxylic acid, and this intermediate can react to form several products. The intermediate can react directly with the amine to form the amide. The by-product from this reaction is dicyclohexylurea (DCU)

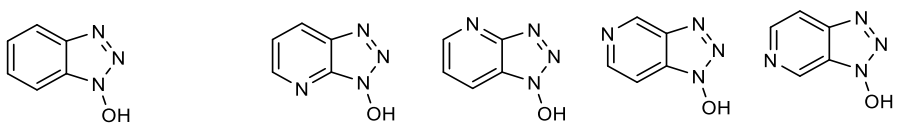
that is insoluble in most organic solvents and water and is therefore easily removed by filtration. The second possible product involves the rearrangement of the *O*-acylurea to form the stable *N*-acylurea as a main undesired product. The third is the formation of the carboxylic acid anhydride that may then react with the amine to form the desired amide product. Since in some cases traces of the DCU by-product are difficult to remove, other carbodiimide reagents have been developed, including diisopropylcarbodiimide **15** (DIC) and *N*-ethyl-*N'*-(3-dimethylamino propyl)carbodiimide **16** (EDC), that has a water-soluble urea by-product that can be removed upon work up (Figure 11).



DCC, **14** DIC, **15** EDC, **16**

Figure 11. Structures of DCC, DIC, EDC

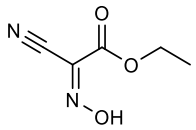
Additives such as *N*-hydroxy derivates (Figure 12) are used to increase the efficiency of these reactions. Koenig and Geiger first introduced the 1-hydroxy-1*H*-benzotriazole **17** (HOBt) additive to improve yields and decrease the amount of epimerisation within reactions.[69] HOBt supresses the formation of the *N*-acylurea and also protonates the *O*-acylisourea preventing the rearrangement and shifting the reaction towards the formation of corresponding active esters that stabilise the approach of the amine *via* hydrogen bonding. In 1994 a related compound 1-hydroxy-7-azabenzotriazole **18** (HOAt) was reported.[70] HOAt showed improved reaction rates and lower degrees of epimerisation than HOBt due to the nitrogen atom at the 7-position of the benzotriazole. This nitrogen is electron-withdrawing and therefore provides a better leaving group, improving the reactivity. It was also shown by Bienert *et al*. that the neighbouring group effect in 7-HOAt increases the reactivity and reduces the loss of conformational integrity significantly when compared with 6-HOAt **21**, 5-HOAt **20** and 4-HOAt **19**.[71]



HOBt, **17** HOAt, **18** 4-HOAt, **19** 5-HOAt, **20** 6-HOAt, **21**

Figure 12. Structure of *N*-hydroxy additives

The most recent additive ethyl-2-cyano-2-(hydroxyimino)acetate or Oxyma **22** (Figure 13) is a safe and efficient reagent used in carbodiimide peptide coupling.[72] It supresses base catalysed side reactions including racemisation more effectively than both HOBt and HOAt and also showed improved coupling efficiency. Calorimetry studies demonstrated a lower risk of explosion when compared to the benzotriazole compounds, as both HOBt and HOAt exhibit explosive properties.[72]

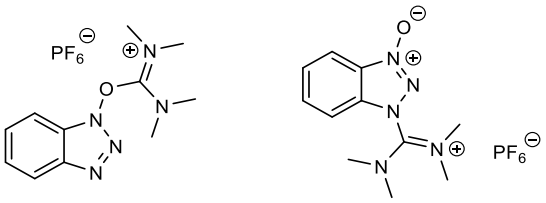


22

Figure 13. Structure of Oxyma

1.6.1.2 Phosphonium and Aminium/Uronium Salts

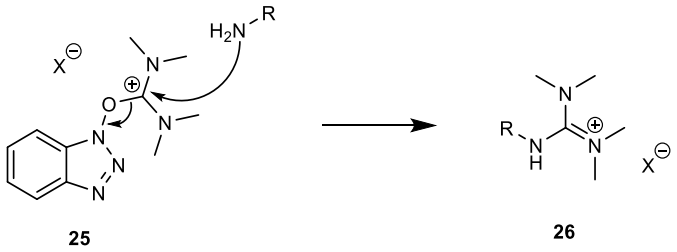
Uronium **23** and aminium **24** (Figure 14) peptide coupling reagents based on the benzotriazole additives **17** and **18** are also commonly used. These include reagents such as 1-[bis(dimethylamino)methylene]-1H-1,2,3-triazolo[4,5-b]pyridinium-3-oxid hexafluoro phosphate (HATU) and 2-(1*H*-benzotriazol-1-yl)-1,1,3,3-tetramethyluronium hexafluorophosphate (HBTU). Coupling reagents based on uronium salts were originally reported as the *O*-isomer though it was later determined by X-ray analysis that their true structure was that of the guanidium salt.[73]



23 **24**

Figure 14. Structure of the uronium (left) and aminium (right) isomers

These reagents are capable of forming the same active ester as in the carbodiimide reactions and differ only in the rate of the initial activation step. In these reactions timing of addition of reagents and the order of addition are crucial as a common side reaction involves the amine reacting with the coupling reagent to form a guanidinium by-product **26** (Scheme 3).



Scheme 3. Formation of the guanidinium by-product **26**

The use of phosphonium salts as coupling reagents was first reported by Gawne *et al*. in 1969 however, they were only widely adopted after studies conducted by Castro and Coste who introduced (benzotriazole-1-yloxy)tris(dimethylamino)phosphonium hexafluorophosphate **27** (BOP, Figure 15) and (benzotriazole-1-yloxy)tris(pyrrolidino)phosphonium hexafluorophosphate **28** (PyBOP, Figure 15) respectively.[74–76] BOP is a commonly used reagent in peptide synthesis, however, its coupling liberates hexamethylphosphorotriamide (HMPA) which is classified as a human carcinogen. This led to the development of PyBOP that retains the rapid coupling of BOP but results in less harmful by-products.

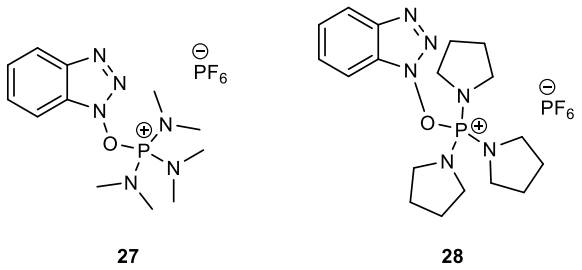
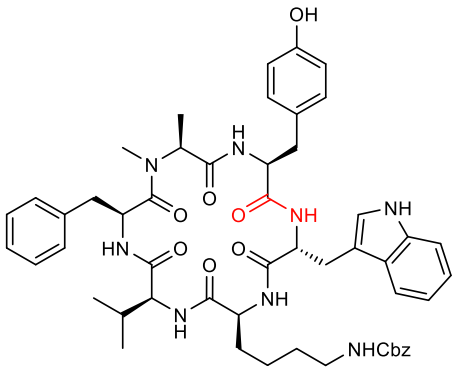


Figure 15. Structure of BOP and PyBOP

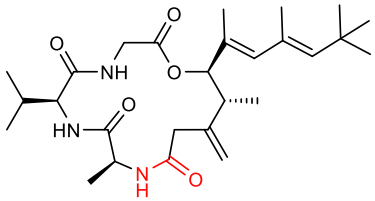
Phosphonium salts react with the carboxylate and therefore a minimum of one equivalent of base is required. The mechanism of the reaction involving the acyloxyphosphonium salt has been proposed by several authors including Kim and Patel who reported that this intermediate can exist at -20 °C when BOP is used in the absence of excess HOBt.[77] Conversely, Castro and Dormoy suggested this species is unstable even at low temperatures and immediately undergoes a reaction with carboxylate ions present to form the anhydride.[75] Alongside this Coste and Campagne theorise that this intermediate is highly unstable and undergoes conversion to the active ester.[78] In spite of this, it is widely accepted that when phosphonium salts containing nucleophilic derivates are used the active species is an ester. An advantage of phosphonium salts over the aminium/uronium salts is that the phosphonium does not react with amine preventing guanidylation.

1.6.1.3 Organophosphorus Reagents

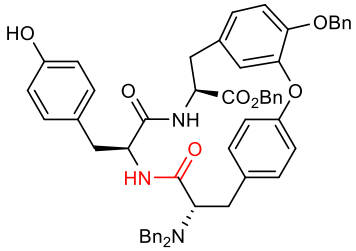
In 1972, Yamada introduced the mixed carboxylic-phosphoric anhydride method to peptide chemistry using diphenylphosphoryl azide **29** (DPPA, Figure 17), synthesised from diphenylphosphorochloridate and sodium azide.[79] DPPA is an effective peptide coupling reagent that shows little racemisation in reactions and is also inactive to the functional groups present in serine and threonine, asparagine and glutamine, histidine, tryptophan, methionine, and nitroarginine.[80] Consequently, peptide couplings involving these functional groups proceed without any side reactions. In 1979, Veber *et al*. reported a simple procedure that allows rapid isolation of cyclic peptides using DPPA.[81] Peptides with varying ring sizes were synthesised in amounts up to 50 g, and subsequently DPPA has been used frequently for lactamisation of macrocyclic peptides (Figure 16). The highly potent cyclic hexapeptide analogue of somatostatin **30** was synthesised using solution-phase peptide synthesis. Cyclisation was achieved using DPPA and sodium hydrogen carbonate as a base at 0 °C in 77% yield, followed by deprotection to give **30** in >99% purity in batches of 40-50 g.[82] DPPA was also used for macrocyclisation of the natural product (4*R*, 5*R*)-antillatoxin **31** in 63% yield and the K13 precursor **32** in 60% yield.[83,84]



30



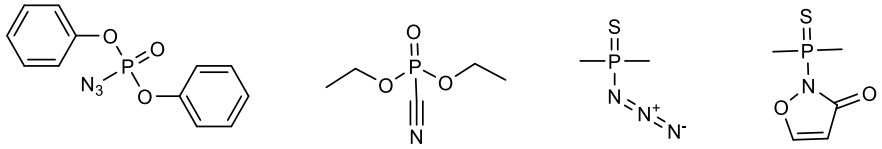
31



32

Figure 16. Cyclic peptides obtained by macrolatamisation with DPPA. Bonds in red show the cyclisation point.

Modification of DPPA has led to the development of analogues such as diethyl phosphorocyanidate **33** (DEPC) as well as thiophosphinic-type coupling reagents including MPTA **34** and MPTO **35** (Figure 17).[85,86] MPTA is crystalline and stable for long term storage, yet side reactions associated with azide and DPPA methods including the formation of carbamoyl azide and urea derivatives could not be avoided. Therefore, 3-dimethylphosphinothioyl-2(3H)-oxazolone (MPTO) was synthesised and successfully avoided the side reactions specific to the azide method.



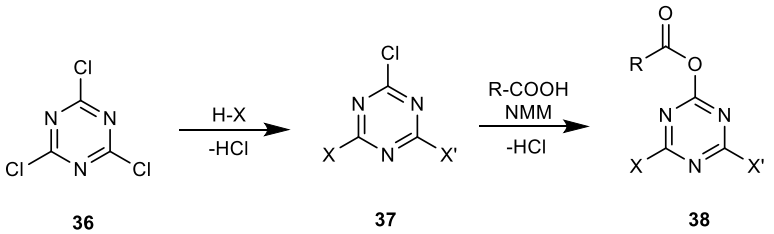
29 **33** **34** **35**

Figure 17. Structures of DPPA (**29**), DEPC (**33**), MPTA (**34**), MPTO (**35**)

1.6.1.4 Triazine Coupling Reagents

1,3,5-Triazines have also been successfully used as coupling reagents. The highly reactive 2,4,6-trichloro-1,3,5-triazine **36** or cyanuric chloride, is produced in the millions of tonnes per year and is amongst one of the lowest priced reagents. The high reactivity of **36** creates difficulties when used in the synthesis of multifunctional compounds. However, the presence of three chlorine atoms makes it an interesting template for the attachment of a chiral auxiliary.

Further studies by Kaminski showed that substitution of the chlorine atoms of **36** with methoxy or phenoxy groups changed the reaction with carboxylic acids.[87] Rather than the acyl chloride the reaction gives the intermediate **37** that under further treatment with amines or alcohols gave the corresponding amides and esters (Scheme 4). Preliminary results showed the substituents on the triazine ring affected the acylating ability of **37**. The reactivities decreased starting from X = Cl, X' = OMe > X, X' = OMe > X, X' = OPh with the most reactive giving esters and amides in 74-98% yield.

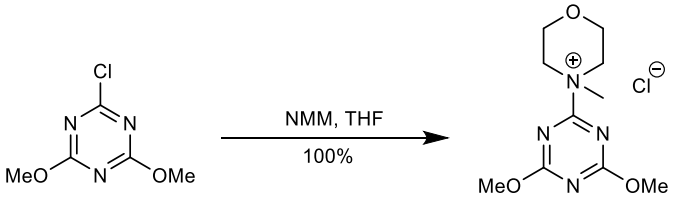


36 **37** **38**

Scheme 4. Substitution of the chlorine atom of **36** to control reactivity. X, X' = Cl, OMe, OPh

The reactive 2-chloro-4,6-dimethoxy-1,3,5-triazine **39** (CDMT) analogue has been widely used in peptide synthesis and has shown to be a useful reagent in terms of stability, mild reaction conditions and cost. *N*-Methylmorpholine (NMM) is typically used as the base in coupling reactions with CDMT, with an inert solvent such as dichloromethane, acetonitrile or tetrahydrofuran, and under these conditions low levels of racemisation (<5%) are typically observed.[88]

The triazine 4-(4,6-dimethoxy-1,3,5-triazin-2-yl)-4-methylmorpholinium **40** (DMTMM, Scheme 5) derived from the reaction of CDMT and NMM can also be used for the synthesis of amides.[89] The advantage of DMTMM is that it enables a one-pot condensation of carboxylic acids and amines in protic solvents such as methanol or water as well as a variety of aprotic organic solvents. The by-products of the reaction are highly water-soluble and are therefore easily removed upon washing with water. Tani *et al*. investigated the levels of racemisation when DMTMM is used for the coupling of 4-methoxybenzyloxycarbonyl (Z(OMe))-Gly-L-Ala-OH and H-L-Phe-OBzl in various solvents.[90] No racemisation was observed in ethyl acetate, THF, DMF or acetonitrile and slight racemisation (<2%) was seen in dimethylsulfoxide, methanol and ethanol.

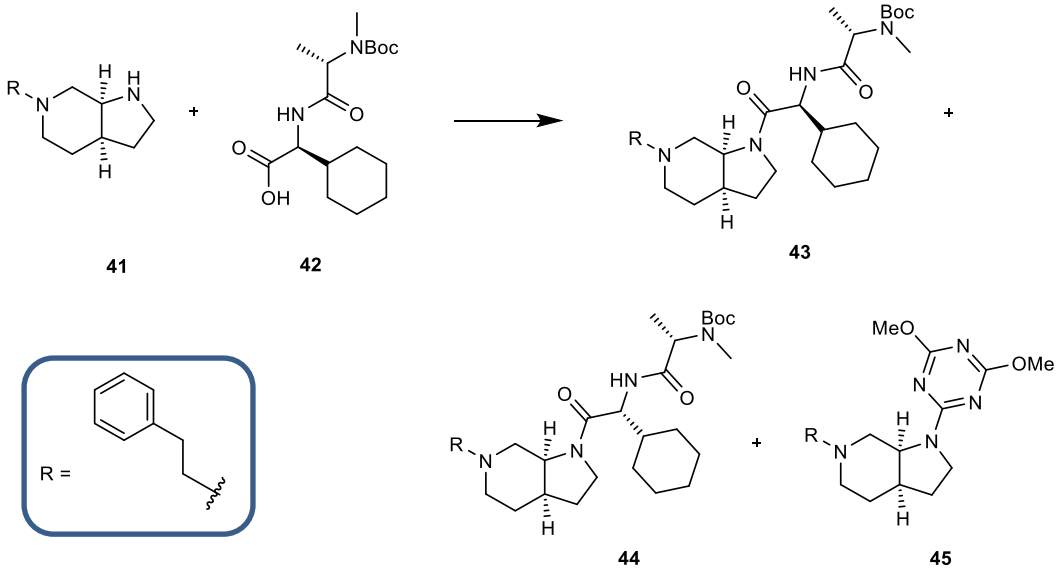


CDMT, **39** DMTMM, **40**

Scheme 5. Reaction of CDMT to form DMTMM[89]

DMTMM **40** has also shown to be the preferable coupling reagent in cases such as for sterically hindered amines. Shieh *et al*. the use of DMTMM for coupling of sterically hindered peptidomimetics compared to other coupling reagents such as CDMT **39**, HBTU/HOBt and BOP.[91] In the reaction shown below (Scheme 6) DMTMM gave the desired peptide **43** in 97%

yield, with <1% of the diastereomer **44** and 2% of the *N*-arylated product **45**. In contrast, CDMT gave only 25% yield of the desired product **43** and 75% of **44** and HBTU/HOBt gave 75% yield of **43** and 25% of the diastereomer **44**. BOP, a reagent well-known for supressing racemisation with sterically hindered amines gave 1.5% racemisation, comparable to that of DMTMM, however, a lower yield of desired product **43** of 94% was observed as 4% of an unidentified by-product was found. These results were repeated with other sterically hindered amines demonstrating DMTMM as a versatile reagent.



Reagents	43 (%) Desired product	44 (%) Racemisation	45 (%) *N*-Arylation
HBTU/HOBt	75	25	0
CDMT	25	0	75
DMTMM	97	<1	2
BOP-Cl	94	2	0

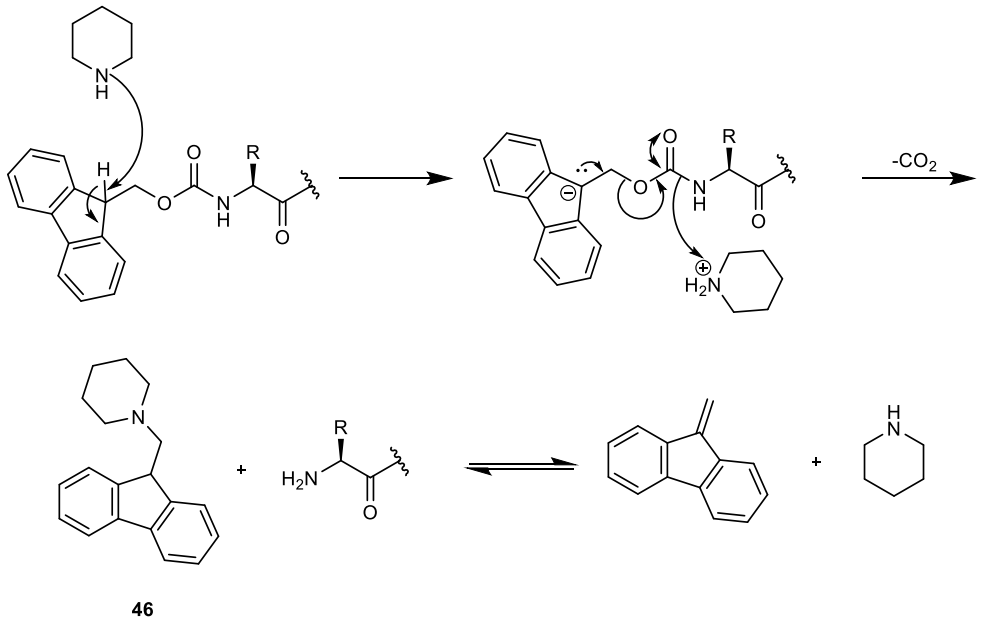
Scheme 6. Coupling of **41** and **42** with a variety of coupling reagents to compare racemisation.[91]

1.7 Solid Phase Peptide Synthesis

Solution phase peptide synthesis is successful in the synthesis of short chain peptides, however, as the number of amino acids increases, difficulties with solubility and purification become challenging. The synthesis of larger and more complex peptides has been made possible by the evolution of solid phase peptide synthesis, first introduced by Bruce Merrifield in 1963.[92] The process works by attaching the first amino acid in a chain to a solid polymer through a covalent bond, followed by the addition of the subsequent amino acids

one at a time in a step-wise manner, before removing from the solid support when synthesis is completed. While the peptide is attached to the insoluble solid polymer it can be filtered and washed free of any reagents or by-products, thereby avoiding the large losses which are normally encountered during isolation and purification of the intermediate peptides. This not only simplifies the synthesis of long chain peptides but also shortens the amount of time required to synthesise them.

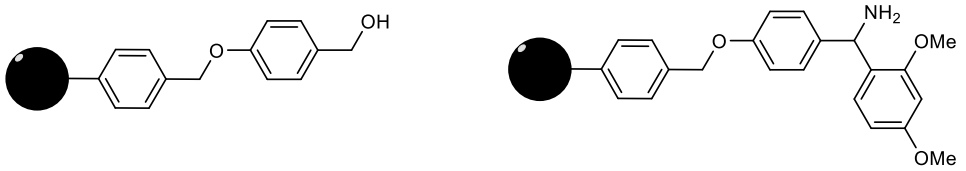
The strategies that have been developed for solution phase peptide synthesis can be adapted to solid phase. However, it does also present some new challenges. The *C*-terminal of the first amino acid is attached to a resin and protecting groups are required for the *N*-terminal end as well as any side chain groups. The two most widely used *N*-terminal protecting groups are the *tert*-butoxycarbonyl (Boc) group that is removed by acids, such as trifluoroacetic acid, and the fluoren-9-methyloxycarbonyl (Fmoc) group that is removed by bases such as piperidine. The Fmoc group is the most commonly used *N*-terminal protecting group used in solid phase synthesis as it can be removed under milder conditions. The Fmoc group can also be used to monitor the coupling of amino acids by simple UV spectrophotometry analysis. When deprotected with 20% piperidine in DMF, a known quantity a dibenzofulvene-piperidine adduct **46** (Scheme 7) is formed that has a unique UV absorbance at 301 nm. The loading of the amino may then be calculated using this absorbance and that of the same piperidine solution used for deprotection.



Scheme 7. Fmoc deprotection mechanism

Polystyrene is the most common resin used in solid phase synthesis and most of these supports contain 1-2% divinylbenzene (DVB) as a cross-linking reagent. These resins are made up of small beads of one of two sizes of 100-200 mesh (75-150 microns) and 200-400 mesh (35-75 microns). The swelling of this polystyrene material is key step in solid phase synthesis as it affects the diffusion and accessibility of the reagents into the core of the polymer, thereby influencing the reaction efficiency. The swelling factor is dependent on the type of resin and the solvent used. The swelling factor of 1% DVB cross-linked resin is typically 5-6 times in dichloromethane, THF or toluene, four times in DMF, two times in acetonitrile or ethanol and no swelling in water. Conversely, 2% DVB cross-linked resin swells only 2-4 times in dichloromethane. Merrifield observed that the swelling was highest in dichloromethane, however, it is not compatible with piperidine, used for Fmoc deprotection, due to the formation of piperidine hydrochloride. Therefore, when a polystyrene resin is used, dichloromethane is typically used at the start of the synthesis and is sometimes used as the cleavage solvent. DMF is classically the solvent used for peptide couplings in solid phase synthesis.[93]

A resin is composed of this polymeric solid support and also a linker that facilitates the temporary anchoring of the first amino acid to the solid support. A linker should be able to immobilise the first amino acid in high yield, be stable to the reagents used in synthesis, and have a high yielding cleavage of the peptide without leading to the formation of unwanted by-products. Most linkers use acidic conditions for cleavage and release the peptide as *C*-terminal acids and amides, the most common examples being the Wang **47** and Rink-amide **48** linkers respectively (Figure 18).

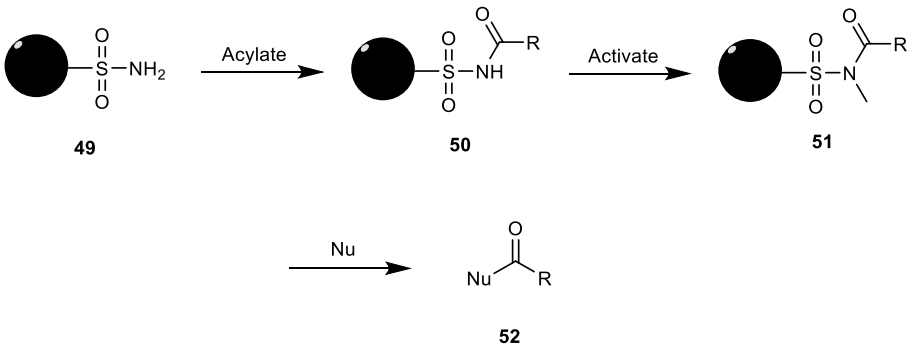


Wang Resin, **47** Rink Amide Resin, **48**

Figure 18. Structures of linkers

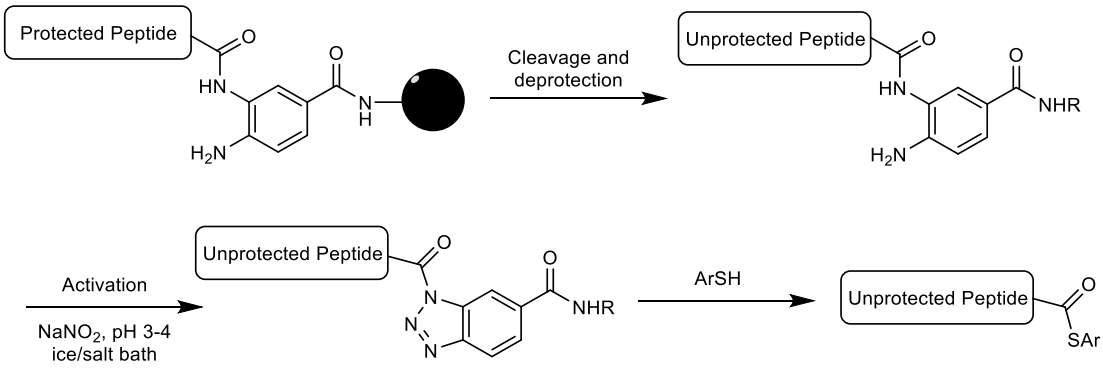
There are several specialised linkers that have been developed that can release the peptides as esters, thioesters or secondary amines. First introduced by Kenner in 1971, safety catch linkers are stable to a large range of reaction conditions and are activated and made labile at the end of a synthesis, releasing the peptide from the resin.[94] Kenner's strategy employed an *N*-acylsulfonamide **50** that is stable to acidic and basic conditions. Activation of **50** through

reaction with diazomethane, gives an *N*,*N*-methylacylsulfonamide **51** that can be cleaved with aminolysis, hydrazinolysis, or saponification to yield primary amides, hydrazones or carboxylic acids respectively (Scheme 8).



Scheme 8. Kenner's safety catch linker[94]

Another strategy for *C*-terminal modification is the introduction of a labile group between the *C*-terminus of the peptide and the solid support. However, the reaction scope is limited by the stability of this labile group to a variety of conditions. Therefore, an alternative approach is the use of a stable moiety between the resin and the *C*-terminus, that can be activated to a more labile group at the cleavage step. Off-resin activation techniques are often plagued by side-product formation and complicated preparation procedures. Lui *et al*. developed a method for synthesising peptide thioesters using a benzotriazole moiety.[95] In this method, *o*-aminoanilide is used as a linker in between the peptide and the solid support, and using standard solid phase conditions a peptide chain can be extended from this (Scheme 9). The unprotected peptide *o*-aminoanilide was then cleaved from the resin and activated to the benzotriazole linker using $NaNO_2$, before undergoing thiolysis to give the resulting thioester. Nevertheless, this approach requires off-resin cyclisation of the 3,4-diaminobenzoic acid linker and is limited to aqueous buffer conditions incompatible with protected peptides.



Scheme 9. Activation of a peptide *via o*-aminoanilides[95]

On-resin functionalisation of the *C*-terminal of peptides is a more effective approach, with the cleavage and incorporation of a functional group at the *C*-terminus occurring simultaneously. In 2016, Raj *et al*. developed a universal method for on-resin functionalisation.[96] This technique requires a *C*-terminal serine residue that upon activation gives a cyclic urethane moiety, predisposing the amide backbone to nucleophilic displacement by a variety of nucleophiles, resulting in modified acids, esters, *N*-aryl amides, and alcohols (Figure 19). This method allows elongation of a peptide chain to be carried out under standard conditions and only activated peptide chains are released from the solid support, without racemisation, subsequently giving highly pure *C*-terminally modified peptides.

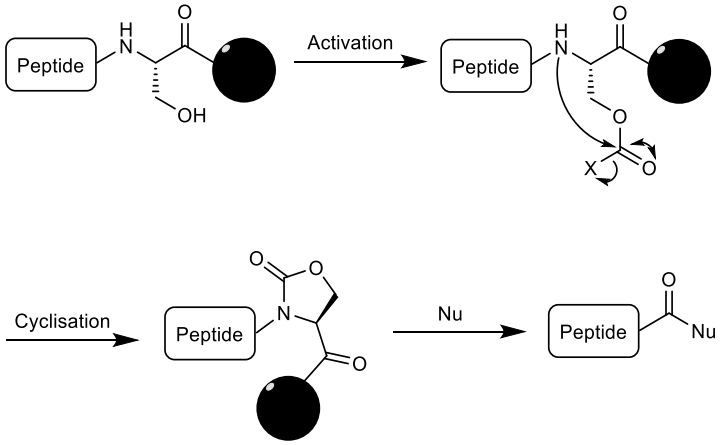


Figure 19. Synthesis of *C*-terminal modified peptides by nucleophilic displacement of a cyclic urethane moiety.[96]

1.8 Cyclic Peptides

Cyclic peptides have been extensively studied over the past few decades and have a range of applications including drug discovery, in the agricultural industry and nanomaterials. They

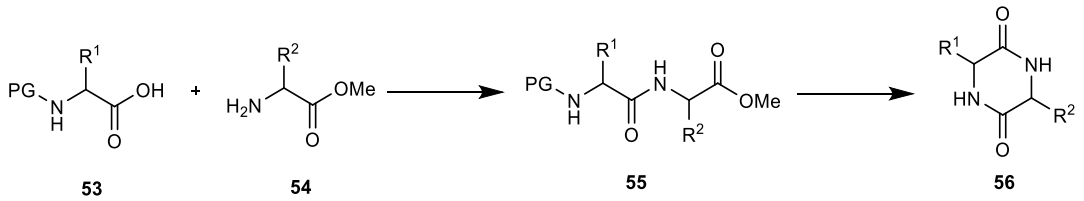
can be classed as homodetic cyclic peptides that comprise purely of normal peptide bonds, isopeptides that contain one or more non α-carbon peptide bonds, depsipeptides that contain a lactone bond in place of an amide bond, and bicyclics that are connected *via* a bridging group.

Cyclisation rigidifies the backbone of the peptide locking it in its active conformation and reduces the entropy loss upon binding with its target, improving the biological activity compared to its linear counterpart. Cyclic peptides have resistance to exopeptidases, that cleave the terminal or penultimate amino acid residue from a chain, and as their structure is less flexible, they can also show enhanced resistance to endopeptidases.

1.8.1 Diketopiperazines

2,5-Diketopiperazines (DKPs) represent the smallest class of cyclic peptides and although often considered a side reaction in peptide synthesis, showed the first example of peptide bond formation through heating glycine in CO_2 and HCl gas to give cyclo-[Gly-Gly].[97] DKPs are found in numerous natural products both alone and as part of larger, more complex structures and are often also found as the degradation products of polypeptides. In terms of drug discovery these small molecules are attractive starting points. They provide constrained, heterocyclic scaffolds that can mimic peptide conformation without the unfavourable physical properties or high metabolism of peptides. The ring has potential for six points of diversity and contains multiple sp^3 centres, which may allow for alternative binding interactions when compared to planar pharmaceuticals currently on the market.

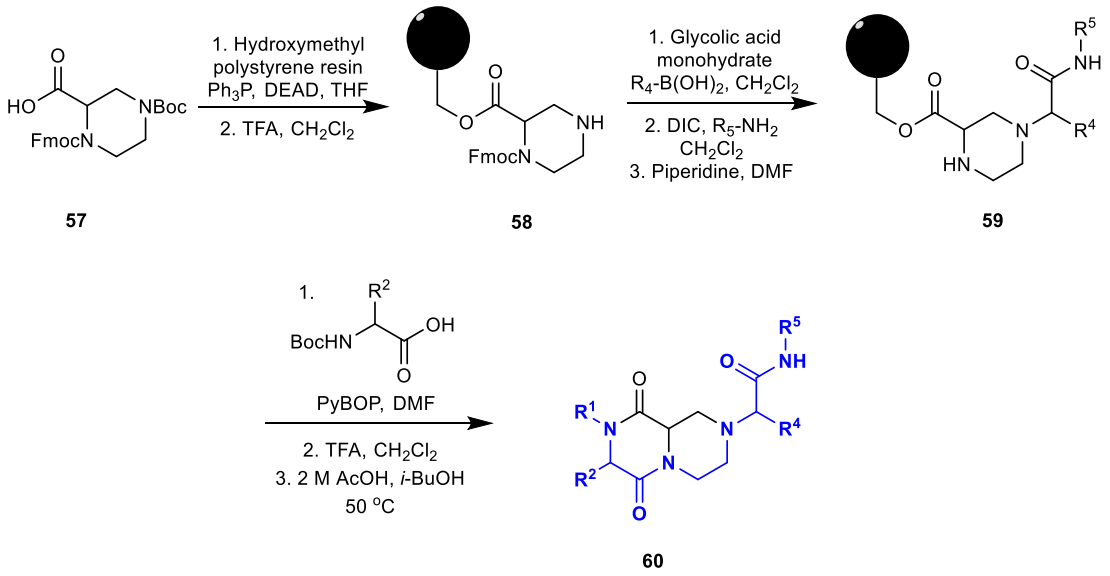
Due to efforts in drug discovery and natural product synthesis, methods for the synthesis of DKPs continue to emerge. The most common method for synthesising DKPs uses an α-amino acid ester as well as an α-amino acid with a protected nitrogen group to first give the dipeptide **55** that can then cyclise *in situ* to give the DKP **56** (Scheme 10).[98] In order for cyclisation to occur the amide bond of the dipeptide must be in the *cis* conformation, and if this is sterically or electronically unfavourable it may inhibit the yield of the reaction. Heating in an acidic or basic environment may help to circumvent this.



Scheme 10. General approach for the formation of a DKP

In 2006, Luthman *et al*. described a general and efficient synthesis of DKPs using microwave assisted heating with water as the solvent. The reactions were typically run for only 10 minutes with the product precipitating in the reaction, giving moderate to good yields of 63-97%.[99] This method uses microwave irradiation to deprotect the dipeptides to promote cyclisation to the DKP in an efficient manner and can also be used to give trisubstituted derivatives or indolyl-2,5-diketopiperazine analogues without solvent.

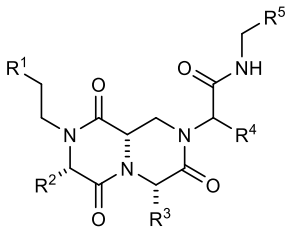
An application of DKPs that has gained importance is their use as templates for inducing defined secondary structures into peptide sequences. Internal β-turn mimics include scaffolds that display side chains that mimic a peptide reverse turn. Golebiowski *et al*. designed a bicyclic system using resin bound piperazinic acid as a core fragment to mimic this β-turn structure (Scheme 11).[100] Functionalisation of the β-nitrogen *via* the Petasis reaction followed by an amide coupling using DIC led to the incorporation of the R^4 and R^5 substituents. After Fmoc deprotection, **59** was then coupled to an *N*-Boc-protected-α-amino acid, and deprotected before cyclative cleavage from the resin. This introduced the remaining R^1 and R^2 side chains to give the bicyclic product **60**. Using this protocol Golebiowski *et al*. were able to synthesise a library of compounds. They showed that various amines (R^5 substituent) could be used successfully, including anilines, and that most commercially available boronic acids (R^4 substituent) could be used in this synthesis, though boronic acids bearing a basic nitrogen did not work. The R^1 and R^2 substituents originate from the amino acids used and are introduced in the amidation reaction.



57 **58** **59** **60**

Scheme 11. Synthesis of a β-turn mimic[100]

Later work from this group also showed the incorporation of the R^3 group by developing a solid phase protocol based on the Ugi reaction between the resin ester of an α-*N*-Boc-diaminopropionic acid, α-bromo acid, aldehyde, and isocyanide (Figure 20).[101]



61

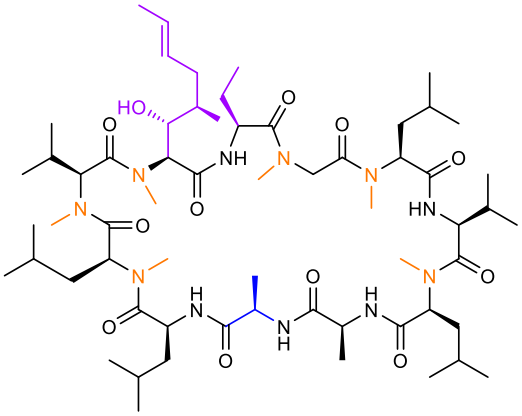
Figure 20. Structure of a β-turn mimic using DKPs[101]

1.8.2 Macrocyclisation of Peptides

More than half of the 'beyond the rule-of-five' drugs that target the flat surfaces of protein-protein interfaces are macrocycles, many of which are generated from natural products. The diversity found in these cyclic peptide natural products reflects the diversity of their targets, and so it follows that any structural similarities between these molecules may provide insight into the requirements for permeability and even bioavailability. Numerous orally bioavailable and cell permeable macrocyclic products are polyketides, and many of them show antimicrobial or immunosuppressive properties. Though there have been a number of polyketides that have been successful in the clinic, their synthesis provides its own challenge

and so cyclic peptides provide a more direct route to targeting novel human disease-related targets.

Cyclosporin A **62** (Figure 21) is a cyclic peptide made up of 11 amino acids first isolated from the fungus *Tolypocladium inflatum* in 1971. Used as an immunosuppressant medication for the treatment of diseases such as rheumatoid arthritis and Crohn's disease, it is taken orally. This oral bioavailability is due to the conformational changes cyclosporin undergoes in different solvent environments, as shown by NMR spectroscopy and computational studies.[102] In cyclosporin, seven of its peptide amide N-H are replaced with *N*-methyls. In non-aqueous media the lipophilic N-methyls project out into the medium and its hydrophilic polar functionality is buried inside the molecule. When placed in aqueous media, it is the lipophilic portion of the molecule that is kept within the interior and the hydrophilic polar functionality that projects out into the media.



62

Figure 21. Structure of cyclosporin A

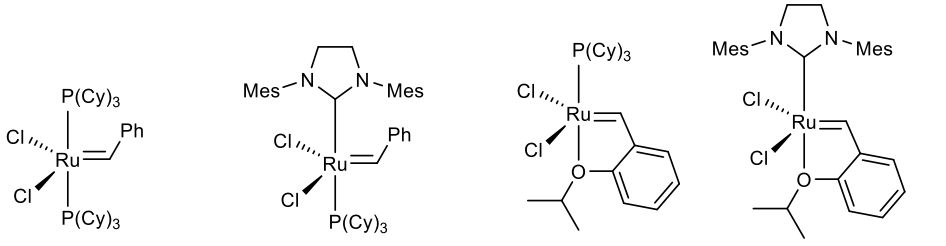
The cyclisation to form macrocycles is often a critical step in the synthesis and different approaches have been developed. Classical methods include head-to-tail lactamisation, internal disulfide bond formation, ring closing metathesis (RCM), and copper-catalysed azide-alkyne cycloaddition.

Difficulties with backbone cyclisations of peptides include the formation of dimers and oligomers as well as the long reaction times may lead to racemisation of the *C*-terminus. Placing a proline or glycine residue at the *C*-terminus can overcome this problem, though if this is not possible, the choice of coupling reagent needs to be investigated. Intramolecular cyclisations are inherently slow reactions and are favoured in high dilutions (10^{-3} – 10^{-4} M), avoiding the formation of oligomers. Thakkar *et al*. screened combinatorial peptide libraries

to analyse the cyclisation efficiency of over two million peptide sequences to determine the effect of ring size, peptide sequence, and solvents.[103] They found that cyclisation of medium and large rings (typically ≥6 amino acids) cyclised efficiently using their conditions of PyBOP, HOBt, DIPEA in DMF. However, formation of smaller rings, such as four or five amino acids, proved to be more difficult, and significant amounts of dimerisation were observed. An alternative route to these smaller ring sizes may use alternative macrocyclisation methods, such as RCM or click chemistry.

1.8.3 Ring Closing Metathesis (RCM)

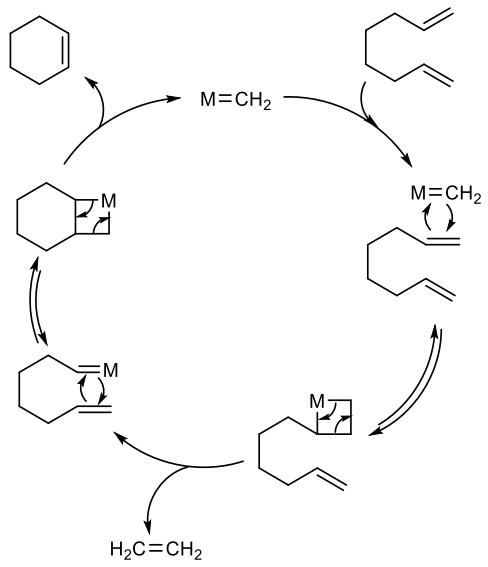
Olefin metathesis has emerged as a powerful tool for the formation of C-C bonds, and also allows for the replacement of disulfide bridges with more stable dicarba bridges. The most commonly synthesised rings are between five to seven atoms, however, macrocycles of up to 90 atoms have been reported.[104] Stereoselectivity in these reactions is dependent on the catalyst, ring strain and the starting diene, with *Z* isomers predominating in smaller rings to minimise ring strain, and *E* isomers often being the more stable product in large macrocycles. The success of this reaction is due to the high catalytic activity and remarkable functional group tolerance of the ruthenium-alkylidene catalysts used in this transformation (Figure 22). These ruthenium catalysts are air stable, tolerant to a wide range of functional groups and are compatible with a range of solvents, making them an attractive way of ring closing within highly functionalised peptide structures. Early work by Grubbs on the synthesis of amino acid derivatives containing various ring sizes and the stabilisation of β-turns in small cyclic peptides using these catalysts[105], inspired this research area. However, there were several transformations that could not be completed using the first-generation Grubbs catalyst, including the cross-metathesis of sterically hindered or electronically deactivated alkenes, and so the second-generation Grubbs catalyst was developed to tackle this problem. A similar catalyst was also created by the Hoveyda group[106], with the second-generation catalyst being published in the following year (Figure 22)[107].



Grubbs I, **63** Grubbs II, **64** Hoveyda-Grubbs I, **65** Hoveyda-Grubbs II, **66**

Figure 22. Structures of Grubbs catalysts and Hoveyda-Grubbs catalysts

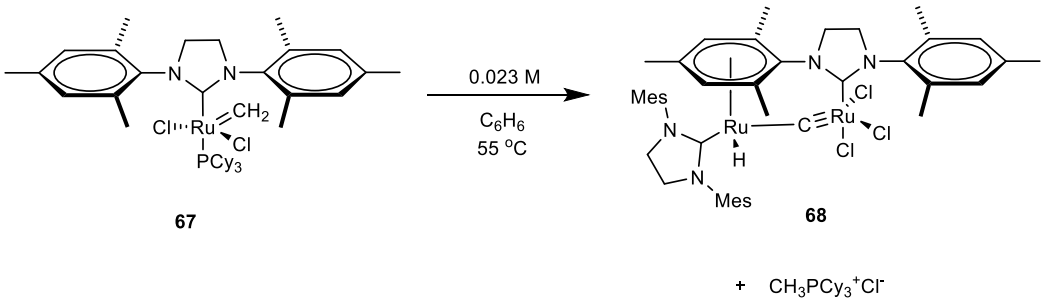
The reactions of are often carried out at high dilution of the substrate, typically between 10-50 μM to prevent polymerisation, heated, and with catalyst loadings of up to 10 mol%. The mechanism for the reaction was proposed by Chauvin in 1971, and proceeds with the formation of a metallacyclobutane intermediate through a [2+2] cycloaddition (Scheme 12).[108] Initiation of the catalytic cycle begins with substitution of the metal catalyst alkene with the substrate and upon cycloaddition affords the metallacyclobutane intermediate. Cycloreversion then results in the formation of ethylene and an alkylidene which undergoes an intramolecular [2+2] cycloaddition with the second terminal alkene on the same molecule, giving a new metallacyclobutane. This then undergoes cycloreversion to expel the metal carbene and a cyclic alkene. The key intermediates are the metallacyclobutane which can go to either starting materials or products by cycloreversion. However, when the alkenes are terminal, the entropic driving force for the reaction is the formation of gaseous ethylene (Scheme 12).



Scheme 12. Reaction mechanism for ring closing metathesis

Ring closing metathesis has shown to be successful in the synthesis of structurally complex molecules that contain groups such as epoxides, ketones, alcohols, esters, amines and amides. Tri- and tetra-substituted alkenes have also been used in the reaction to give substituted olefinic products.[109] However, some metathesis reactions are perturbed by migration of the newly formed alkene and these side products are often difficult to remove by standard purification techniques. While the mechanism for this isomerisation is currently unknown, work by Grubbs in 2004 indicated that a ruthenium hydride species **68**, formed from the decomposition of the metathesis catalyst, can catalyse the migration of alkenes

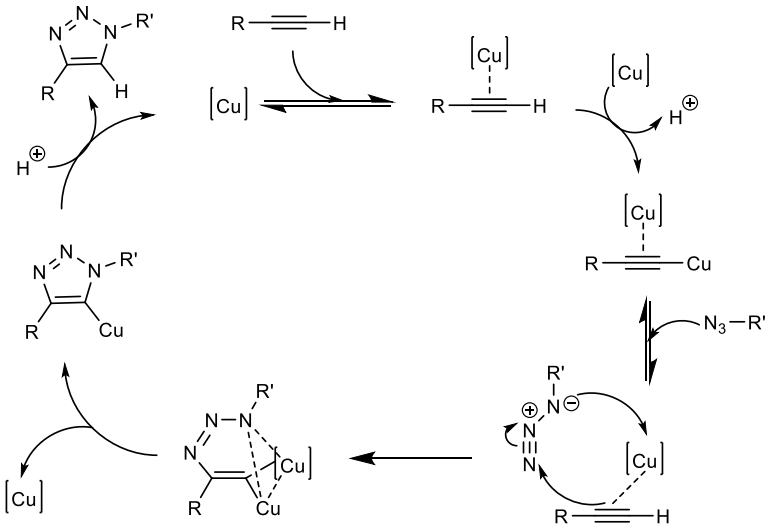
(Scheme 13).[110] In the study, **67** was monitored by ^{31}P NMR while heated at 55 °C in benzene for 72 h. During this time a new peak at δ 34.5 ppm was observed, while the peak corresponding to the methylidene **67** at δ 38.6 ppm decreased. An orange crystalline solid of **68** precipitated from solution and was isolated in 46% yield. Following on from this in 2004, Grubbs *et al*. showed that additives such as 1,4-benzoquinones prevent this isomerisation in a number of allylic ethers and long chain aliphatic alkenes under ruthenium metathesis conditions.[111]



Scheme 13. Formation of ruthenium hydride species **68**[110]

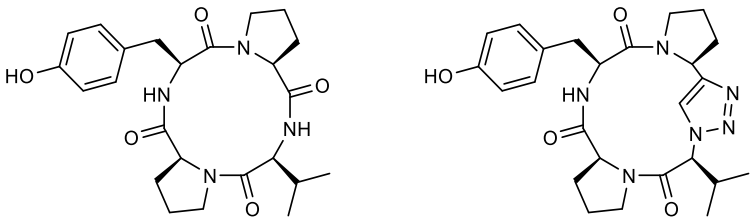
1.8.4 Alkyne-Azide Cycloaddition

Sharpless introduced the term 'click chemistry' in 2001 to describe reactions that are high yielding, stereospecific, wide in scope, generate minimal by-products, and can be conducted in benign solvents in one pot.[112] This 1,3-dipolar cycloaddition of an azide and an alkyne to give a 1,2,3-triazole was developed by Huisgen, however, this reaction required elevated reaction temperatures and results in the formation of two regioisomers when using unsymmetrical alkynes.[113] The copper-catalysed version of this reaction established by Sharpless gives only the 1,4-isomer and can be performed at room temperature under aqueous conditions. The mechanism of the reaction involves a bimetallic structure of π-complexation to the σ-alkynyl-Cu^{I} species which increases the reactivity of the alkynyl ligand by decreasing electron density on the sp carbon atom (Scheme 14). Subsequent azide attack is followed by the formation of a Cu^{III} vinylidene metallacycle and then ring contraction to a triazoyl-Cu derivative. This can then be protonated to give the triazole and close the catalytic cycle. The active Cu^{I} catalyst can either be generated from Cu^{I} salts or Cu^{II} salts with the use of sodium ascorbate as the reducing agent, together with a base or amine ligand to inhibit aerobic oxidation to Cu^{II} or Cu^{0}.



Scheme 14. Mechanism of the click reaction

1,2,3-Triazoles are found commonly within pharmaceutical and bioactive molecules. They possess similar atom placement and electronic properties to an amide bond, while also providing geometry comparable to that of a β-turn.[114] This reaction has been used effectively numerous times in the cyclisation of peptides. One example is the synthesis of the potent tyrosinase inhibitor *cyclo*-[*L*-Pro-*L*-Tyr-*L*-Pro-*L*-Val] **69** that proved difficult by cyclisation through peptide bond formation (Figure 23). As this peptide was too strained for cyclisation *via* lactamisation, Bock *et al*. used the 1,2,3-triazole moiety as an amide bond surrogate and cyclisation aid.[115] The target tetrapeptide **70** was isolated in 70% yield by heating the linear peptide with a Cu(I) catalyst under reflux at 100 °C for 16 h, demonstrating the proficiency of this reaction where lactamisation failed.

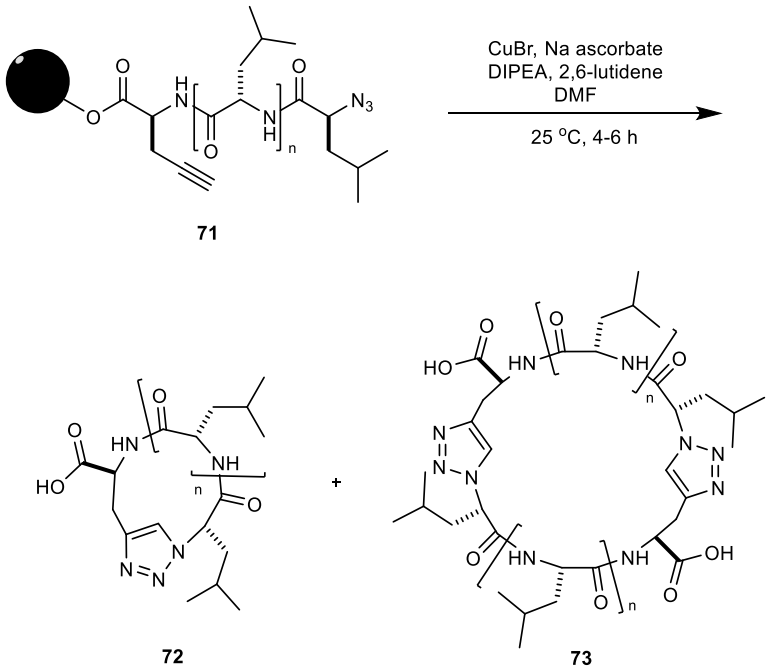


69 **70**

Figure 23. Structure of *cyclo*-[*L*-Pro-*L*-Tyr-*L*-Pro-*L*-Val] and its triazole analogue[115]

Lokey *et al*. examined the use of the click reaction in the macrocyclisation of resin bound tetra-, penta-, hexa- and heptapeptides that lacked β-turn-promoting structures such as proline or *D*-amino acids.[116] *L*-Propargyl glycine was used at the *C*-terminal of the peptide and *L*-azido leucine was placed on the *N*-terminal with a variety of intermediary amino acids **71**.

The cyclisations were performed using stoichiometric amounts of CuBr (1 eq.) and an excess of sodium ascorbate, with DIPEA and 2,6-lutidine in DMF and were typically complete within 4-6 h (Scheme 15). The reactions resulted in clean cyclomonomer **72** and cyclodimer **73** products in differing ratios. Due to the mild conditions, the reaction tolerates most amino acid side chains and therefore it would be possible to carry out the cyclisations in without any side chain protecting groups.



Scheme 15. Solid phase Cu catalysed cyclisation reactions[116]

1.9 Conclusion to Introduction

Development of peptides and peptidomimetics that target specific PPIs has been supported by advances in the synthesis and applications of cyclic peptides and organopeptide hybrids. This, along with chemical strategies for constraining peptide secondary structure, has led to macrocyclic ligands that are not only efficacious, but also show improved bioavailability and enhanced physicochemical properties. In order to continue this advancement in PPI modulators for potential therapeutic use, efforts also need to be made into understanding the protein target, and how its structure and characteristics can be used to guide the development of more effective macrocyclic ligands.

1.10 Project Aims and Objectives

This project aims to develop peptidomimetic inhibitors of the protein-protein interaction of Keap1 and Nrf2. There are multiple ligands that bind to Keap1 through the same binding site as Nrf2, with differing affinities. Of these ligands, this project focuses on p62, which binds to Keap1 through the amino acid sequence 349-DPSTGE-354. In this project, a section of the more potent sequence Ac-DPETGEL-OH is synthesised and cyclised using non-peptide linkers. By forming the cyclic peptides, the natural conformation of the β-hairpin structure of the ligands that bind to Keap1 is mimicked and conformational rigidity is also induced which may help with binding. From the peptide sequence, the tripeptide proline-glutamic acid-threonine (PET) was chosen as it includes the key interaction of the glutamic acid which binds to the Kelch domain. Threonine may aid in cyclisation, as it is key in forming intramolecular hydrogen bonds with both proline and glutamic acid, and proline with its distinctive side chain structure induces conformational rigidity and aids in the formation of β-turns.

Cyclisation of peptides can be attempted using a variety of techniques including ring-closing metathesis and azide-alkyne cycloaddition, as well as head-to-tail cyclisation of the PET tripeptide. Other methods aim to include the formation of heterocycles, such as pyrazoles, as the linker between the *N*- and *C*-termini of the peptide.

Analysis of the cyclic compounds will be conducted by performing conformational studies by NMR spectroscopy and also molecular modelling of the compounds can be carried out to assess the potential binding of these compounds to the Keap1 protein.

2. Solution Phase Peptide Synthesis

2.1 Cyclisation by Ring Closing Metathesis

Cyclisation is an effective way to reduce the flexibility of a peptide, stabilising its secondary structure, which may increase its affinity towards a receptor. The first aim of this project was to synthesise a set of cyclic compounds that had aliphatic linkers of different lengths that could be cyclised *via* ring-closing metathesis (Figure 24).

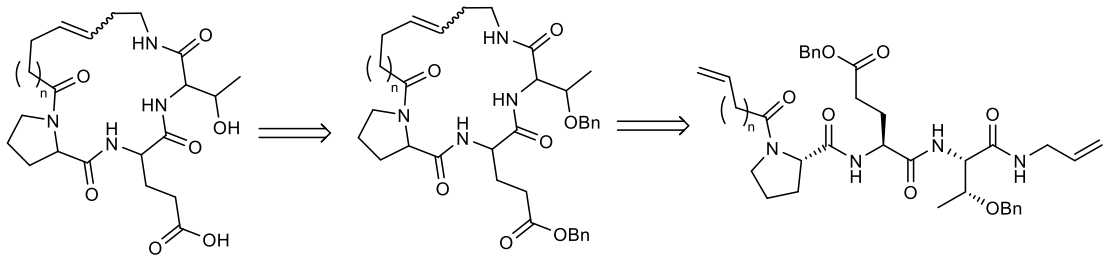
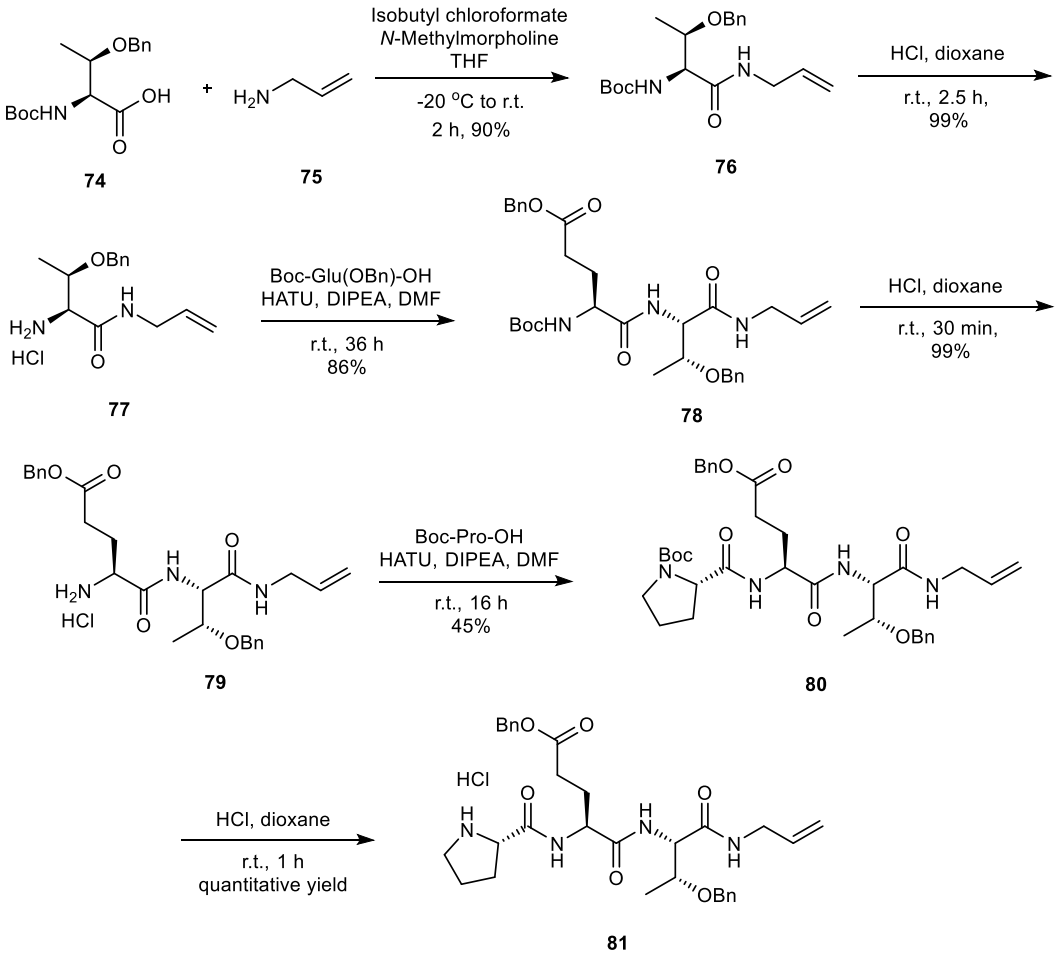


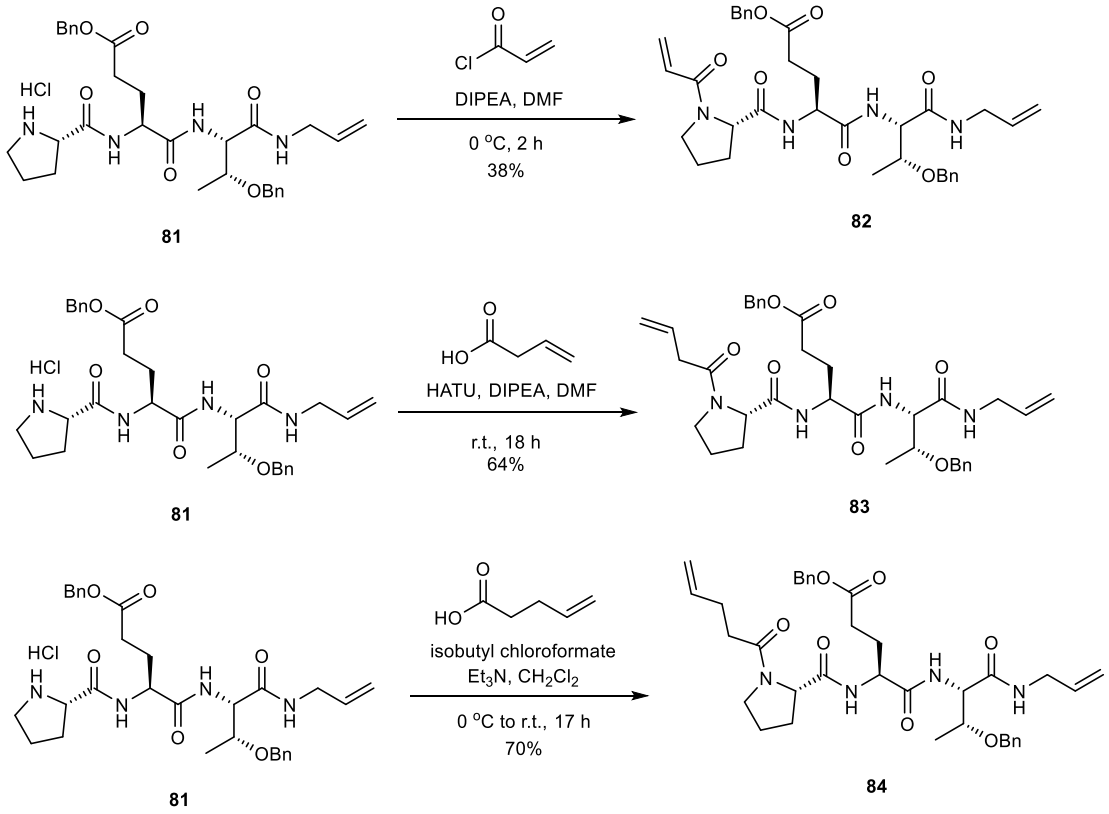
Figure 24. Retrosynthetic analysis of cyclic peptides using aliphatic linkers where n = 1, 2, 3

In this approach, instead of using a protecting group on the *C*-terminal, an allyl group was placed on the *C*-terminal, whilst the *N*-terminal could still be protected using a Boc group, allowing for variation at this end of the chain. Allylamine **75** was reacted with Boc-threonine **74** and isobutyl chloroformate to give compound **76** in 90% yield (Scheme 16). Isobutyl chloroformate was added to the deprotonated carboxylate salt of **74** and reacted to form the mixed anhydride before undergoing aminolysis with the amine to give **76** in excellent yield. Subsequently the Boc group was removed using HCl in dioxane to give the HCl salt **77**. Coupling of the deprotected threonine **77** to glutamic acid used standard amide coupling conditions of 1-[bis(dimethylamino)methylene]-1*H*-1,2,3-triazolo[4,5-*b*] pyridinium 3-oxide hexafluorophosphate (HATU) and diisopropylethylamine (DIPEA) in DMF. HATU was chosen as the coupling reagent due to its high reaction rates, with few side reactions and low probability of epimerisation of the product peptide. The resulting compound **78** was Boc deprotected to **79** and then coupled to proline to give tripeptide **80** in a 39% overall yield. The *N*-terminal of the tripeptide was then deprotected with HCl to give **81**, allowing for the *N*-substituent to be varied.



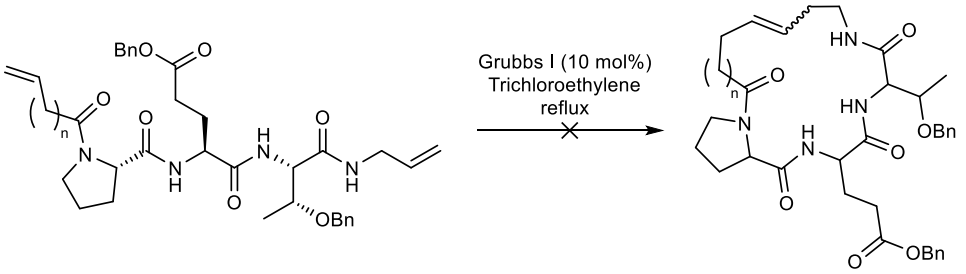
Scheme 16. Synthesis of tripeptide **80**

The free amine of proline was reacted with several acids to allow for different carbon chain lengths to be installed. Tripeptide **81** was reacted with acryloyl chloride, vinyl acetic acid and 4-pentenoic acid under different conditions to give three analogue precursors **82**, **83**, and **84** (Scheme 17). For each analogue reaction conditions were taken from the literature for coupling onto proline.[117–119] The reaction with acryloyl chloride showed no epimerisation of any stereocentre, although the yield was low at 38%. This reaction was also trialled using acrylic acid and a number of different coupling reagents including HATU and *N*-ethyl-*N*'-(3-dimethylaminopropyl)carbodiimide hydrochloride (EDC), but each showed lower yields than the reaction using acryloyl chloride. HATU, conversely, was used for the coupling of vinyl acetic acid in moderate 64% yield and isobutyl chloroformate was used for the coupling of 4-pentenoic acid in 70% yield (Scheme 17).



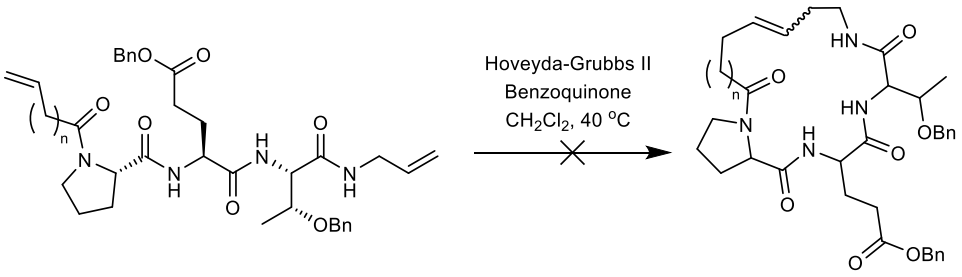
Scheme 17. Synthesis of aliphatic linker analogues

The penultimate step in the synthesis of these analogues was ring closing metathesis. This reaction allows for the synthesis of up to 30-membered cyclic alkenes, with the *E* and *Z* selectivity dependent on ring strain. For the cyclisation of compounds **82**, **83**, and **84**, two different catalysts were used – Grubbs first-generation and Hoveyda-Grubbs second-generation. Literature precedent for ring closing metathesis of peptides used Grubbs I at a catalyst loading of 10 mol% in trichloroethylene at 20 µM under reflux (Scheme 18)[120]. However, under these conditions each of the three peptides **82**, **83**, **84** failed to cyclise and only starting material was recovered from the reaction. Extending the reaction times up to 72 h also had no effect.



Scheme 18. Ring closing metathesis of tripeptide using Grubbs I

Hoveyda-Grubbs II shows enhanced reactivity compared to that of Grubbs I, including towards highly electron-deficient substrates and initiates at lower temperatures. The reactions of the peptides **82**, **83**, **84** using Hoveyda-Grubbs II were performed in dichloromethane at 40 °C with an initial catalyst loading of 10 mol% (Scheme 19). 1,4-Benzoquinone was also added to the reaction mixture and can be used to prevent the isomerisation of aliphatic alkenes during ring closing metathesis[121].



Scheme 19. Ring closing metathesis using Hoveyda-Grubbs II

Upon catalyst loading of 10 mol% once again only starting material was isolated from the reaction mixture as evident by both mass spectrometry and the ^{1}H NMR spectrum (Table 3, Entry 1, 3, 5). To try and initiate the reaction the catalyst loading for each peptide was increased. The metathesis of peptide **82** was done using 15 mol% of catalyst and a longer reaction time of 48 h (Table 3, Entry 2), but only starting material was obtained. For peptides **83** and **84** the catalyst loading was increased to 20 mol% (Table 3, Entry 4 and 6), but after 72 h none of the starting material or desired product was seen after purification by column chromatography.

Entry	Compound	Hoveyda-Grubbs II loading (mol%)	Reaction Time	Yield (%)
1	**82**	10.0	16 h	Starting material
2		15.0	48 h	Starting material
3	**83**	10.0	16 h	Starting material
4		20.0	72 h	Complex mixture
5	**84**	10.0	16 h	Starting material
6		20.0	72 h	Complex mixture

Table 3. Reaction conditions for ring closing metathesis using Hoveyda-Grubbs II

2.2 Peptide Protecting Groups

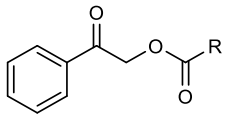
In synthesis it is often necessary to temporarily mask or protect a functional group to allow for bond formation elsewhere in the molecule. This concept was originally proposed by Bergmann *et al*. who developed the first protecting group, benzyloxycarbonyl (Cbz), that protects amines and overcomes their inherent nucleophilic properties.[122] Ultimately a protecting group should be easily introduced, stable to a wide range of reaction conditions, and then simply and reliably removed when required. In peptide synthesis there is often a high amount of functionality with either the *N*- or *C*-terminal requiring protection as well as any side chain functional groups. Therefore, it is often important to have the ability to remove any protecting group, in any order, in the presence of the others. In 1977, Merrifield introduced the concept of orthogonality for amino groups in peptide synthesis. It allowed for the manipulation of multiple protecting groups that could be removed independently of one another by a distinct mechanism.[123]

In order to synthesise the tripeptide in this project and be able to alter the terminal ends or side chains independently of one another, an orthogonal protecting group strategy was needed. A common protecting group combination employed in both solution and solid phase peptide synthesis is *N*-terminal protection using *tert*-butyloxycarbonyl (Boc) and side chain protection using the benzyl (Bn) protecting group, as both groups can be removed easily and cleanly. *N*-Boc-amino acids tend to be crystalline solids, which are acid labile, with the most common conditions for Boc deprotection being 25-50% trifluoroacetic acid (TFA) in dichloromethane. However, they can also be removed using other acids such as hydrochloric acid, trimethylsilyl chloride and methanesulfonic acid.[124,125] The Boc group is stable to catalytic hydrogenation, bases, and nucleophiles, making it a suitable protecting group in conjunction with benzyl groups. The benzyl group is most commonly removed by palladium-catalysed hydrogenolysis. However, it can also be removed under harsher conditions such as strong acids, or oxidising agents such as chromium trioxide and acetic acid, or ozone.

The protection of the *C*-terminal carboxylic acid differs between solid and solution phase peptide synthesis. In solid phase the *C*-terminal is most commonly bound to the solid support, with the linker or handle acting as a protecting group, but in solution phase this is not possible. For the solution synthesis of this peptide a protecting group would be required that was stable to acidic conditions and would not affect the integrity of either Boc or benzyl groups upon removal.

In Greene and Wuts book titled 'Protecting Groups in Organic Synthesis', of the 83 protecting groups listed for carboxylic acids, 72 of them are esters.[126] Methyl or ethyl esters are the most common protecting groups used for acids, however, they require basic conditions for their removal, and this may have also resulted in partial deprotection of the benzyl protecting group present on the side chain of glutamic acid. This also excluded any base labile *C*-terminal protecting groups, as the unhindered benzyl ester can be susceptible to both acid and base hydrolysis. Alternatively, the *tert*-butyl ester may be used to protect the *C*-terminal. Removal of the *tert*-butyl ester can be achieved under acidic conditions, usually requiring more forcing conditions than removal of the Boc group, allowing the Boc group to be removed independently in the presence of the ester. Despite this, *tert*-butyl *C*-terminal protected threonine is not commercially available and its synthesis can be problematic, requiring either gaseous isobutylene or perchloric acid.

Phenacyl esters are more readily cleaved by nucleophiles than benzyl esters and are also stable to acid hydrolysis. Consequently, it was decided that the phenacyl (Pac, Figure 25) group would be a suitable *C*-terminal protecting group. The Pac group is not only stable to acid but also basic conditions as well as hydrogenolysis, making it a suitable orthogonal protecting group. It can be removed by either reduction using zinc in acetic acid or nucleophiles such as sodium thiophenolate and is also photocleavable with either UV or visible light. This considerable functional group tolerance and mild deprotection conditions make it an attractive protecting group for peptide synthesis, and it has been used in biological studies for more than 50 years.[127]



85

Figure 25. Structure of the phenacyl (Pac) group.

However, Pac-protected amino acids are more electrophilic than their methyl ester equivalent. In rare cases this may lead to racemisation during coupling *via* a reversible cyclisation mechanism (Figure 26).

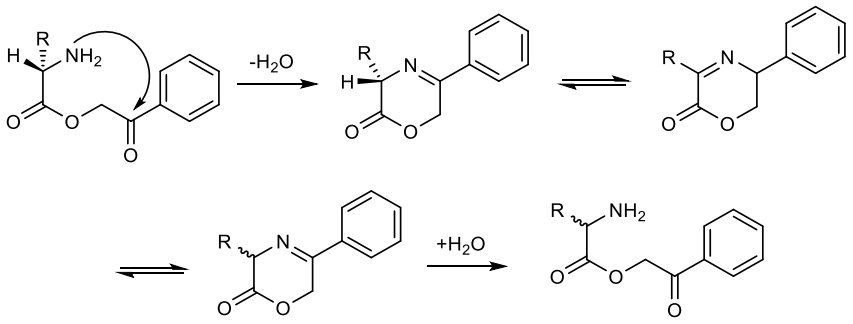
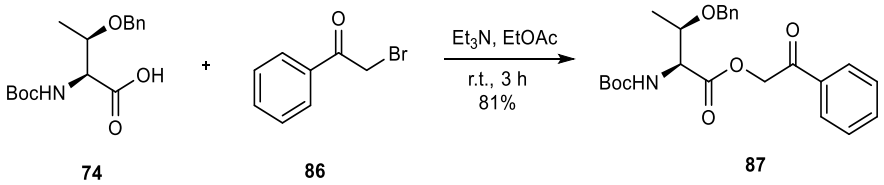


Figure 26. Racemisation of amino acids with the Pac protecting group

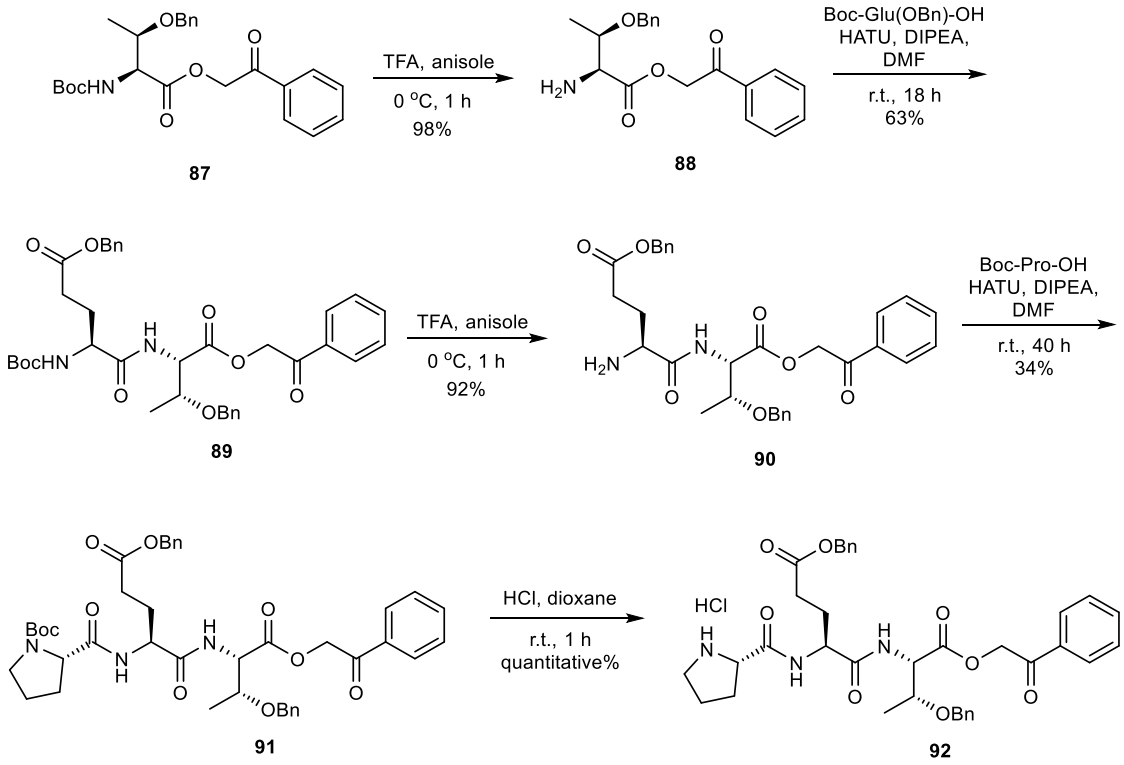
For the synthesis of the tripeptide Pro-Glu-Thr, commercially available Boc and benzyl protected threonine, Boc-Thr(OBn)-OH **74**, first needed to be Pac protected on the *C*-terminus. Reaction of **74** with phenacyl bromide **86** and triethylamine at room temperature for 3 h gave **87** in 81% yield after purification (Scheme 20).



Scheme 20. Protection of Boc-Thr(OBn)-OH with the phenacyl ester

Initial attempts at Boc-deprotection of **87** using trifluoroacetic acid (TFA) in dichloromethane yielded only starting material. A literature search revealed Munekata *et al.* had used anisole as a solvent when Boc deprotecting amino acids using TFA in the presence of the Pac group.[128] After 1 h in an ice bath they removed the excess acid *in vacuo* allowing them to then triturate the product in diethyl ether. This was successfully repeated for the deprotection of **87** with the use of anisole as both the *tert*-butyl scavenger and solvent, at 0 °C took the reaction to completion in 1 h. After concentrating the reaction mixture under reduced pressure, addition of diethyl ether resulted in the precipitation of the product **88** as a colourless solid in 98% yield (Scheme 21).

Coupling of the deprotected threonine **88** to Boc-Glu(OBn)-OH used the standard amide coupling conditions of HATU and DIPEA in DMF. Deprotection of the dipeptide **89** was performed using TFA in anisole and amide coupling to Boc-proline was also completed using HATU to give the fully protected tripeptide **91** in 31% yield over the two steps. The amino Boc group was deprotected using hydrochloric acid and isolated as the HCl salt, **92** (Scheme 21).



Scheme 21. Synthesis of the tripeptide Pro-Glu-Thr

As expected with peptide synthesis using HATU, no epimerisation of any stereocentre occurred during the synthesis of tripeptide **91**. This is demonstrated from the ^{1}H NMR spectra of **91** (Figure 27). The NMR spectra shown in Figure 3 displays the presence of only one diastereomer, as can be seen most evidently from the sharp peaks corresponding to the *N*-terminal Boc group at δ 1.44 ppm and the doublet from the CH_3 group of the side chain of threonine at δ 1.28 ppm. As there was no doubling up of these peaks can be assumed that no epimerisation of **91** had occurred.

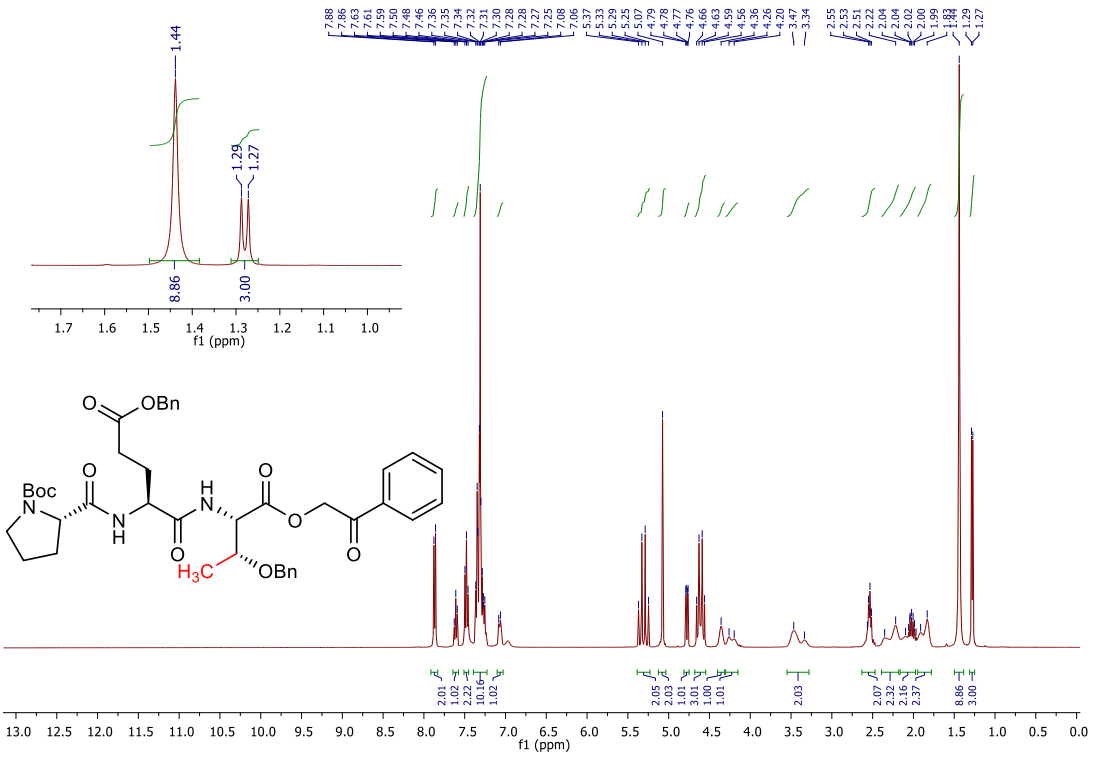


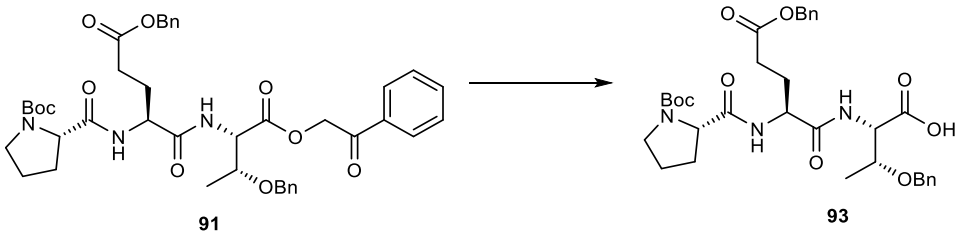
Figure 27. NMR of tripeptide **91**

2.3 Removal of the Pac Protecting Group

To synthesise cyclic analogues of the tripeptide sequence, the protecting groups from each end of the chain needed to be removed. The phenacyl group is particularly useful due to the fact its cleavage conditions are not regularly encountered in deprotections. In 1969, Hendrikson and Kandall used zinc in glacial or dilute aqueous acetic acid to cleave Pac esters at room temperature in good yields and often without the need for purification.[129] A typical procedure for deprotection was to add several equivalents of zinc dust to the Pac ester or ether in acetic acid, and after 1 h filtering the solution to give the product.

However, when applied to this tripeptide sequence **91** the yields were much lower than expected (Table 4). Zinc in acetic acid (Table 4, Entry 1) gave 13% yield, while dilution with DMF and ethyl acetate (Table 4, Entry 2 and 3) for improved solubility proved to be even lower yielding at <10%, with varying equivalents of zinc appearing to have no effect. The highest yield obtained was 22% (Table 4, Entry 4), using water as the solvent. It was thought that the zinc powder may be the cause of the low yields due to the formation of zinc carbonate on the surface by reaction with carbon dioxide in the air, preventing reduction at the zinc surface. Therefore, activated zinc was made by stirring in dilute hydrochloric acid for 1 h prior to the reaction, then washed with water, ethanol and diethyl ether before rigorous

drying. This activated zinc was then used in the deprotection reaction with a 90% solution of acetic acid in water (Table 4, Entry 5), improving the yield to 38% which was still not ideal for a deprotection reaction. Another approach was to change acetic acid to a milder acidic solution such as ammonium chloride in water[130] (Table 4, Entry 6); yet, this did not increase the yield.



Entry	Conditions	Equivalents	Yield 93 (%)
1	Zn, AcOH	16.0	13
2	Zn, AcOH, DMF	20.0	<10
3	Zn, AcOH, EtOAc	6.0	<10
4	Zn, AcOH, H_2O	6.0	22
5	Activated Zn, AcOH (90%)	15.0	38
6	Zn, NH_4Cl, H_2O, THF	5.0	17

Table 4. Reaction conditions for the deprotection of the Pac group using Zn

Due to the low yields recorded for the deprotection of the Pac group, other methods were investigated. Removal of the phenacyl group can be achieved using nucleophiles. The mechanism by which nucleophiles attack the phenacyl group is thought to be through an S_N2 type reaction at the CH_2 group, with stabilisation by the overlapping p-orbitals of the transition state and the ketone (Figure 28).[131]

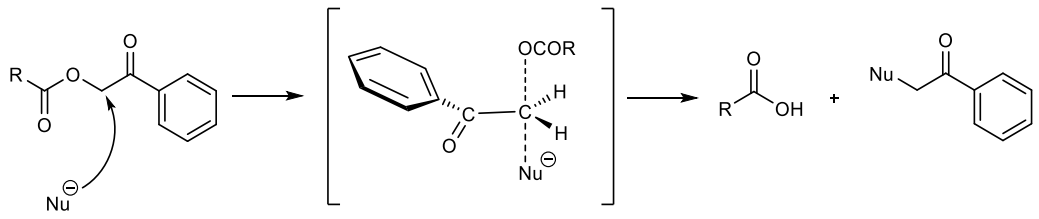
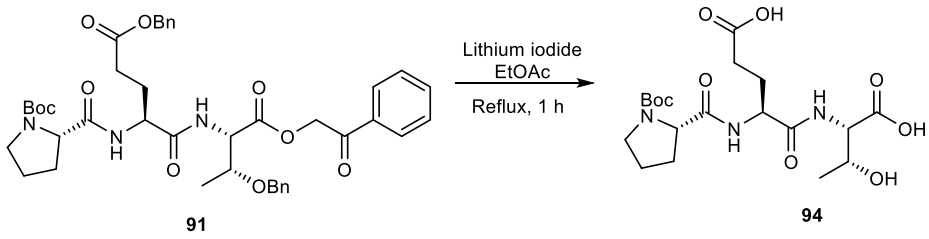


Figure 28. Reaction mechanism of deprotection of the phenacyl group using nucleophiles

Sodium thiophenolate cleaves the alkyl-oxygen bond of the Pac ester to give the corresponding sodium carboxylate. This transformation takes place in inert solvent such as DMF, at or below room temperature.[132] Sodium thiophenolate was reacted with **91**, but only

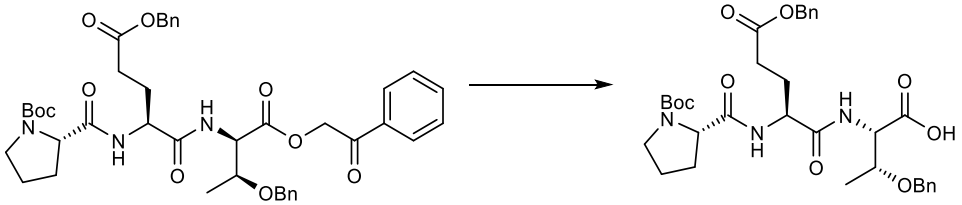
starting material was recovered from the reaction mixture with no apparent removal of the Pac group (Table 5, Entry 1). The number of equivalents of sodium thiophenolate used were increased from 5.0 to 10.0 and the reaction was heated to 50 °C overnight (Table 5, Entry 2), yet again only starting material was recovered. The nucleophile was changed to lithium iodide and the reaction was performed at reflux for 1 h in ethyl acetate (Table 5, Entry 3). This cleaved the Pac group and gave **94** in 55% yield, however, removal of the benzyl protecting groups on the side chain was also observed (Scheme 22).



91 **94**

Scheme 22. Removal of the Pac and Bn groups using lithium iodide

Tetra-*N*-butylammonium fluoride has been widely used for the deprotection of silyl ethers and esters but can also be used for the removal of protecting groups that are labile to hard bases. The Pac ester has been reported to be cleaved rapidly using TBAF in good yields.[133] When reacted with the tripeptide degradation of the starting material was seen by ^{1}H NMR spectroscopy (Table 5, entry 4).



91 **93**

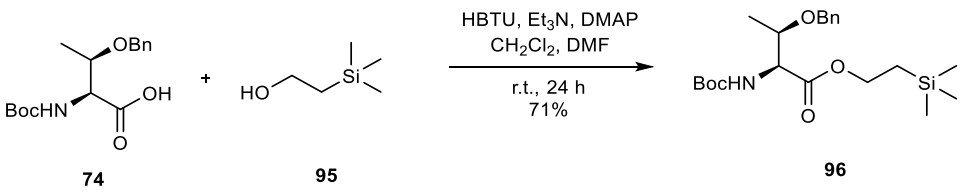
Entry	Conditions	Equivalents	Yield 93 (%)
1	Sodium thiophenolate, DMF	5.0	Starting material
2	(r.t. then 50 °C)	10.0	Starting material
3	LiI, EtOAc (reflux)	15.0	55
4	TBAF, DMF	3.0	Degradation of starting material

Table 5. Reaction conditions for the deprotection of the Pac group using nucleophiles

2.4 New Protecting Group Strategy

As the previous approach had failed to the give deprotected tripeptide in good yield, an improved protecting group strategy was needed. The Boc and benzyl protecting groups on the *N*-terminal and side chains were ideal as the protected amino acids are commercially available and they provide a clean and efficient way of deprotection. Therefore, a new protecting group for the *C*-terminal was necessary. The trimethylsilylethyl (TMSE) group was first reported as an α-carboxylate protecting group in solution synthesis by Sieber in 1977.[134] These esters were shown to be synthesised in good yields from Boc protected amino acids and 2-trimethylsilyl ethanol using dicyclohexylcarbodiimide (DCC) with pyridine and are stable to a wide variety of reaction and work up conditions. Deprotection occurs upon treatment with a fluoride source, most commonly a quaternary ammonium fluoride in DMF. The mild conditions also prevent racemisation from occurring. In 1993 the TMSE ester was reported as a side chain protecting group in solid phase peptide synthesis in conjunction with *N*-terminal Fmoc protected amino acids. Most resin bound peptide cyclisations that used TFA labile resin required either allyl based protection that uses air sensitive $Pd(Ph_3P)_4$ to achieve deprotection, or the acid labile dimethoxybenzyl (Dmb) ester, that uses 1% TFA for cleavage. As a result, there is a need to balance side chain deprotection and cleavage from the resin. By using the TMSE ester as a side chain protecting group both issues could be avoided, and it was shown to be an effective protecting group in the solid phase synthesis of cyclic peptides.[135]

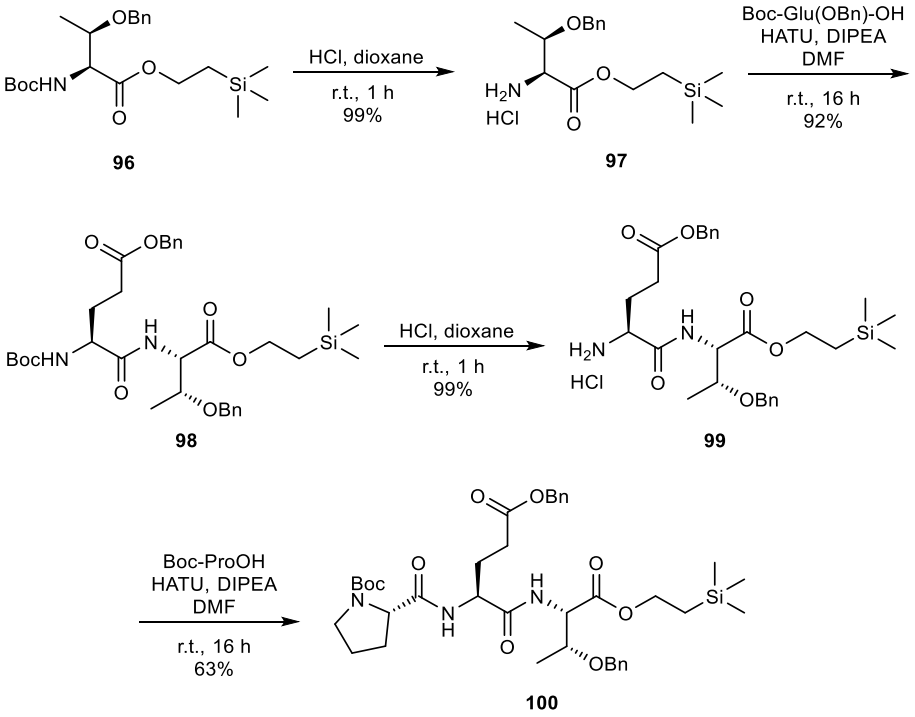
The desired threonine TMSE ester **96** was synthesised from Boc-Thr(OBn)-OH **74** and 2-trimethylsilylethanol **95** in the presence of triethylamine and 4-dimethylaminopyridine (DMAP) in 71% yield (Scheme 23).



Scheme 23. Protection of threonine with the TMSE group

The tripeptide was synthesised using the same conditions previously used of HATU mediated coupling with DIPEA in DMF giving **100** in an overall yield of 57%. However, due to the presence of the TMSE ester, deprotection of the Boc groups had to be completed using HCl

in dioxane rather than trifluoroacetic acid as this would have resulted in the deprotection of both the Boc and TMSE groups (Scheme 24).



Scheme 24. Synthesis of tripeptide sequence

As shown in the ^{1}H NMR (Figure 29), the linear tripeptide **100** showed no epimerisation during the synthesis. Only single peaks are present in the spectra, most evidently for the *N*-terminal Boc group and CH_3 group on the side chain of threonine, showing the presence of only one diastereomer.

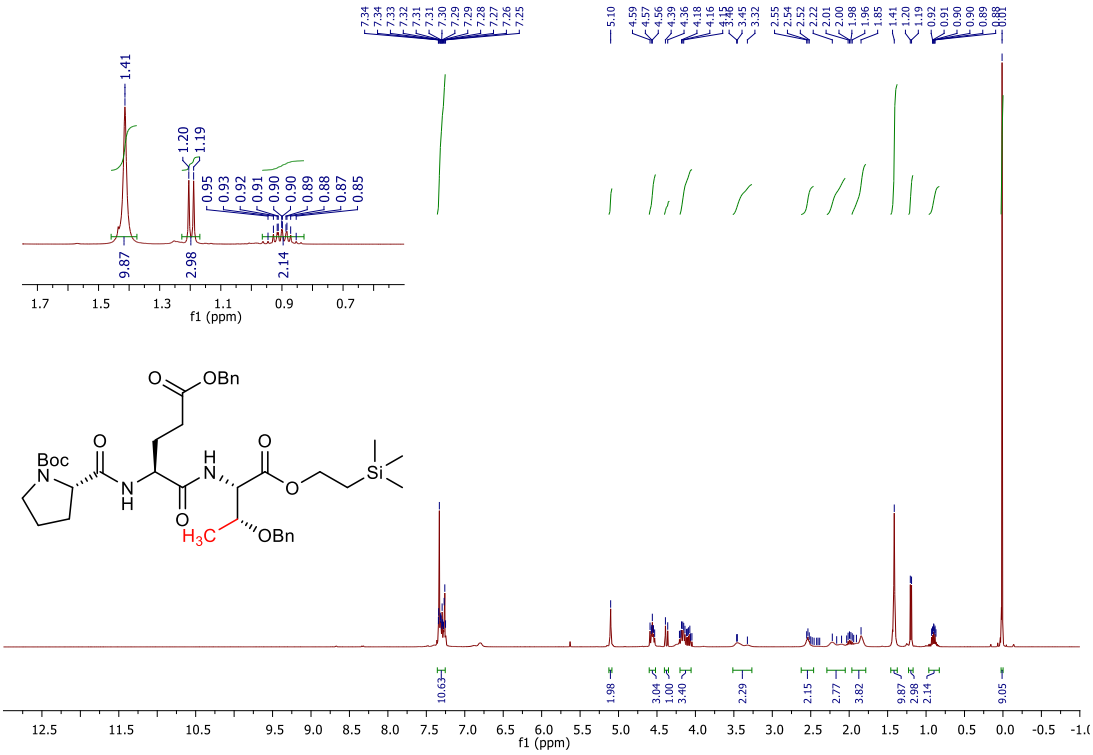


Figure 29. ^{1}H NMR spectra of the tripeptide **100**

Deprotection of the TMSE protecting group requires a fluoride source for its removal. In the literature, the most common method for cleavage is using tetrabutylammonium fluoride (TBAF). For tripeptide **100**, the first deprotection conditions attempted used a similar fluoride source of tetrabutylammonium triphenyldifluorosilicate (TBAT, Figure 30) in DMF at room temperature (Table 6); however, only starting material was recovered (Table 6, Entry 1). Other sources of fluorine such as hexafluorosilicic acid (H_2SiF_6) and triethylamine-HF (Table 6, Entry 2 and 3) gave only starting material. A more nucleophilic source of fluorine was trialled with pyridine-HF (Table 6, Entry 4) though this resulted in removal of the Boc group, leaving the TMSE group in place. Trifluoroacetic acid was then attempted, but as expected it cleaved both protecting groups (Table 6, Entry 5).

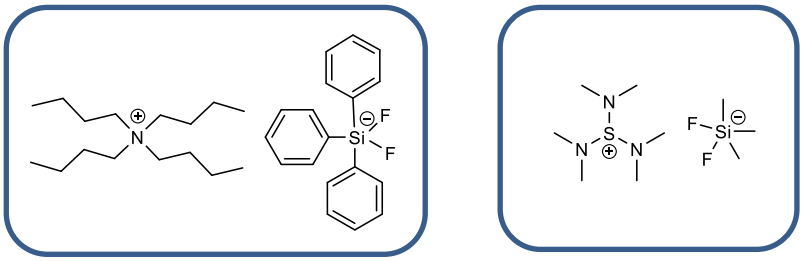
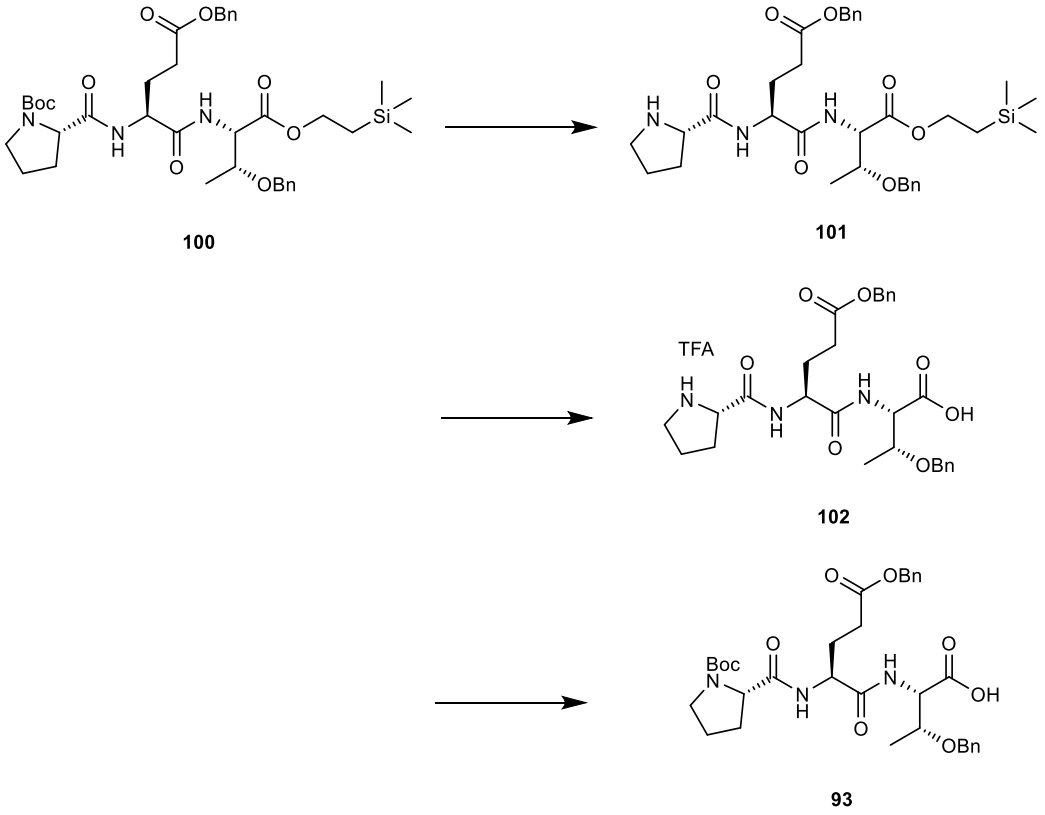


Figure 30. Structures of TBAT (left) and TASF (right)

Tris(dimethylamino)sulfonium difluorotrimethylsilicate (TASF) is an organic source of fluoride ions with high reactivity and it has the advantage over quaternary ammonium fluorides in that it is a source of anhydrous fluoride ions (Figure 30). It has been shown to successfully cleave a range of silyl ethers, (trimethylsilyl)ethyl carbamates and esters.[136] TASF removed the TMSE group in excellent yield over 16 h at room temperature (Table 6, Entry 6).



100 **101** **102** **93**

Entry	Conditions	Equivalents	Yield (%)
1	TBAT, DMF	3.0	Starting material
2	H_2SiF_6, MeCN	20.0	Starting material
3	Triethylamine-HF, CH_2Cl_2	3.0	Starting material
4	Pyridine-HF, CH_2Cl_2	3.0	**101**
5	TFA, CH_2Cl_2	-	**102**, 99
6	TASF, DMF	2.0	**93**, 98

Table 6. Reaction conditions for the deprotection of TMSE ester

2.5 Synthesis of Analogues

As the Boc/Bn/TMSE protecting group strategy in solution phase was working efficiently the next step was to synthesise the cyclic analogues. This approach to making cyclic analogues

coupled a long chain amino acid derivative in a lactamisation method termed the 'head to tail' approach (Figure 31).

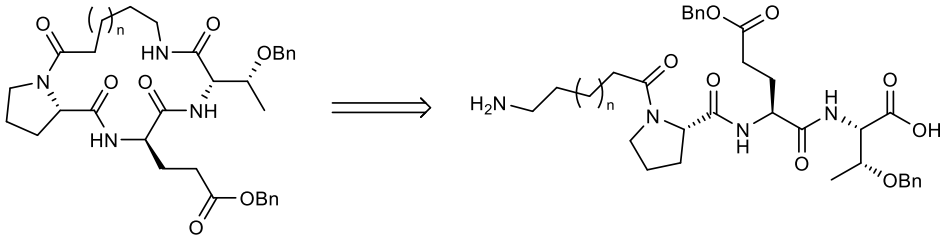


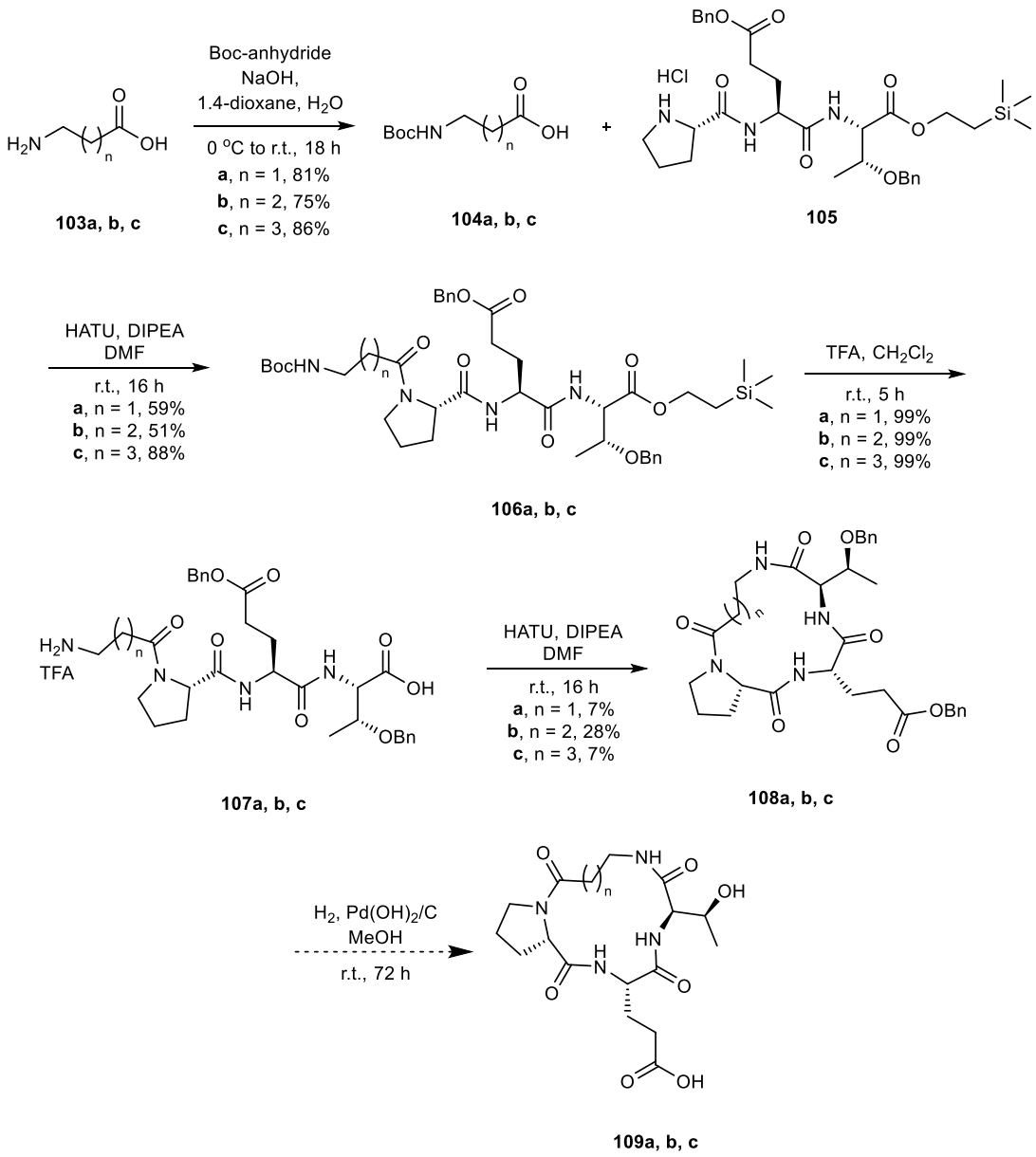
Figure 31. 'Head to tail' approach of cyclisation

2.5.1 Investigation of Cyclisation Conditions

Through this method a variety of ring sizes could be synthesised by varying the chain length of the amino acid derivative, thereby exploring which ring sizes are preferred for this tripeptide. The first analogue to be synthesised was the tripeptide Pro-Glu-Thr cyclised with 5-aminovaleric acid **103c**. 5-Aminovaleric acid **103c** was first Boc-protected using di-*tert*-butyl dicarbonate and sodium hydroxide to give **104c** in 86% yield (Scheme 25).

Compound **104c** was then reacted with the Boc-deprotected tripeptide **105** in a HATU mediated amide coupling to give compound **106c** in 88% yield. This was then fully deprotected using trifluoroacetic acid, which cleaved both the Boc group and the TMSE group to give the deprotected *N*- and *C*-terminal peptide. The next step was cyclisation, first attempted using HATU and DIPEA in DMF, giving the cyclised peptide in 7% yield. The final step for the synthesis of this analogue would be the removal of the benzyl side chain protecting groups. However, the yield of the cyclisation step was not ideal and there also appeared to be racemisation of the threonine centre upon cyclisation. This was evident from both the ^{1}H and ^{13}C NMR spectra of **108c** as multiple related compounds were observed in the NMR spectra.

Two remaining analogues **108a** and **108b** were also synthesised using the same method. These analogues included the β-alanine **103a** and γ-aminobutyric acid **103b** as the linkers, and once again as well as being low yielding, racemisation of threonine was observed upon cyclisation.



Scheme 25. Synthesis of cyclic fragments **108a**, **108b** and **108c**

The racemisation upon cyclisation is most clearly illustrated in the synthesis of compound **108b**. Formation of the linear peptide **106b** proceeded well, with no apparent epimerisation and was deprotected to **107b**, the ^{1}H NMR spectra of which is shown in Figure 32. This deprotected peptide shows only one doublet for the side chain CH_3 group of threonine. However, after cyclisation with HATU, the ^{1}H NMR spectra of **108b** (Figure 33) shows two doublets, the major at δ 1.18 ppm and another at δ 1.23 ppm. The ratio of these signals is 1 : 3 and this ratio remains the same after debenzylation to **109b** (Figure 34). The two diastereomers were unable to be separated by preparative HPLC and the reaction was also low yielding. Formation of diastereomers was also seen with both other analogues **109a** and **109c**.

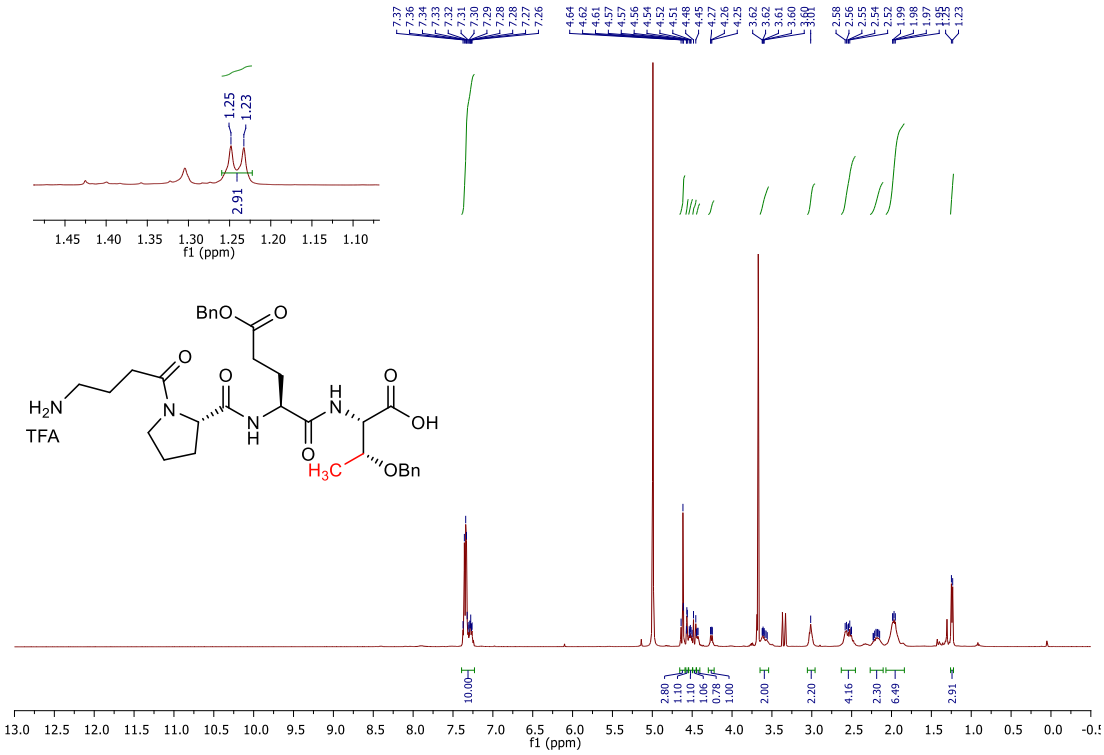


Figure 32. ^{1}H spectra NMR in CD_3OD for the deprotected linear peptide **107b**

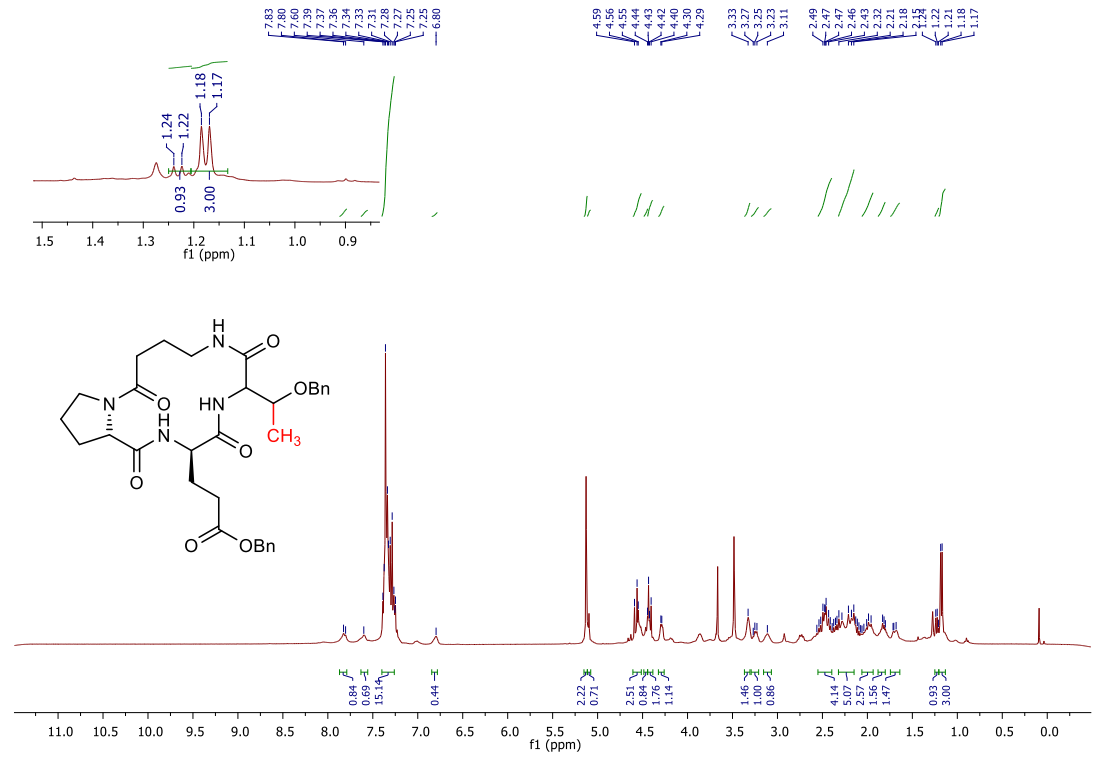


Figure 33. ^{1}H NMR spectra in $CDCl_3$ for the cyclic peptide **108b**

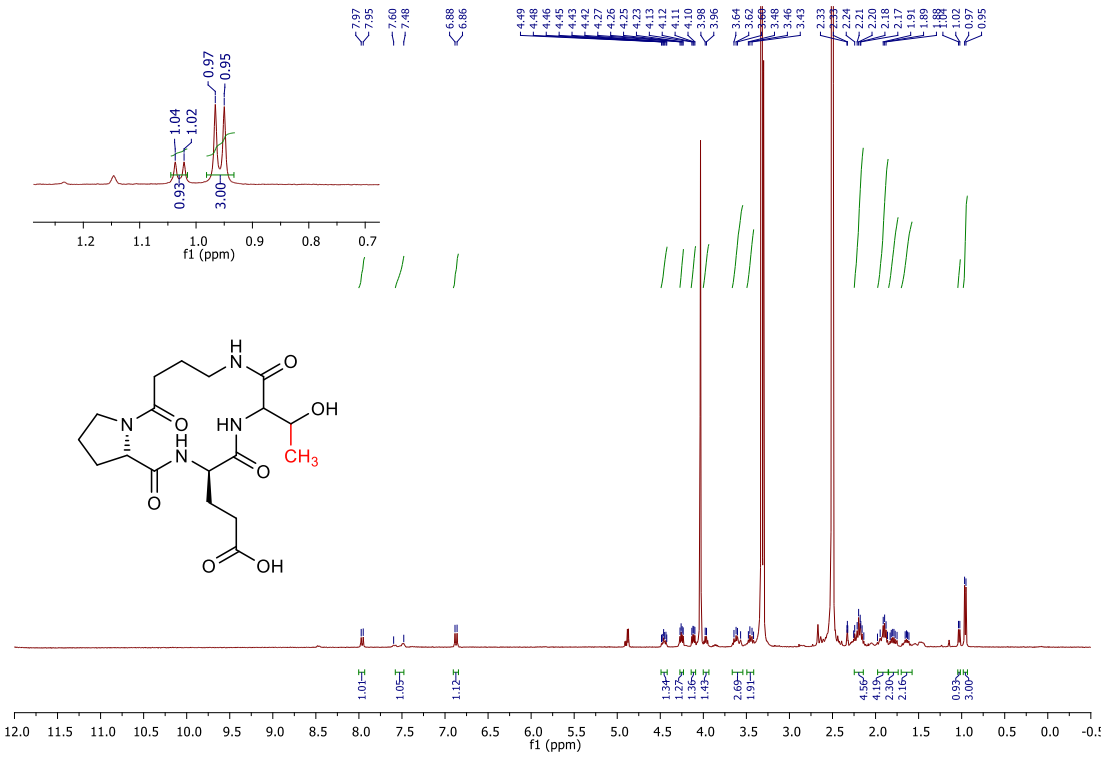
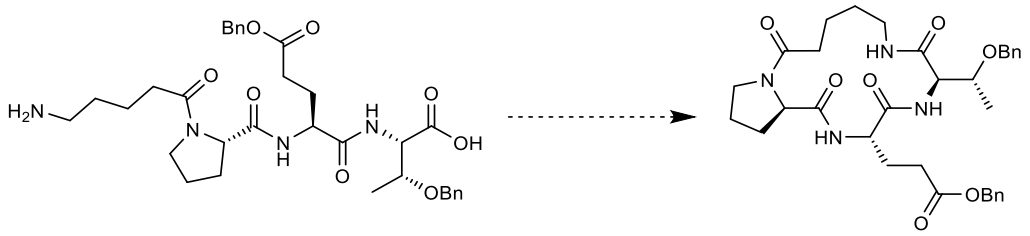


Figure 34. ^{1}H NMR spectra in DMSO-*d*6 for the deprotected cyclic peptide **109b**

After cyclisation using HATU as the coupling reagent, it was thought that the compounds observed in the NMR spectrum were diastereomers due to racemisation of the threonine stereocentre. However, after NMR experiments performed on related cyclic compounds synthesised in Chapter 3, it has been inferred that the diastereomers present in these compounds are more likely to be due to cis/trans isomerisation around the proline residue. Further investigation into this proposal is discussed in Chapter 3.

Due to the formation of multiple compounds, a range of coupling reagents were trialled for the cyclisation step of **107c** with 5-aminovaleric acid as the linker (Table 7). Initially, EDCI.HCl (Table 7, Entry 1) and DCC (Table 7, Entry 2) were trialled, both of which are carbodiimides that give water soluble and insoluble by-products respectively. EDCI gave an even lower yield of <5% for the cyclisation step compared to HATU and coupling with DCC resulted in no product being isolated. Diphenylphosphoryl azide (DPPA, Table 7, Entry 3) gave a slightly higher yield than EDCI but the product still contained numerous impurities after column chromatography.

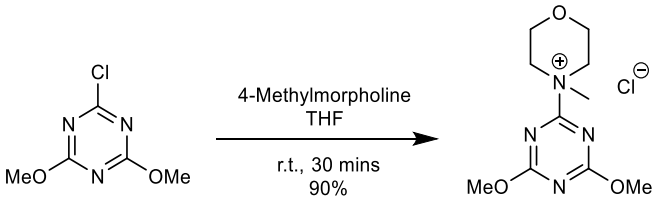


107c 108c

Entry	Reaction Conditions	Yield (%)
1	EDCI.HCl, HOBt, DIPEA, DMF, 16 h	<5
2	DCC, HOBt, Et_3N, CH_2Cl_2, 16 h	No product recovered
3	DPPA, Et_3N, DMF, 16 h	Impure

Table 7. Reaction conditions for cyclisation of **107c**

The coupling reagent 4-(4,6-dimethoxy-1,3,5-triazin-2-yl)-4-methyl morpholinium chloride or DMTMM (Scheme 26) is an organic triazine that is commonly used in amide coupling reactions but has also been used to synthesise other carboxylic functional groups such as esters and anhydrides (Chapter 1). For the cyclisation of **107c**, DMTMM **40** first needed to be synthesised from CDMT **39** (Scheme 26). This reaction proceeded well with DMTMM **40** precipitating from solution after 30 mins to give the colourless solid in 90% yield.

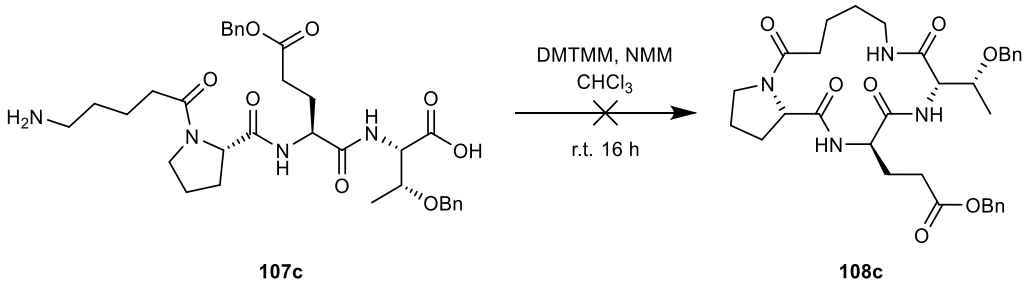


CDMT, **39** DMTMM, **40**

Scheme 26. Synthesis of DMTMM

The cyclisation of **107c** was performed under basic conditions in chloroform, following a procedure previously successful for peptide cyclisation within the group (Scheme 27).[137] No product was isolated from this reaction after 16 h at room temperature. This may be due to demethylation at the morpholinium nitrogen to 4-(4,6-dimethoxy-1,3,5-triazin-2-yl) morpholine (DMTM) which has shown to decompose almost completely when placed in chloroform at room temperature for 3 h. Therefore, the extended reaction times required for cyclisation were not compatible with using chloroform as the solvent. DMTMM can be stirred in THF for 13 h at room temperature with almost complete recovery.[89] Nevertheless,

the linear peptide **107c** was shown not to be soluble in THF and therefore the cyclisation conditions were kept to HATU and DIPEA in DMF as these showed to be the most reliable.

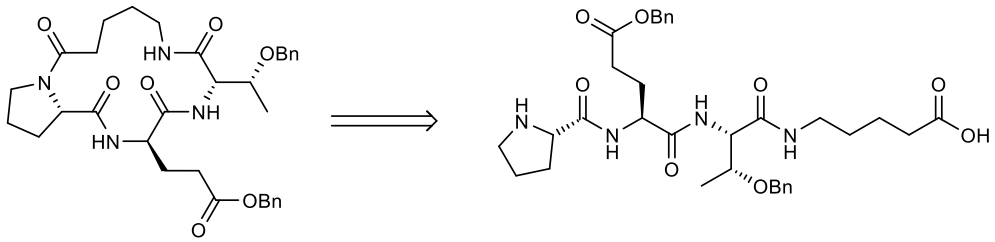


107c **108c**

Scheme 27. Cyclisation using DMTMM

2.5.2 Reverse Coupling

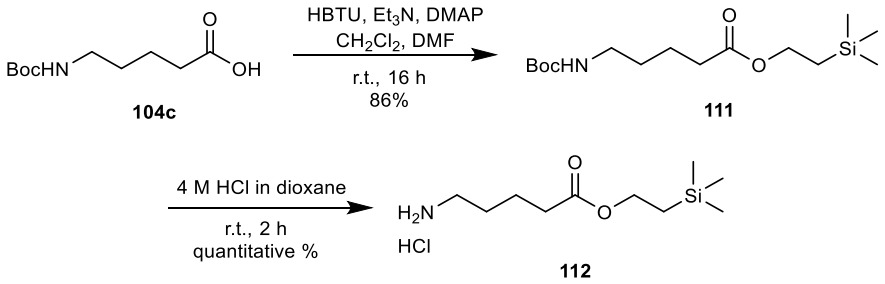
As the cyclisation using HATU was resulting in the formation of diastereomers a different approach was attempted. It was thought that the ring closing step between threonine and 5-aminovaleric acid would be the higher yielding, as the alternative cyclisation onto proline involves its secondary amine which is more sterically hindered and less reactive (Figure 35).



108c **110**

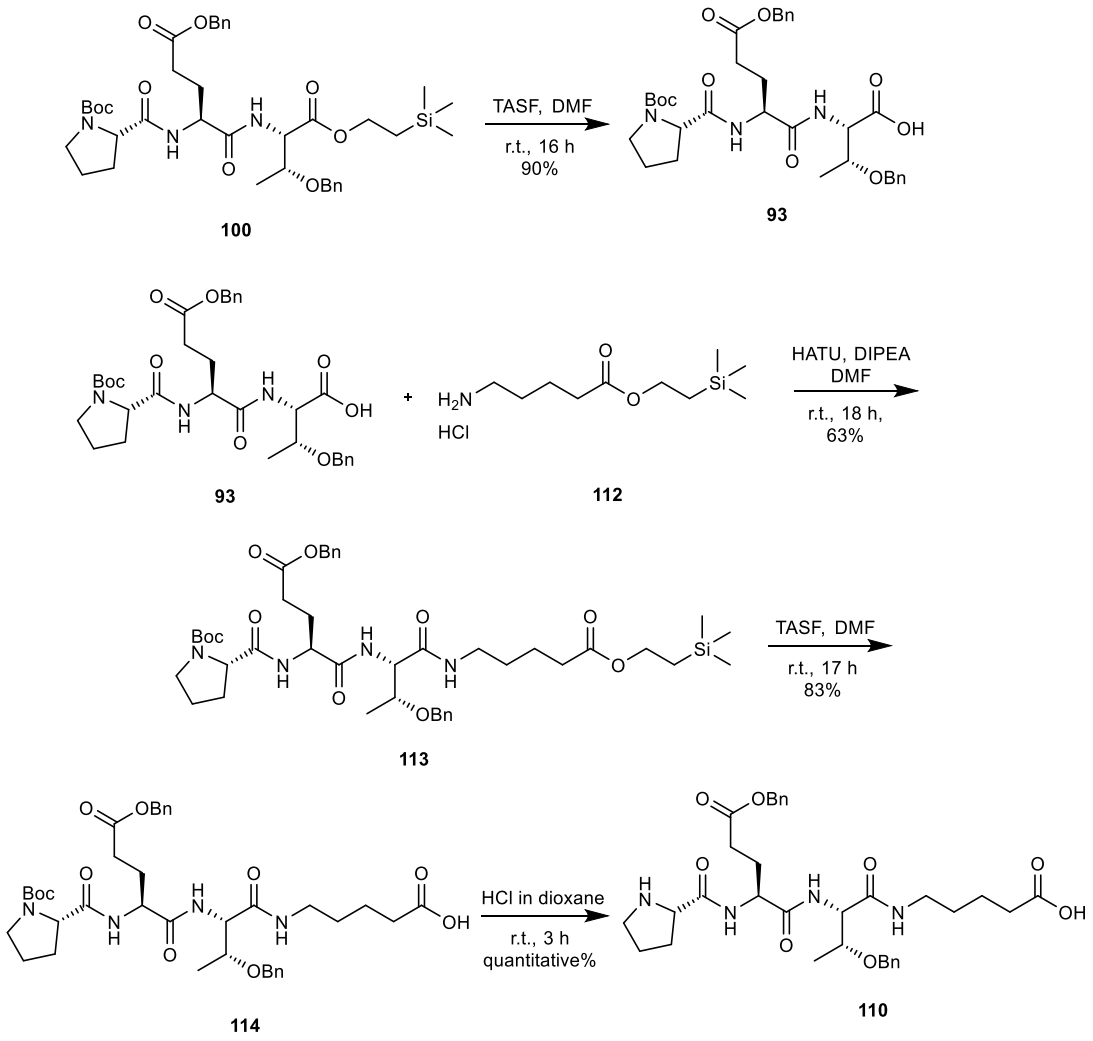
Figure 35. Reverse coupling of **110**

Amine **112** was synthesised from the starting acid Boc-5-aminovaleric acid **104c**. TMSE protection was achieved using the previous conditions of HBTU, triethylamine and DMAP (Scheme 28). This gave **111** in 86% yield, which was treated with 4 M HCl in dioxane to remove the Boc protecting group to give **112** as the HCl salt in quantitative yield.



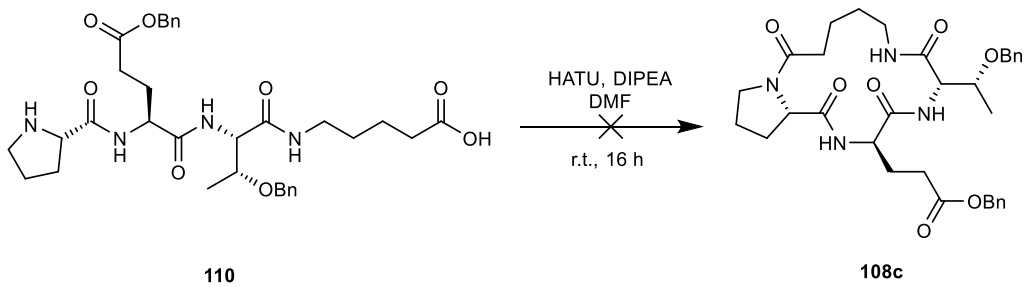
Scheme 28. Synthesis of **112**

The tripeptide **100** was TMSE deprotected to give the free *C*-terminal in 90% yield and subsequently coupled to the HCl salt of the amine **112** (Scheme 29). Coupling of **112** onto the deprotected tripeptide **93** proceeded in moderate 63% yield. Deprotection of the termini was performed sequentially, first using TASF to deprotect the ester, followed by Boc deprotection using HCl to give **110** as the HCl salt and a crystalline solid. The removal of both protecting groups could also be achieved using TFA, though, the formation of a TFA salt had given an oil and therefore the HCl salt was preferred due to the ease of handling.



Scheme 29. Synthesis of **110**

Cyclisation of **110** was then performed using HATU (Scheme 30). The cyclised product **108c** was isolated with a low crude yield and after column chromatography still contained impurities. It was therefore concluded that as cyclisation onto proline did not improve the yield or prevent the formation of diastereomers, that coupling onto threonine was the more reliable route.



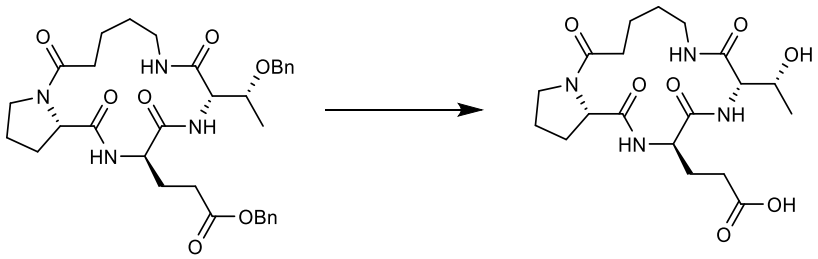
Scheme 30. Reverse coupling of **110**

2.5.3 Deprotection of the Benzyl Side Chain Protecting Groups

The final step for the synthesis of the cyclic products was the removal of the benzyl protecting groups on the side chains. The benzyl group is a robust group for the protection of carboxylic acids and alcohols. The reactivity of the benzylic C-H bond is comparable to that of an alkene and this enhanced reactivity can be attributed to a lower bond dissociation energy due to the stability of the benzyl radical that is stabilised by the aromatic ring.

After synthesising compounds **108a**, **108b** and **108c** it was decided to cleave the remaining protecting groups and purify the products by preparative HPLC to try and separate out the diastereomers which were seen after the cyclisation. The most widely used *O*-debenzylation methods used in organic synthesis are either palladium on carbon (Pd/C) or palladium hydroxide on carbon ($Pd(OH)_2/C$). The first set of conditions that were attempted to debenzylate compound **108c** were 10 mol% Pd/C in methanol (Table 8, Entry 1). However, after 16 h only the more labile benzyl ester from glutamic acid had been removed. Addition of acetic acid (Table 8, Entry 2) to try and promote the deprotection reaction also only resulted in the cleavage of the benzyl ester. Changing the solvent to 1 : 1 dichloromethane : methanol and increasing the reaction time to 20 h (Table 8, Entry 3) also failed to cleave the benzyl ether on threonine. As increasing the reaction time had no effect for cleaving both the benzyl ester and the benzyl ether bonds, the catalyst loading of Pd/C was increased from 10 mol% to 20 mol% in methanol (Table 8, entry 4). However, this resulted in a complex mixture of products being formed.

As a range of Pd/C conditions had been trialled and no product was formed cleanly, the palladium catalyst was changed to $Pd(OH)_2/C$. Attempting the reaction in methanol (Table 8, Entry 5) over 16 h, resulted in a mixture of products. Upon preparative HPLC several compounds were isolated, including the mono-debenzylated product. A range of solvents for the reaction were also trialled including dichloromethane, trifluoroethanol, ethyl acetate, and ethanol. However, starting material **108c** was insoluble in each of these solvents.

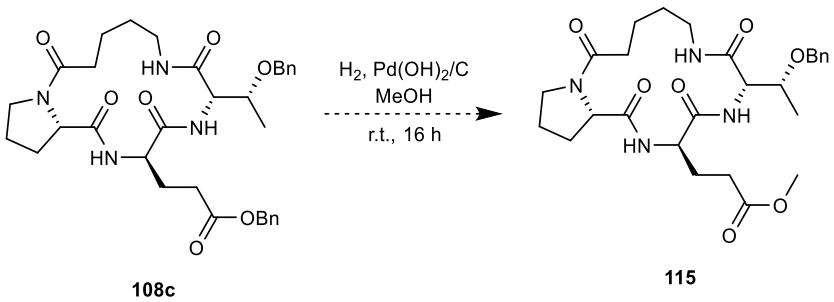


108c 109c

Entry	Compound	Reaction Conditions	Catalyst Loading (mol%)	Outcome
1	**108c**	H_2, Pd/C, MeOH	10	Only one Bn group removed
2		H_2, Pd/C, AcOH, MeOH	10	Only one Bn group removed
3		H_2, Pd/C, 1 : 1 CH_2Cl_2: MeOH	20	Only one Bn group removed
4		H_2, Pd/C, MeOH	20	Mixture of products
5		H_2, $Pd(OH)_2$/C, MeOH	30	Mixture of products

Table 8. Benzyl deprotection conditions performed on cyclic products

The main product of the debenzylation with $Pd(OH)_2$/C in methanol was compound **115** (Scheme 31). The formation of the methyl ester on glutamic acid can be attributed to the extended reaction times required for the cleavage of the benzyl ether on threonine. Hydrolysis of the methyl ester using lithium hydroxide would have required an aqueous work up, and as the benzyl ether was still proving challenging to cleave, other debenzylation conditions were trialled.



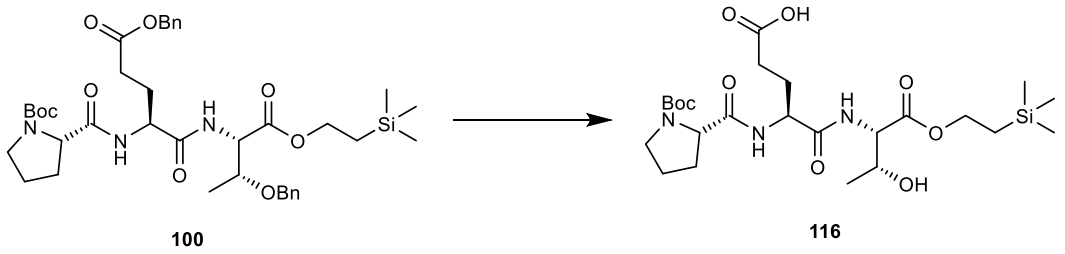
108c 115

Scheme 31. Potential product of the debenzylation of **108c**

As the cyclisation of **108c** was low yielding there was a limited amount of cyclic compound to test debenzylation conditions on. Consequently, the following reactions were completed on the linear tripeptide **100**. Transfer hydrogenation is the addition of hydrogen to a molecule without the use of gaseous H_2 and is a powerful and versatile method to access a variety of hydrogenated compounds. The catalysts used are readily available, and neither air or water sensitive, and the hydrogen donors are inexpensive and easy to handle. For these reasons transfer hydrogenation is an attractive alternative to direct hydrogenation, particularly for the removal of protecting groups in peptide synthesis. In 2001, Gowda *et al*. employed zinc as a catalyst with either formic acid or ammonium formate for the reduction of nitro-containing compounds to amines.[138] Following on from this work in 2002, they published an investigation into other low-cost metals that could be used for catalytic transfer hydrogenation and developed a system that utilises magnesium as the catalyst and hydrazinium monoformate as the hydrogen donor.[139] Hydrazinium monoformate was pre-formed prior to the reaction from formic acid and hydrazine hydrate, which is miscible in most organic solvents, including methanol that was used in the debenzylation reaction. In the paper, Gowda reports the debenzylation of threonine and glutamic acid were complete within 1 h at room temperature in 90% and 95% yields respectively. These conditions of Mg and hydrazinium monoformate in methanol were tested on the tripeptide **100**. However, after 1.5 h under these conditions only starting material was recovered (Table 9, Entry 1). The reaction was tried again, this time heating to 50 ^{o}C for 5 h (Table 9, Entry 2), but again only starting material was observed.

The use of hydrogen bromide in acetic acid for debenzylation was first demonstrated by Ben-Ishai and Berger in 1952.[140] They showed that benzyl esters and Cbz-protected amines are cleaved with hydrogen bromide in glacial acetic acid at room temperature within 1 h. This method was later developed by Merrifield for use in solid phase peptide synthesis.[92] However, when a solution of 33% hydrobromic acid in glacial acetic acid was used to deprotect **100**, the starting material degraded completely within 4 h (Table 9, Entry 3). Lewis acidic reagents including boron trihalides are mild and effective reagents for ether cleavage. Boeckman showed the use of catechol boron trihalides for the deprotection of benzyl ethers, as well as methoxymethyl (MOM) and the 2-methoxyethoxymethyl (MEM) ethers, in good yields.[141] In 1993, Ward *et al.* reported the use of boron trichloride dimethyl sulfide ($BCl_3.SMe_2$) complex to selectively cleave benzyl ethers in the presence of cyclic and silyl ethers, esters, lactones, alkenes and alkynes.[142] Various substrates were treated with $BCl_3.SMe_2$ and all deprotection reactions were complete within 4 h without any side

reactions. They found that debenzylation typically occurred quicker when dichloromethane was used as a solvent when compared to diethyl ether. When these conditions were applied to **100** for 4 h debenzylation failed to occur and instead the tripeptide was Boc-deprotected, as was demonstrated by ^{1}H NMR (Table 9, Entry 4).

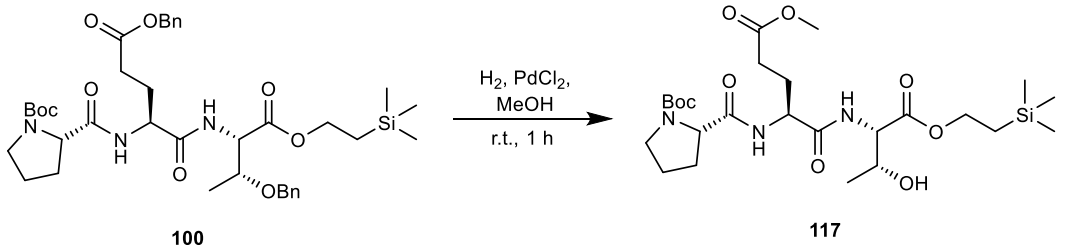


100 **116**

Entry	Reaction Conditions	Outcome
1	Hydrazinium monformate, Mg, MeOH, r.t., 1.5 h	Starting material isolated
2	Hydrazinium monformate, Mg, MeOH, 50 °C, 5 h	Starting material isolated
3	HBr, AcOH, 4 h	Degraded starting material
4	$BCl_3 \cdot Me_2S$, CH_2Cl_2, 4 h	Removed Boc group instead of Bn

Table 9. Deprotection conditions on linear tripeptide

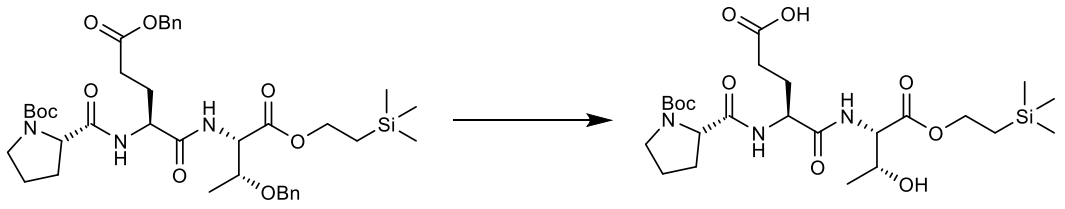
Attention then returned to using other palladium catalysts to remove the benzyl groups. Palladium black in methanol cleaved the benzyl ester on glutamic acid after 20 h, leaving the benzyl ether on threonine in place (Table 10, Entry 1). Repeating the reaction for 41 h (Table 10, Entry 2) resulted in a complex mixture of products. Surprisingly, after 1 h with palladium chloride as the catalyst the benzyl ether was completely cleaved from threonine and the product isolated was the methylated glutamic ester **117** in 94% yield (Table 10, Entry 3). The methylation of the ester can be attributed to the formation of HCl in the deprotection reaction from methanol and $PdCl_2$, which then catalyses the esterification (Scheme 32).



100 **117**

Scheme 32. Debenzylation of **100** in methanol

By changing the solvent of the reaction from protic methanol to aprotic DMF the formation of HCl was avoided (Table 10, Entry 4) and consequently, after removing the solvent, debenzylated **116** was isolated in 93% yield.



100 **116**

Entry	Reaction Conditions	Outcome
1	H_2, Pd black (30 mol%), MeOH, 20 h	Cleaved Glu Bn but not Thr Bn group
2	H_2, Pd black (30 mol%), MeOH, 41 h	Mixture of products
3	H_2, $PdCl_2$ (30 mol%), MeOH, 1 h	**117**, 94% yield
4	H_2, $PdCl_2$ (30 mol%), DMF, 3 h	**116**, 93% yield

Table 10. Deprotection conditions on linear tripeptide. All Pd conditions are at 30mol%

2.6 Conclusion

Ring closing metathesis was an approach to making cyclic compounds. Synthesis of the linear peptides proceeded well, yet cyclisation often proved unsuccessful with multiple Grubbs catalysts, as starting material or a complex mixture were isolated.

In the solution phase synthesis of the cyclic peptides, a range of protecting group strategies has been investigated. The major difficulty arose from the protection of the *C*-terminal of the tripeptide. The phenacyl ester showed promise and the protection reaction occurred in good yield, along with the synthesis of the linear tripeptide. However, problems developed upon removal of the group which failed to give yield higher than 38%.

The final protecting group strategy employed the TMSE ester on the *C*-terminal. After investigating a variety of deprotection conditions, cleavage occurred in the highest yield with the fluorine source TASF, in 98%. It was the Boc/Bn/TMSE protecting group strategy carried forward for the remainder of the solution phase peptide synthesis.

Although the protecting group strategy had now been solved, there remained the problem of the formation of diastereomers in the cyclisation step. Changing the coupling reagent from

HATU showed no improvement on yield or in the formation of diastereomers and varying the point of cyclisation resulted in a massive decrease in yield.

Debenzylation of both cyclic and linear peptide proved problematic. Both transfer hydrogenation conditions and catalytic hydrogenolysis using gaseous H_2 were tested, however, it was removal of the benzyl ether of threonine that was shown to be the hardest to cleave. After testing a range of palladium catalysts for different reaction times in multiple solvents, $PdCl_2$ in DMF gave clean product in 93% yield.

However, the problem of the formation of diastereoisomers on cyclisation was still problematic and therefore another approach was trialled for the synthesis of the tripeptide and cyclisation that involved solid phase peptide synthesis.

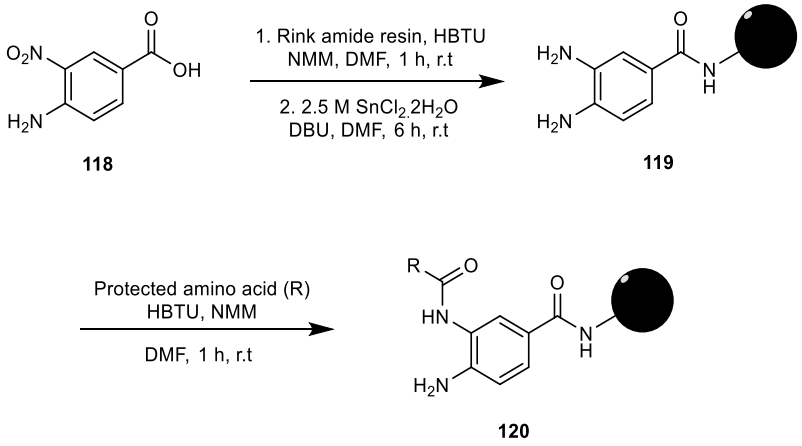
3. Solid Phase Peptide Synthesis

As the solution phase approach to the synthesis of the cyclic peptides proved problematic, attention turned to solid phase peptide synthesis as a potential solution. While most cyclic peptides have traditionally been synthesised in solution phase, solid phase head-to-tail cyclisation offers a number of advantages. Macrocyclisation should proceed with higher efficiency as there is minimal risk of polymerisation of the peptide, and it provides precise control over the structure or post-synthetic modifications.

3.1 Synthesis Using Labile Linkers

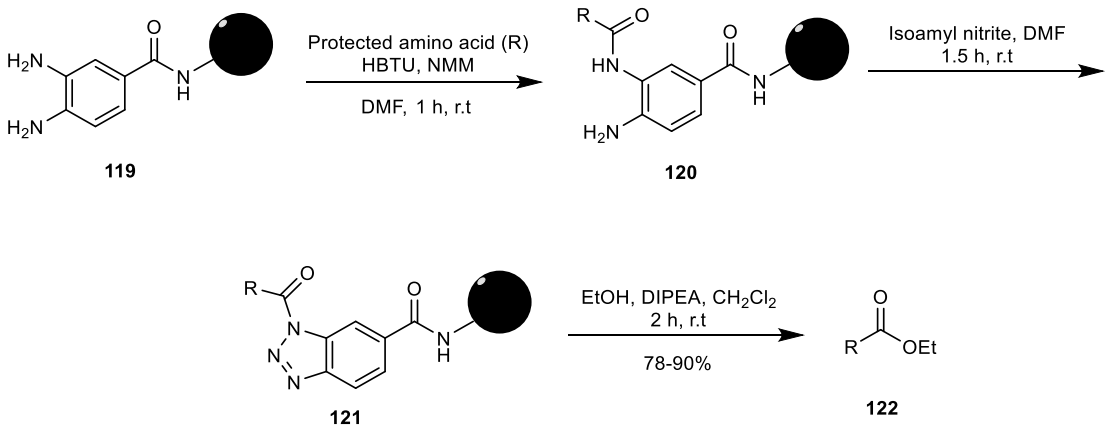
In solid phase peptide synthesis, peptides are usually synthesised from *C*-terminus to the *N*-terminus, consequently making functionalisation of the *C*-terminal difficult. As briefly discussed in Chapter 1, linkers or a labile group can be placed in between the solid-support and the synthetic peptide. However, labile linkers limit the number of reaction conditions available for the synthesis. Instead linkers that are stable to a wide range of reaction conditions and are then activated at the cleavage step provide an alternative route that is more reliable.

The benzotriazole group is compatible with many synthetic conditions and transformations and has been used as a traceless linker in the synthesis of multiple compounds. In 2018, Selvaraj *et al*. reported a method for on-resin *C*-terminal modification of synthetic peptides.[143] This method uses a diaminobenzoic acid derivative as the linker for peptide elongation and is then activated to the benzotriazole upon treatment with isoamyl nitrite. This technique can be used with a diverse number of nucleophiles to release *C*-terminally modified peptides from the resin in a short time. The diaminobenzoic acid linker **119** is synthesised from 4-amino-3-nitrobenzoic acid **118** which was first coupled onto the Rink amide resin using HBTU (Scheme 33). The nitro group was then reduced using tin chloride to give **119**. The first amino acid of the sequence could then be coupled onto **119**, followed by the remaining sequence, before activation of **120** to the benzotriazole.



Scheme 33. Literature synthesis of the diaminobenzoic acid linker[143]

The benzotriazole linker has been used in a number of solid-phase syntheses, though conditions for its preparation are often harsh, and are not compatible with any side chain protecting groups that may be present in the peptide. Consequently, for activation of the diaminobenzoic acid linker **119** to the benzotriazole **121**, Selvaraj *et al*. trialled both sodium nitrite and isoamyl nitrite for cyclisation at the *o*-aminoanilide. Of the two conditions, isoamyl nitrite gave better results, with the reaction completing in 90 min to 3 h with 85-99% conversion. Investigation into the solvents for the reaction showed DMF gave the highest yield of 99%. The compatibility of this reaction was then assessed by synthesising several peptides with differing *C*-terminal amino acids attached to the linker. Using the procedure described above, peptides with the *C*-terminal amino acid including glutamic acid, histidine, cysteine, tryptophan and phenylalanine were all synthesised in high purity and yield (78-90%). A variety of side chain protecting groups were also stable to this procedure, including *tert*-butyl, trityl, Boc and 2,2,4,6,7-pentamethyldihydrobenzofuran-5-sulfonyl (Pbf) group (Scheme 34).



Scheme 34. Literature investigation into the scope of the reaction[143]

R = amino acid residue or peptide chain

Selveraj *et al*. then demonstrated that this method could be used to synthesise the cyclic peptide sunflower trypsin inhibitor-1 **123** (SFTI-1). SFTI-1 is a potent Bowman-Birk protein family inhibitor and is made up of 14 amino acids (Figure 36). Previous syntheses of this compound and its analogues has required elevated temperatures and a long reaction time, resulting in a 35% yield after purification. Using the diaminobenzoic acid linker, the linear peptide was synthesised, followed by removal of the *N*-terminal Fmoc group and activation using isoamyl nitrite to give the benzotriazole linker. The *N*-terminal amine can then act as a nucleophile to both cyclise the peptide and subsequently cleave it from the resin. This cyclisation reaction was shown to be completed in 5 h, before deprotecting the amino acid side chains. This deprotection triggered formation of the intramolecular disulfide bridge to give SFTI-1 in 42% yield and 94% purity.

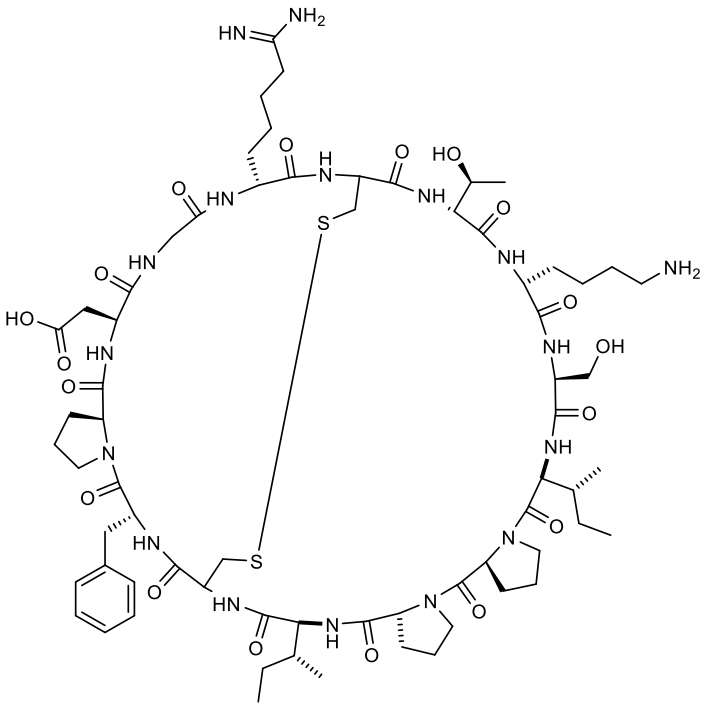
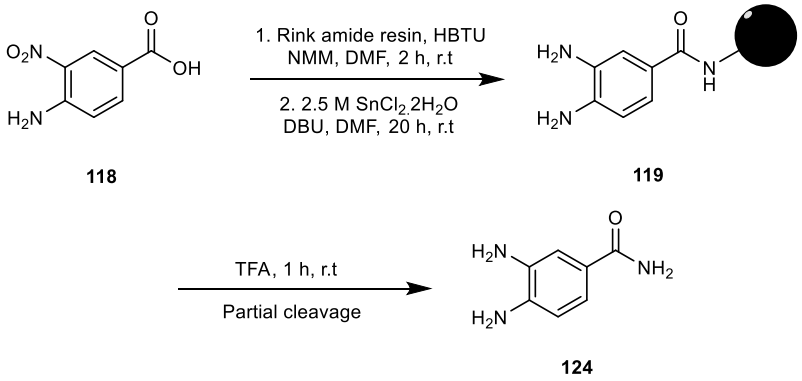


Figure 36. Structure of sunflower trypsin inhibitor-1 (SFTI-1), **123** [143]

Attention then turned to applying this method to the synthesis of the peptide in the current project. To synthesise the proline-glutamic acid-threonine peptide, the protecting group strategy of the amino acids was changed to Fmoc for the *N*-terminus and *tert*-butyl for the side chains. This eliminated the need for the debenzylation reaction that had been problematic during solution phase synthesis.

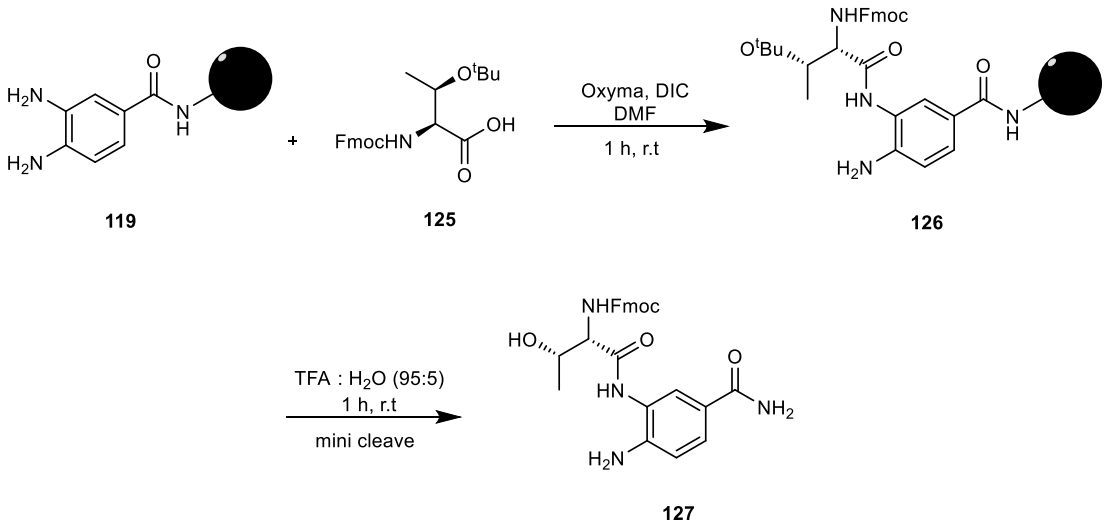
Following the procedure outlined by Selvaraj *et al*. commercially available 4-amino-3-nitrobenzoic acid was coupled onto the Rink Amide MBHA resin. This resin comprises the modified Rink amide linker attached to the MBHA resin. This coupling was completed using HBTU as the coupling reagent with *N*-methylmorpholine (NMM) as the base in DMF. Coupling was complete in 2 h (Scheme 35). The next step was to reduce the aromatic nitro group to the aniline. Tin(II) chloride is widely used as a reducing agent and provides mild conditions under aqueous acid to reduce nitro groups in the presence of other reducible groups, such as aldehydes or phenyl groups. However, in 1984 Bellamy *et al*. developed a general and inexpensive method for the selective reduction of aromatic nitro compounds in non-acidic and non-aqueous media.[144] Using $SnCl_2 \cdot H_2O$ in ethanol or ethyl acetate, allowed for the reduction of a wide variety of substituted nitrobenzenes in almost quantitative yields. Reduction of the nitro group of **118** was performed using $SnCl_2 \cdot H_2O$ and DBU in DMF for 20 h, before a small amount of resin was removed for cleavage to check the coupling and reduction

were successful. Cleavage was done using TFA for 1 h, and mass spectrometry confirmed the structure of **124**.



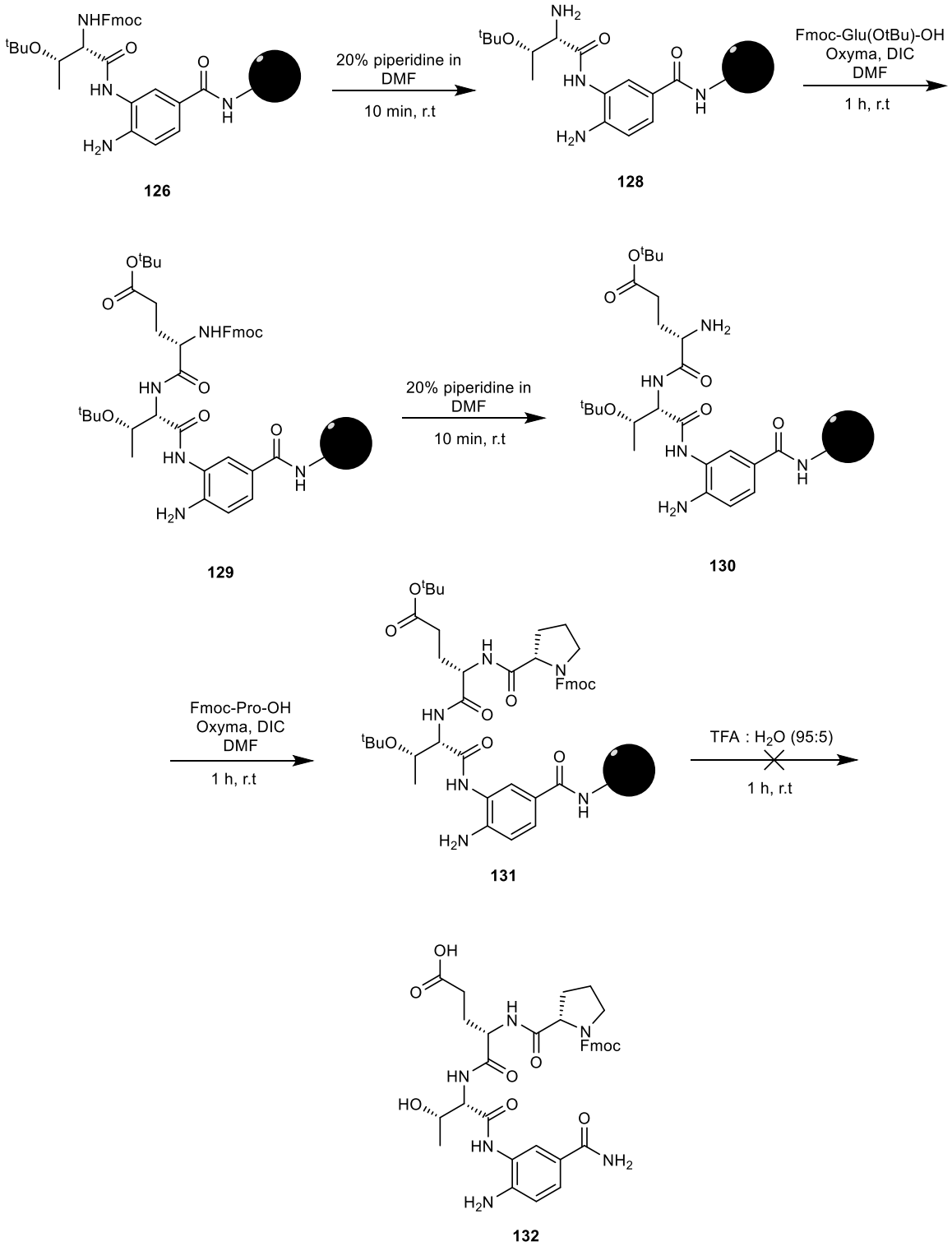
Scheme 35. Preparation of the diaminobenzoic acid linker

The next step was to couple on the first amino acid in the sequence. Coupling of Fmoc-Thr(O^{t}Bu)-OH was initially performed using Oxyma and DIC in DMF (Scheme 36). Oxyma, first introduced in Chapter 1, is a safe and efficient reagent used in carbodiimide peptide coupling chemistry. The carbodiimide DIC is used as an alternative coupling reagent to DCC in peptide synthesis. DIC is a liquid, and therefore is easier to handle than the waxy solid of DCC, and the *N,N'*-diisopropylurea by-product formed in the reaction is soluble in most organic solvents, thereby facilitating the work-up procedures performed in solid phase synthesis. The additive Oxyma has been shown to outperform both HOBt/DIC, HBTU and PyBOP in terms of purity and yield, and has consequently become one of the reagents of choice for synthesis of peptides.[145] In this synthesis, four equivalents of Fmoc-Thr(O^{t}Bu)-OH, Oxyma and DIC were used and the reaction was conducted in DMF. The reaction mixture was shaken at room temperature for 1 h before conducting a partial cleavage of the resin **126** using a TFA : H_2O (95:5) mixture. Once again mass spectrometry was used to confirm the structure of **127** and that coupling of the first amino acid onto the linker had been successful.



Scheme 36. Loading of the first amino acid, Fmoc-Thr(O^{t}Bu)-OH onto the linker

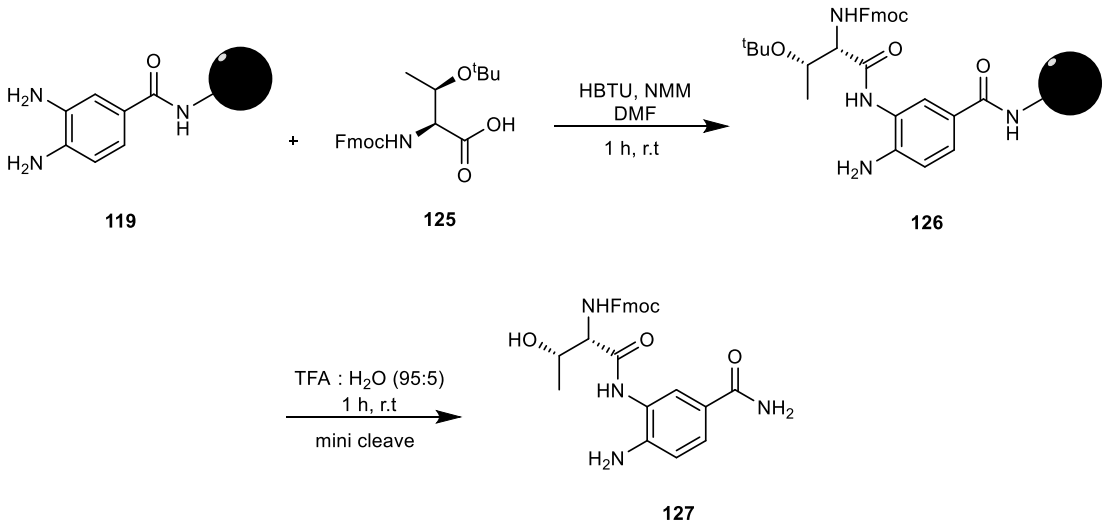
Following on from the successful first coupling, **126** was Fmoc deprotected using 20% piperidine in DMF and then coupled to Fmoc-Glu(O^{t}Bu)-OH using Oxyma and DIC in DMF, before Fmoc deprotection once again and the final coupling to Fmoc-Pro to give **131** (Scheme 37). At this stage the amount of peptide **131** bound to the resin was quantified. This method uses the UV spectrophotometry analysis described in Chapter 1. By using a known quantity of 20% piperidine in DMF, the loading of the peptide was calculated using the absorbance of the dibenzofulvene-piperidine adduct compared to that of the same piperidine solution used for deprotection. Upon conducting this procedure, the loading of the peptide onto the resin was much lower than expected, and so partial cleavage of the resin was done to confirm the structure of the peptide attached to the resin. However, the structure of **132** was not found by mass spectrometry and so a different approach for the coupling was attempted.



126 **128** **129** **130** **131** **132**

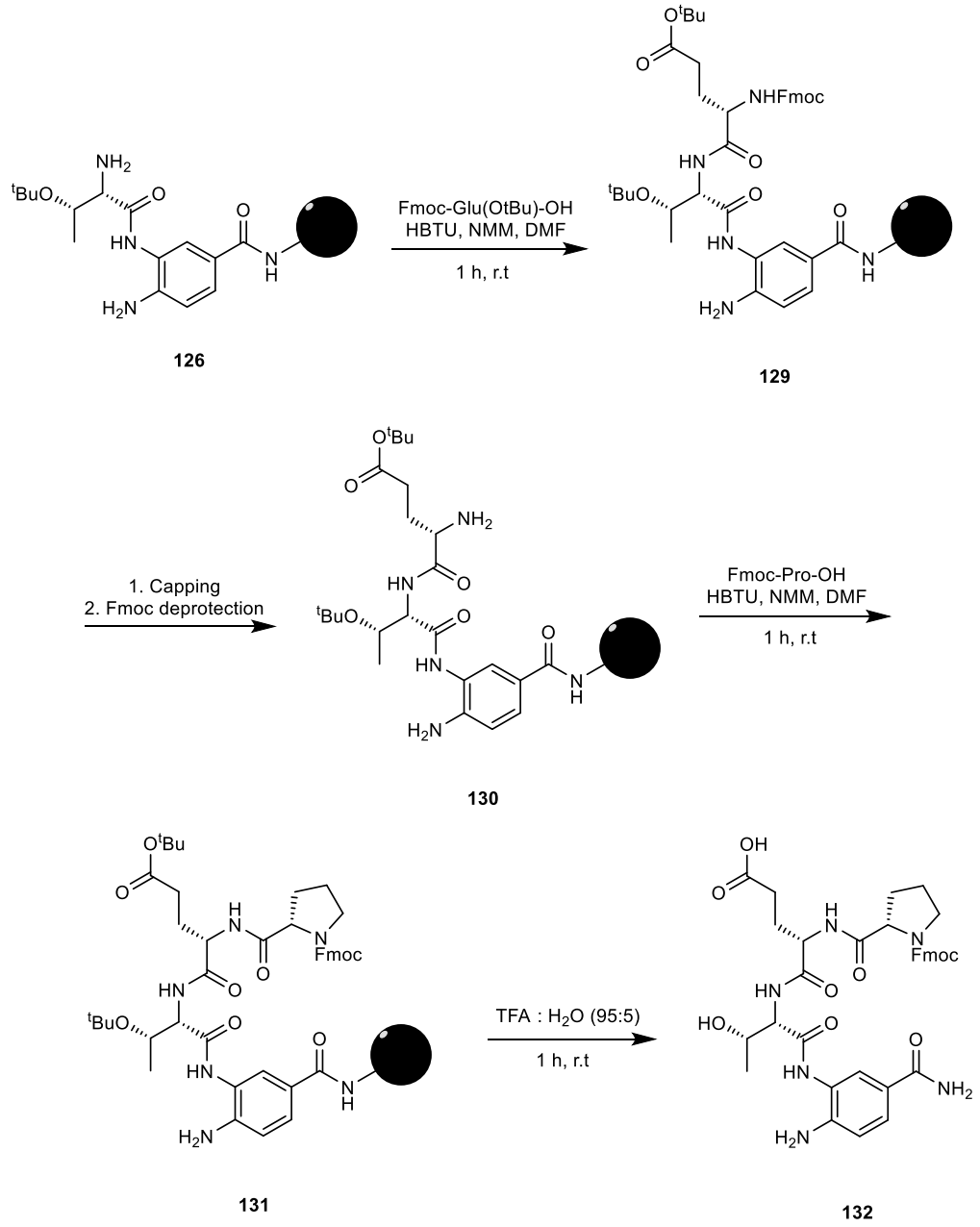
Scheme 37. Solid phase synthesis of the tripeptide-linker adducts. **132** was not observed

As the synthesis of the peptide using Oxyma and DIC was proving to be problematic, attention returned to the conditions used in the procedure by Selvaraj *et al*. (see Scheme 34). These conditions were used for the coupling of Fmoc-Thr(O^{t}Bu)-OH **125** onto the linker (Scheme 38). Once again, a partial cleavage was performed to verify the first coupling was successful.



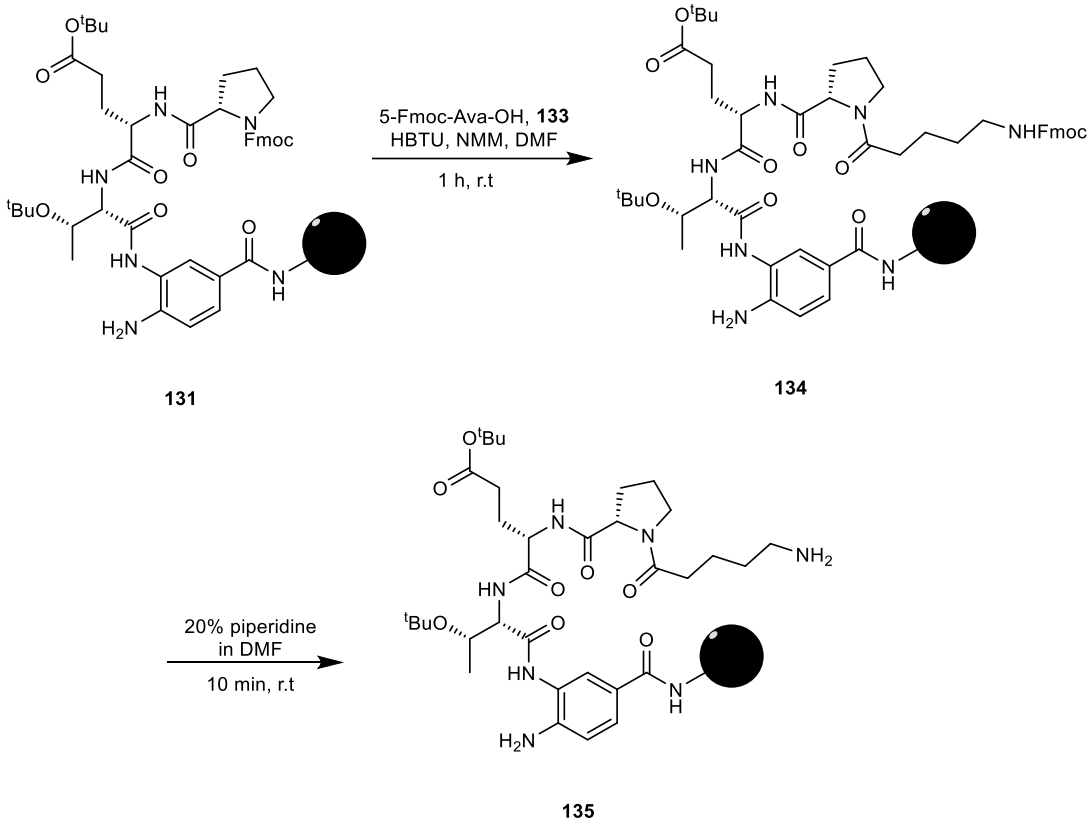
Scheme 38. Coupling of Fmoc-Thr(O^{t}Bu)-OH onto the linker using HBTU

The remainder of the peptide sequence was then coupled onto the resin using HBTU and NMM (Scheme 39). Fmoc-Glu(OtBu)-OH and Fmoc-Pro-OH were coupled onto the resin to give compound **131**. A capping step was introduced into this synthesis, using acetic anhydride and pyridine and was performed after each coupling before subsequent Fmoc deprotection. This capping step transfers an acetyl group from acetic anhydride onto any free NH on the resin, and in so doing acylates any unreacted peptide, preventing it from reacting on in the next coupling step. Consequently, introducing a capping step into the peptide synthesis can help to prevent any unwanted side reactions. This step was followed by Fmoc deprotection using 20% piperidine in DMF. After the synthesis of the tripeptide was complete, a partial cleavage of the peptide from the resin was performed, with the structure of **132** confirmed by mass spectrometry.



Scheme 39. Solid phase synthesis of peptide **131**, followed by cleavage of peptide from resin to give **132**

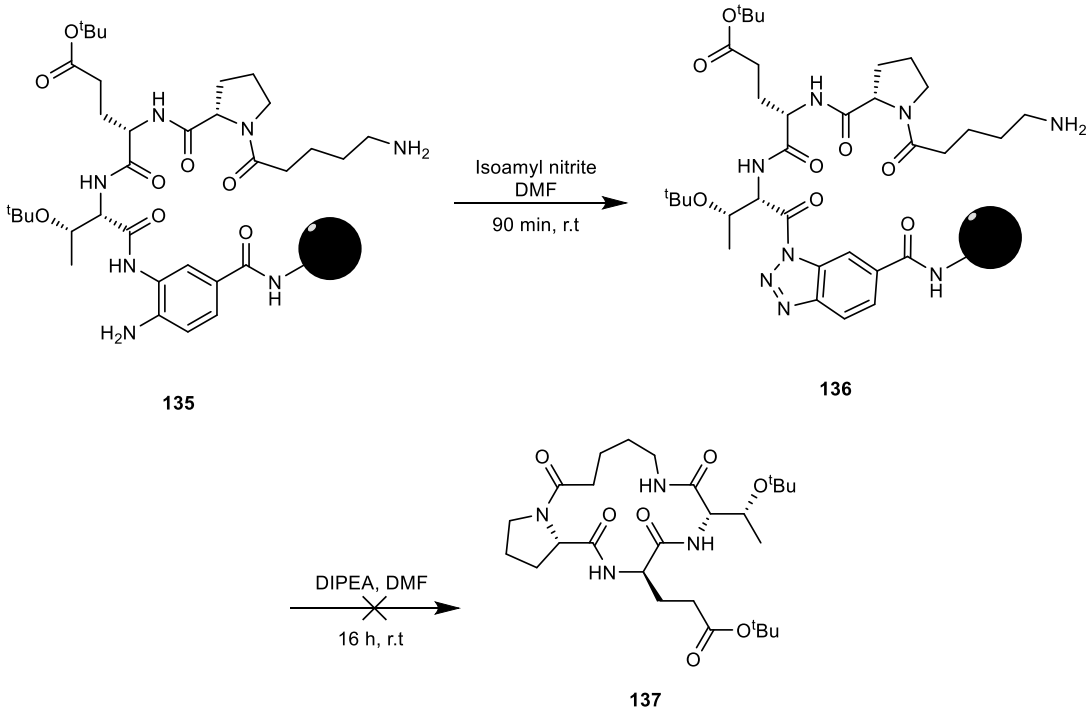
The next step in the synthesis was to couple Fmoc-aminovaleric acid **133** onto proline. Once again this was done using HBTU and NMM, followed by Fmoc deprotection to give **135** (Scheme 40).



Scheme 40. Solid phase synthesis of **135**

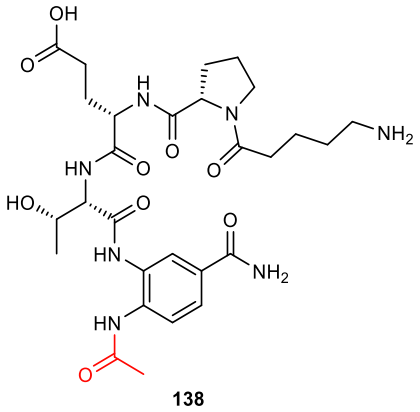
Activation of the diaminobenzoic acid linker was then attempted using isoamyl nitrite before the cyclisation reaction. The free *N*-terminal amine resin-bound o-aminoanilide-peptide **135** was activated with isoamyl nitrite (10 equivalents) at room temperature for 90 min (Scheme 41). Alkyl nitrites, such as isoamyl nitrite, are inexpensive and mild esters of nitrous acid that can be easily prepared. Initially used as vasodilators, it was observed that alkyl nitrites were useful chemical reagents and an efficient source of nitric oxide (NO).

Subsequently, the on-resin *N*-terminal amine was then reacted with *C*-terminal acid and cleaved from resin in the presence of DIPEA (4 equivalents) in DMF for 16 h at room temperature (Scheme 41).



Scheme 41. Activation and cyclisation attempt of the linker

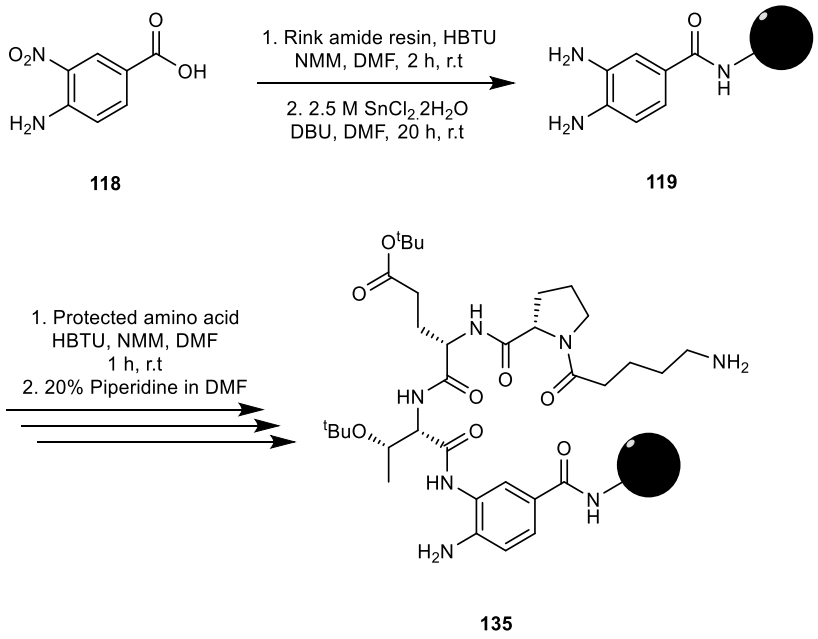
However, after 16 h the cyclisation reaction failed to yield any cleaved cyclic peptide and so a Kaiser test was performed. A Kaiser test is typically used to monitor the completeness of a peptide coupling reaction in solid phase synthesis. An intense blue colour is generated from the reaction of ninhydrin with any free primary aliphatic amine present on the resin after deprotection. It should be stated that the Kaiser test is not applicable in the case of aromatic amines, and so would not result in a false positive if the activation to the benzotriazole has not been successful. The results from the Kaiser test indicated there was still peptide attached to the resin and so part of the resin was cleaved using TFA in water. Using mass spectrometry, the major compound cleaved from the resin was determined to be **138** (Figure 37). This compound had been formed due to the capping steps performed after each coupling reaction, transferring an acetyl group onto the free amine on the diaminobenzoic acid ring. This acetylation prevented the activation step to the benzotriazole, and therefore cyclisation of the peptide. In order to stop the acetylation from occurring, the synthesis of the peptide was repeated, with the capping steps omitted.



138

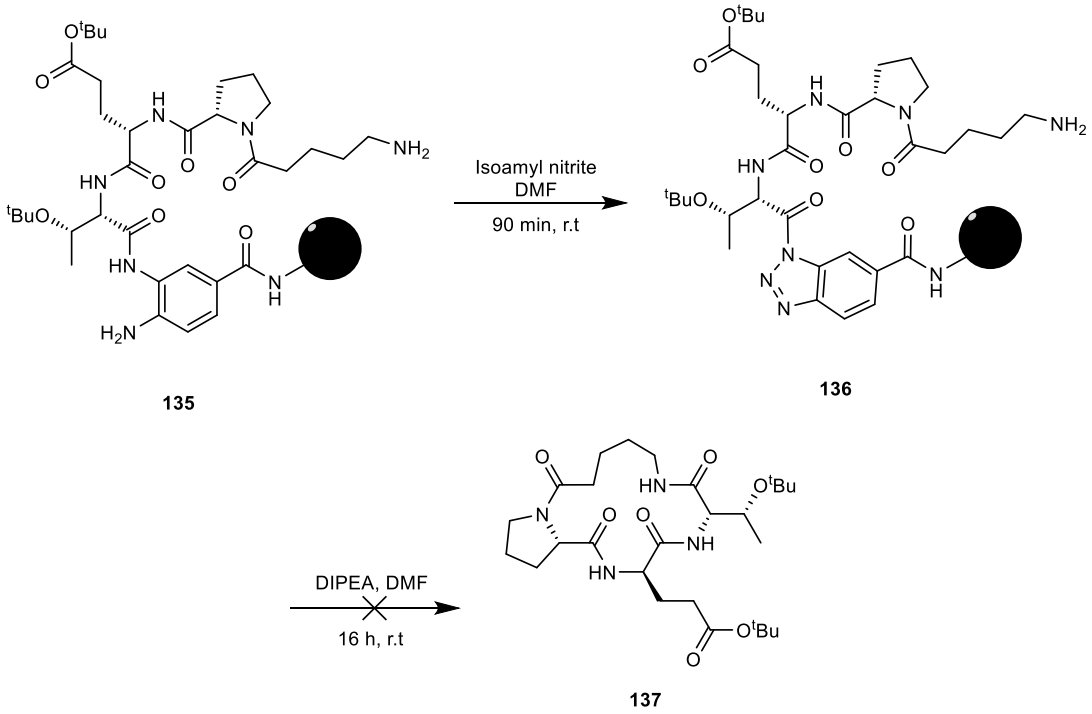
Figure 37. Structure of the peptide **138** cleaved from the resin

The peptide synthesis proceeded as previously described, with first coupling and reducing the linker to give **119**, then completing the couplings of Fmoc-Thr(O^{t}Bu)-OH, Fmoc-Glu(O^{t}Bu)-OH, Fmoc-Pro-OH and Fmoc-aminovaleric acid to give **135** (Scheme 42). Fmoc deprotections were performed using 20% piperidine after each coupling, before washing the resin and completing the next step.



Scheme 42. Synthesis of **135** without any capping steps

Once peptide **135** had been synthesised, the activation and cyclisation steps were attempted (Scheme 43). However, only a minor amount of cyclic peptide **137** was isolated and when the resin was tested using a Kaiser test, no peptide was shown to be present on the resin.

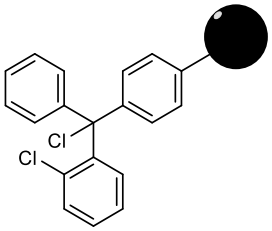


Scheme 43. Activation and cyclisation

As this method yielded an insufficient amount of cyclic peptide, a different solid phase technique was attempted. This method involved the use of a different resin for the synthesis of the linear peptide followed by cyclisation in the solution phase.

3.2 Solid Phase Synthesis of Cyclic Peptides Using Solution Phase Cyclisation

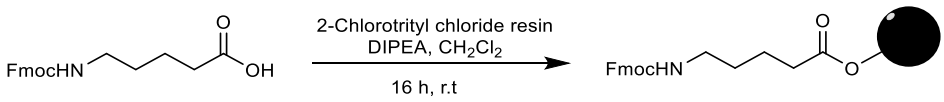
The chlorotrityl chloride resin **139** (Figure 38) is one of the most useful resins for solid phase synthesis of *C*-terminal acid peptides and can be used in the synthesis of both protected and unprotected peptides. Cleavage of the chlorotrityl chloride resin can be achieved under mild acidic conditions when compared to other acid labile resins, by using 0.5% TFA or hexafluoroisopropanol (HFIP). An advantage of this resin is that it minimises both the formation of diketopiperazines and racemisation upon loading of the first amino acid. This is due to both steric factors, and that no coupling reagents or activation is required for loading of the first amino acid, it can simply be completed using a base such as DIPEA.



139

Figure 38. Structure of the chlorotrityl chloride resin

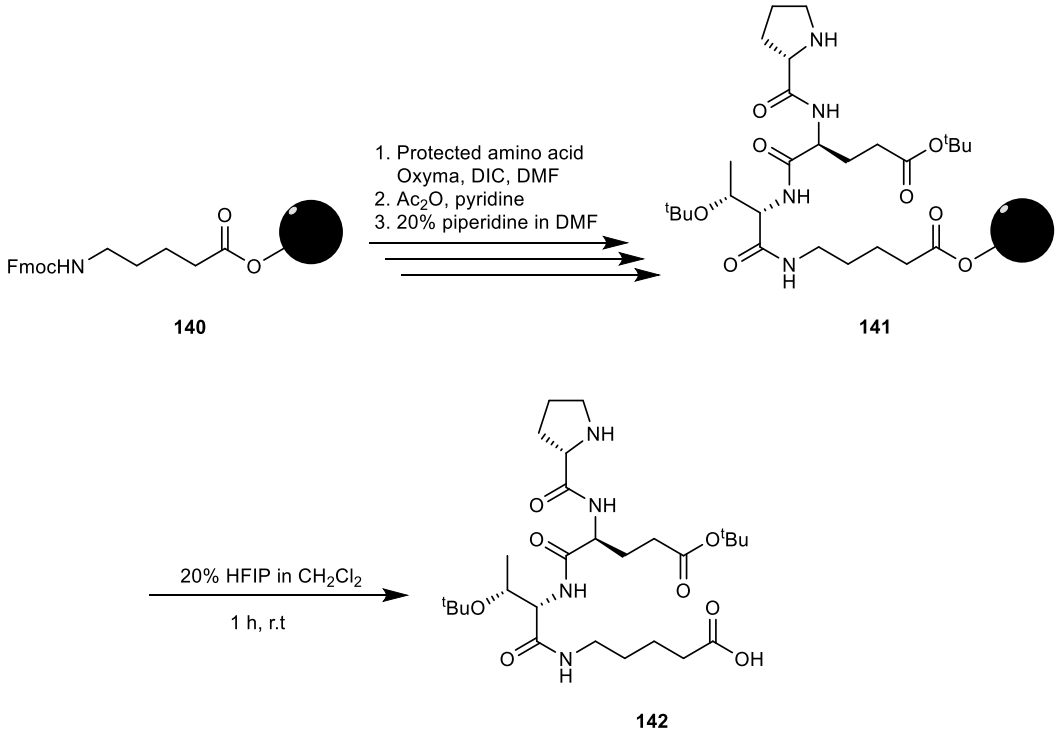
Automated synthesis of the tripeptide in this project used 2-chlorotrityl chloride resin as a solid support to construct the linear peptides by use of a Biotage Initiator+ Alstra Synthesiser. In order to do this, the first amino acid had to be loaded onto the resin manually using DIPEA in dichloromethane (Scheme 44). As difficulties had previously arisen with racemisation of threonine, the linker chain of Fmoc-aminovaleric acid **133** was loaded onto the resin first to keep any potential racemisation during the synthesis to a minimum.



133 **140**

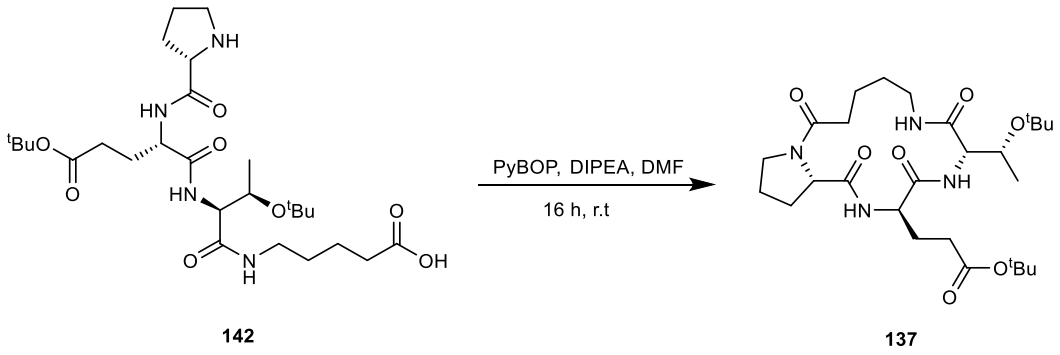
Scheme 44. Loading of **133** onto the 2-chlorotrityl chloride resin

The remaining coupling steps of Fmoc-Thr(O^{t}Bu)-OH, Fmoc-Glu(O^{t}Bu)-OH, Fmoc-Pro-OH were completed on the Biotage Initiator+ Alstra Peptide Synthesiser, followed by cleavage from the resin using 20% HFIP in dichloromethane (Scheme 45). The linear peptide **142** was isolated as a single diastereomer.



Scheme 45. Synthesis of **142** using the 2-chlorotrityl chloride resin

Following cleavage from the resin, cyclisation was attempted using solution phase conditions (Scheme 46). PyBOP was used as the coupling reagent and the reaction was conducted at high dilution in DMF. Cyclisation was proved successful by mass spectrometry, however, the formation multiple compounds were once again observed in this reaction and separation of these compounds were unable to be separated by preparative HPLC.

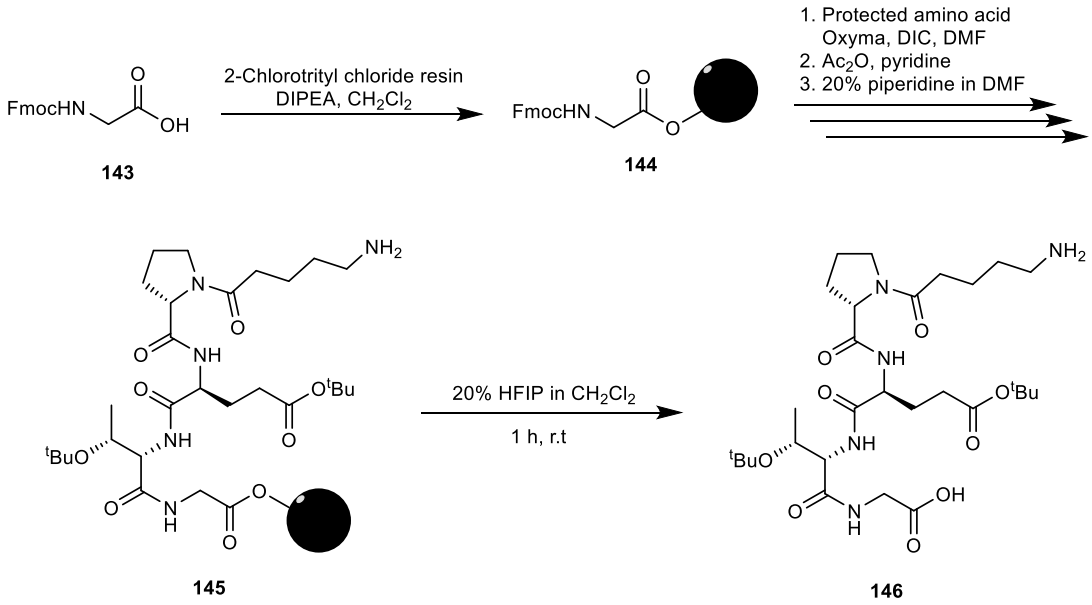


Scheme 46. Solution phase cyclisation of **142**

As the cyclisation step had resulted in the formation of multiple compounds, as it had done previously, modifications were made to the peptide sequence. In the peptide sequences screened by Wells *et al*. (Table 1, Chapter 1), from which this project identified the tripeptide sequence Pro-Glu-Thr, the amino acid following threonine was glycine. The addition of

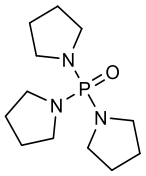
glycine onto the *C*-terminal of the peptide, this would result in the cyclisation step being a coupling between glycine and the linker. As both of these residues are not chiral, the cyclisation step should proceed without racemisation.

Using the 2-chlorotrityl chloride resin, glycine was first loaded onto the resin using DIPEA in dichloromethane for 16 h to give **144** (Scheme 47). Automated synthesis, using Oxyma and DIC for the couplings, was then used for the remainder of the peptide sequence and coupling of the linker. The linear peptide **146** was then cleaved from the resin using 20% HFIP in dichloromethane as a single diastereomer (Scheme 47).



Scheme 47. Automated synthesis of peptide **146**

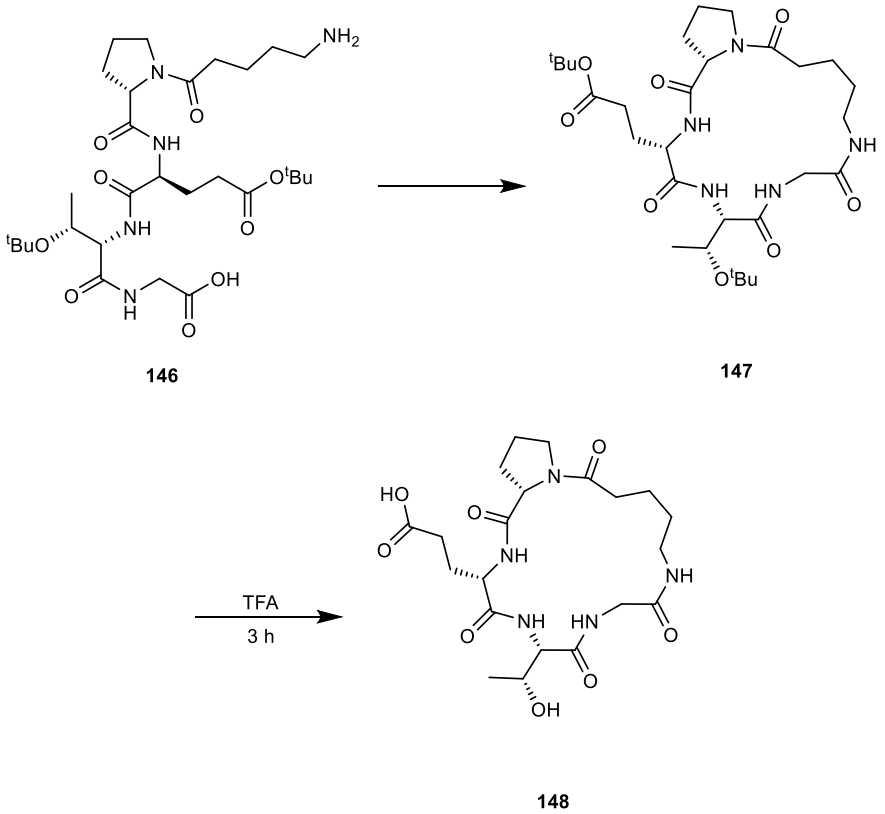
Several cyclisation conditions were attempted, followed by side chain deprotection of the product using TFA (Table 11). Cyclisation performed with PyBOP and DIPEA in DMF (Table 11, Entry 1) showed formation of **147** with subsequent TFA deprotection giving the crude **148** without any discernible racemisation. However, upon purification of **148** by preparative HPLC, the cyclic product could not be isolated pure. A by-product of PyBOP **149** (Figure 39) from the reaction was shown to be present in the product after purification and after attempting a number of different gradients on the HPLC, as well as repeating the reaction and including an aqueous work up, failed to improve the purity of the final product.



149

Figure 39. Structure of the PyBOP by-product

The next set of conditions attempted were EDCI and DMAP in DMF (Table 11, Entry 2), though after 18 h no product was shown to be formed in the crude reaction mixture. DMTMM was also tried as a coupling reagent in the cyclisation reaction, followed by TFA deprotection to give **148** (Table 11, Entry 3). When these conditions were first attempted once again by-products from the DMTMM coupling were present in the final product **148**. However, by adding in an aqueous work up before the deprotection step, this allowed **148** to be isolated in 93% purity after purification and in a 5% overall yield. Therefore, these reaction conditions were taken forward for the synthesis of the two remaining analogues **149a** and **149b** with differing linker lengths (Scheme 48).

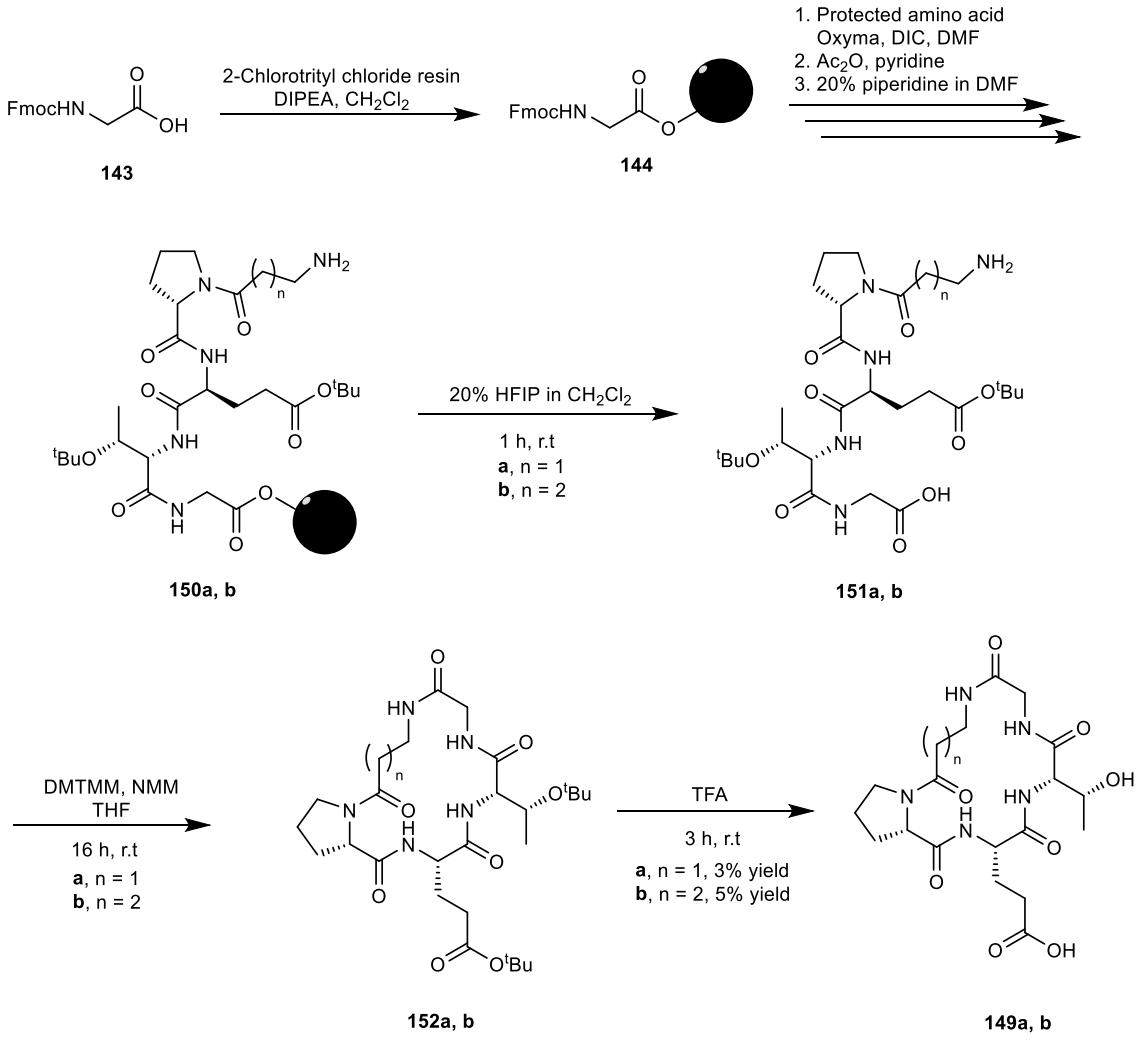


146 147 148

Entry	Reaction Conditions	Yield (%)
1	PyBOP, DIPEA, DMF, 16 h	Unable to remove PyBOP impurity
2	EDCI, DMAP, DMF, 18 h	No product isolated
3	DMTMM, NMM, THF, 16 h	5 (after purification)

Table 11. Cyclisation conditions. Each set of reaction conditions was followed by TFA deprotection

The remaining analogues included peptides with the linkers β-alanine and γ-aminobutyric acid. These analogues were synthesised following the previous procedure (Scheme 48). Fmoc-glycine was first coupled manually onto the chlorotrityl chloride resin to give **144**, with the remainder of the linear peptide constructed using automated synthesis. The peptide was then cleaved from the resin and cyclised using DMTMM over 16 h. At this stage an aqueous work-up was performed to remove impurities and the resulting product was treated with TFA over 3 h to remove the side chain *tert*-butyl groups. After purification compound **149a** was isolated in 3% yield and compound **149b** was isolated in 5% yield. The purities of both of these analogues were >90%, as determined by HPLC.



Scheme 48. Synthesis of cyclic analogues **149a** and **149b**

3.3 NMR Spectroscopy and Molecular Modelling Studies

After successfully synthesising three cyclic compounds **148**, **149a** and **149b**, conformational studies by NMR spectroscopy and molecular modelling studies will be carried out to see how they may differ from one another.

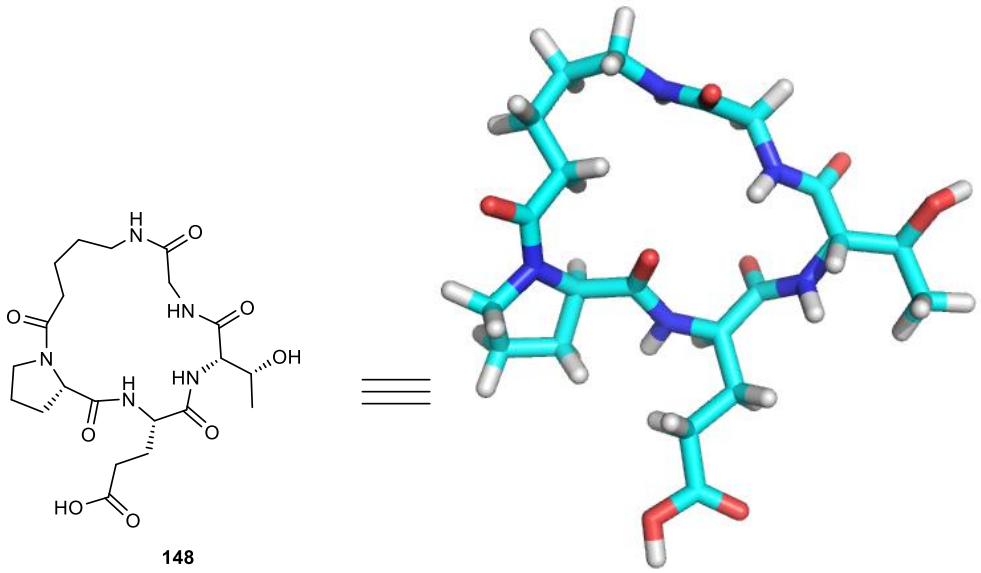
3.3.1 Molecular Modelling

Molecular modelling encompasses all theoretical and computational methods used to mimic the structure and behaviour of molecules. This can range from small chemical systems to large biological assemblies including protein folding, enzyme catalysis, and conformational changes associated with biomolecular function. Performing molecular modelling studies on peptides is beneficial as they provide simpler models of larger and more complex proteins. It can also help to provide rationalisations of their function in terms of structure, dynamics and

interactions with the environment. Due to the smaller size of peptides, they tend to be more flexible than proteins and thus dynamics plays a greater role in peptide properties in solution. Therefore, peptide modelling considers characterisation of a range of possible structures and predicting their populations, as well as the rates of interconversion between them.

In this project, the molecular editor and visualiser, Avogadro (Version 1.2.0)[146], was used to construct and view the synthesised peptides in 3D. The structures of the peptides were first built, and the energy of the molecules minimised. Constraints were added to the peptide backbone, fixing the distance between the bonds. The bond distances for the backbone were synonymous to the peptide backbone in the crystal structure of the phosphorylated sequence of p62 in complex with Keap1 (PDB reference: 3WDZ).[147] Optimisations were then performed around these bond constraints and a general AMBER force field (GAFF) was applied to the system.[148]

The first cyclic structure to be analysed was that of compound **148** (Figure 40). The proposed energy minimised 3D structure is shown below.



148

Figure 40. Proposed structure of **148**

The possible structure of our peptide **148** (blue) was then compared to the natural binding sequence of p62 using PyMOL v2.0 and importing the peptide from PDB (Figure 41).[149] The peptide (green) shown below is from the crystal structure of Keap1 in complex with phosphorylated p62 (PDB: 3WDZ). The backbones of each of the peptides were lined up by eye as closely as possible. From the three views shown it can be seen that the proline and glutamic acid residues of our peptide **148** align with the proline and phosphorylated serine residue of p62. As the key interaction with Keap1 is from the phosphorylated serine to an

arginine residue in the binding site Keap1, it can be inferred that this key interaction may still occur in our cyclic peptide. However, the position of the threonine residue differs from the p62 peptide, with the side chain positioned in the opposite direction.

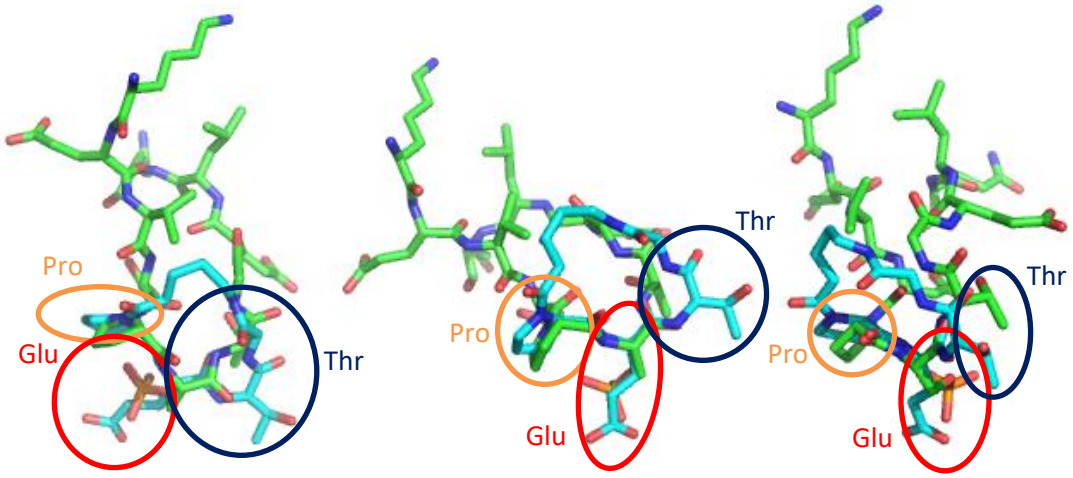


Figure 41. Structure of our peptide (blue) compared with the phosphorylated p62 sequence (green). Structures aligned by eye in PyMOL[149]

When both of these peptides are placed in the binding site of Keap1, it can be seen they have similar binding motifs (Figure 42). The image was created in PyMOL and the backbones of the two peptides were aligned by eye. From Figure 36B it can be seen that the glutamic acid residue of the cyclic peptide **148** extends into a similar space as the phosphorylated serine residue of the Wells peptide. This residue may therefore interact favourably with Arg-483 in the Keap1 protein, a key interaction for the binding of similar peptides to Keap1. The proline residues of each of the peptides are also positioned in a similar space, however, the threonine residues are not. The threonine residue of the cyclic peptide **148** is positioned in the opposite direction to the p62-like peptide synthesised by Wells *et al.* and this is resulting in a steric clash with the backbone of both Ala-536 and Ser-555 in the Keap1 protein. This unfavourable interaction may result in a loss of binding. This brief modelling only showed one possible conformation of the cyclic peptide **148** but there are many possible conformations of this peptide in solution, and the conformation of the cyclic peptide **148** may also change upon binding to the protein, and therefore it is not definitive whether this interaction would result in the cyclic peptide **148** not binding to Keap1.

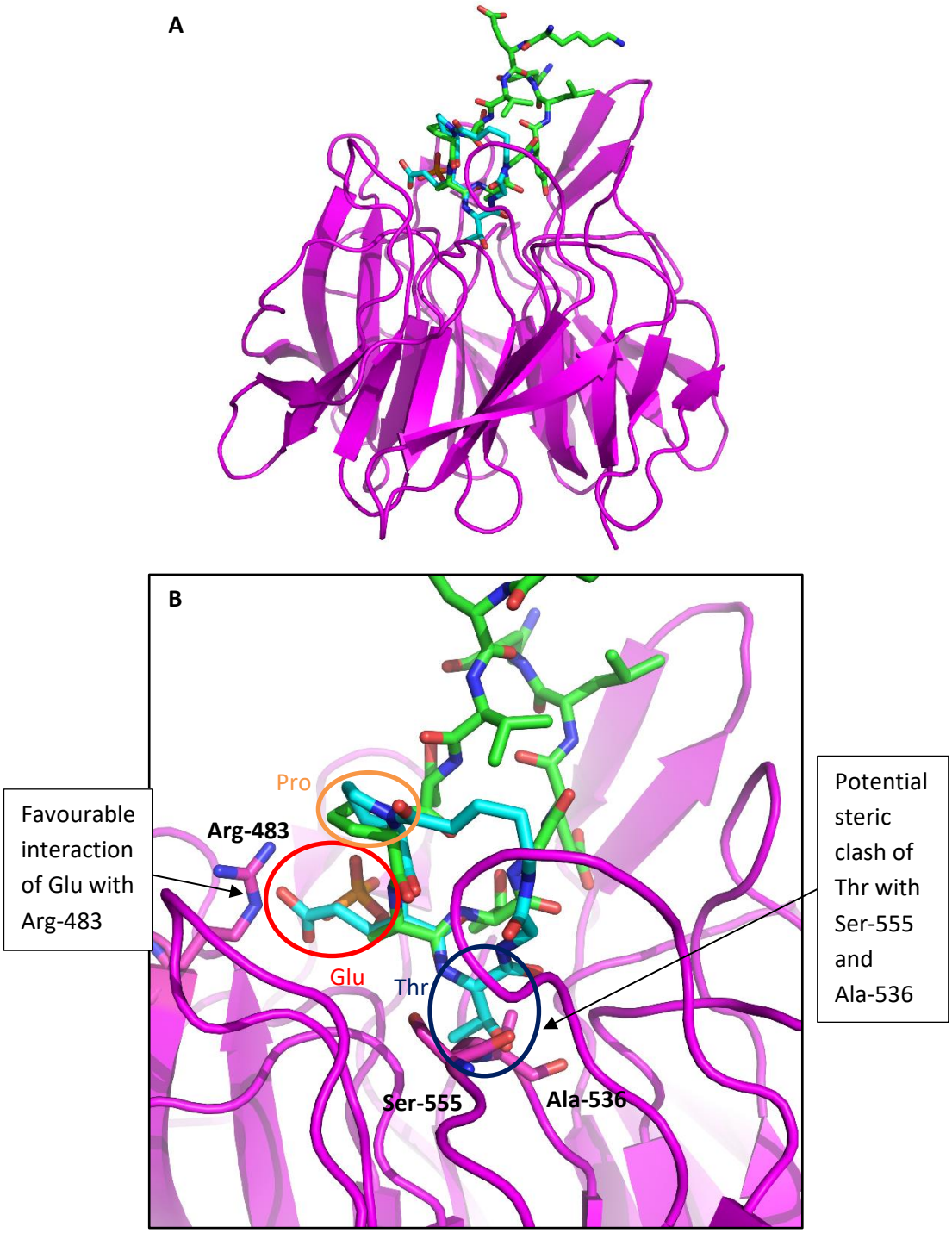


Figure 42. **A**. Binding of p62 analogue (green) and cyclic peptide **148** (blue) to Keap1 (pink). **B**. Closer view of cyclic peptide interactions with Keap1. Generated in PyMOL and importing the protein structure from PDB (3WDZ).

These studies were also performed on cyclic peptides **149a** and **149b**. The proposed energy minimised 3D conformation of each of the peptides is shown below (Figure 43). These structures may be more constrained due to the smaller linker lengths when compared to **148**.

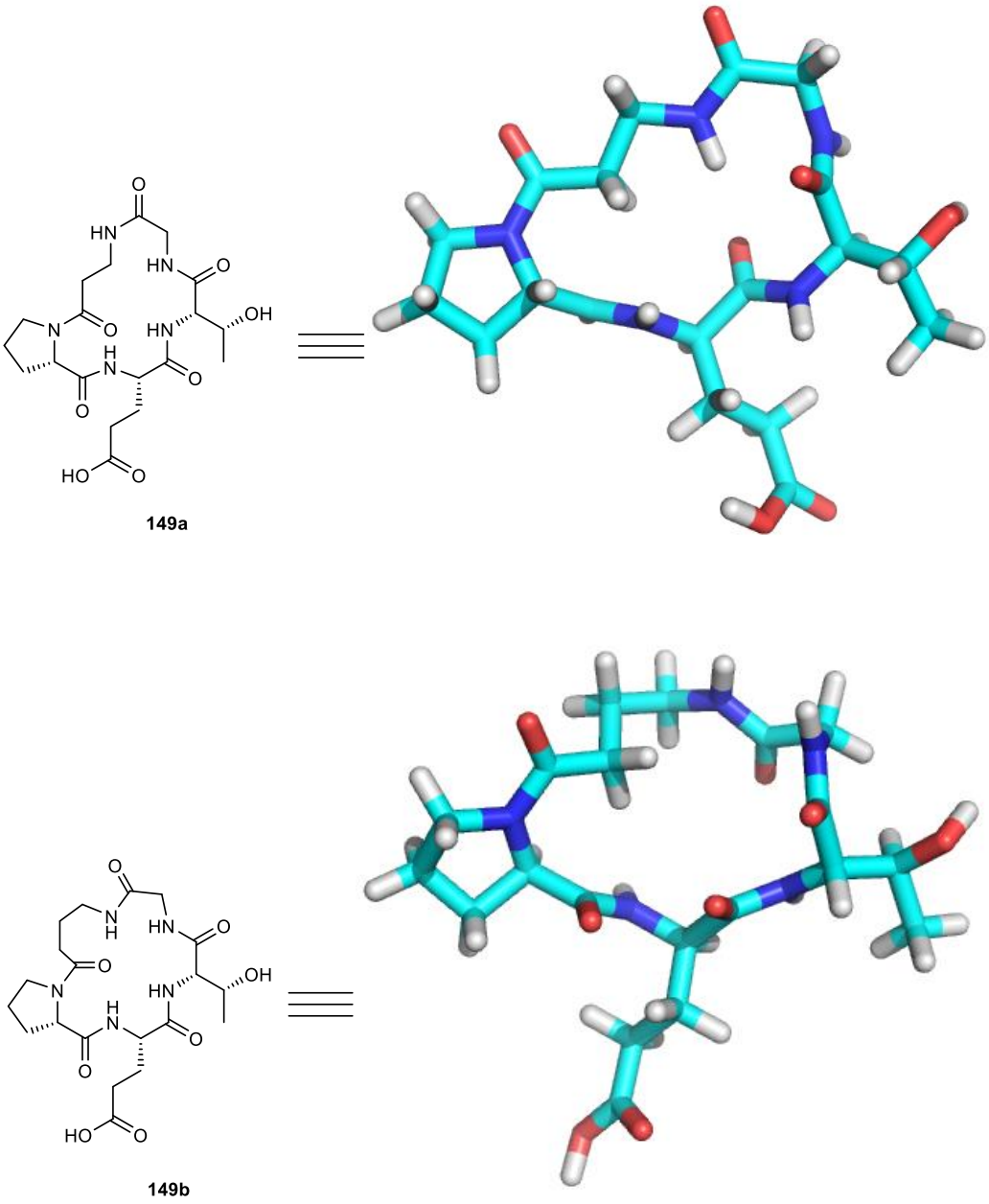
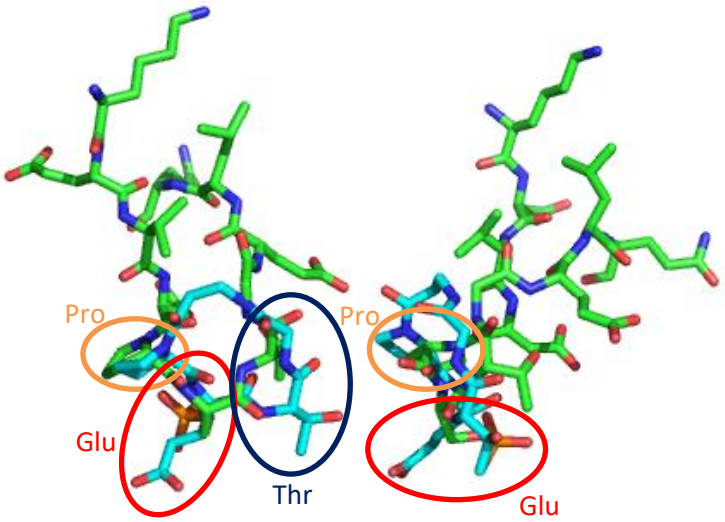


Figure 43. Proposed structure of peptide **149a** and **149b**

Comparison of each of these possible conformations with the natural analogue of p62 (green) are shown below (Figure 44). In these more constrained rings, it was more difficult to align the backbones of the peptides with the natural sequence. As was previously seen with compound **148**, the threonine residue does not lie in the same chemical space as the native threonine. Also seen within these peptides, were changes in the positioning of the glutamic acid residue in **149b** and both the proline and glutamic acid residues in **149a**. In both peptides the glutamic acid residue extended into a different region of chemical space (Figure 44a/b), and in **149b** the proline residue adopted a different conformation entirely (Figure 44b).

a)



b)

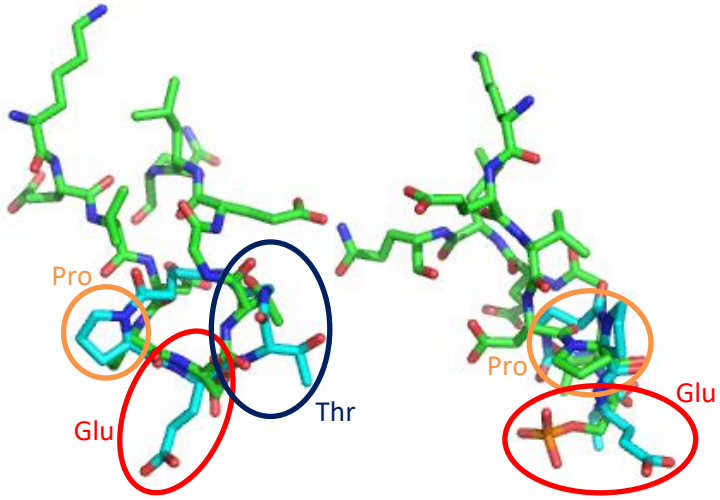


Figure 44. Cyclic peptides **149a** (blue, Figure a) and **149b** (blue, Figure b) aligned by eye with a p62 analogue (green)

Both cyclic peptides **149a** and **149b** were placed in the binding site of Keap1. Due to the different conformations of these peptides when compared to **148**, there was an increased number of potential steric clashes with Keap1, which may inhibit binding. Figure 45B shows the p62-like peptide synthesised by Wells *et al.* (green) and the cyclic peptide **149-b** synthesised in this project (blue) in the binding site of Keap1 (pink). This image shows the conformation of **149-b** may be markedly different from that of the Wells peptide. The glutamic acid residue of **149-b** is located in a different position to that of the phosphorylated serine of the Wells peptide. As a result of this, the glutamic acid residue of **149-b** is creating a steric clash with the side chain of Tyr-525, rather than a favourable interaction with Arg-483. The threonine residues of each peptide are once again located in opposite directions, however, this time the threonine residue of **149-b** is not resulting in any unfavourable interactions.

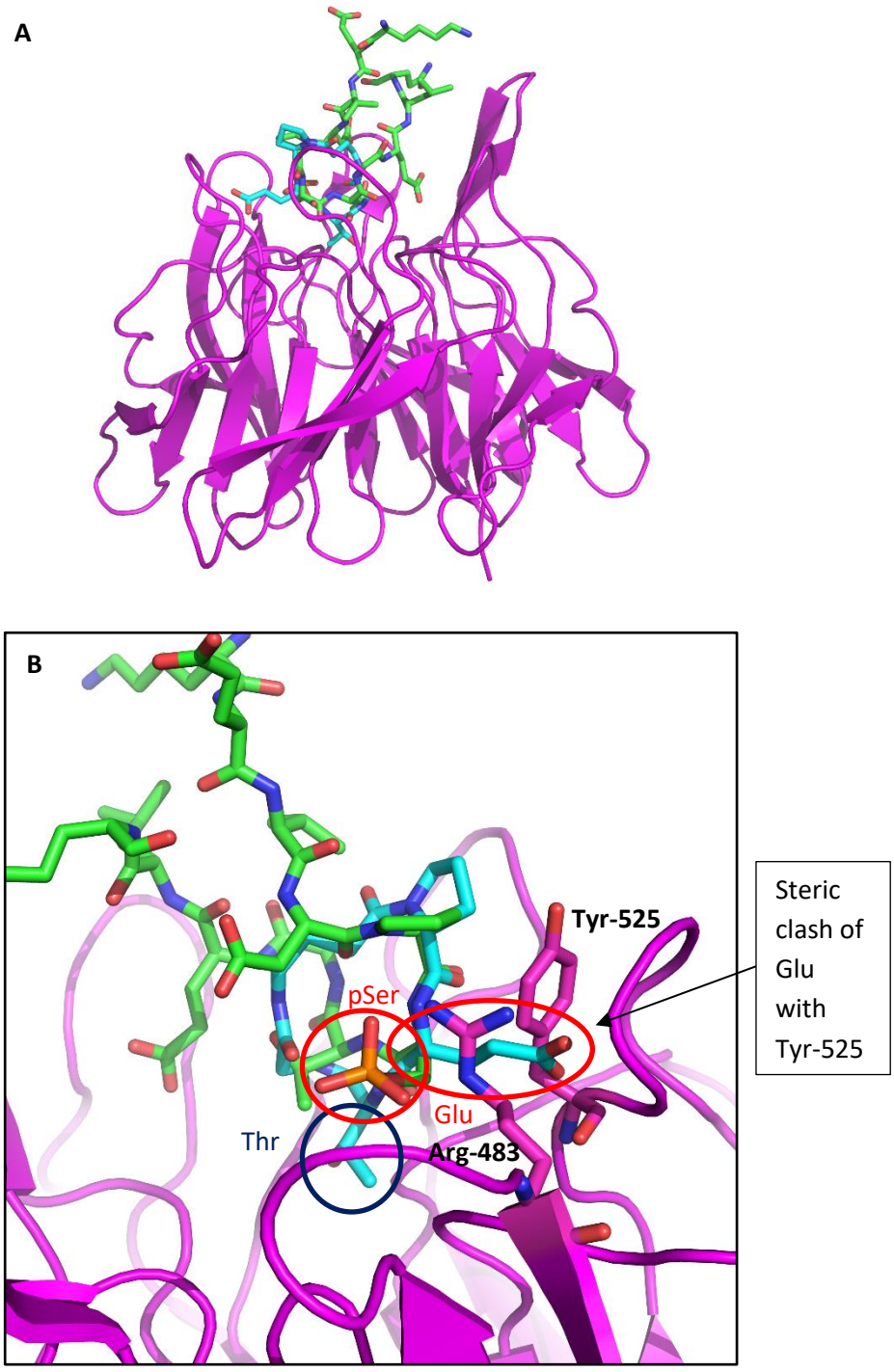


Figure 45. **A**. Binding of p62 analogue (green) and cyclic peptide **149b** (blue) to Keap1 (pink). **B**. Closer view of cyclic peptide interactions with Keap1. Generated in PyMOL and importing the protein structure from PDB (3WDZ).

Figure 46 and 47 show the p62-like peptide synthesised by Wells *et al.* (green) and the cyclic peptide **149-a** synthesised in this project (blue) in the binding site of Keap1 (pink). The conformation of **149-a** was the most challenging to align to the Wells peptide as the backbone was the most constrained. Once again, the steric clash of the glutamic acid residue

of **149-a** with Tyr-525 was observed and the threonine of **149-a** was also positioned in the opposite direction but did not appear to result in any unfavourable interactions.

A



Figure 46. **A**. Binding of p62 analogue (green) and cyclic peptide **149a** (blue) to Keap1 (pink). Generated in PyMOL and importing the protein structure from PDB (3WDZ).

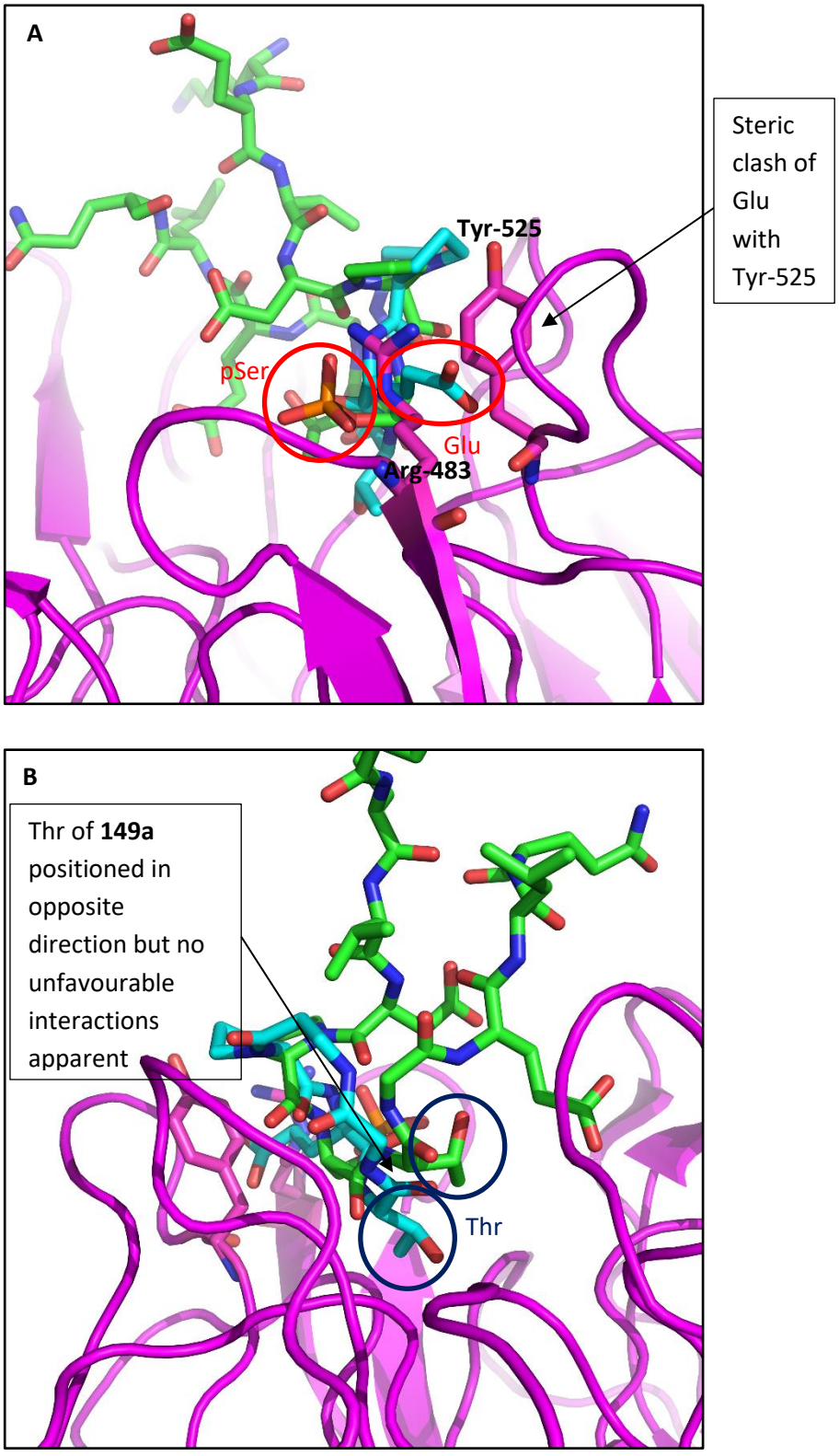


Figure 47. **A** and **B**. Closer view of cyclic peptide interactions with Keap1. Generated in PyMOL and importing the protein structure from PDB (3WDZ).

Molecular modelling of the cyclic peptides prepared in this project has provided an insight into their potential conformations and how they may bind to Keap1. It should be kept in mind

that these studies were cursory and consequently a more in-depth approach would be needed to generate more accurate results.

3.3.2 NMR Spectroscopy

Analysis of the ^{1}H NMR and 2D NMR spectra of the cyclic peptides **148**, **149a** and **149b** showed the presence of two related compounds. The HPLC traces for each compound displayed a single peak and the mass spectra were pure with only the desired product *m/z* ion present. As the linear peptide precursors for each of the compounds were a single diastereomer, epimerisation during cyclisation *via* an amide coupling between the *C*-terminal glycine and the linker residue was unlikely. Epimerisation usually occurs when the terminal acid is activated by the coupling reagent, leading to the formation of an oxazolone, that then reacts with a nucleophile leading to the racemisation of the chiral centre. However, as the terminal acid in this case was glycine, which does not possess chirality, therefore would not result in racemisation. However, this does not rule out the presence of conformers. An explanation for the perceived presence of two compounds in the NMR spectra may be due to restricted rotation around the amide bonds due to the double bond character, leading to rotamers. One way to investigate this hypothesis is through variable-temperature (VT) NMR spectroscopy. VT NMR experiments heat the sample to overcome the barrier to rotation, resulting in coalescence of the peaks seen in the NMR spectrum. In this case, experiments were run on a Bruker AVIII600 with a Bruker smart probe with compound **148** at a concentration of 9.4 mM in a 2% DMSO in a 10% D_2O in H_2O solution. The temperature was varied at 5 ^{o}C increments from 25 ^{o}C to 85 ^{o}C. The room temperature NMR spectrum of **148** showed the presence of two magnetically different compounds, which can be seen most evidently from the methyl group of the threonine residue highlighted in Figure 48.

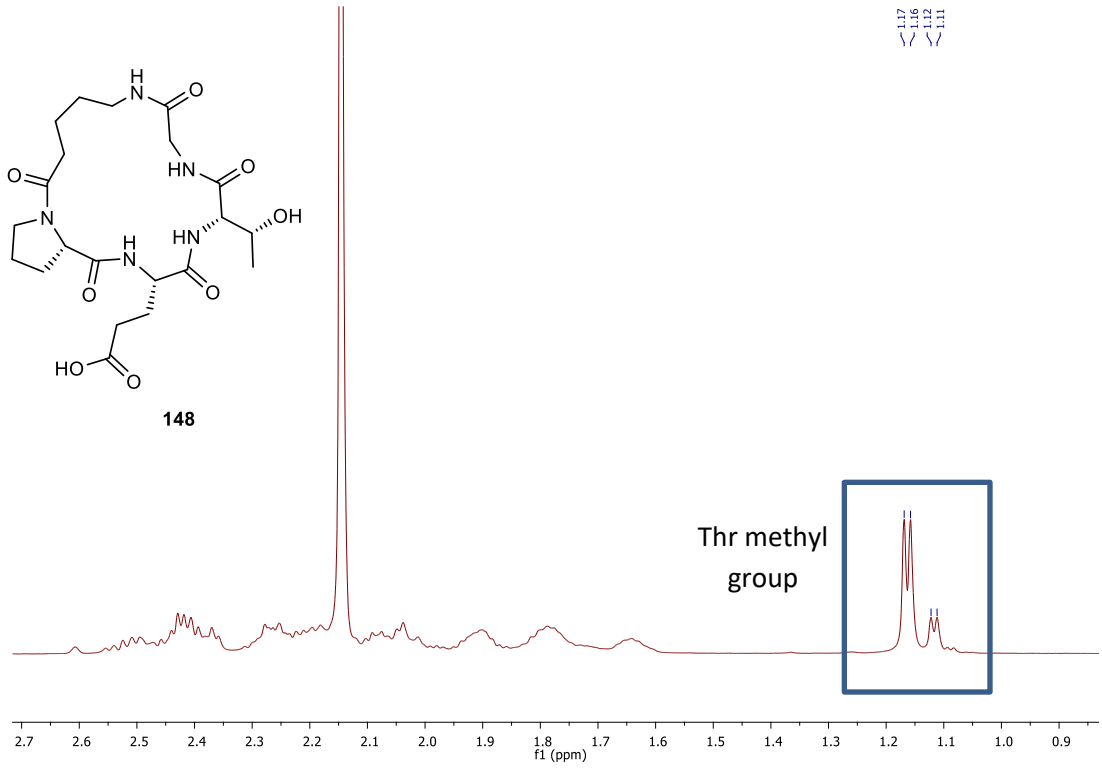


Figure 48. Partial ^{1}H NMR spectrum of **148** run at 25 ^{o}C. Thr methyl group is boxed

As the temperature of the NMR experiment was raised the signals became broader with the two threonine peaks no longer existing as distinct doublets (Figure 49). This broadening continued as the temperature was raised to 85 ^{o}C where the two threonine signals became a broad singlet (Figure 50). It cannot be said conclusively whether this coalescence was due to overcoming the rotation barrier of the peptide or simply the broadening of the signals swamped both doublets. However, as the ratio of the two peaks for the threonine methyl groups did not change as the temperature was slowly raised, it suggested that the most likely reason for the apparent coalescence was the broadening of the NMR signals.

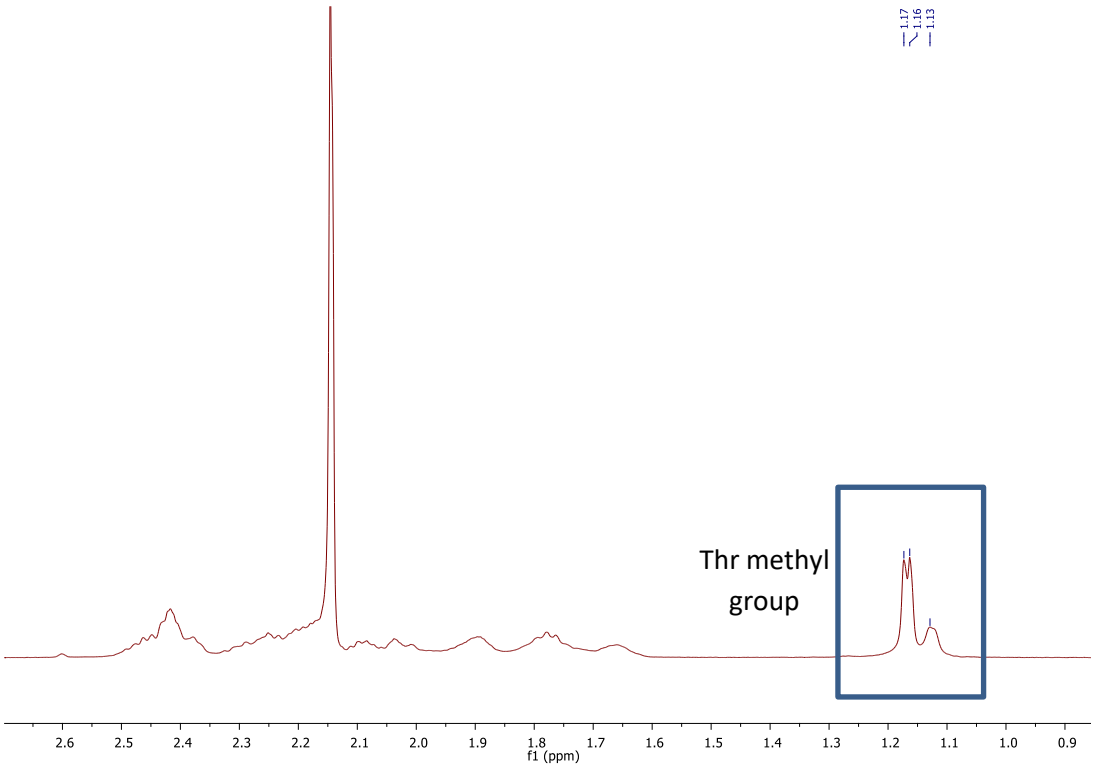


Figure 49. ^{1}H NMR spectrum of **148** run at 60 °C

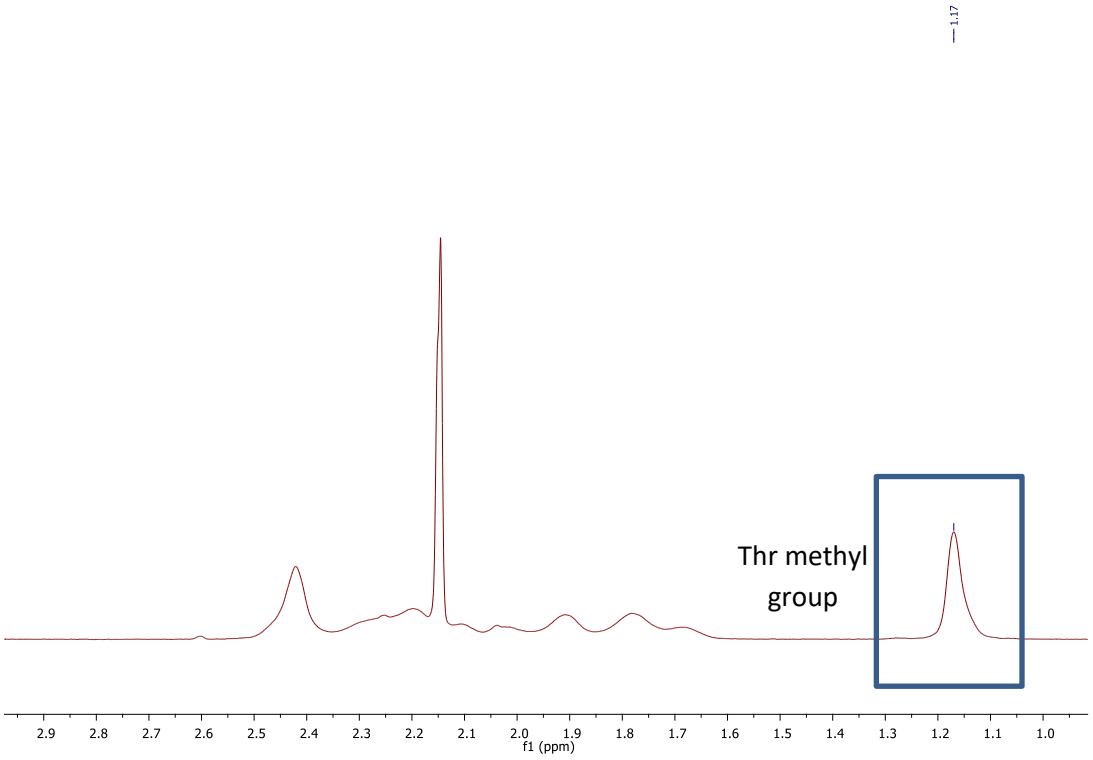
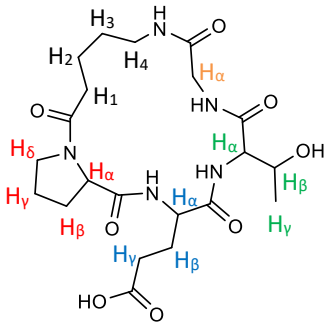


Figure 50. ^{1}H NMR spectrum of **148** run at 85 °C

Another explanation for the presence of two distinct compounds in the NMR spectra may be *cis*/*trans* isomerisation of the proline peptide bond. Most peptide bonds typically adopt the *trans* isomer to minimise steric repulsion, though both AA-Pro (where AA is any amino acid) *cis* and *trans* isomers are subjected to this repulsion and consequently have a much lower energy difference. The fraction of *cis* Pro bonds is dependent on the preceding amino acid, with glycine and aromatic residues resulting in up to 40% *cis* isomer.[150]

To investigate this theory several NMR experiments were run. ^{1}H and 2D NMR experiments including NOESY, TOCSY and HSQC were run on a Bruker AVIII 800 spectrometer with a QCI cryoprobe. ^{1}H NMR experiments were obtained with 2048 by 256 points and 16 transients; HSQC experiments were obtained with 1024 by 128 points and 8 transients. Data processed with zero filling and squared shifted sine bell function and base line corrected as appropriate. Solvent suppression was achieved using excitation sculpting method. Samples were run at 25 ^{o}C in 2% DMSO in a 10% D_2O in H_2O solution. Concentration of samples were **148** 9.4 mM, **149b** 9.7 mM, **149a** 3.3 mM, dependent on the amount of sample available.

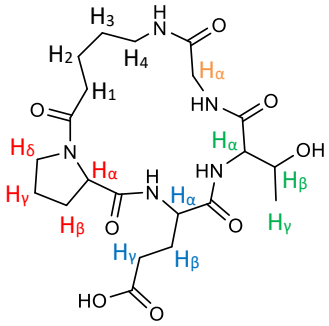
Complete assignment of **148**, **149a** and **149b** from NOESY and TOCSY data is shown below. Each of **148**, **149a** and **149b** has an assignment table for the major component in the NMR, labelled **148-A**, **149a-A** and **149b-A** (Tables 12, 14, and 16 respectively) and a second table for the second minor entity that was present. The assignments for the minor component are labelled **148-B**, **149a-B** and **149b-B** (Tables 13, 15, and 17 respectively).



148-A

Amino Acid	NH	H_α	H_β	H_γ	H_δ
Pro	-	4.38	2.25, 1.84	2.00, 1.76	3.54, 3.39
Glu	8.30	4.45	2.17, 2.05	2.50, 2.40	-
Thr	8.35	4.06	3.88	1.14	-
Gly	8.68	4.02, 3.58	-	-	-
	NH	**H_1**	**H_2**	**H_3**	**H_4**
Linker	7.78	2.51	1.77	1.62	3.19

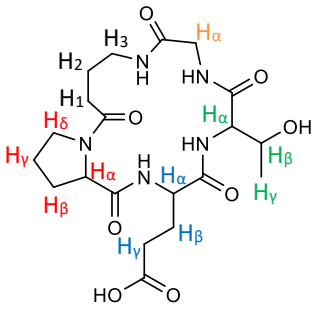
Table 12. Assignment of **148-A**



148-B

Amino Acid	NH	H_α	H_β	H_γ	H_δ
Pro	-	4.21	2.22, 2.19	2.00, 1.84	3.57, 3.56
Glu	8.40	4.19	2.20, 2.15	2.38, 2.32	-
Thr	8.19	4.31	4.27	1.09	-
Gly	8.44	3.88, 3.71	-	-	-
	NH	**H_1**	**H_2**	**H_3**	**H_4**
Linker	8.20	2.43	1.80	1.70	3.18

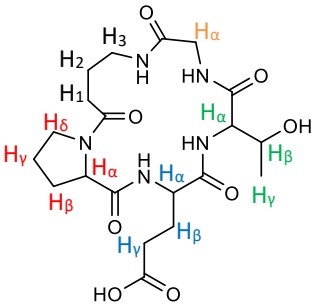
Table 13. Assignment of **148-B**



149b-A

Amino Acid	NH	H_α	H_β	H_γ	H_δ
Pro	-	4.24	2.22, 1.90	1.95, 1.84	3.61, 3.50
Glu	8.06	4.30	2.16, 2.04	2.40, 2.31	-
Thr	8.23	4.14	3.69	1.10	-
Gly	8.31	3.87, 3.72	-	-	-
	NH	**H_1**	**H_2**	**H_3**	-
Linker	7.46	3.28	2.55	3.58	-

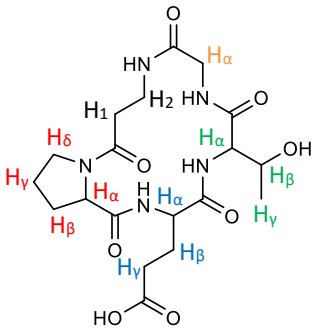
Table 14. Assignment of **149b-A**



149b-B

Amino Acid	NH	H_α	H_β	H_γ	H_δ
Pro	-	4.29	2.17, 1.83	2.34, 2.10	3.52, 3.45
Glu	8.61	4.28	2.22, 2.11	2.39, 2.30	-
Thr	7.79	4.11	3.94	1.19	-
Gly	8.52	3.89, 3.75	-	-	-
	NH	**H_1**	**H_2**	**H_3**	-
Linker	6.82	2.92	2.45	4.06	-

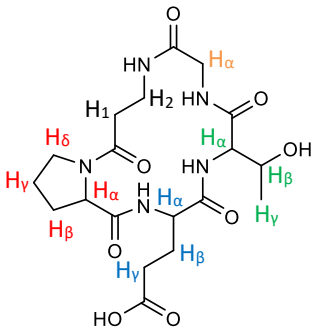
Table 15. Assignment of **149b-B**



149a-A

Amino Acid	NH	H_α	H_β	H_γ	H_δ
Pro	-	4.29	2.19, 1.83	1.92, 1.71	3.67, 3.55
Glu	7.86	4.52	2.15, 1.94	2.32, 2.24	-
Thr	8.04	4.10	3.59	1.10	-
Gly	8.66	4.00, 3.59	-	-	-
	NH	**H_1**	**H_2**	-	-
Linker	7.59	1.54	3.08	-	-

Table 16. Assignment of **149a-A**



149a-B

Amino Acid	NH	H_α	H_β	H_γ	H_δ
Pro	-	4.32	2.24, 1.86	2.08, 1.73	3.65, 3.57
Glu	8.38	4.34	2.07, 2.00	2.37, 2.18	-
Thr	7.99	4.12	3.63	1.09	-
Gly	8.70	4.01, 3.57	-	-	-
	NH	**H_1**	**H_2**	-	-
Linker	7.74	1.46	3.11	-	-

Table 17. Assignment of **149a-B**

Comparison of the chemical shift data between the two compounds present in each NMR spectra is not sufficient evidence to confirm the presence of *cis*/*trans* isomers. There are only minor differences in chemical shifts between the **A** and **B** sets of data in each case and so this data proves inconclusive. However, more information can be inferred from the NOESY spectra (Figure 51). In a NOSEY spectrum of compound **148** there is a cross-peak (circled in green) between the H_α of proline (circled in red) and the H_1 of the linker (circled in yellow) of the major compound **148-A**, showing them to be close in space. However, this cross-peak is not present in the minor compound **148-B**, indicating that the linker in this compound may be positioned in the opposite conformation. This may be evidence that the two compounds present in the NMR spectra for the cyclic compounds are *cis*/*trans* isomers around the proline residue.

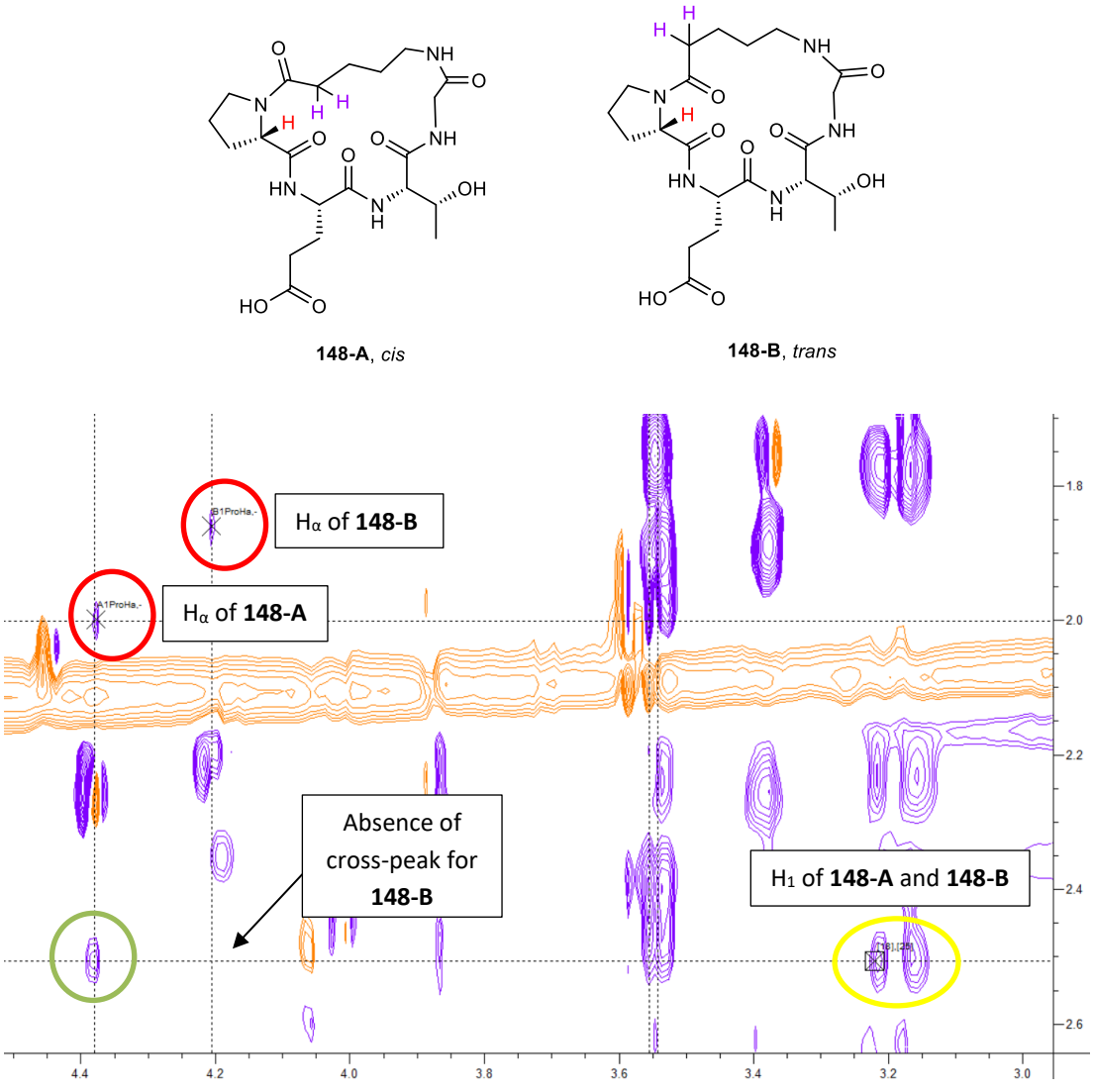


Figure 51. NOESY spectrum of **148**.

3.4 Conclusion

Due to the difficulties that had arisen in the solution phase synthesis of the tripeptide Pro-Glu-Thr (Chapter 2), solid phase synthesis was thought to be another viable option. First attempted was synthesis using on-resin cyclisation *via* the use of a labile linker in the form of a benzotriazole, that had been shown to be successful in the cyclisation of peptides. In the synthesis of this peptide, the capping steps needed to be omitted due to acylation of the aniline that prevents the formation of the active benzotriazole. However, even when the synthesis was repeated, with successful activation, only a minor amount of the desired cyclic peptide was formed.

Due to the insufficient amount of peptide synthesised in the previous method, solid phase synthesis of the linear peptide followed by solution phase cyclisation was attempted. This method used the 2-chlorotrityl chloride resin and an automated synthesiser to construct the linear peptide and then several solution phase cyclisation conditions were used. The main difficulty with this synthesis was not racemisation, but removal of by-products formed in the reaction. By using the coupling reagent DMTMM, and subsequent aqueous work up of the reaction, followed by TFA deprotection and purification, three analogues were isolated all in >90% purity allowing for studies to be conducted on these compounds.

Molecular modelling studies provided an insight into the potential 3D conformations of these peptides. Of the studies conducted it can be predicted that compound **148** may result in the most effective binding of the three peptides due to the most favourable binding interactions and least steric clashes with Keap1. It was also the peptide that most closely matched the conformation of the analogue of the native p62 protein.

Full assignment of each peptide including both the major and minor compounds present in the NMR spectra was completed using data form NOESY and TOCSY experiments. VT NMR experiments were performed on sample **148**, however, the results were inconclusive. Signals in the spectra broadened as the temperature was raised and it was unclear as to whether the signals coalesced or not. Comparison of the chemical shifts between the two compounds present also was unable to provide information as to where the conformational difference might lie. However, NOESY spectrum provided an insight into the possible conformations of the two compounds. A cross-peak between the H_α of proline and the first CH_2 of the linker is present with one of the compounds and not the other, showing that there may be *cis*/*trans* isomerisation around the proline. More work is required to better establish the conformational difference.

4. Macrocyclic Peptides with Heterocyclic Linkers

There are many examples of biologically active structures isolated from nature that consist of cyclic peptides embedded with heterocyclic structures. An example is the natural antibiotic Plantazolicin (Figure 52). It was first isolated from the bacterium *Bacillus amyloliquefaciens* in 2011 and is currently used as an antibacterial treatment against a small number of species, including *Bacillus anthracis*.[151] Introduction of heterocycles into peptides not only increases structural diversity, but also by incorporating linkers that stabilise secondary structures, such as helices, this may lead to improved cellular permeability.[152] By modifying the intramolecular hydrogen bonding network in cyclic peptides, through incorporation of non-natural residues, this may mask the polar surface area, enhancing passive membrane permeability and can also lead to the formation of non-covalent interactions that are important in molecular recognition. These interactions can be classified as hydrogen bonds, cation-π interactions, ion-pair interactions and London dispersion forces. Variation of the heterocyclic moiety can allow for the design of peptides that are selective or have affinities for specific anions, allowing for stronger interactions with the target.[153]

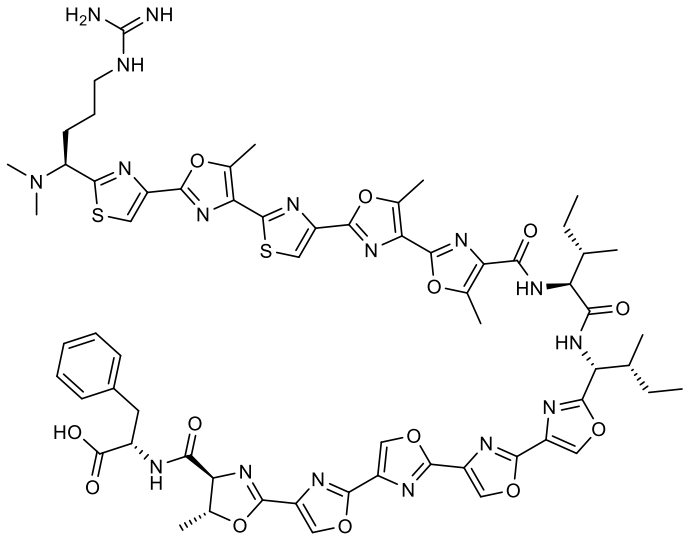
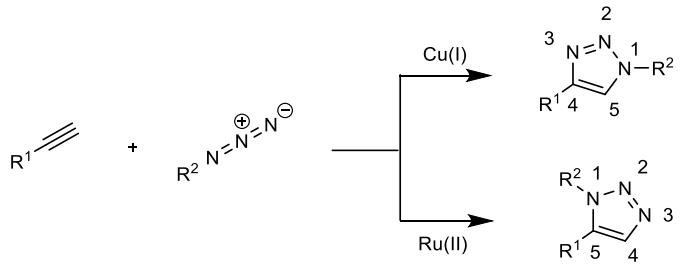


Figure 52. Structure of the antibiotic plantazolicin

4.1 Triazole Linkers

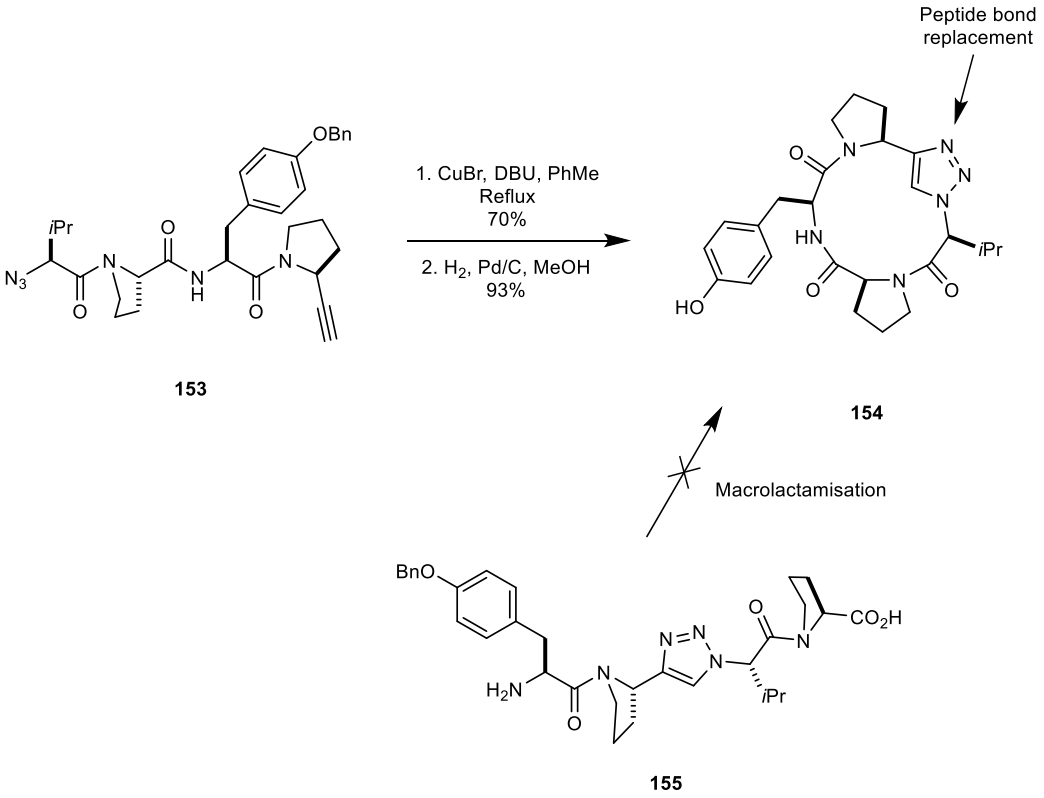
1,2,3-Triazoles are an interesting group in peptidomimetics. They are a class of heterocycles that closely resemble amide bonds, in size, H-bonding capability and planarity, while also being stable to degradation *via* enzymes. The emergence of copper-catalysed azide alkyne cycloaddition (CuAAC) has allowed an improved and selective route to 1,4-substituted triazoles, followed by work in 2005 by Fokin *et al*. that used ruthenium catalysis (RuAAC) for

the synthesis of 1,5-triazoles (Scheme 49).[154] The 1,4- and 1,5-triazoles synthesised can be used as *trans* and *cis* peptide bond mimics respectively.



Scheme 49. Synthesis of 1,4- and 1,5-triazoles using CuAAC and RuAAC

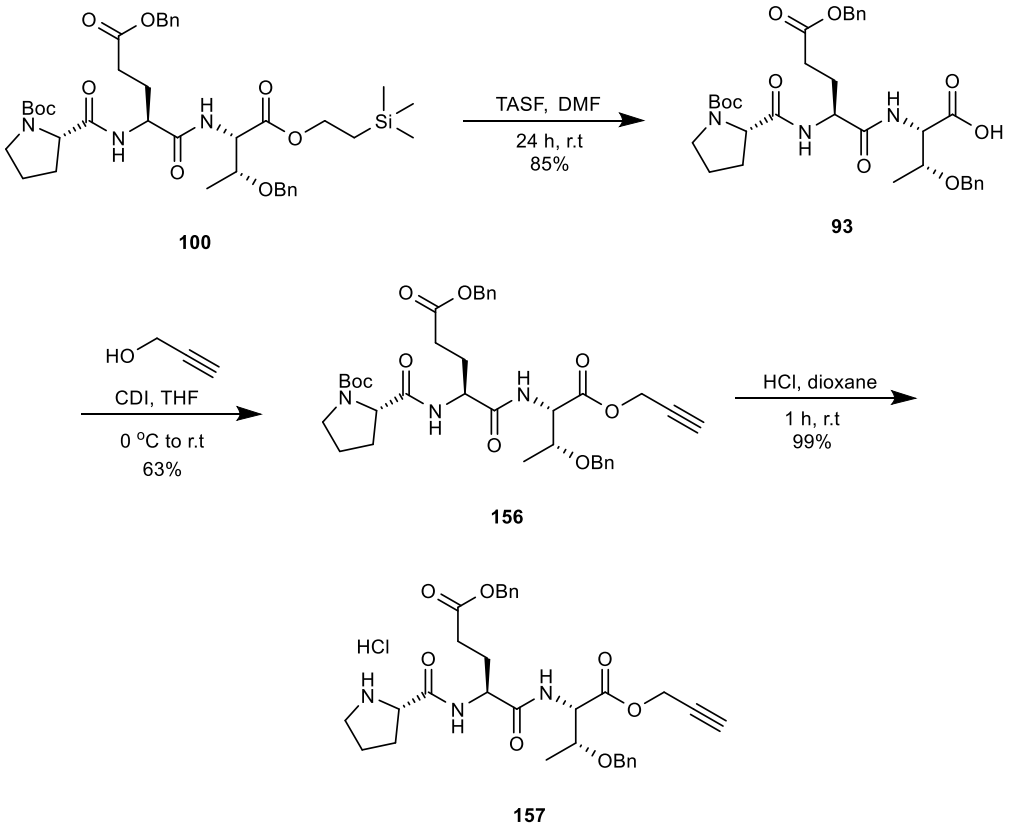
The triazole moiety may be incorporated into the peptide backbone or side chain by the reaction of an acetylene or azido-substituted amino acid and provides a convenient way to access cyclic peptidomimetics. However, one major drawback of this reaction in cyclic peptidomimetics is the formation of cyclo-homodimers, that may account for reported low yields with this reaction. Regardless of this, CuAAC can be used in the formation of otherwise challenging products. An example of this is the synthesis of the highly strained tetrapeptide analogue **154** that cannot be attained *via* lactamisation but can through CuAAC (Scheme 50).[155] Not only was the peptide **154** able to be attained through CuAAC but also proved to be approximately three-fold more potent against mushroom tyrosinase than the natural product it is derived from, signifying that 1,4-triazoles are useful amide bond mimics.



Scheme 50. Literature synthesis of tetrapeptide **154** by CuAAC.[155]

To use CuAAC to perform a head-to-tail cyclisation of our tripeptide Pro-Glu-Thr, initially the acetylene and azide substituted peptide needed to be synthesised. Using the solution phase conditions in Chapter 2, and the Boc/Bn/TMSE protecting group strategy, peptide **100** was successfully synthesised. Removal of the TMSE group from the *C*-terminus with TASF gave compound **93**, and this was reacted with propargyl alcohol and 1,1'-carbonyldiimidazole (CDI) to give ester **156** in 63% yield (Scheme 51). The ester **156** was then Boc deprotected using HCl in dioxane to give **157** in a quantitative yield.

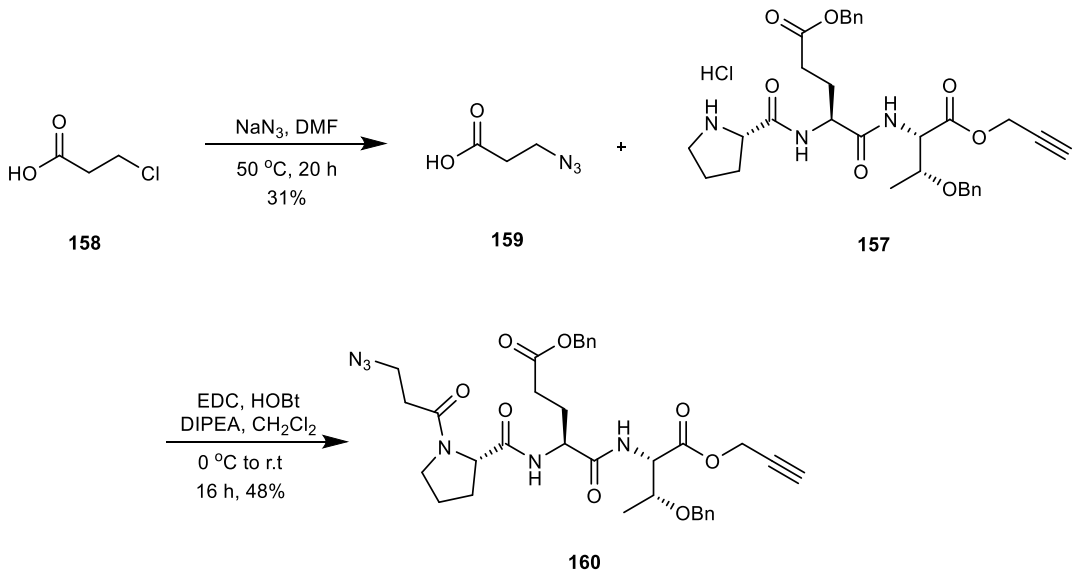
CDI is predominantly used as a coupling reagent for peptide synthesis; however, it can also be used to convert carboxylic acids into esters, ureas, and carbamates.[156] It is a useful alternative reagent to highly toxic phosgene as it possesses similar synthetic utility and exists as a solid. The by-products produced by a reaction of CDI, CO_2 and imidazole, are relatively benign, and the production of the imidazole anion during the reaction often means that a base is not required for the reaction.



100 93 156 157

Scheme 51. Synthesis of ester **157**

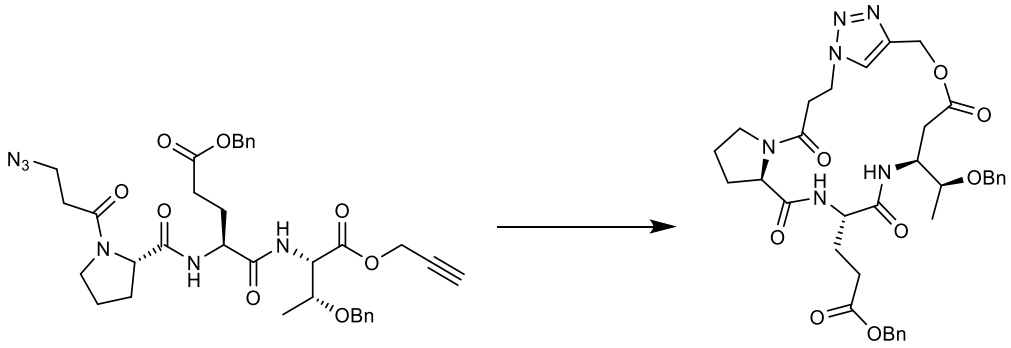
The linker of the peptide was converted into the azide portion of the molecule to react with the alkyne of **157**. 3-Chloropropionic acid **158** was reacted with sodium azide in DMF at 50 °C for 20 h to give **159** in 31% yield (Scheme 52). The azide **159** was then reacted with peptide **157** using EDC as the coupling reagent to give **160** in a 48% yield.



158 159 157 160

Scheme 52. Synthesis of **160**

The copper-catalysed intramolecular azide-alkyne cycloaddition was then attempted on substrate **160** using several different reaction conditions (Table 18). The reaction of copper(I) bromide and DBU with **160** (Table 18, Entry 1) failed to give any desired product **161**. The reaction may have been affected by the purity of the CuBr that has a significant influence over both the reaction rate and completion.[157] It has also been shown that the presence of iodide, bromide, and iodide inhibit CuAAC, with iodide exerting the most detrimental effect.[158] For this reason the copper catalyst used in the reaction was changed to copper(II) sulfate (Table 18, Entry 2 and 3). The most common conditions used for this reaction are aqueous conditions employing $CuSO_4$ and a reducing agent such as sodium ascorbate. A $CuSO_4$/sodium ascorbate system (Table 18, Entry 2) in dichloromethane/water mixture at room temperature did result in the formation of desired product **161**. However, multiple purification methods failed to remove all the copper impurities. Changing the solvent to a *tert*-butanol : water (1:2) mixture (Table 18, Entry 3), improved the yield of the reaction, though unfortunately the product **161** was not isolated pure.[159]

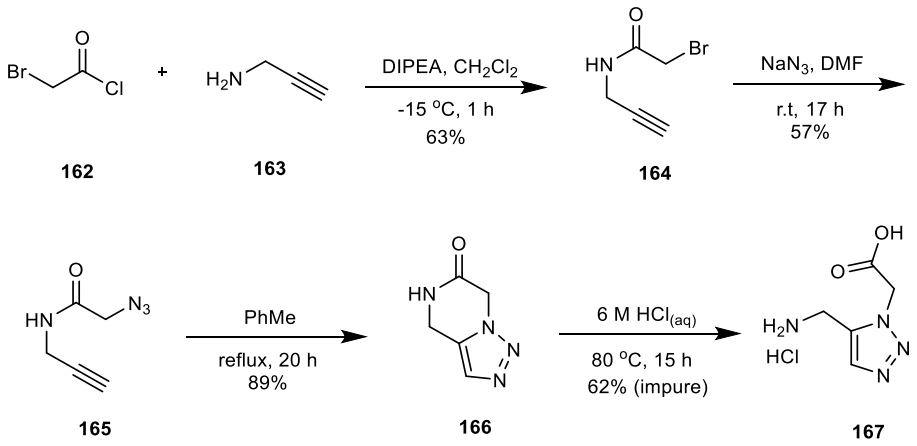


Entry	Reaction Conditions	Outcome
1	CuBr, DBU, PhMe, reflux, 16 h	No product formed
2	$CuSO_4$, sodium ascorbate, CH_2Cl_2, H_2O, 16 h	Could not remove Cu
3	$CuSO_4 \cdot 5H_2O$ sodium ascorbate, ^tBuOH, H_2O, 16 h	Could not remove Cu

Table 18. Reaction conditions for CuAAC

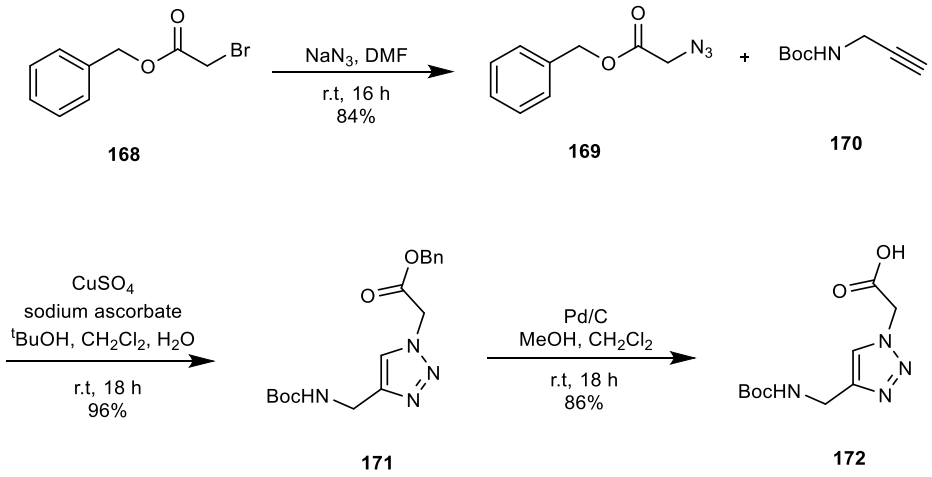
Following on from the difficulties encountered implementing CuAAC as the ring closing step, a second attempt to synthesise the triazole product **161** was to first synthesise the linker and then perform a head-to-tail cyclisation. To do this, two different regioisomers **167** and **172** were synthesised to mimic the geometries of both *cis* and *trans* amide bonds. In 2007, Pokorski *et at*. developed a gram scale route to the 1,5-substitution pattern by utilising a ring-constrained Huisgen cycloaddition.[160] Following the procedure outlined in this work,

acylation of propargyl amine **163** using bromoacetyl chloride **162** at -15 °C gave compound **164** in 63% yield (Scheme 53). The bromoacetamide was then converted into the azide with sodium azide in a 57% yield, and the subsequent Huisgen cycloaddition heated under reflux for 20 h gave the bicyclic triazole **166** in an 89% yield. All steps proceeded without the need for purification. The ring opening step conducted under strongly acidic conditions yielded **167**, however, due to its insolubility, purification proved challenging and protection of the amine using Boc or Fmoc groups resulted in very low yields of desired protected product.



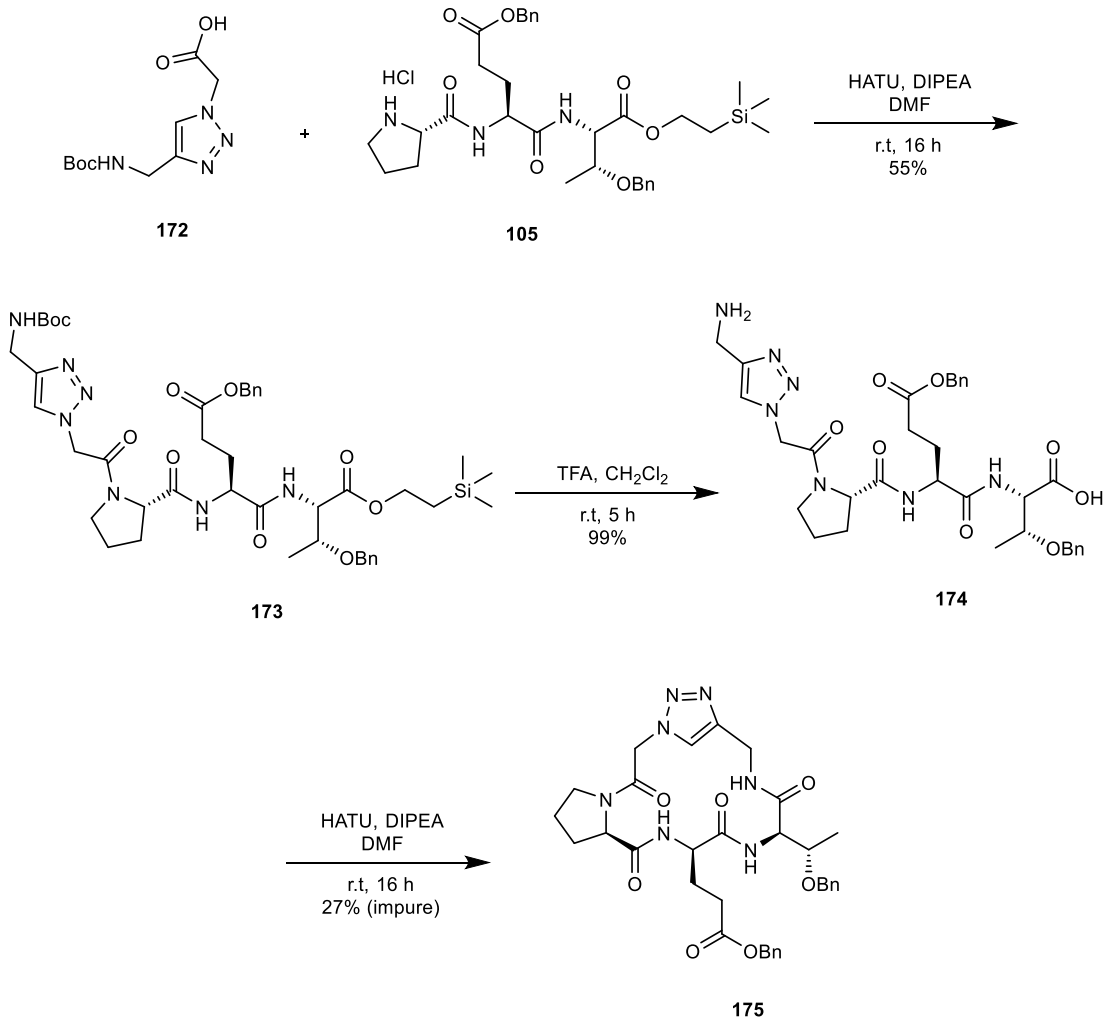
Scheme 53. Synthesis of the 1,5-regioisomer **167**

Pokorski *et at*. also synthesised of the 1,4-regioisomer using a copper-catalysed Huisgen cycloaddition.[160] Following their procedure, with a modification in protecting groups, benzyl bromoacetate **168** was converted into the azide **169** in excellent yield under the previous conditions outlined (Scheme 54). The cycloaddition reaction was performed using copper(II) sulfate and sodium ascorbate in a 1:1:1 mixture of *tert*-butanol, dichloromethane, and water. This reaction gave the fully protected triazole **171** in a 96% yield after purification. Debenzylation of **171** was conducted using 10% Pd/C and after 18 h gave **172** in excellent yield.



Scheme 54. Synthesis of the 1,4-regioisomer **172**

After this deprotection of the acid, **172** was then coupled to the *N*-terminally deprotected peptide **105** using HATU (Scheme 55). This reaction proceeded with moderate yield before both the *N*- and *C*-termini of the peptide were deprotected simultaneously using TFA in dichloromethane to give **174**. The cyclisation step was then attempted using HATU and after 16 h at room temperature, product was seen by both NMR spectroscopy and mass spectrometry. However, as **175** was an extremely polar molecule standard column chromatography conditions were not effective in purification, and so reverse phase preparative HPLC was attempted on the compound. Regrettably, from this only a 27% yield of impure cyclic compound **175** was obtained, with unidentified impurities failed to be removed by both column chromatography and preparative HPLC.



172 105 173 174 175

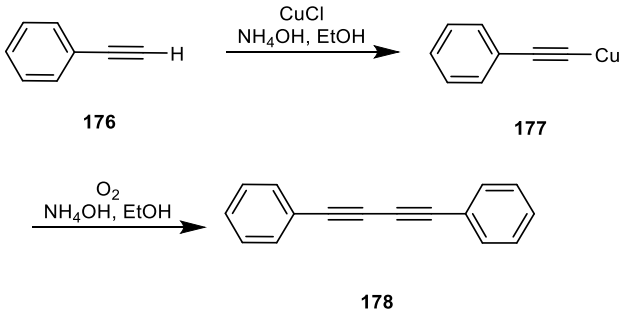
Scheme 55. Coupling of **172** to the peptide and subsequent deprotection

4.2 Cyclisation Through Formation of a Diyne

The most common methods used for peptide macrocyclisation are through the formation of disulfide bridges, lactamisation, ring-closing metathesis or azide-alkyne cycloaddition, all of which have been shown to be highly effective methods in the literature. Even so, there is still a need for methods that afford macrocyclisation under mild conditions and allow for further functionalisation of the introduced macrocyclic tether. Oxidative alkyne-alkyne coupling introduces a 1,3-diyne unit that can be used for post-cyclisation modifications in the peptide. One potential modification is the introduction of peptidomimetic macrocycles, resulting in a variety of cyclic peptides, with potentially differing conformations, from one parent compound.

Glaser reported the first synthesis of symmetrical diynes in 1869, where it was observed that copper(I) phenylacetylide **177** when exposed to air dimerised to diphenyldiacetylene **178**

(Scheme 56).[161] The Glaser coupling was applied to a variety of terminal alkynes and gave the corresponding diynes in moderate yields. Aromatic ethynyl compounds resulted in good yields, though aliphatic alkynes gave unsatisfactory yields.



Scheme 56. Glaser coupling[161]

In order to improve this, several modifications to the Glaser coupling were carried out. In 1956, Eglinton and Galbraith found that the use of excess $Cu(OAc)_2$ in methanolic pyridine accelerated the dimerisation of alkynes.[162] This was followed by Hay in 1962, who showed the certain amines, such as *N*,*N*,*N'*,*N'*-tetramethylethylenediamine **179** (TMEDA, Figure 53), were better ligands for the dimerisation.[163] In this procedure, only a catalytic amount of CuCl was required to achieve good yields of diynes, as better solubility of the Cu(I)-TMEDA complex was believed to improve the reaction rate.

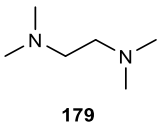
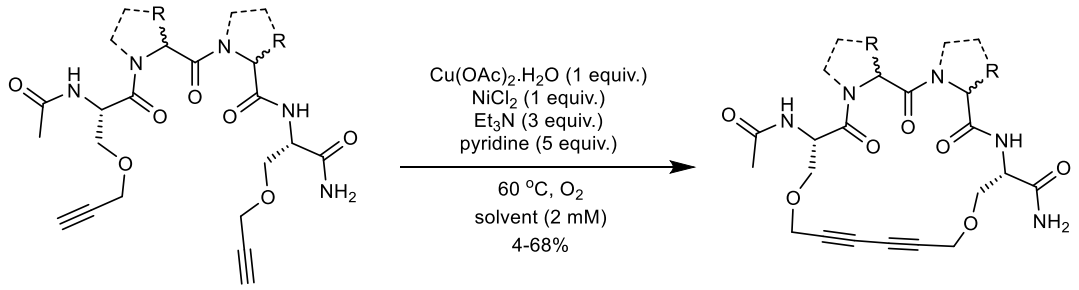


Figure 53. Structure of TMEDA

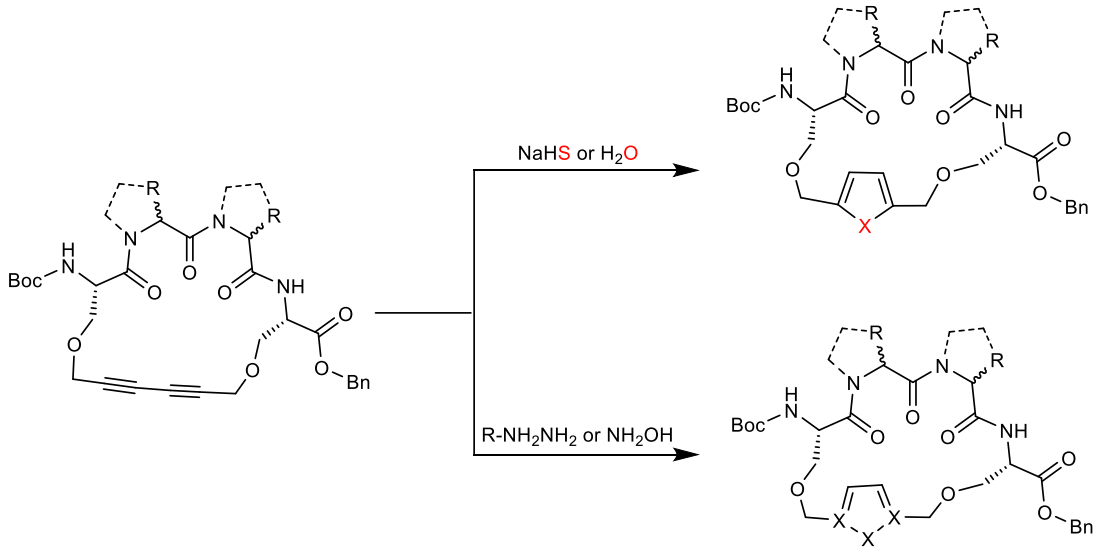
Alkyne-alkyne coupling reactions have been used to construct macrocyclic rings in peptidic applications. Mallet *et al*. reported the synthesis of cyclic peptides using a Glaser-Eglinton reaction between two either *C*- or *N*-propargylglycine residues, leading to cyclic hexa- and octa-peptides constrained with a butadiyne bridge.[164] The reactions were performed on a solid support and under microwave activation for each peptide, and then the three dimensional structure of the peptides were analysed by NMR spectroscopy and molecular mechanics. In this study, it was shown that 1,3-butadiene cyclisation expands the range of constrained peptides and can be successfully incorporated into peptides to stabilise secondary structures.

In 2015, Verlinden *et al*. used Glaser-Hay diyne coupling to synthesise a variety of tetrapeptide-based macrocyclic 1,3-diynes from *O*-propargylated serine and tyrosine residues.[165] After trialling over 50 reaction conditions, the most effective cyclisation conditions were shown to use $Cu(OAc)_2 \cdot H_2O$ and $NiCl_2$ as a co-catalyst which improved yields and reduced reaction times. In addition, triethylamine was used as a base (3 equiv.) and pyridine as a ligand (5 equiv.) at 60 °C under an O_2 atmosphere (Scheme 57). Tetrapeptides synthesised included *N*-methylated amino acids and less hydrophobic residues such as glutamic acid and lysine. Corresponding macrocycles were obtained efficiently with low to moderate yields.



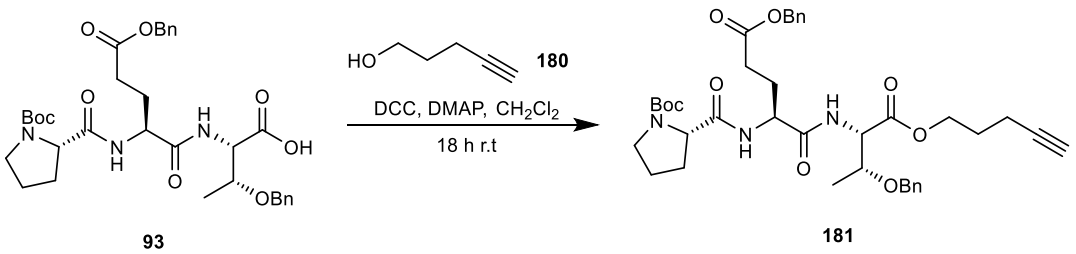
Scheme 57. Oxidative diyne macrocyclisation[165]

Following on from this work, Verlinden *et al*. then successfully showed that the 1,3-diyne could be used as a handle to introduce heterocycles into the macrocyclic structure.[166] Various heterocycles were synthesised using this method including thiophene, furan, pyrazole, and isoxazole, under mild conditions. The 1,3-diynes were transformed into various heterocycles through nucleophilic attack upon treatment with NaHS or H_2O to yield thiophenes and furans or use of hydrazines and hydroxylamine gave rise to pyrazole and isoxazoles (Scheme 58).



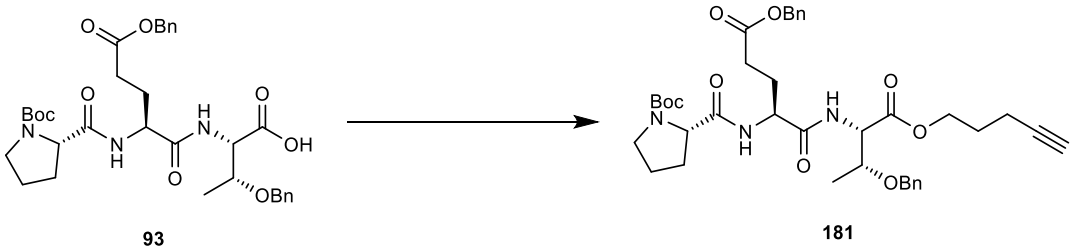
Scheme 58. Synthesis of heterocycles. When using hydrazines and hydroxylamines, a mixture of regioisomers was obtained. R = *D*-Pro, *D*-Ala, *L*-Pro, *L*-Ala[166]

To apply this method to the peptide used in this project, both the *C*- and *N*-termini of the peptide were propargylated. Initial techniques to add an alkyne residue to the *C*-terminus involved coupling of 4-pentyn-1-ol **180** to the *C*-terminally deprotected tripeptide **93** using DCC and DMAP in dichloromethane in a Steglich esterification (Scheme 59).[167] The addition of DMAP in catalytic amounts helps to reduce the amount of *N*-acylurea formation by creating an acyl pyridinium species that is incapable of intramolecular by-product formation. However, purification of **181** proved difficult as traces of the dicyclohexylurea by-product of DCC were still present after both filtration of the reaction mixture and column chromatography.



Scheme 59. Synthesis of **181**

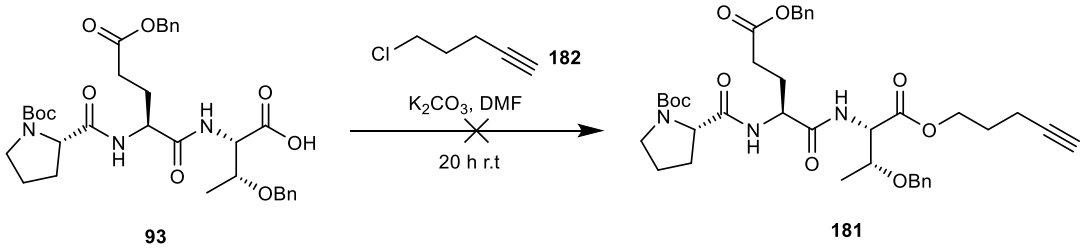
The reaction was repeated using EDC in place of DCC (Table 19, Entry 1). EDC and its by-product are water-soluble and therefore removed during the aqueous work-up, though in this case the esterification proved to be low yielding. Addition of HOBt (Table 19, Entry 2), which is once again used to supress the formation of *N*-acylurea, improved the yield of the reaction slightly, but not to a desirable level.



Entry	Reaction Conditions	Outcome
1	**180**, EDCI, DMAP, CH_2Cl_2, 0 °C to r.t	<3% yield
2	**180**, EDCI, HOBt, DMAP, CH_2Cl_2, 0 °C to r.t	<5% yield

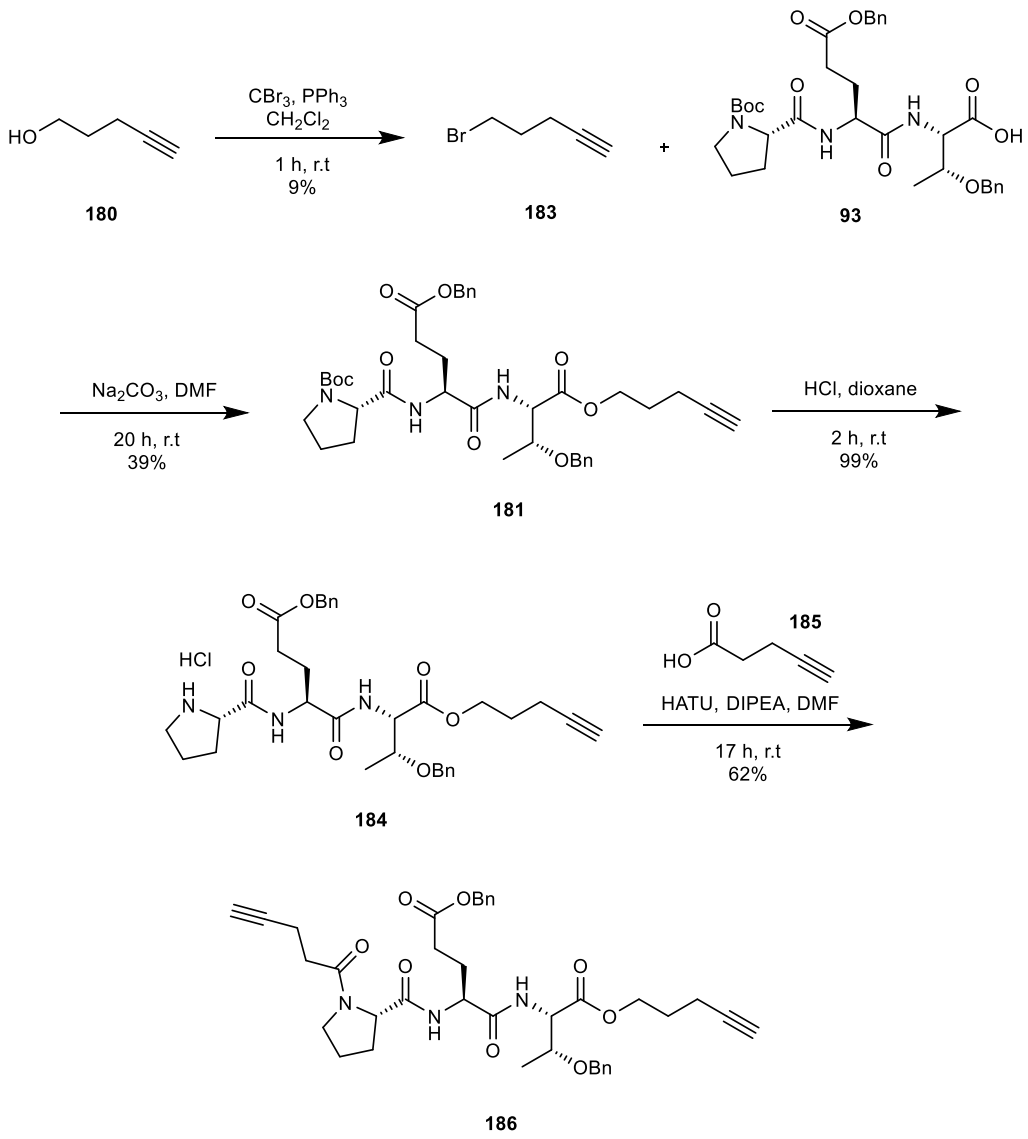
Table 19. Conditions for esterification of **93**

Following on from the issues encountered when using carbodiimides for the esterification reaction, alkylation of the peptide using 5-chloro-1-pentyne **182** was then attempted (Scheme 60). However, only a small amount of product **181** was isolated from the reaction with the majority of the material recovered being starting material **93**.



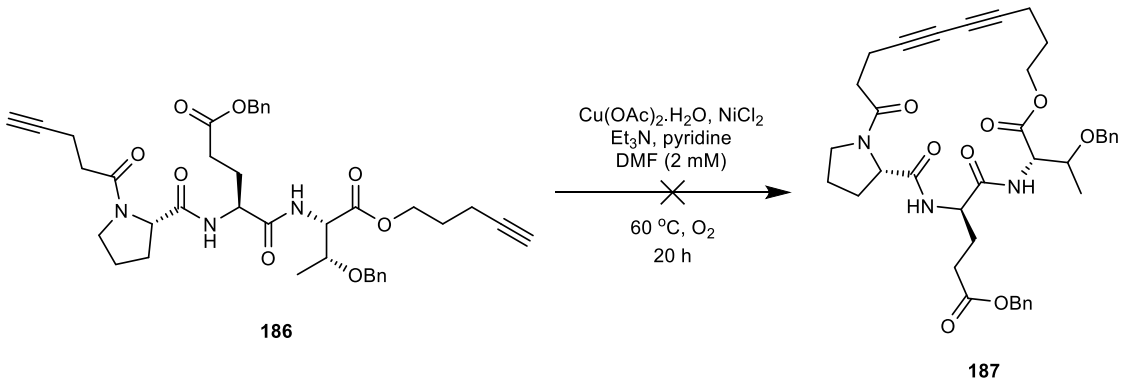
Scheme 60. Synthesis of **181**

Changing the alkylating reagent to 5-bromo-1-pentyne **183** increased the reactivity of the alkylating reagent from the chloro compound **182**, though **183** first needed to be synthesised from 4-pentyn-1-ol **180** (Scheme 61). Using triphenylphosphine and carbon tetrabromide, **180** was converted into the alkyl bromide **183** in an Appel reaction.[168] This compound was then reacted with the peptide **93** under basic conditions, and gave **181** in a 39% yield, and subsequent Boc deprotection using HCl in dioxane allowed for coupling on the *N*-terminal (Scheme 61). Reaction of 4-pentynoic acid **185** with the peptide **184** using HATU gave the diyne compound **186** in 62% yield.



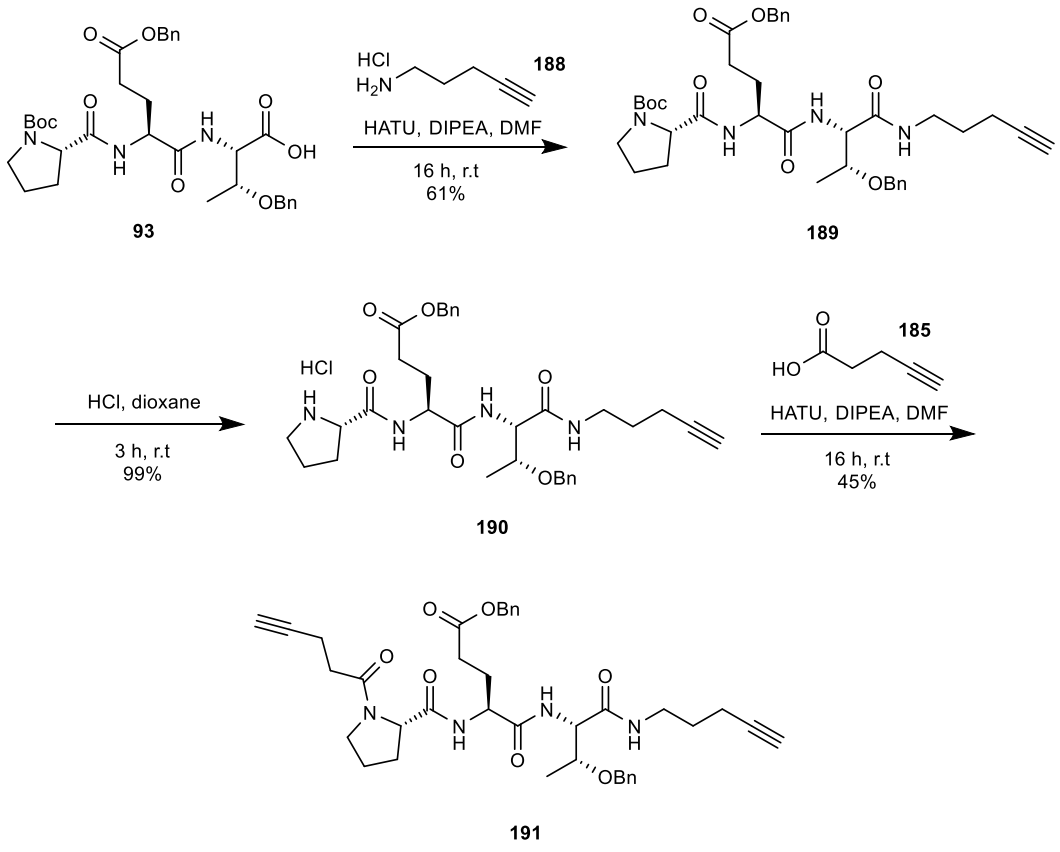
Scheme 61. Synthesis of the diyne compound **186**

The peptide **186** was then subjected to the Glaser-Hay diyne coupling conditions used by Verlinden *et al*. (Scheme 62). DMF was used as the solvent for the reaction as opposed to ethanol due to the solubility of the peptide and the reaction was conducted at a 2 mM concentration. However, after 20 h heating to 60 °C, no product was isolated and significantly, no starting material was isolated, suggesting possible degradation of the starting material may have occurred during the reaction.



Scheme 62. Glaser-Hay diyne coupling

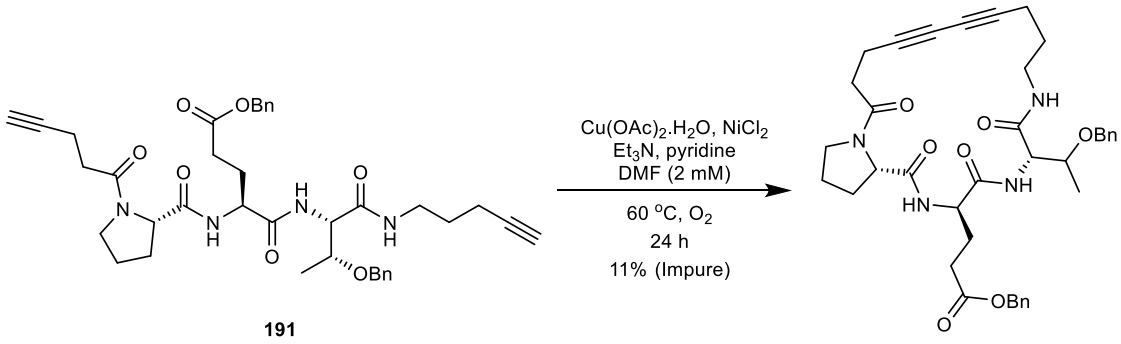
Due to this possible degradation, the corresponding amide analogue of the ester **186** was then synthesised. 4-Pentyn-1-amine hydrochloride **188** was reacted with peptide **93** in a HATU coupling reaction, followed by Boc deprotection and subsequent coupling to 4-pentynoic acid **185** to give peptide **191** in a 27% yield over the three steps (Scheme 63).



Scheme 63. Synthesis of the amide analogue **191**

The cyclisation reaction was then attempted on **191** (Scheme 64). The reaction was shown to be successful by mass spectrometry, although purification of the cyclic compound proved difficult. Upon attempting purification with both column chromatography and preparative

HPLC, copper salts from the reaction mixture co-eluted with the highly polar diyne tethered cyclic peptide **192**. A chelating agent, trisodium phosphate (Na_3PO_4), was used by Verlinden *et al*. to remove the copper salts prior to purification, enabling isolation of their peptides as white solids.[165] However, when these conditions were used to improve purity of **192**, a number of unidentified impurities still remained after purification by column chromatography, resulting in a crude yield of 11%. Although the ^{13}C NMR of **192** contained impurities, disappearance of the terminal alkyne CH groups was seen in the crude spectra of the product, indicating lack of starting material **191** and the possible formation of the cyclic diyne. The mass ion of the product **192** was also seen in the mass spectrum.



Scheme 64. Cyclisation of **191** using Glaser-Hay coupling conditions

Due to low yields and difficulties with purification in the diyne reaction, attention was focused on other methods of cyclisation.

4.3 Cyclisation Through Formation of an Oxadiazole

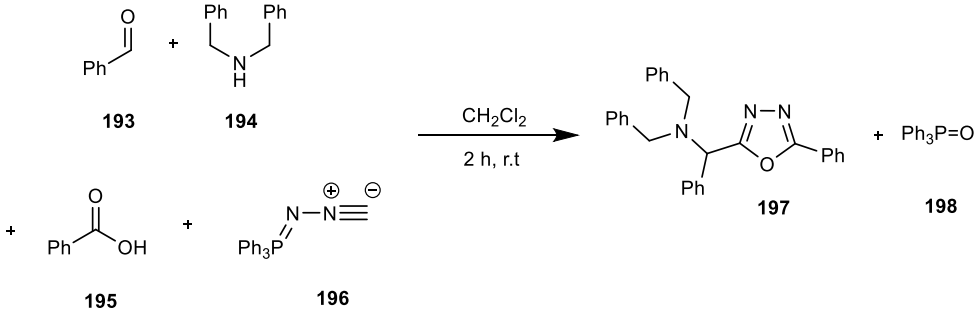
Oxadiazoles are a class of heterocyclic compounds that have been widely used in the search for new therapeutics. Of the four possible isomers, the 1,3,4-oxadiazole most frequently appears in drug molecules and has shown a wide range of properties including antibacterial, antimalarial and anti-inflammatory characteristics (Figure 54)[169–171]



Figure 54. Structure of 1,3,4-oxadiazole

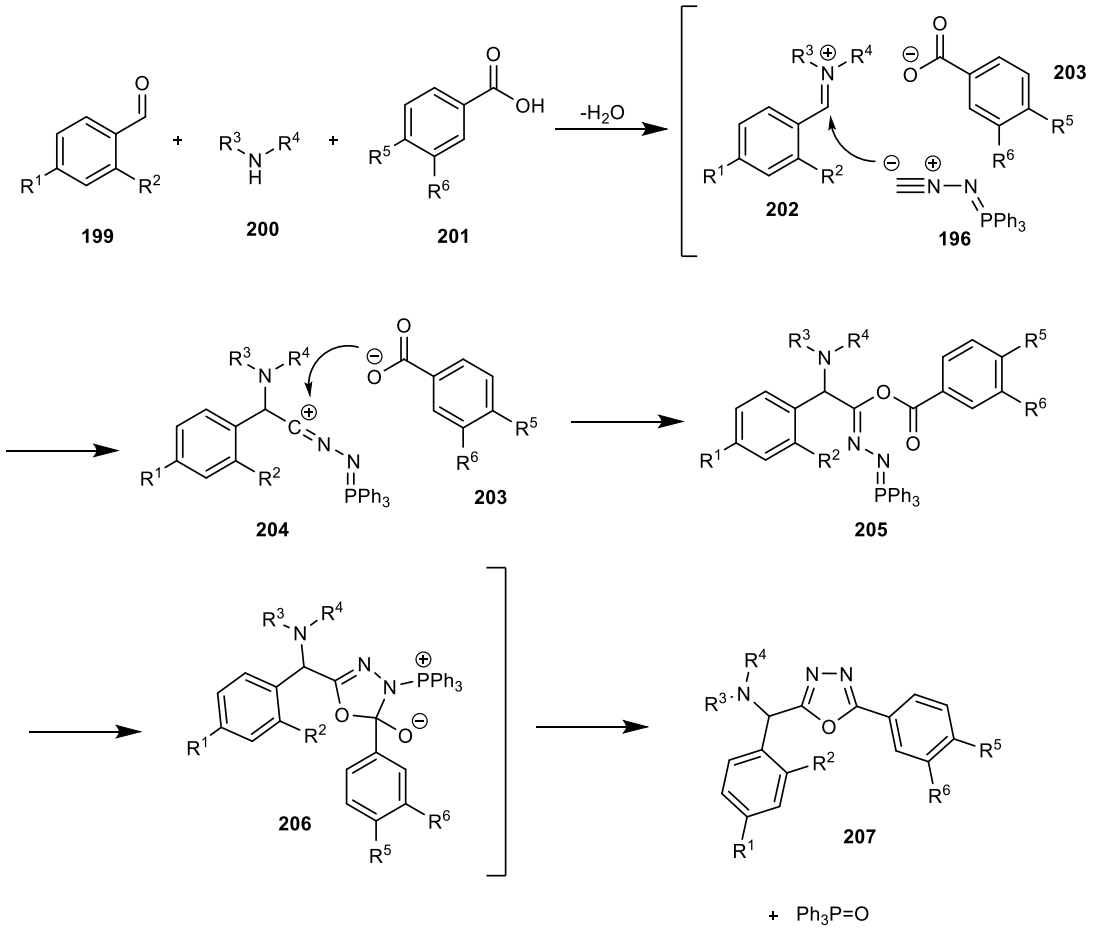
There have been a number of methods reported in the literature for the synthesis of 1,3,4-oxadiazoles, however, the majority of these methods are multi-step and often require harsh reaction conditions.[172,173] In 2010, Ramazani *et al*. reported an efficient synthesis of

2,5-disubstituted 1,3,4-oxadiazole derivatives using (*N*-isocyanimino)triphenylphosphorane **196**, a secondary amine, a carboxylic acid, and aromatic aldehyde, without the need for catalyst or activation (Scheme 65).[174] (*N*-Isocyanimino)phosphoranes, such as **196**, are bench stable reagents that incorporate both a nucleophilic amino group and an isocyanide into a single species and are important reagents in synthetic chemistry.



Scheme 65. Synthesis of 2,5-disubstituted 1,3,4-oxadiazole derivatives[174]

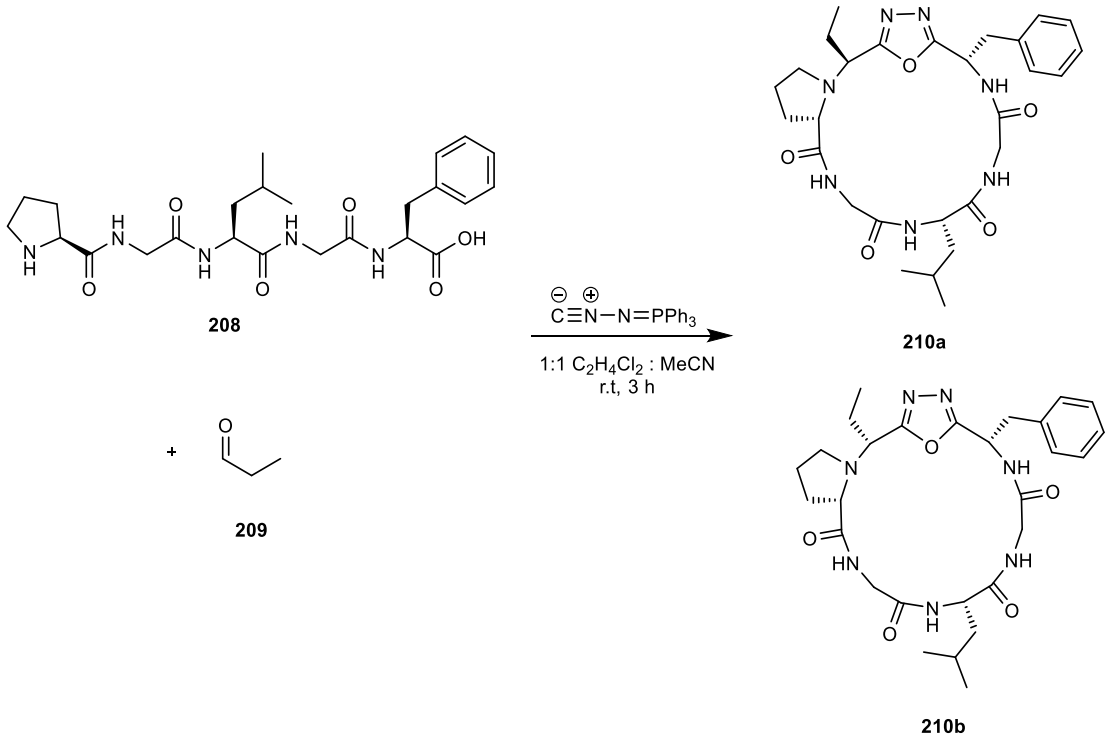
This synthesis of 1,3,4-oxadiazoles by a multicomponent reaction is followed by an *aza*-Wittig cyclisation, generating several derivatives in both high yield and purity. The proposed mechanism proceeds *via* the formation of an intermediate iminium ion **202** from the condensation of benzaldehyde **199**, secondary amine **200**, and the carboxylic acid **201** (Scheme 66). Nucleophilic addition of (*N*-isocyanimino)triphenylphosphorane **196** to **202** gives the nitrilium intermediate **204**, that may be attacked by the conjugate base of **201** to give adduct **205**. This then undergoes an intramolecular *aza*-Wittig cyclisation to give **207** with removal of triphenylphosphine oxide as the by-product.



Scheme 66. Potential mechanism for formation of 1,3,4-oxadiazole derivatives[174]

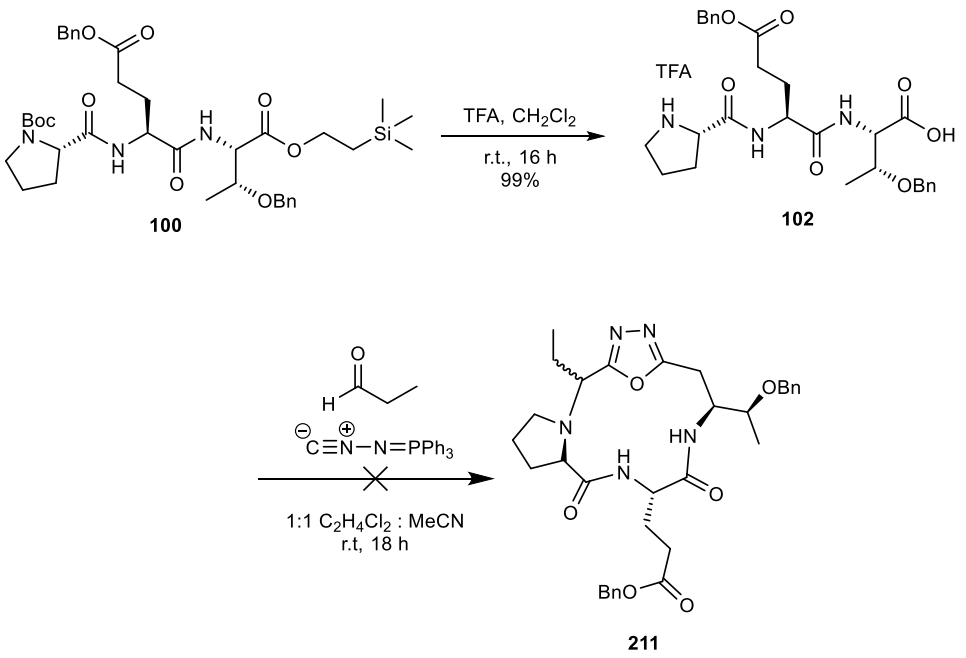
Due to the neutral ring closing conditions and variety of potential reagents this approach has been used in the synthesis of various 2,5-disubstituted 1,3,4-oxadiazole derivatives. In 2016, Frost *et al*. used (*N*-isocyanimino)triphenylphosphorane **196** in reactions of linear peptides and aldehydes to form peptide macrocycles *via* generation of a 1,3,4-oxadiazole in the peptide backbone.[175] One example of these reactions involves the reaction of the linear pentapeptide Pro-Gly-Leu-Gly-Phe **208** with propionaldehyde **209** and (*N*-isocyanimino)triphenylphosphorane in a 1:1 mixture of dichloroethane and acetonitrile (Scheme 67). This solvent mixture was shown to be most suitable for solubility of each of the three components. Completion of the reaction occurred after 3 h at room temperature and the target macrocycle **210** was isolated in a 2:1 mixture of diastereomers and were separated by reverse-phase chromatography. The substrate scope of this reaction was then expanded to include a variety of amino acids without the presence of proline at the *N*-terminus, as well as different sequence lengths containing four, six and seven residues. The aldehyde component of the reaction was also varied to include phenylacetaldehyde and isovaleraldehyde to mimic the side chain of amino acids. Therefore, this could potentially be

used to improve engagement with a biological target, in comparable yields to that of propionaldehyde.



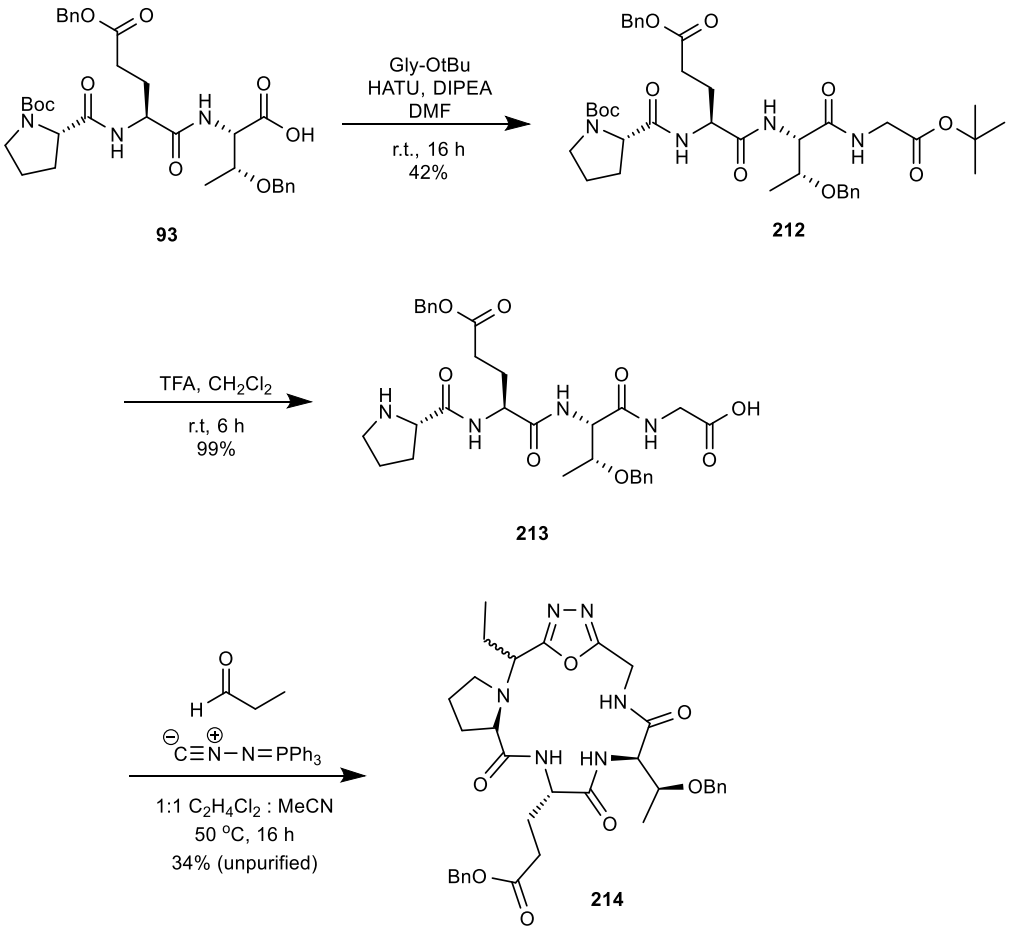
Scheme 67. Cyclisation of PGLGF **208** with propionaldehyde **209** [175]

These reaction conditions were then used to attempt to cyclise our tripeptide Pro-Glu-Thr. The tripeptide **100** was first deprotected using trifluoroacetic acid to give **102** and cyclisation was performed with propionaldehyde and (*N*-isocyanimino)triphenylphosphorane in dichloroethane and acetonitrile mixture (Scheme 68). No product was formed after 16 h so the reaction was heated to 50 °C, however, once again no desired product **211** was observed by mass spectrometry or NMR spectroscopy .



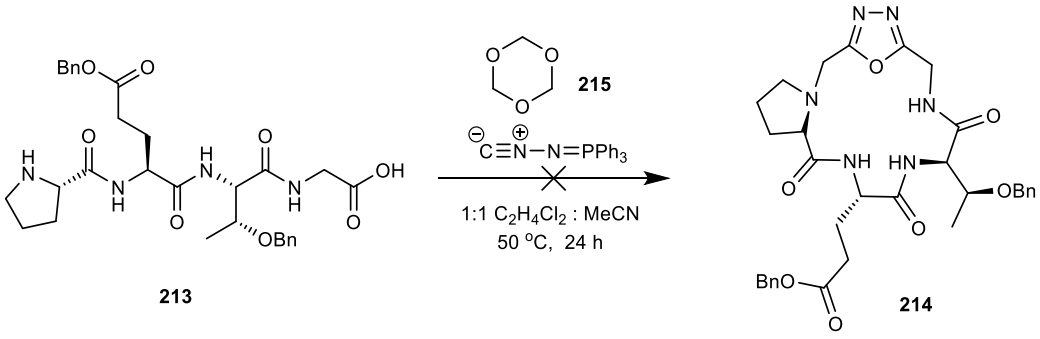
Scheme 68. Attempted cyclisation to form **211**

Cyclisation of the tripeptide **102** failed to result in any desired product possibly because the ring being formed was too constrained, thus disfavouring the cyclisation. The smallest amino acid sequence successfully cyclised with these conditions by Frost *et al*. was a tetrapeptide. Therefore, the same conditions were trialled on the tetrapeptide Pro-Glu-Thr-Gly, through the addition of glycine on to the *C*-terminal, as it is the next amino acid in the native peptide sequence of p62. Gly-O^{t}Bu was coupled to the tripeptide **93** using HATU giving the tetrapeptide **212** in a 42% yield (Scheme 69). This peptide was then deprotected using trifluoroacetic acid in dichloromethane, washed with a sodium hydrogen carbonate solution to remove the TFA salt and reacted on using the previous conditions to give the cyclic product **214** in moderate crude yield. However, removal of the triphenylphosphine oxide by-product proved difficult and so the cyclic peptide **214** was not isolated pure. Formation of product failed upon repetition of this reaction and so other related reaction conditions were trialled.



Scheme 69. Tetrapeptide cyclisation

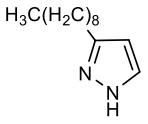
As well as using propionaldehyde in the cyclisation of the tetrapeptide **213**, 1,3,5-trioxane was also used. 1,3,5-Trioxane **215** provides an anhydrous source of formaldehyde, and so under these conditions would introduce formaldehyde into the peptide, avoiding the formation of another chiral centre in the molecule. Unfortunately, when these conditions by Frost *et al*. were attempted no product was isolated from the reaction (Scheme 70).



Scheme 70. Cyclisation of **213** using 1,3,5-trioxane

4.4 Pyrazole Linkers

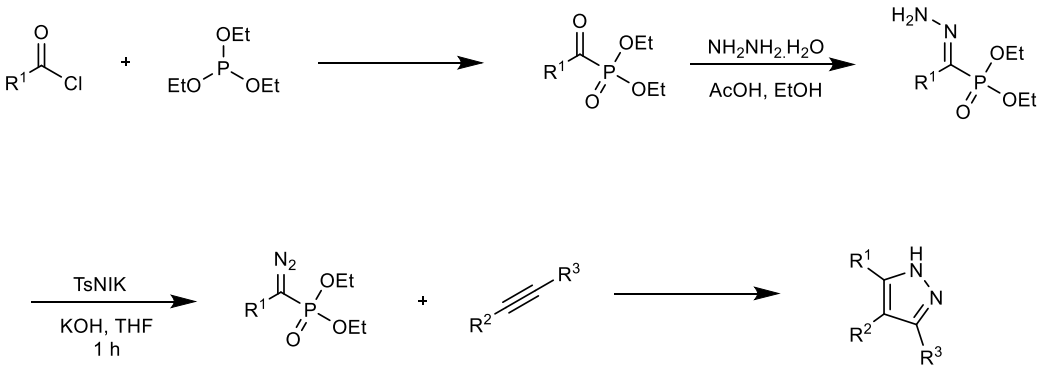
Pyrazoles are aromatic heterocycles consisting of a five-membered ring with two adjacent nitrogen atoms. The first pyrazole isolated from nature was 3-nonyl-1*H*-pyrazole **216** from the plant *Houttuynia cordata* found in tropical Asia (Figure 55). Though pyrazoles are not widespread in nature, a large number of pyrazoles have been synthesised and approved for use not only in drug molecules, but also food colouring and agrochemicals.[176]



216

Figure 55. Structure of 3-nonyl-1*H*-pyrazole

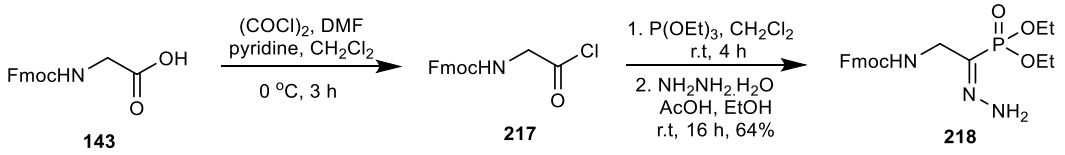
In this project, the pyrazole analogue of the cyclic peptide aimed to be comparable to the triazole linker previously discussed. The synthesis of this linker was based on work published in the group in 2014, using the oxidising reagent *N*-iodo *p*-toluenesulfonamide (TsNIK) that was shown to successfully generate diazo compounds from hydrazones.[177] These diazo compounds are then used in a 1,3-dipolar cycloaddition onto alkynes to yield pyrazoles (Scheme 71). Detail on this approach for the synthesis of pyrazoles is discussed in Chapter 5.



Scheme 71. Synthesis of pyrazoles

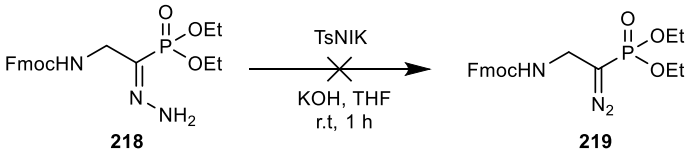
In this approach, the initial starting material used for synthesis of a hydrazone was Fmoc-Gly **143**. The commercially available acid **143** was converted into the acid chloride using oxalyl chloride, DMF and pyridine in dichloromethane at 0 °C (Scheme 72). Completion of the reaction was monitored by IR spectroscopy for disappearance of the OH peak of the acid, and after 3 h, the acid chloride **217** was reacted on without purification. Addition of triethyl phosphite to **217** was first attempted as a solvent-free reaction. However, insolubility of **217** and the requirement of the addition of one equivalent of triethyl phosphite to prevent

formation of the bisphosphonate, meant that the reaction was repeated with the addition of anhydrous dichloromethane. The formation of the α-ketophosphonate was followed by mass spectrometry and after completion of the reaction, it was added to a solution containing hydrazine hydrate. The hydrazone **218** was isolated after purification as a colourless solid in a 64% yield.



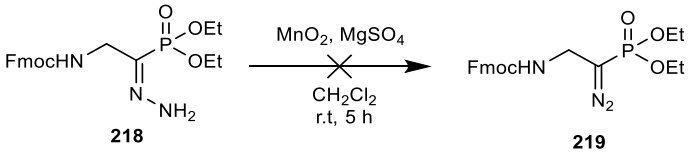
Scheme 72. Synthesis of hydrazone **218**

Oxidation of the hydrazone **218** to the diazo compound **219** was then attempted using the reagent TsNIK (Scheme 73). However, the reaction failed to yield any diazo compound or isolate any starting material. This unsuccessful oxidation may be due to the use of KOH in the reaction. The presence of this base may have cleaved the Fmoc group from glycine, resulting in degradation of the free amine molecule.



Scheme 73. Attempted oxidation of **218** to its diazo compound

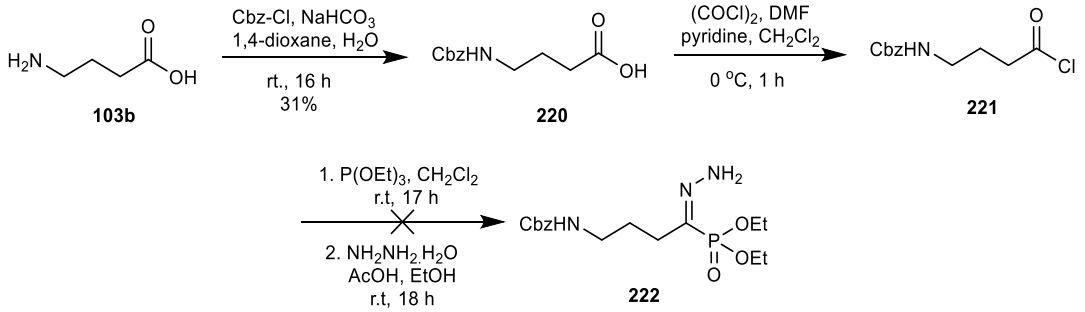
A second method of oxidation was trialled on **218** using MnO_2 and $MgSO_4$ in dichloromethane (Scheme 74).[178] Once again, no product or starting material were isolated from the reaction mixture.



Scheme 74. Attempted oxidation of **218** using MnO_2

Another strategy was to change both the protecting group and the starting material. The Cbz group is a base stable protecting group and is typically removed using hydrogenolysis. In this case, γ-aminobutyric acid **103b** was used as the starting material and was Cbz protected under basic conditions with benzyl chloroformate to give **220** in 31% yield (Scheme 75). The

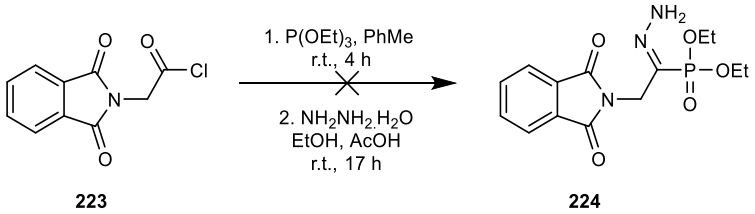
acid chloride **221** was then synthesised using oxalyl chloride, before reacting on with triethylphosphite, followed by hydrazine hydrate to give the hydrazone **222**. However, upon work-up of the reaction, no product or starting material was isolated. The acid chloride reaction was monitored by IR and so this reaction was thought to have reached completion, and generation of the mass ion for the α-ketophosphonate was also shown to be present in the mass spectrum. Nevertheless, the reaction to form the hydrazone **222** was ineffective.



103b **220** **221** **222**

Scheme 75. Synthesis of **222**

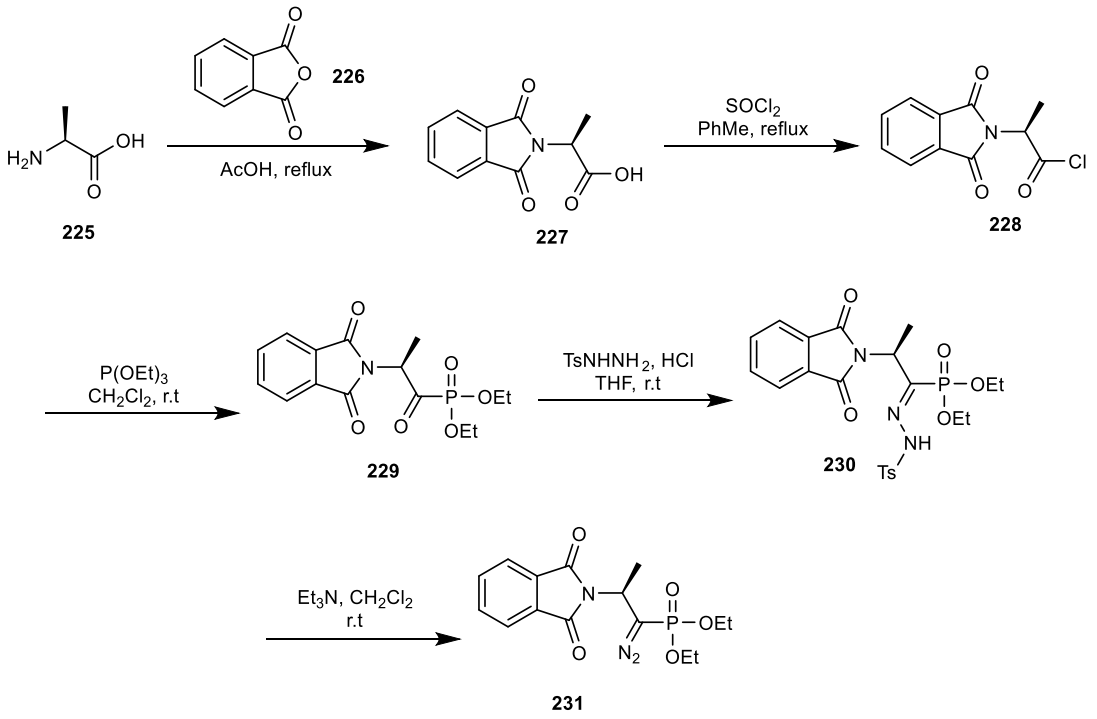
Due to issues encountered while using the Fmoc and Cbz protecting groups, it was decided to change the protecting group on the nitrogen to a phthaloyl group. Particularly in peptide synthesis, phthaloyl groups are beneficial as they block both hydrogens on the primary amine and can therefore be effective in preventing racemisation. In this case it would improve stability of the linker. Phthalylglycyl chloride **223** is a commercially available reagent used in the synthesis of the pyrazole linker. Phthalylglycyl chloride **223** was first reacted with triethylphosphite and was then used to form the hydrazone **224** (Scheme 76). However, difficulties with solubility of the starting material **223** hindered the formation of the α-ketophosphonate, thereby also preventing formation of the hydrazone. Addition of toluene to the initial reaction was shown to improve solubility of phthalylglycyl chloride and consequently production of the intermediary α-ketophosphonate.[179] In spite of this, formation of the hydrazone **224** also proved problematic. The use of hydrazine is one of the major methods through which phthaloyl groups are removed and so in this case also led to deprotection of the primary amine, and subsequent degradation of material.



223 **224**

Scheme 76. Synthesis using the phthaloyl group

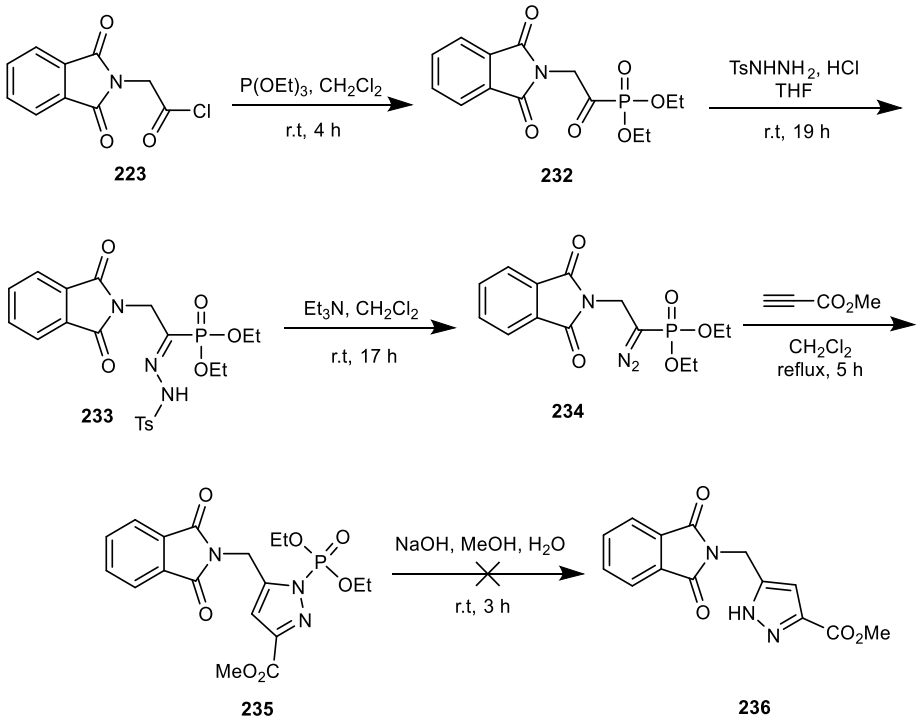
In 2013, Cai *et al*. developed a method for the synthesis of α-diazophosphonyl compounds derived from amino acids.[180] A number of amino acids were used as examples in this synthesis including *L*-alanine (Scheme 77). The first step in the synthesis was condensation of *L*-alanine **225** with phthalic anhydride **226** in acetic acid and heated under reflux, proceeded by formation of the corresponding acid chloride using thionyl chloride. The Arbuzov reaction followed, forming the α-ketophosphonate **229** that was then converted to the tosylhydrazone phosphonate **230** using *p*-toluene sulfonohydrazide at room temperature. Formation of the desired α-diazophosphonyl compound **231** was performed *via* elimination from **230** using triethylamine in an overall reported 42% yield.[180]



Scheme 77. Synthesis of α-diazophosphonyl compounds[180]

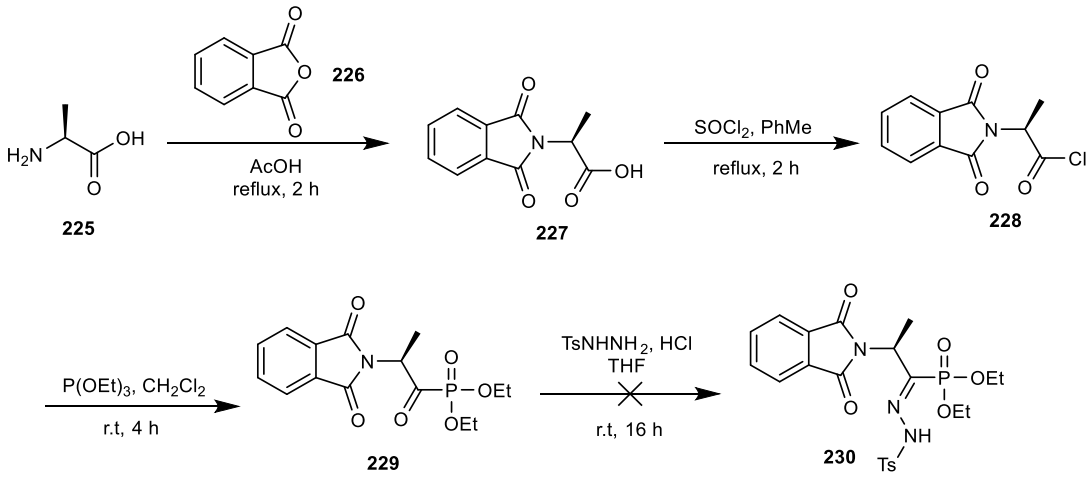
Using phthalylglycyl chloride **223** as the starting point with the conditions demonstrated by Cai *et al*., formation of **232** at room temperature in dichloromethane was shown to be successful by mass spectrometry (Scheme 78). Synthesis of the tosylhydrazone phosphonate **233** also proceeded well, and was once again reacted on without purification to give the diazo compound **234**, which was then immediately reacted on with methyl propiolate in dichloromethane, heated to reflux for 5 h. Formation of the phosphorylated pyrazole **235** was shown by mass spectrometry, and so to hydrolyse this compound to **236**, NaOH in aqueous methanol was used. However, upon hydrolysis none of the pyrazole compound **236** was isolated. The phthaloyl group may have also been removed under the basic hydrolysis

conditions, though, the pyrazole should have been stable enough to avoid degradation, even with removal of the phthaloyl group. Synthesis of the α-diazophosphonyl compound **234** was attempted on a larger scale, but formation and isolation of **234** could not be repeated.



Scheme 78. Attempted synthesis of the α-diazophosphonyl compound **234** and subsequent pyrazole formation

As difficulties occurred in the formation of the glycine analogue of the conditions introduced by Cai *et al*., synthesis of the alanine equivalent that was shown to be successful in their publication was then attempted. The *N*-terminal of *L*-alanine was first protected using phthalic anhydride **226** under reflux for 2 h (Scheme 79). The acid chloride was synthesised using thionyl chloride again under reflux for 2 h, before using triethylphosphite in dichloromethane to form the α-ketophosphonate **229**. *p*-Toluene sulfonohydrazide converted **229** into the tosylhydrazone phosphonate **230** after 16 h at room temperature, before forming the diazo compound **231** after 16 h. All reactions were performed without any purification steps and monitored by both TLC and mass spectrometry, however, formation of the tosylhydrazone phosphonate compound **230** failed and therefore was not isolated.



Scheme 79. Synthesis of the alanine analogue of **230**

As the hydrazone **230** was not synthesised, the reaction mixture was analysed by mass spectrometry, and the major component was shown to be the bisphosphonate compound **237** (Figure 56). Formation of this compound prevented reaction of *p*-toluene sulfonohydrazide, and consequently synthesis of the desired **230**. Due to time constraints on this project, repetition of this reaction and investigation into the formation of the bisphosphonate was not conducted and provides future work that needs to be undertaken on the formation of this linker.

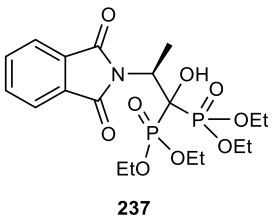


Figure 56. Structure of the bisphosphonate

4.5 Conclusion

In this Chapter a number of different heterocyclic rings were shown as potential linkers for the cyclic peptide Pro-Glu-Thr and all syntheses were based on literature precedent. Synthetic peptides that include heterocycles provide several advantages over peptide drugs alone, including improved pharmacological properties, metabolic stability, oral bioavailability, and permeability.

Performing a copper-catalysed azide alkyne cycloaddition to simultaneously ring close and form a 1,2,3-triazole proved challenging and so the triazole linker was first synthesised and

then used to cyclise the peptide. The triazole was formed using literature conditions, and subsequently deprotected before coupling to the linear peptide. Cyclisation proved successful, though difficulties were encountered upon removal of copper salts from the reaction mixture and so the cyclic compound was unable to be isolated pure.

Cyclisation through the formation of a diyne as demonstrated by Verlinden *et al*. used Glaser-Hay diyne coupling to synthesise a variety of tetrapeptide-based macrocyclic 1,3-diynes.[166] Using these conditions on the *N*- and *C*-propargylated ester of the tripeptide was attempted to be cyclised, though degradation of the starting material occurred. Therefore, the more stable amide analogue was then synthesised and successfully cyclised, though difficult purification and low yields meant that this method was no longer investigated.

Another cyclisation method that was attempted was through the formation of a 2,5-disubstituted 1,3,4-oxadiazole. Cyclisation using this method on the tripeptide failed due to the potential high amount of ring-strain generated upon cyclisation. Therefore, the reaction conditions were attempted once again, this time on a tetrapeptide with the addition of glycine to the tripeptide. Cyclisation *via* this approach was shown to be successful by mass spectrometry, though the results could not be replicated upon repetition of the reaction.

The final method used a pyrazole linker, in which the background of the chemistry is discussed in detail in Chapter 5. The protecting groups used in this synthesis proved to be problematic, with both Fmoc and Cbz groups failing to enable the generation of the diazo compound required for the 1,3-dipolar cycloaddition onto alkynes to yield pyrazoles. Converting the protecting group to a phthaloyl group created problems upon formation of the hydrazone, and using conditions developed by Cai *et al*. for the synthesis of α-diazophosphonyl compounds that utilised *p*-toluene sulfonohydrazide yielded the desired diazo compound, though reaction to form the pyrazole was unsuccessful. Repetition of this reaction was ineffective, and so the alanine analogue was attempted to be synthesised but unfortunately time constraints on this project did not allow for this method to be fully studied.

5. Synthesis of Pyrazoles Through Catalyst-Free Cycloaddition of Diazo Compounds to Alkynes

5.1 Introduction

Pyrazole is a five-membered ring consisting of three carbon atoms and two adjacent nitrogen atoms. It is a weak base that was first reported by Ludwig Knorr in 1883.[181] The nitrogen atoms in pyrazoles have differing reactivities; one nitrogen atom (N1) existing as 'pyrrole-like' as its unshared electrons are conjugated with the aromatic system (Figure 57). The other nitrogen atom (N2) is described as 'pyridine-like' as it contributes just one electron to the aromatic π-system and has a basic lone pair of electrons in the sp^2 orbital in the plane of the ring. Consequently, pyrazoles react with both acids and bases.

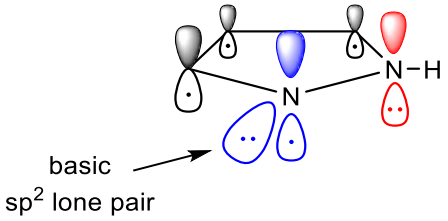
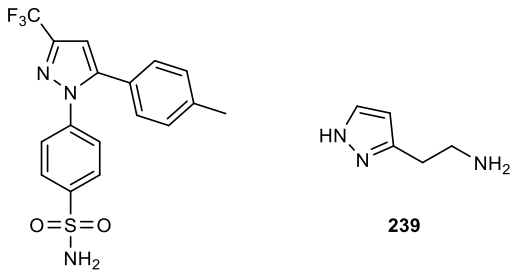


Figure 57. Structure of pyrazoles showing the difference between N1 (red) and N2 (blue)

Pyrazoles have been greatly studied and consequently a large number of syntheses and analogues have been reported. They possess a diverse range of applications and properties, including anti-inflammatory, kinase inhibitors, antibacterial, analgesic and anticonvulsant agents.[182–186] The pyrazole core is also present in numerous leading drugs. Examples include the anti-inflammatory drug Celebrex **238** and the histamine H_2 receptor agonist Betazole **239** (Figure 58).



238 **239**

Figure 58. Structure of the drugs Celebrex **238** (left) and Betazole **239** (right)

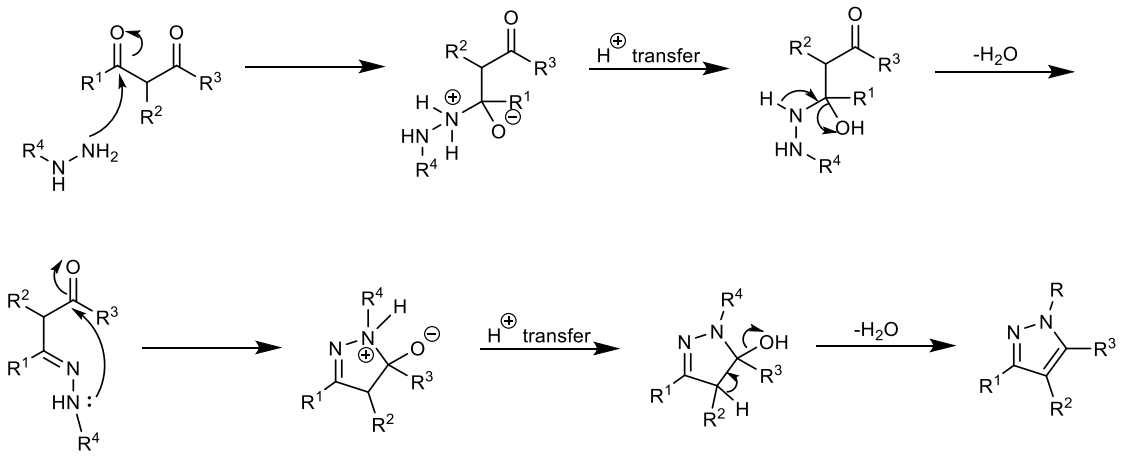
Derivatives of pyrazoles, including aminopyrazoles, can be used as a building block for more complex moieties. Novel 3-aminopyrazole inhibitors of the MK-2 kinase were successfully

developed through a scaffold hopping strategy.[187] These compounds showed potent inhibition of MK-2 activity as well as cellular activity.

5.1.1 Classical Methods for the Synthesis of Pyrazoles

5.1.1.1 Cyclocondensation of Hydrazine with Carbonyl Compounds

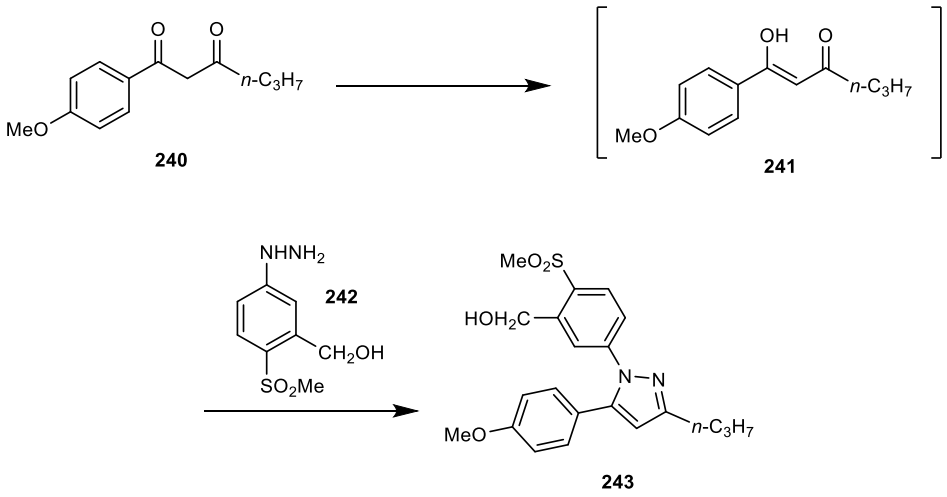
Due to the interesting and varied activities of pyrazoles, considerable attention has been focussed on their synthesis. Classical methods involve approaches based on cyclo-condensations of hydrazine with 1,3-dicarbonyl compounds or 1,3-dielectrophiles such as the Knorr synthesis. The mechanism of the Knorr pyrazole synthesis begins with imine formation, with attack occurring on either of the carbonyls (Scheme 80). The second nitrogen of hydrazine then attacks the other carbonyl group to form a second imine, resulting in a diimine that is deprotonated and gives the pyrazole product.



Scheme 80. Mechanism for the Knorr pyrazole synthesis

The Knorr synthesis was typically performed under reflux using polar protic solvents such as methanol, ethanol or isopropanol and addition of acid or using acetic acid as a solvent in the reaction was commonly used to help decrease the reaction times. The substituent on the hydrazine can be widely varied to include alkylhydrazines, arylhydrazines, and acylhydrazines, and when reacting with symmetrical dicarbonyl compounds result in a single isomer, or unsymmetrically substituted dicarbonyls, a mixture of two regioisomers. Several steric and experimental factors influence the preferential formation of one isomer over another. Singh *et al*. reported factors that that affect the regiochemical outcome in the synthesis of 1,3,5-trisubstituted pyrazoles.[188] Simple reaction of the dicarbonyl **240** with the HCl salt of the arylhydrazine **242** gave regioisomers in a 52:48 ratio. Addition of triethylamine

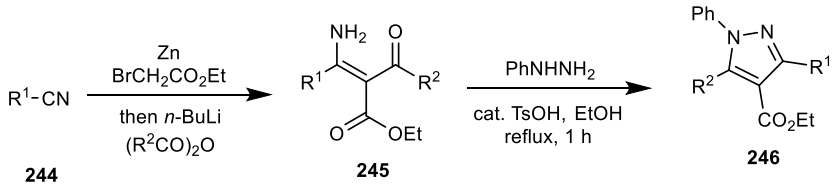
to the reaction resulted in the sole formation of compound **243**, and the same result was seen when using the free arylhydrazine **242** (Scheme 81). This outcome might be due to the preferred enol form **241** that the arylhydrazine attacks the ketone under neutral conditions to regioselectively generate pyrazole **243**. The HCl salt of arylhydrazine **242** may be in equilibrium between the free and protonated forms, leading to fluctuating nucleophilicity of the NH_2, giving poor regio-control.



Scheme 81. Regioselectivity when using Et_3N or the free arylhydrazine[188]

Another highly selective modification to the reaction was reported by Gosselin *et al*.[189] In this publication it was found that cyclocondensations of arylhydrazine hydrochlorides and 1,3-diketones gave excellent regioselectivities in aprotic solvents with strong dipole moments and dielectric constants, such as *N,N'*-dimethylacetamide, DMF, or *N*-methylpyrrolidinone (NMP). Conversely, when the solvent was changed to a polar protic solvent, such as ethanol, the same reaction resulted in poor regioselectivity.

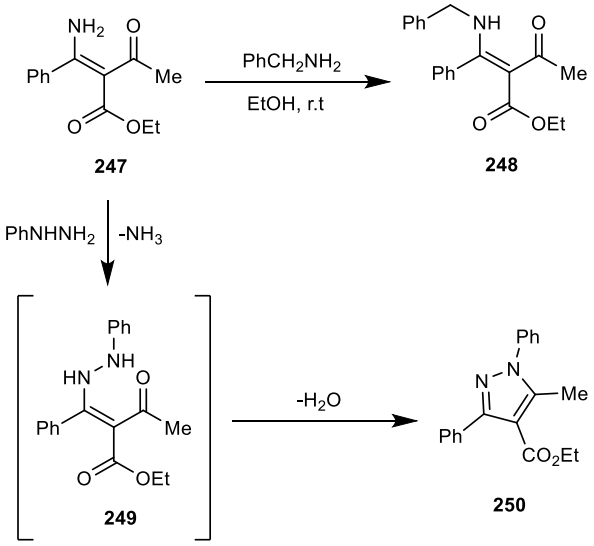
The use of 1,3-dicarbonyl surrogates can also help to improve the regioselectivity in the synthesis of pyrazoles, and of these β-enaminones are the most commonly employed. However, only a handful of precedents have been reported for their synthesis. In 2009, Ko *et al*. developed a broad and general route for the regioselective synthesis of 1-phenyl pyrazoles **246** from β-enaminoketoesters **245** prepared by tandem Blaise-acylation.[190] It was reported that the Blaise reaction intermediate, the zinc bromide complexes of β-enaminoketoesters, could be activated by the addition of *n*-BuLi *in situ* to result in chemoselective C2-acylation and consequently provide various β-enaminoketoesters that were then used in the synthesis of pyrazoles (Scheme 82). This method was broad in substrate scope and included a mixture of aryl, alkyl, diaryl and dialkyl substituents.



244 **245** **246**

Scheme 82. Tandem Blaise-acylation and regioselective synthesis of 1-phenyl pyrazoles[190]

Reaction of the β-enaminoketoester **247** with benzylamine resulted in isolation of the Michael addition product **248** in 64% yield (Scheme 83). This supported the mechanism that Michael addition of the unsubstituted nitrogen of the phenyl hydrazine at the β-carbon carrying the electronegative amine group is followed by intramolecular cyclocondensation (Scheme 83).[190]



247 **248** **249** **250**

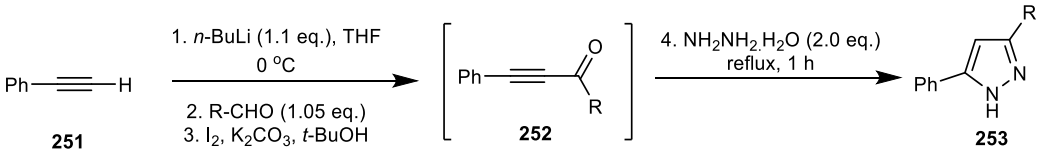
Scheme 83. Proposed pathway for regioselective pyrazole formation[190]

5.1.1.2 Multicomponent Reactions

Pyrazoles may also be synthesised through multicomponent reactions. A multicomponent reaction (MCR) is a reaction comprised of three or more starting materials that react to form a single product. Most or all the atoms present in the starting materials are also present in the formed product. These types of reactions offer significant advantages over bimolecular reactions. They allow for the synthesis of complex molecules by forming multiple bonds in a single step from simple starting materials, without the need for isolation of intermediates. Using MCRs in solvent-free conditions presents an almost benign process in this regard.

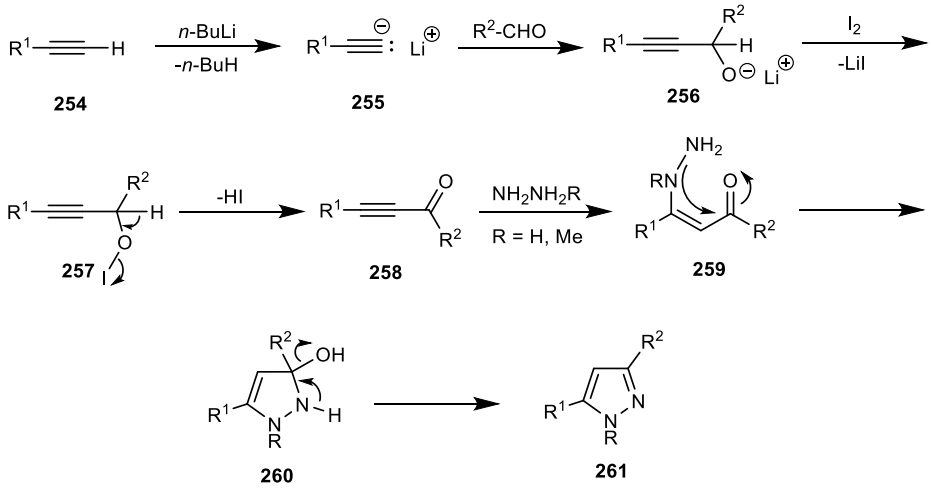
In 2014, Harigae *et al*. reported a method for the synthesis of 3,5-disubstituted pyrazoles in one pot by treatment of terminal alkynes with aromatic aldehydes, molecular iodine, and

hydrazines (Scheme 84).[191] Reactions were reported in good yields (68-99%), and high regioselectivity.



Scheme 84. Multicomponent synthesis of pyrazoles. R = Ph, 4-MeOPh, 4-MePh, 3-MePh, 2-MePh, 4-Cl, 4-CF_3Ph[191]

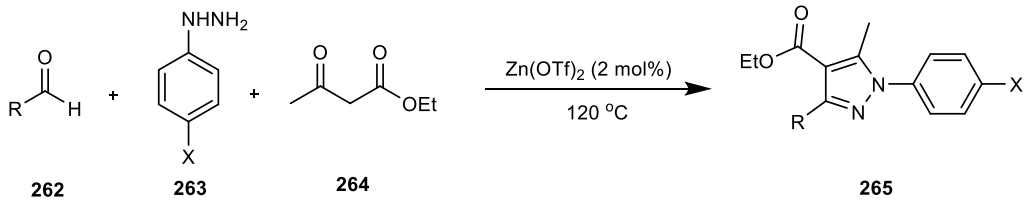
The proposed mechanism of the reaction begins with formation of the lithium acetylide **255** that then reacts with the aldehyde to give the propargyl secondary alkoxide **256** (Scheme 85). This is then oxidised by iodine with K_2CO_3, resulting in an α-alkynyl ketone **258**, which subsequently reacts with hydrazine through a Michael-type addition to give the pyrazole **261**.



Scheme 85. Proposed mechanism for regioselective synthesis of pyrazoles using multicomponent reactions[191]

An example of a solvent-free MCR for the synthesis of pyrazoles was developed by Safaei *et al* (Scheme 86).[192] In this method, fully substituted pyrazoles as well as symmetrical and unsymmetrical bispyrazoles were synthesised using $Zn(OTf)_2$ as a catalyst. Aldehydes, arylhydrazines, and ethyl acetoacetate were reacted under solvent-free conditions at 120 °C, with a variety of Lewis acids and as a result $Zn(OTf)_2$ was shown to be the most effective in the reaction. The reaction failed to give the desired product in the absence of the $Zn(OTf)_2$ catalyst even with extended reaction times, and increasing the temperature or amount of catalyst above 2 mol% did not increase the yield of the reaction. Reactions were all high-yielding (>80%) with no side-product formation. Starting materials included aldehydes with

electron-withdrawing and electron-donating groups on the aromatic ring, such as halogens, aldehydes and cyano groups, as well methoxy groups. The reaction was also shown to be successful using aliphatic aldehydes.

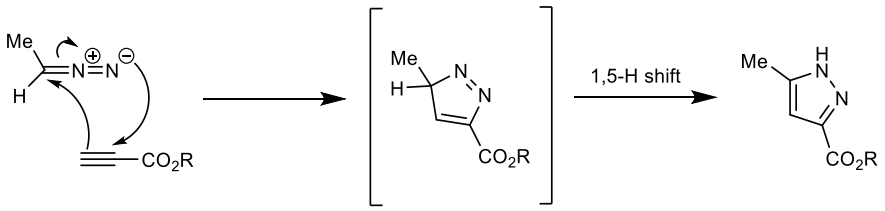


Scheme 86. Solvent-free synthesis of fully substituted pyrazoles using $Zn(OTf)_2$. R = aryl, heteroaryl, alkyl; X = H, Cl, Me.[192]

5.1.1.3 1,3-Dipolar Cycloadditions

1,3-Dipolar cycloadditions were first described in the 19th century, though mechanistic studies and synthetic applications were established by Huisgen in 1963.[193] They involve chemical reactions between a 1,3-dipole and a dipolarophile to form a five-membered ring. Dipolarophiles are typically alkenes or alkynes and often result in the formation of heteroaromatic rings. 1,3-Dipole compounds contain one or more heteroatoms in their structure and share four electrons in the π-system over three atoms. Examples of 1,3-dipole compounds include azides, diazoalkanes, and nitrile oxides.

1,3-Dipolar cycloadditions are pericyclic reactions that are usually determined by the interaction between the highest occupied molecular orbital (HOMO) of the 1,3-dipole and the lowest unoccupied molecular orbital (LUMO) of the dipolarophile. The mechanism proceeds by a concerted pericyclic cycloaddition mechanism originally proposed by Huisgen (Scheme 87).[194]

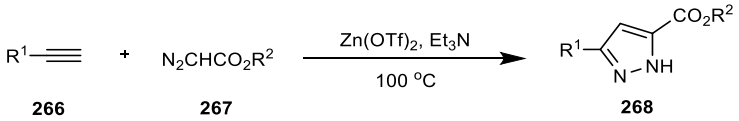


Scheme 87. Concerted pericyclic cycloaddition

In some cases, 1,3-dipoles can react with dipolarophiles without any activation, for example in the case of ozonolysis of alkenes. However, typically the reaction of diazocarbonyl compounds with alkenes or alkynes proceeds slowly, or with need of thermal activation. One

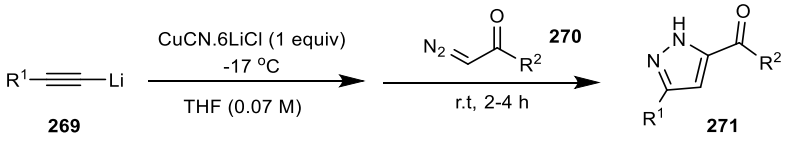
of the methods used to accelerate pyrazole formation *via* a [3+2] cycloaddition is using catalysts, and in particular Lewis acids and bases. Lewis acids, such as $Zn(OTf)_2$, are believed to coordinate to the unsaturated compound lowering the energy of the LUMO, and thereby increasing the electrophilicity and reactivity of the dipolarophile.

An example of this was reported by He *et al*. in 2009, by using $Zn(OTf)_2$ promoted 1,3-dipolar cycloadditions of diazoacetate compounds to terminal alkynes to form a series of pyrazoles in good yields (Scheme 88).[195] This simple procedure was successfully performed using a variety of alkynes, including arylalkynes and alkylalkynes.



Scheme 88. 1,3-Dipolar cycloaddition of diazocarbonyl compounds to terminal alkynes[195]

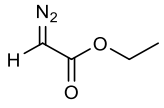
Another method to accelerate the reaction between 1,3-dipoles and dipolarophiles is to use additives that increase the electron density of the dipolarophile, increasing the rate of reaction by raising its HOMO. Although this method is not often used it is, most notably, used in the copper-catalysed synthesis of triazoles from azides and alkynes. Ready *et al*. reported examples of this cycloaddition with an inverse electron demand in 2007, and it was shown to be effective in the synthesis of pyrazoles by reaction of copper acetylides with diazocarbonyl compounds (Scheme 89).[196] Lithium phenylacetylide was first treated with several copper(I) sources, followed by benzyl diazoacetate. Variation of the copper source and base led to CuCN·6LiCl which gave the highest yields with least formation of by-products. This reaction displayed great variation in both the alkyne and diazocarbonyl components and resulted in the formation of a single regioisomer. Both electron-poor and electron-rich aryl acetylenes performed well, along with a variety of substituted terminal alkynes that included halides, amino groups, esters and nitriles. The diazocarbonyl component was also differed from benzyl diazoacetate to ethyl and *tert*-butyl diazoesters as well as Weinreb amides.



Scheme 89. Copper promoted reaction of lithium acetylides with diazocarbonyl compounds[196]

5.1.2 Diazo Compounds

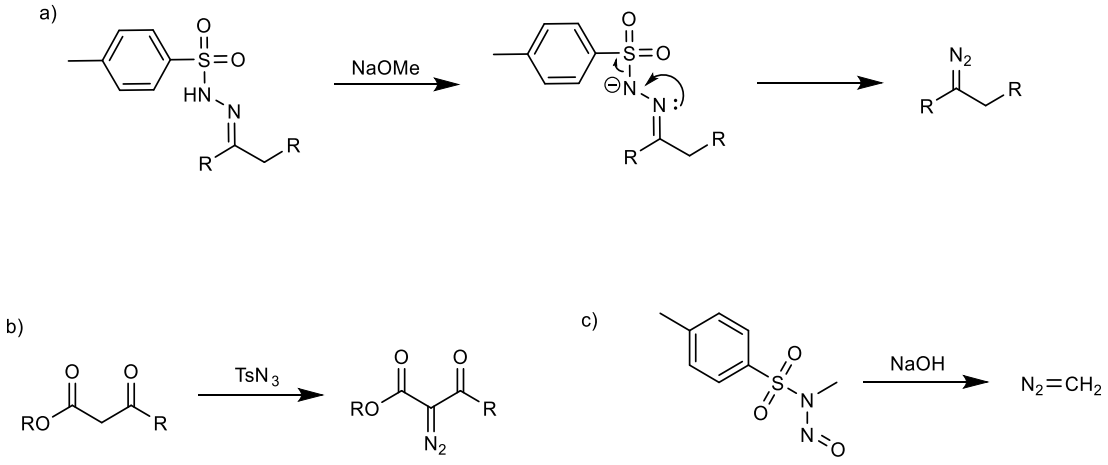
Diazoalkanes or diazo compounds are one of the earliest 1,3-dipoles described in history and are extensively used in cycloaddition reactions. They consist of two linked nitrogen atoms bound to a carbon atom with an overall neutral charge and can be described by the general formula $R_2C=N^+=N^-$. Diazo compounds, including diazomethane, are explosive however, they can be stabilised through the addition of an electron-withdrawing carbonyl group. This allows the electron density to delocalise further, increasing the stability of the compound. Such an example is the commercially available compound ethyl diazoacetate **272** (Figure 59).



272

Figure 59. Structure of ethyl diazoacetate

The diazo compounds diazomethane and ethyl diazoacetate were first synthesised in 1883 and 1894 respectively.[197,198] Since then there has been a considerable number of syntheses published for the synthesis of a large variety of diazo compounds. These include oxidation of hydrazones, diazo group transfer from azides, and base mediated cleavage of *N*-alkyl-*N*-nitroso sulfonamides (Scheme 90).



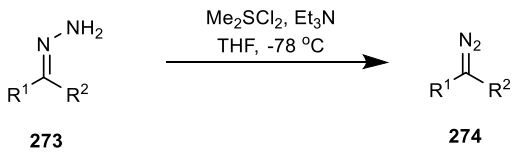
Scheme 90. Synthesis of diazo compounds: a) oxidation of hydrazones; b) transfer from azides; c) base-mediated cleavage of *N*-alkyl-*N*-nitroso sulfonamides

Diazo group transfer is a common synthesis of diazo compounds from a sulfonyl azide, such as tosyl azide, to an active methylene substrate in a Regitz diazo transfer.[199] Using this method diazo derivatives of cyclopentadienes, 1,3-dicarbonyl and 1,3-disulfonyl compounds,

ketones, carbonic acid esters, and β-iminoketones can be synthesised in high yields. However, the potential explosion hazard of this method, typically using tosyl azide, has led to the development of safer alternatives such as *p*-acetamidobenzenesulfonyl azide. This diazo group transfer has been shown to not only succeed when the methylene compound bears two strong acceptor substituents such as acyl, cyano, sulfonyl, or phosphoyl groups, but also aryl, heteroaryl and vinylacetate substituents.[200]

Diazo compounds can also be synthesised through the oxidation of hydrazones. Stoichiometric quantities of toxic heavy metal salts, such as mercury(II) oxide and lead(IV) acetate, are often used for this process.[201] These reagents tend to be hazardous as well as environmentally unfriendly and can also result in difficulties with isolation and purification leading to potentially dangerous handling of diazo solutions. Therefore, a number of metal-free alternative procedures have been published.

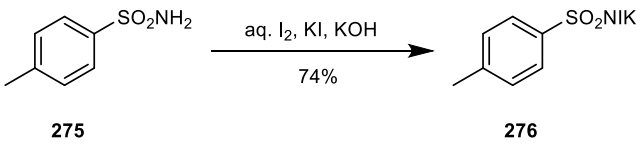
In 2007, Javed *et al*. showed that use of chlorodimethylsulfonium chloride allowed for the preparation of 2-diazo-1,2-diphenylethanone, as well as diazocyclohexane and several aryl- and alkyl-substituted derivatives of diazomethane in moderate to good yields (Scheme 91).[202] Chlorodimethylsulfonium chloride is generated *in situ* from DMSO and oxalyl chloride in the presence of triethylamine to give this 'activated' DMSO reagent. Changing the solvent from THF to a 9:1 mixture of diethyl ether and dichloromethane prevented solvent participation in the reaction allowing for unstable diazoalkanes to be subsequently used without isolation.



273 **274**

Scheme 91. Metal-free synthesis of diazo compounds using 'activated' DMSO[202]

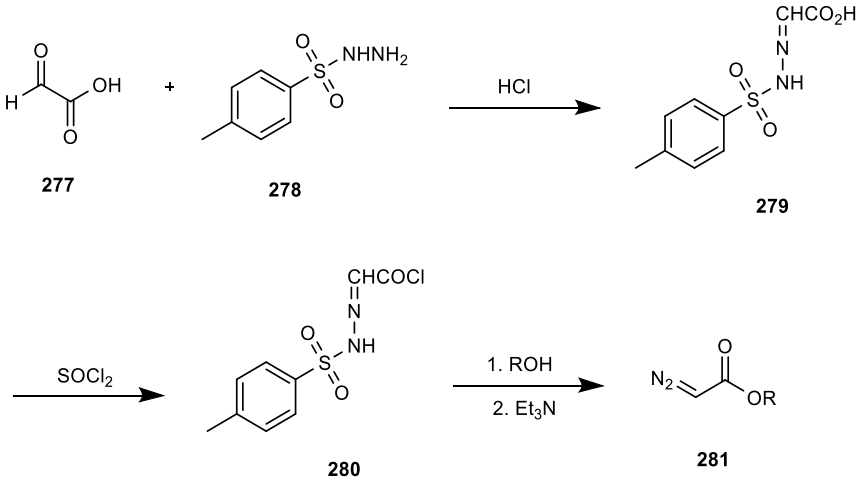
In 2014, a paper was published from the Moody group that detailed a new reagent for the oxidation of hydrazones to diazo compounds.[203] This method built upon work from Barton *et al*. using molecular iodine and a base for oxidation of hydrazones.[204] Investigation into mild iodinating reagents led to the *N*-iodo potassium *p*-toluenesulfonamide salt **276**, also known as TsNIK. This reagent was synthesised from *p*-toluenesulfonamide **275** rapidly and in multi-gram quantity using iodine in a mixture of aqueous potassium iodide and potassium hydroxide and is isolated *via* filtration (Scheme 92).



Scheme 92. Preparation of TsNIK[203]

The reaction conditions used for the diazo formation used TsNIK (1.1 equiv.) in a 4:1 mixture of THF:KOH at room temperature for 1 h. This allowed for high yields of the desired diazo products that were pure after a simple work-up and required no further purification. Compounds prepared using this method included stabilised diazo compounds such as diazoesters, diazoamides, diazoketones, diazophosphonates and diphenyldiazomethane in high yields.

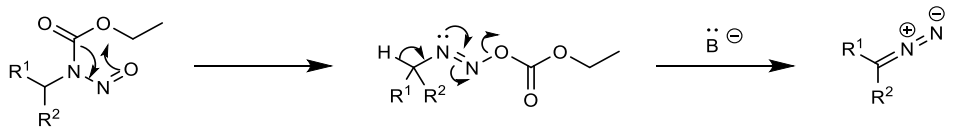
Another widely used method for the synthesis of diazo compounds from hydrazones is cleavage of toluenesulfonyl hydrazones, known as the Bamford-Stevens reaction.[205] Cleavage of tosylhydrazones is conducted under basic conditions to give the corresponding diazocarbonyl compounds. This reaction was later modified by House *et al*. for the preparation of α-diazoesters.[206] This method was based on conversion of glyoxylic acid **277** to its tosylhydrazone **279**, and subsequent reaction with thionyl chloride, which is then reacted with an alcohol to give the hydrazone ester (Scheme 93). This ester is then decomposed using triethylamine to yield the diazoester **281**.



Scheme 93. House synthesis of α-diazoesters[206]

One of the classical methods for the synthesis of diazomethane involved base-catalysed decomposition of *N*-alkyl-*N*-nitroso derivatives from sulfonamides, ureas, carbamates, and ketones. *N*-Methyl-*N*-nitroso-*p*-toluenesulfonamide or Diazald is used as a common

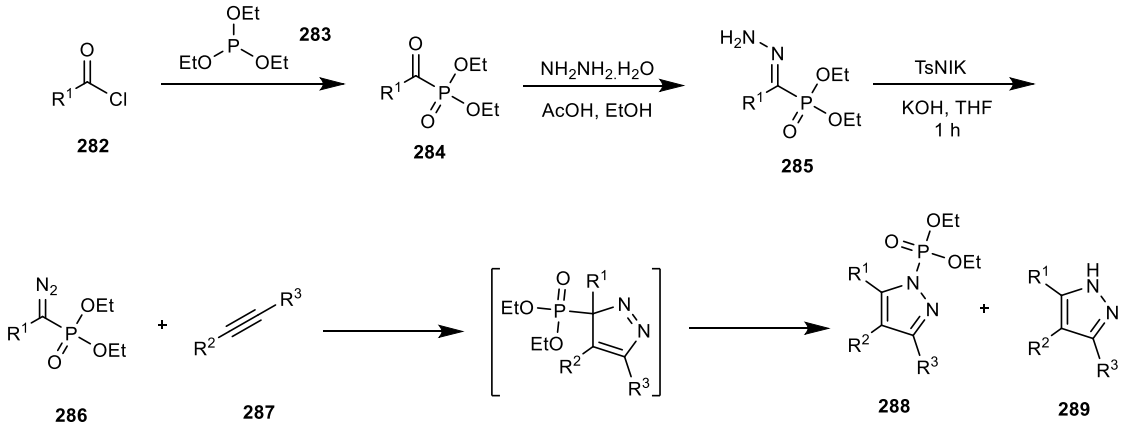
precursor for the generation of diazomethane and, although *N*-nitroso compounds are highly carcinogenic, it is favoured over reagents such as *N*-methyl-*N*-nitrosourea that are less stable. *N*-alkyl-*N*-nitroso compounds are used to form diazo compounds under basic conditions in a mechanism such as the one shown below (Scheme 94). This method is used in the generation and *in-situ* consumption of diazomethane in a multi-molar process as described in a patent in 1998 where cleavage of Diazald is achieved in a two-phase system containing a phase-transfer catalyst.[207]



Scheme 94. Base mediated elimination reaction of *N*-alkyl-*N*-nitroso compounds

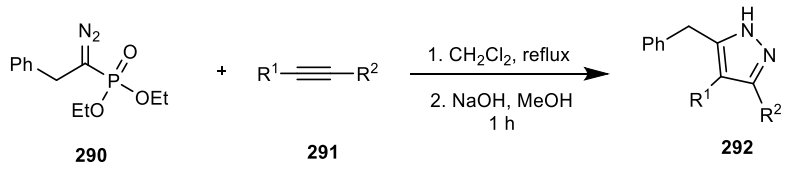
5.2 Previous Work Completed in the Group

Previous work published within the group developed a new reagent, TsNIK, was used for the synthesis of stabilised diazo compounds, as is discussed in Section 5.1.2.[203] In this paper, α-ketophosphonate hydrazones were generated using an adaption of a known procedure of a Michaelis-Arbuzov reaction followed by a one-pot condensation with hydrazine hydrate under acidic conditions.[208] These α-ketophosphonate hydrazones **285** were then oxidised to the corresponding stabilised α-diazophosphonate **286** using TsNIK in high yields and purities (Scheme 95). A 1,3-dipolar cycloaddition with an alkyne **287** followed by a 1,5-shift gives a mixture of compounds **288** and **289**. Using this methodology, a new synthesis of functionalised pyrazoles through catalyst-free cycloaddition of diazo compounds to alkynes is described.



Scheme 95. Synthesis of pyrazoles

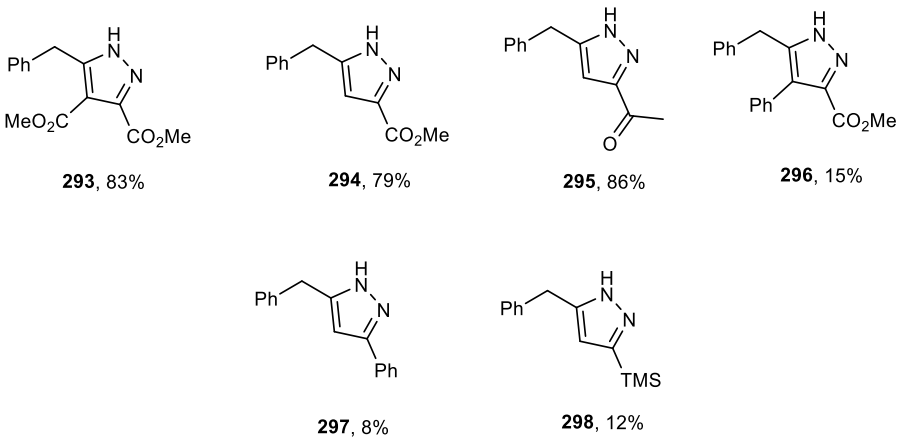
A previous member of the Moody group, Katie Ruffell, had performed some initial reactions using the above conditions. These included the formation of a number of both intra- and intermolecular cycloaddition products. After formation of the diazophosphonate starting material **290**, the intermolecular cycloaddition products synthesis followed the general scheme shown below (Scheme 96). Products obtained after the cycloaddition contained a mixture of product **292** and phosphorylated product and so a hydrolysis step was introduced immediately after the cycloaddition to ensure isolation of one product.



290 **291** **292**

Scheme 96. Formation of intermolecular cycloaddition products

Alkynes used for this reaction included commercially available dimethyl acetylenedicarboxylate, methyl propiolate, 3-butyn-2-one, methylphenyl propiolate and phenylacetylene, as well as the synthesised alkyne ethynyltrimethylsilane. These alkynes resulted in the products **293**, **294**, **295**, **296**, **297**, and **298** respectively (Figure 60). Yields vary depending on the alkyne in the reaction. Alkynes with electron-withdrawing groups attached, such as **293** and **294**, accelerate the reaction by lowering the LUMO, while those with electron-donating groups, such as **297** and **298**, decelerate the reaction by raising the HOMO.

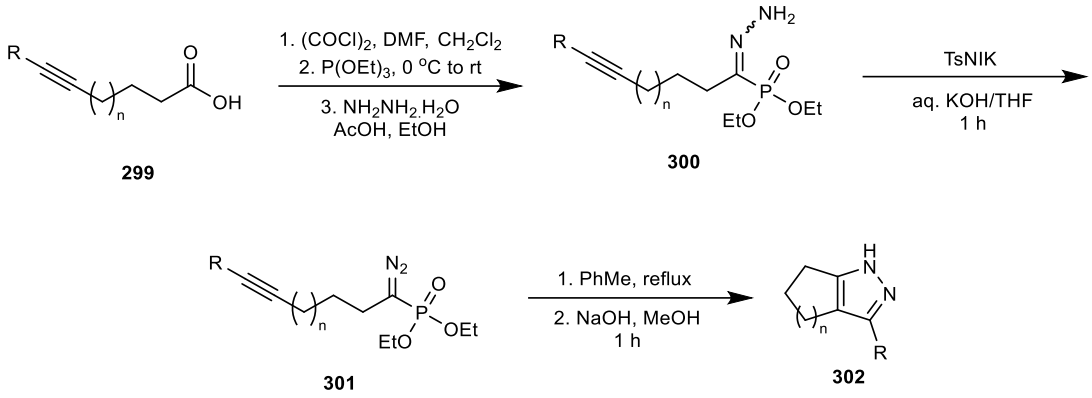


293, 83% **294**, 79% **295**, 86% **296**, 15%

297, 8% **298**, 12%

Figure 60. Intermolecular pyrazole products

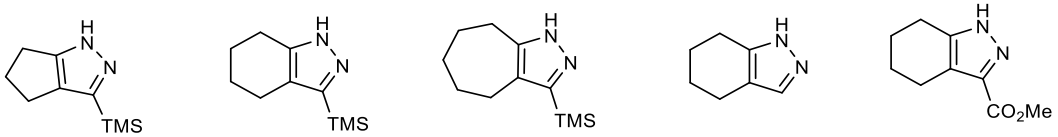
The intramolecular cycloadditions followed the scheme shown below (Scheme 97). The starting materials **299** for these reactions were more complex and so first had to be synthesised, before generating the acid chloride, α-ketophosphonate, hydrazone **300** and diazophosphonate **301** respectively.



299 **300** **301** **302**

Scheme 97. Synthesis of intramolecular pyrazoles

Several bicycles were synthesised from these cycloadditions (Figure 61). Formation of favourable rings such as cyclohexane resulted in high yields with several different alkynes. Cyclisation to the cycloheptane was lower yielding.



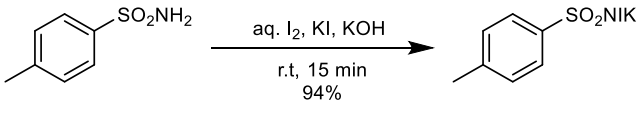
303, 73% **304**. 85% **305**, 15% **306**, 81% **307**, 85%

Figure 61. Intramolecular pyrazole products

The aim of this project was to build upon this preliminary work and extended the substrate scope of the reaction. This includes the preparation of a variety of diazophosphonates and reacting them with several commercial alkynes, as well as strained alkynes.

5.3 Synthesis of Pyrazoles

To synthesise the pyrazoles as in the above procedure, the oxidising reagent TsNIK **276** was first synthesised.[203] TsNIK was prepared from *p*-toluenesulfonamide **275** and aqueous iodine, potassium iodide and potassium hydroxide (Scheme 98). The reaction was filtered after 15 min, to give the pure TsNIK on a 5 g scale in excellent yield.

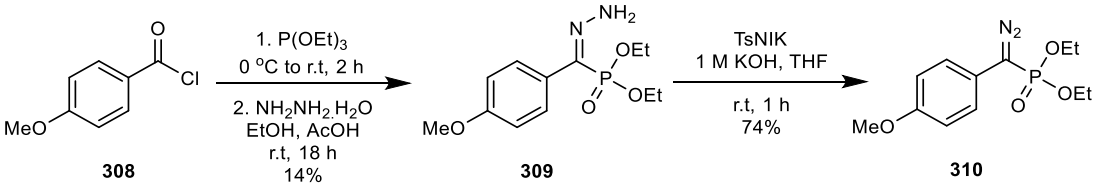


275 **276**

Scheme 98. Synthesis of TsNIK **276**

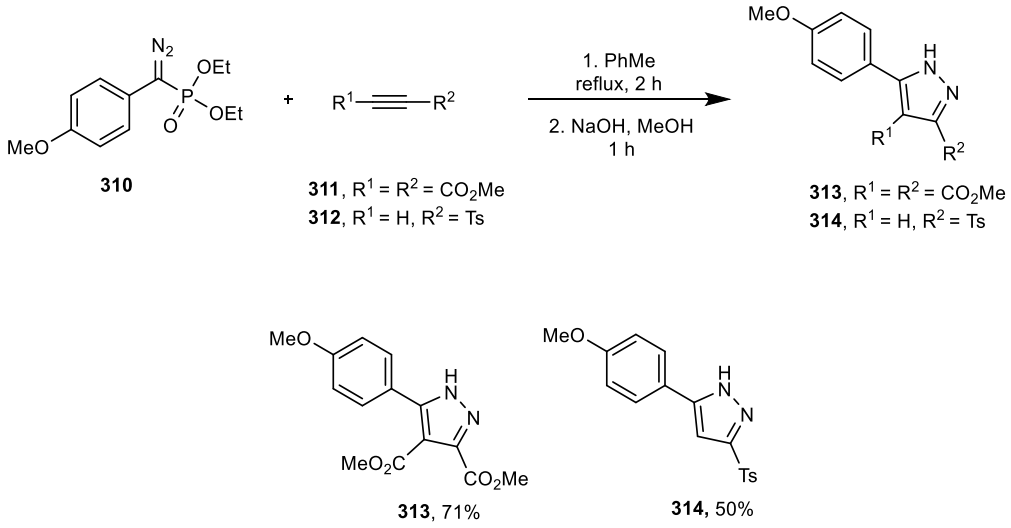
5.3.1 Intermolecular Synthesis of Pyrazoles

The commercially available acid chloride 4-methoxybenzoyl chloride **308** was first reacted to form the α-ketophosphonate in a Michaelis-Arbuzov reaction. The Michaelis-Arbuzov reaction first described in 1898, proceeds *via* nucleophilic attack of the phosphorus of a trialkyl phosphite onto an alkyl halide, followed by halide ion dealkylation of the trialkylphosphonium salt to give the desired phosphonate.[208] After the reaction to form the α-ketophosphonate, this mixture was added to hydrazine hydrate to give the hydrazone **309** in a moderate yield (Scheme 99). TsNIK was then added to a 1:4 solution of 1M KOH:THF and **309** and after 1 h the diazophosphonate **310** was isolated in a 74% yield after purification.



Scheme 99. Synthesis of the diazophosphonate **310**

The diazophosphonate **310** was then reacted with two alkynes to give the corresponding pyrazoles. Dimethyl acetylenedicarboxylate **311** and ethynyl *p*-tolyl sulfone **312** were heated under reflux with the starting material **310** for 2 h. Synthesis of the pyrazoles was followed by hydrolysis using NaOH in a methanol/water mixture to give **313** and **314** respectively in moderate to good yields (Scheme 100).



Scheme 100. Synthesis of the pyrazoles **313** and **314**

To confirm the regioselectivity of the reaction, a crystal structure of the pyrazole **314** was obtained (Figure 62). The regioselectivity in this reaction is controlled by sterics as the less hindered nitrogen of the diazo attacks the side of the alkyne with the tosyl group.

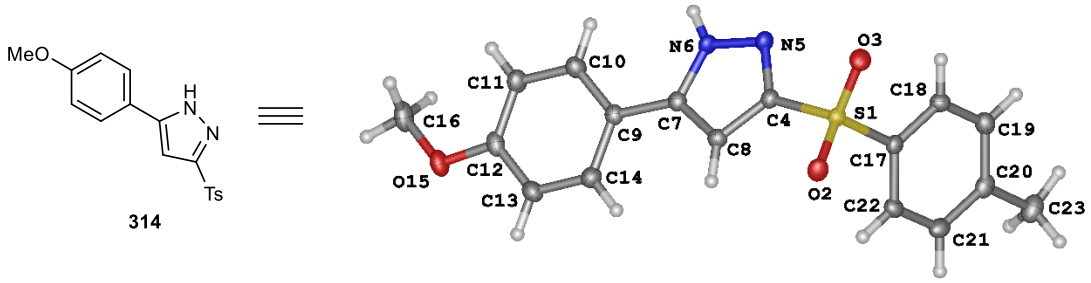
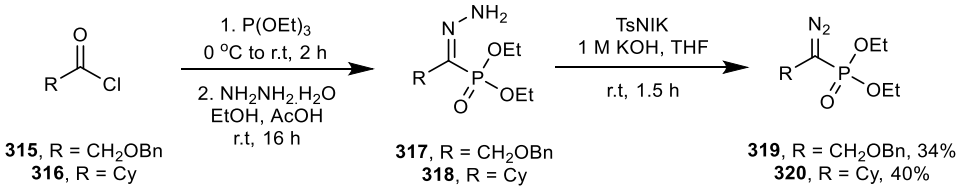


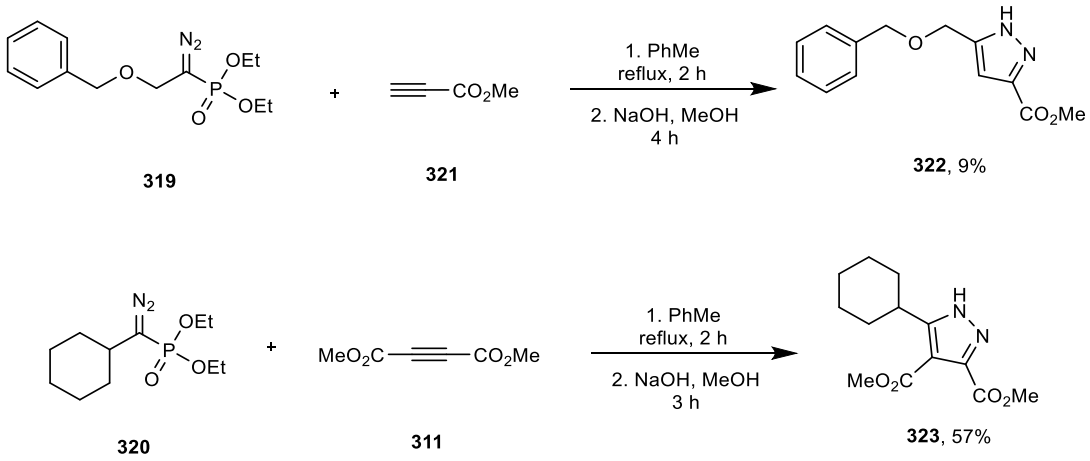
Figure 62. Crystal structure of **314**

Two other pyrazoles were also generated using this procedure. Benzyloxyacetyl chloride **315** and cyclohexanecarbonyl chloride **316** were used as starting materials that were reacted with triethyl phosphite to give the corresponding α-ketophosphonate. The next step formed the hydrazones using hydrazine hydrate and were subsequently oxidised to their diazophosphonate using TsNIK (Scheme 101). All steps were performed without isolation or purification and the reactions were monitored by TLC and mass spectrometry.



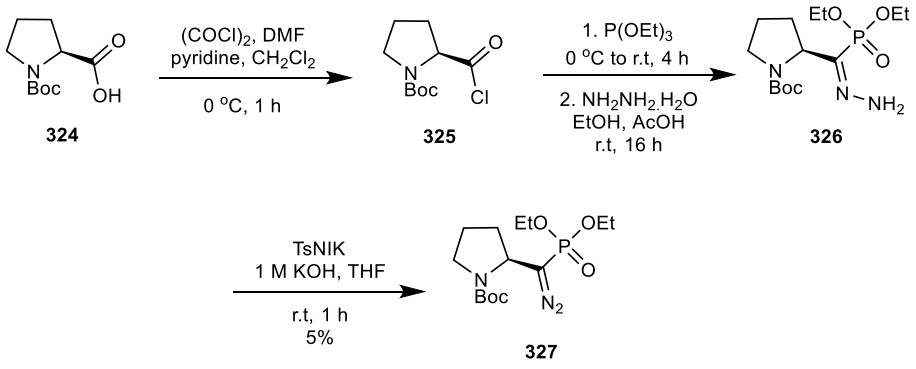
Scheme 101. Synthesis of the diazophosphonates **319** and **320**

The diazophosphonates **319** and **320** were then reacted with methyl propiolate and dimethyl acetylenedicarboxylate respectively to give the corresponding pyrazoles (Scheme 102). Both reactions were conducted in toluene under reflux for 2 h and followed by hydrolysis using NaOH. The pyrazoles **322** and **323** were isolated in moderate yields.



Scheme 102. Synthesis of pyrazoles **322** and **323**

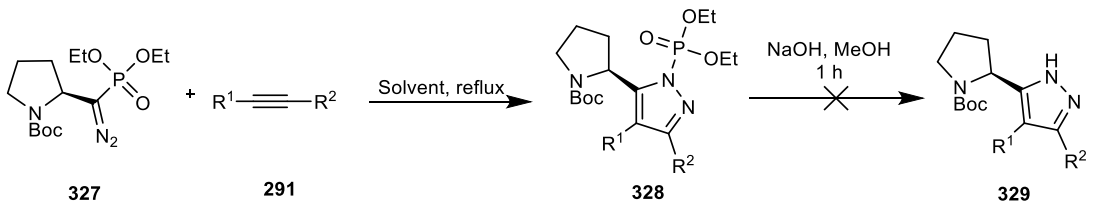
Using *N*-Boc *L*-proline **324**, its equivalent diazo compound was synthesised by following the procedure previously outlined (Scheme 103). One-pot formation of the acid chloride **325**, α-ketophosphonate, hydrazone **326** and then diazo compound **327** was low yielding with an overall yield of 5%.



Scheme 103. Synthesis of diazophosphonate **327**

The diazophosphonate was then subjected to a number of cycloaddition reactions (Table 20). Using methyl propiolate and dimethyl acetylenedicarboxylate as the alkynes in the reactions, **327** was heated under reflux in dichloromethane (Table 20, Entry 1 and 2). After 2 h in each reaction, no product was shown to have been formed by mass spectrometry and so the reaction involving methyl propiolate was left to heat under reflux for 20 h. Though after this increased reaction time, no product was observed. The solvent in this reaction was then changed to toluene so the reaction could be heated to a higher temperature (Table 20, Entry 3 and 4). After 7 h, using methyl propiolate and dimethyl acetylenedicarboxylate, the phosphorylated product **328** was present by mass spectrometry, and so the hydrolysis reaction using NaOH was performed. However, after work up of the hydrolysis reaction, no

desired product or starting material was isolated. The reaction was attempted again, this time using ethynyltrimethylsilane as the dipolarophile in toluene (Table 20, Entry 5). After 5 h, the phosphorylated product was present by mass spectrometry, but upon isolation only a small amount of this compound was acquired. It may follow that the cycloaddition reaction of **327** is low yielding and that as these reactions are performed on small scale that once hydrolysis of the phosphate group has occurred, the remainder of the pyrazole may be lost during work-up and isolation.

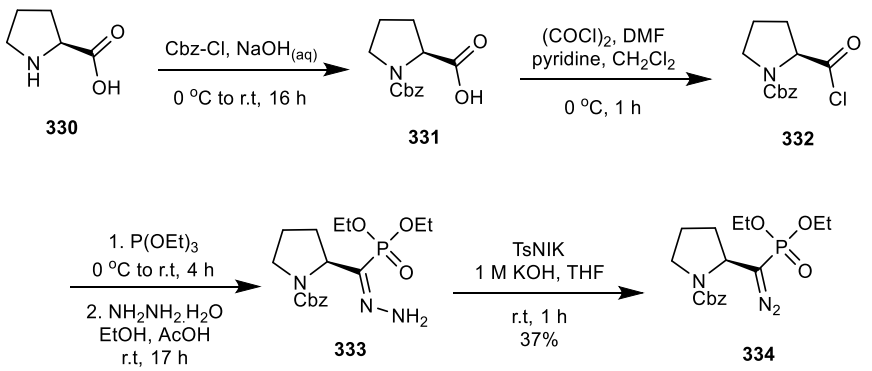


327 **291** **328** **329**

Entry	Reaction Conditions	Outcome
1	Dimethyl acetylenedicarboxylate, CH_2Cl_2, 2 h	**329** not observed by mass spec
2	Methyl propiolate, CH_2Cl_2, 20 h	**329** not observed by mass spec
3	Dimethyl acetylenedicarboxylate, PhMe, 7 h	**328** mass ion seen by mass spec, **329** not isolated after hydrolysis
4	Methyl propiolate, PhMe, 7 h	**328** mass ion seen by mass spec, **329** not isolated after hydrolysis
5	Ethynyltrimethylsilane, PhMe, 5 h	**328** mass ion seen by mass spec, **329** not isolated after hydrolysis

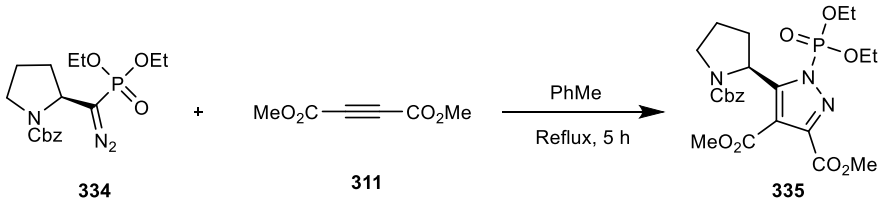
Table 20. Reaction of **327** with alkynes

The instability of the Boc group may also have been a contributing factor to the difficulties in attaining the desired pyrazole product. Therefore, the protecting group on the proline was changed to Cbz. To synthesise this compound, *L*-proline **330** was first Cbz-protected using benzyl chloroformate in aqueous NaOH (Scheme 104). This was then reacted on without purification to form the acid chloride **332**, followed by reaction with triethyl phosphite and hydrazine hydrate to give **333**. The hydrazone was then oxidised to the diazophosphonate using TsNIK in 1 h to give **334** in 37% overall yield.



Scheme 104. Synthesis of diazophosphonate **334**

The diazophosphonate **334** was then reacted with dimethyl acetylenedicarboxylate **311** in toluene under reflux for 5 h (Scheme 105). Formation of the product **335** was seen by mass spectrometry and by ^{1}H NMR, however, the product contained multiple impurities and due to the small amount isolated, purification and hydrolysis was not attempted.



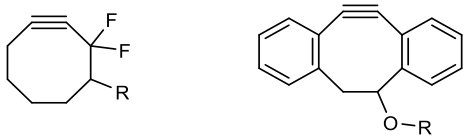
Scheme 105. Synthesis of pyrazole **335**

5.3.2 Strain-Promoted Synthesis of Pyrazoles

Although the cycloadditions to generate pyrazoles using this method are catalyst-free, they require elevated temperatures. For the process to be bioorthogonal, the reactions should be able to take place at room temperature. In 1961, Wittig and Krebs noted that the strained, cyclic alkyne cyclooctyne, reacted violently when in the presence of phenyl azide, resulting in a triazole product.[209] This 1,3-dipolar cycloaddition contrasted with the slow reactions displayed by linear alkynes in a classical Huisgen cycloaddition, and is often referred to as 'Cu-free click chemistry' or strain-promoted azide-alkyne cycloaddition (SPAAC).

These strained alkynes such as difluorinated cyclooctynes (DIFO) **336** or debenzylated cyclooctynes (DIBO) **337** have been shown to have many uses including bioorthogonal labelling for imaging and tracking of biomolecules (Figure 63). Compounds such as these are used in a method known as the bioorthogonal chemical reporter strategy, where a cell's metabolic machinery is used to install a bioorthogonal functional group into target biomolecules. This can then be covalently labelled using a probe such as **336** or **337**. The most

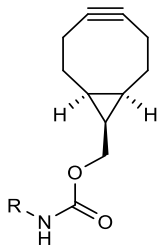
commonly used chemical reporter is an azide due to its small size, metabolic stability and lack of reactivity with natural biofunctionality.



336, DIFO **337**, DIBO

Figure 63. Structures of DIFO and DIBO

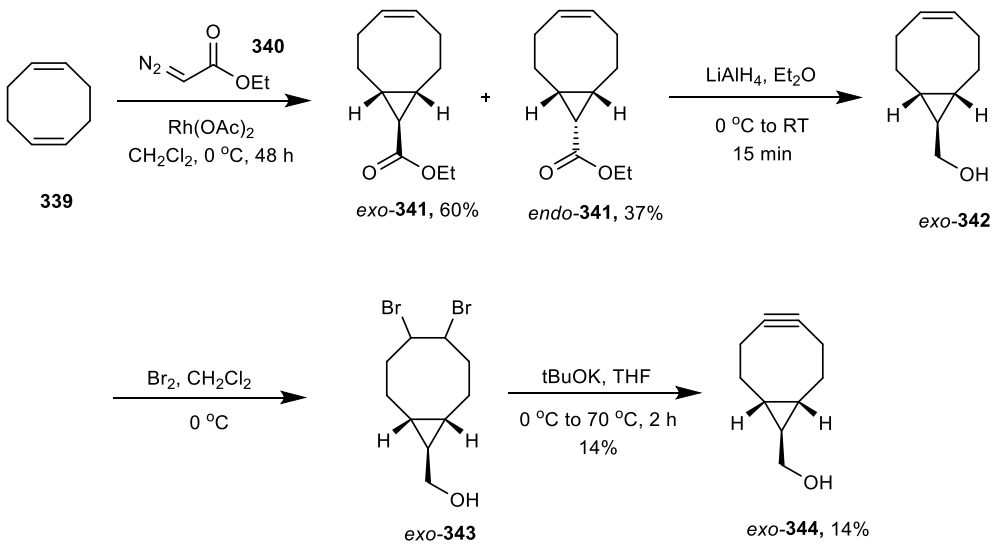
In 2010, Dommerhalt *et al*. reported the synthesis of bicyclo[6.1.0]nonyne (BCN, Figure 64) **338** as a novel ring-strained alkyne prepared through cyclopropanation of 1,5-cyclooctadiene.[210] Derivatives of this alkyne were used in a variety of strain-promoted cycloaddition reactions, and applied in labelling of proteins and glycans. BCN was prepared easily and due to its lack of conformational isomerism, produces sharp peaks in ^{1}H NMR spectra. Another advantage of this symmetrical octyne is that upon cycloaddition only one regioisomer is formed.



338, BCN

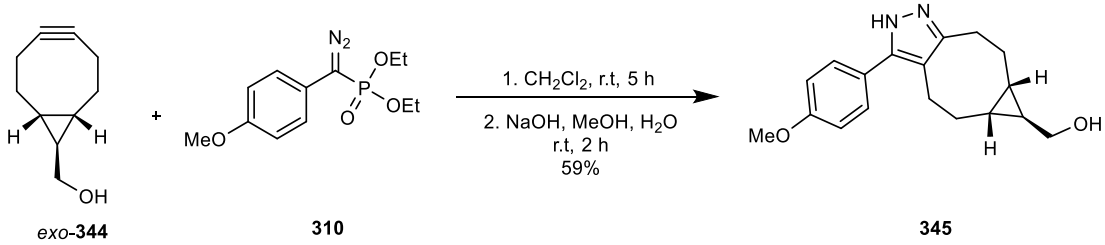
Figure 64. Structure of BCN

By using the procedure outlined by Dommerhalt *et al*., a precursor to BCN allowed for the strain-promoted cycloaddition to be applied to the synthesis of pyrazoles. Synthesis of the octyne began with addition of ethyl diazoacetate **340** to a large excess of 1,5-cyclooctadiene **339** with $Rh_2(OAc)_4$ at 0 ^{o}C (Scheme 106). After 48 h, the reaction mixture was purified, resulting in two diastereomeric compounds *exo*-**341** and *endo*-**341** in 60% and 37% yields respectively. As formation of *exo*-**341** was the higher yielding reaction, this compound was taken forward in the next step. Ester reduction using $LiAlH_4$ was followed by bromination at 0 ^{o}C and finally elimination under reflux to give *exo*-**344** in 14% overall yield. Formation of *exo*-**344** was completed over three steps in under 3 h and required only one purification step.



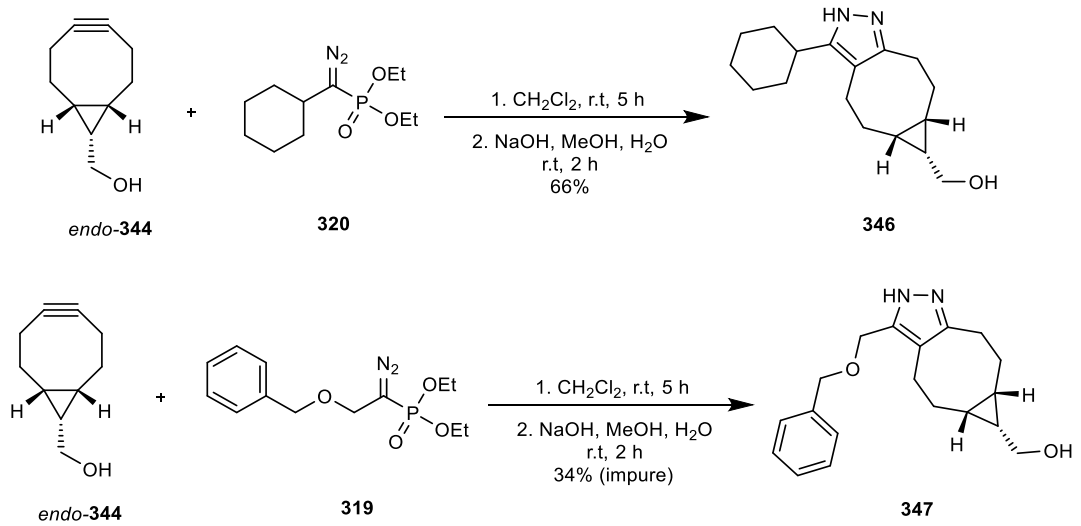
Scheme 106. Synthesis of the strained alkyne *exo*-**344**

The octyne *exo*-**344** was then reacted with the diazophosphonate **310** to give pyrazole **345** (Scheme 107). This cycloaddition reaction was performed at room temperature in under 5 h and was followed by hydrolysis using NaOH. After purification, pyrazole **345** was isolated in a 59% yield, demonstrating the bioorthogonality of this reaction.



Scheme 107. Cycloaddition of *exo*-**344** with diazophosphonate **310**

Formation of octyne *endo*-**341** was completed in a 37% yield compared to 60% of *exo*-**341** (Scheme 106). Due to the time constraints commercially available (1*R*,8*S*,9*s*)-bicyclo[6.1.0]non-4-yn-9-ylmethanol (*endo*-**344**) was used for subsequent reactions. The diazophosphonate compounds **320** and **319** were reacted with *endo*-**341** under the previous conditions to give their corresponding pyrazoles **346** and **347** (Scheme 108). Pyrazole **346** was isolated in a 66% yield after cycloaddition at room temperature and hydrolysis. Pyrazole **347** was isolated in a 34% crude yield after the hydrolysis reaction, however, still had a number of impurities present after multiple purification attempts, and so was not isolated pure.



Scheme 108. Synthesis of pyrazoles **346** and **347**

5.4 Conclusion

The 1,3-dipolar cycloaddition between a 1,3-dipole such as a diazo compound and a dipolarophile such as an alkyne, is an atom-economical strategy for the synthesis of functionalised pyrazoles. Synthesis of stabilised diazocompounds, such as diazophosphonates, were successfully prepared using the procedure developed within the Moody group in 2014 through the use of the oxidising reagent TsNIK. From this procedure, another member of the Moody group, Katie Ruffell, established the methodology for the synthesis of functionalised pyrazoles using these diazophosphonate compounds and alkynes in a catalyst-free approach. Reactions were conducted under reflux in a number of solvents and the was shown to be effective in both intra- and intermolecular cycloadditions.

Expanding the scope of this project to include other intermolecular cycloadditions, required the synthesis of several diazophosphonates that were reacted with a variety of commercially available alkynes. Most of the cycloaddition reactions proceeded well and in good yield, and with the addition of a hydrolysis step immediately after pyrazole formation, resulted in the isolation of one product. Regiochemistry in these examples was controlled by a combination of electronic and steric effects.

This catalyst-free procedure was also shown to be successful in bioorthogonal strain-promoted cycloadditions. Synthesis of the strained alkyne bicyclo[6.1.0]nonyne **338** outlined by Dommerhalt *et al.*, was performed to give the octyne **344** in moderate yield that was then used in a number of cycloaddition reactions. Reactions of the octyne with several diazophosphonates were conducted at room temperature in under 5 h, and as this is also a

catalyst-free approach requiring no external activation, can be classed as a bioorthogonal process.

6. Overall Conclusions and Future Work

Inhibition of the Keap1-Nrf2 protein-protein interaction (PPI) is thought to have therapeutic potential in several diseases including neurodegenerative conditions such as Alzheimer's and Parkinson's, as well as cardiovascular diseases and cancer. Disruption of this interaction results in the upregulation of the transcription factor Nrf2 and subsequently its gene products involved in defence against oxidative stress. The development of direct inhibitors of the PPI of Keap1 and Nrf2 that circumvent toxic off-target effects has progressed rapidly, with *in vitro* potencies of lead small molecules showing promising activities for the progression into *in vivo* studies. However, the development of drug-like PPI inhibitors remains challenging, making it ever more critical to explore new techniques to improve therapeutic potential. This project developed cyclic peptides that provide scaffolds that may display enhanced metabolic stability and induce conformational rigidity that may maximise the peptides interaction with its target. Of the endogenous ligands that bind to Keap1, this project focuses on p62, and its highly potent mutated binding sequence Ac-DPETGEL-OH (Chapter 1, Section 5.2) Portions of this sequence were cyclised through multiple methods as described below.

Chapter 2 focussed on the solution phase synthesis and cyclisation of the tripeptide Pro-Glu-Thr. Initial attempts of cyclisation using ring-closing metathesis proved difficult, with mostly starting material being isolated. After attempting the reaction with several linkers, catalysts and varying the reaction temperature, attention turned to head-to-tail cyclisation *via* amide coupling. This method required an orthogonal protecting group strategy. First developed was the Boc/Bn/Pac protecting group strategy. However, although synthesis of the fully protected peptide proceeded well, removal of the *C*-terminal Pac protecting group proved difficult. Removal of this group was low yielding and therefore the Pac group was replaced with the TMSE ester. Preparation of this fully protected linear peptide also proceeded well, with removal of the ester achieved using the reagent TASF in excellent yields. Removal of the Boc group and debenzylation of the side chains was performed using HCl in dioxane and hydrogenation with a $PdCl_2$ catalyst respectively. Cyclisation of the linear peptide was attempted using a variety of amide coupling conditions. However, racemisation of the *C*-terminal residue, threonine, resulted in the formation of a 3:1 ratio of diastereomers of the cyclic product. Reversing the cyclisation onto proline, resulted in a substantial decrease in yield.

As solution phase synthesis of the cyclic peptides was proving problematic, in Chapter 3 a number of solid phase techniques were investigated. First attempted was on-resin cyclisation using a labile linker in the form of benzotriazole. Literature precedent had been set for the preparation of cyclic peptides in this manner in high yields. Nevertheless, this technique failed to yield any cyclic peptide in this case and so cyclisation was then tried with solid phase synthesis of the linear peptide, followed by solution phase cyclisation. Once again upon cyclisation *via* amide coupling of the tripeptide and linker, racemisation of the threonine residue occurred. At this point in the project it was decided that a glycine residue, the proceeding amino acid in the natural peptide, should be added to the peptide portion of the molecule. Therefore, any cyclisation attempt was then between glycine and the linker preventing epimerisation. Using these linear peptides and the coupling reagent DMTMM, cyclic peptides **148**, **149a** and **149b** were prepared (Chapter 3, Section 3.2). Brief molecular modelling studies were performed on these compounds to show how they may potentially bind to the Keap1 protein (Chapter 3.3.1). NMR studies were also conducted and from these experiments, two distinct compounds were once again seen in the NMR spectra. As these compounds each showed one peak by mass spectrometry and HPLC, 2D NMR experiments were run. Both VT NMR experiments and TOCSY data proved insufficient to prove the presence of *cis*/*trans* isomers around the proline residue. However, data from the NOESY spectrum may have provided an indication that this may be the case (Chapter 3.3.2). Future work on this project would include more in-depth molecular modelling and NMR conformational studies on the three cyclic peptides **148**, **149a** and **149b**. Further work into this area, along with other studies such as electrospray ionisation (ESI), ion mobility spectrometry (IMS) and mass spectrometry may be used to examine the conformation of the peptides.[211,212] In addition to this, the activity of the compounds for inhibiting Keap1 would be tested in a cell based Nrf2 reporter assay. By testing the activity of these peptides to inhibit Keap1, this may help further investigation into other improved peptide inhibitors of this interaction.

As well as the synthesis of chain linkers, such as **148**, **149a** and **149b**, methods to prepare cyclic peptides with heterocyclic linkers was also attempted in Chapter 4. All methods of cyclisation used in this Chapter were also based on literature precedent. Performing a copper-catalysed azide alkyne cycloaddition to simultaneously ring close and form a 1,2,3-triazole proved challenging. Therefore, the triazole linker was first prepared and then coupling onto the linear peptide **174** and cyclised to give **175** (Chapter 4, Section 4.1). Cyclisation proved successful, though difficulties were encountered upon removal of copper

salts from the reaction mixture and so the cyclic compound was unable to be isolated pure. Cyclisation through the formation of a diyne was also performed using Glaser-Hay diyne coupling (Chapter 4, Section 4.2). Once again, difficult purification and low yields meant that this method was no longer investigated. Another cyclisation method that was attempted was through the formation of a 2,5-disubstituted 1,3,4-oxadiazole (Chapter 4, Section 4.3). Cyclisation *via* this approach was shown to be successful by mass spectrometry, though the results could not be replicated. The final method used a pyrazole linker. Preparation of the desired diazo compounds required for the 1,3-dipolar cycloaddition onto alkynes to yield pyrazoles was unsuccessful. Several protecting group strategies and oxidising conditions were attempted, though regrettably no desired product was isolated from these reactions. A different approach using *p*-toluene sulfonohydrazide gave the desired α-diazophosphonyl compound, though reaction to form the pyrazole was unsuccessful (Chapter 4, Section 4.4). The methodology developed for the synthesis of compounds **148**, **149a** and **149b** could also be extended to include some of the heterocyclic compounds where the linker was synthesised prior to cyclisation, such as the triazole linker. This might help to improve the purification issues encountered. Further effort should also be placed into the development of the diyne and pyrazole linkers, whose preparations were hampered by purification difficulties and time constraints.

Chapter 5 detailed the background of the synthesis of the pyrazole linker used in Chapter 4. This method uses a catalyst-free 1,3-dipolar cycloaddition of stabilised diazo compounds onto alkynes (Chapter 5, Section 5.2). Methodology developed in the group for the preparation of α-diazophosphonates employing the oxidising reagent TsNIK, was used to prepare the starting materials in various cycloaddition reactions. Most of the cycloaddition reactions performed proceeded in good yield, though all resulted in two products, the desired pyrazole and the phosphorylated pyrazole (**288** and **289**). Addition of a hydrolysis step immediately after pyrazole formation, pushed the reaction to completion and resulted in the sole isolation of the desired pyrazole. This catalyst-free procedure was also shown to be successful in bioorthogonal strain-promoted cycloadditions. Reactions of a strained octyne with several diazo compounds were conducted at room temperature in under 5 h, and as this is also a catalyst-free approach requiring no external activation, can be classed as a bioorthogonal process.

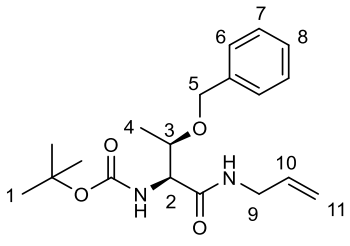
7. Experimental Procedures

7.1 General Experimental

Commercially available reagents were used without further purification unless otherwise stated. Flash chromatography was carried out using silica gel 60 A, with the eluent indicated. Thin layer chromatography was carried out using commercially available aluminium backed plates coated with Merck Kieselgel 60 F_{254} and visualised under UV light or staining with potassium permanganate solution. Preparative HPLC was conducted using Waters 1525 Binary HPLC pump on a reverse phase Waters 19x150 mm column, detecting peaks using wavelengths 210 nm and 280 nm. Automated solid phase peptide synthesis was done using a Biotage Initiator+ Alstra Synthesiser. Proton (400 MHz) and carbon (100 MHz) spectra were recorded on Bruker 400 MHz or 800 MHz instruments using an internal deuterium lock. Chemical shifts are quoted in parts per million (ppm) and coupling constants, *J*, are quoted in Hertz (Hz) and all spectra are referenced using deuterated solvents. The multiplicity of peaks reported with the following abbreviations: s, singlet; br s, broad singlet; d, doublet; t, triplet; q, quartet; quint, quintet; sept, septet; m, multiplet. In ^{13}C NMR, signals corresponding to CH, CH_2 and CH_3 signals were assigned from DEPT spectra. Electrospray ionisation (ESI) mass spectra were carried out on a Bruker microTOF mass spectrometer. Melting points were recorded using Electrothermal IA9200 apparatus. Infrared spectra were recorded on a Bruker Alpha series FT-IR spectrometer over 4000-600 cm^{-1}. Specific rotations were measured on an AA-1000 polarimeter and values are quoted in 10^{-1} $degcm^2g^{-1}$.

7.2 Experimental Procedures

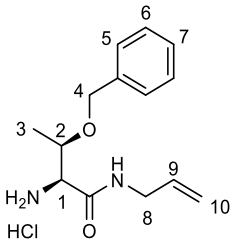
N-(*tert*-Butoxycarbonyl)-threonine(*O*-benzyl)-*O*-allylamide, **76**



N-(*tert*-Butoxycarbonyl)-*O*-benzyl-L-threonine, **74**, (3.00 g, 9.71 mmol) was dissolved in anhydrous THF (15 ml) and cooled to -20 °C. 4-Methylmorpholine (1.10 ml, 9.71 mmol) was added, followed by isobutyl chloroformate (1.25 ml, 9.71 mmol) under vigorous stirring. Allylamine, **75**, (0.8 ml, 10.7 mmol) was added and the mixture was warmed to room temperature and stirred for 2 h. The reaction mixture was concentrated under reduced

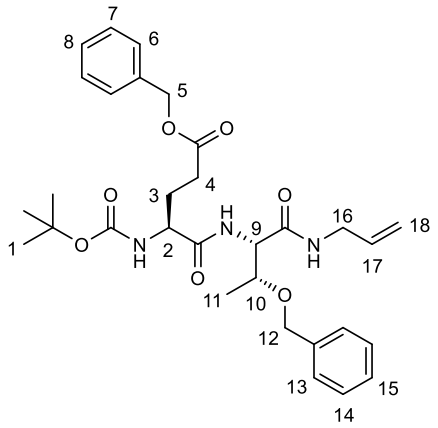
pressure, then water (30 ml) was added along with hydrochloric acid (1 M) adjusting the pH to 1. Ethyl acetate (30 ml) was added, the layers were separated, and the aqueous phase was re-extracted using ethyl acetate (2 x 30 ml). The organic extracts were combined, washed with a saturated solution of $NaHCO_3$ and a saturated solution of brine, dried using $MgSO_4$ and concentrated under reduced pressure to give the *title compound*, **76**, as a colourless solid (3.05 g, 8.76 mmol, 90%). **mp** 67-68 °C; **[α]$_D^{25}$** +9.00 (*c* 1, CH_3OH); **MS** (ESI^+) calcd for $C_{19}H_{28}N_2O$ [M+H] 349.2049, found 349.2125; **υ$_{max}$ (ATR)/cm^{-1}** 3332, 3311 (C-H), 3076, 1686 (C=O), 1645 (C=C), 1523; **^{1}H NMR** (400 MHz; $CDCl_3$) δ 7.36-7.28 (5H, m, ArH, H-6,7,8), 6.60 (1H, br s, NH), 5.88-5.78 (1H, m, CH, H-10), 5.51 (1H, br s, NH), 5.18 (1H, ddq, *J* 17.2, 10.3, 5.5, CH_2, H-11), 5.12 (1H, dq, *J* 11.7, 10.3, 2.8, 1.6, CH_2, H-11), 4.64 (1H, d, *J* 8.0, CH_2, H-5), 4.57 (1H, d, 8.0, CH_2, H-5), 4.30 (1H, br s, CH), 4.23 (1H, qd, *J* 6.3, 2.8, CH), 3.94-3.90 (2H, m, CH_2, H-9), 1.47 (9H, s, CH_3, H-1), 1.20 (3H, d, *J* 4.0, CH_3, H-4); **^{13}C NMR** (100 MHz; $CDCl_3$) δ 169.7 (C=O), 155.9 (C=O), 138.0 (C), 133.9 (CH), 128.4 (CH), 127.8 (CH), 127.7 (CH), 116.3 (CH_2), 80.1 (C), 74.8 (CH), 71.7 (CH_2), 57.8 (CH), 41.8 (CH_2), 28.7 (CH_3), 15.6 (CH_3). Data match literature values.[213]

Threonine(*O*-benzyl)-*O*-allylamide hydrochloride, **77**



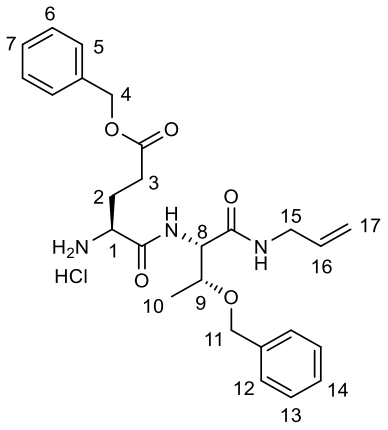
N-(*tert*-Butoxycarbonyl)-threonine(*O*-benzyl)-*O*-allylamide, **76**, (3.05 g, 8.76 mmol) was dissolved in HCl in dioxane (4 M, 10.0 ml) and the solution was stirred at room temperature for 2.5 h. The reaction mixture was concentrated under reduced pressure to give the *title compound*, **77**, as colourless gum (1.97 g, 7.94 mmol, quantitative yield). **[α]$_D^{25}$** +4.50 (*c* 1, CH_3OH); **MS** (ESI^+) calcd for $C_{14}H_{20}N_2O_2$ [M+Na] 271.2049, found 271.1412; **υ$_{max}$ (ATR)/cm^{-1}** 3214 (C-H), 3060, 1988, 1671 (C=O), 1644 (C=C); **^{1}H NMR** (400 MHz; $CDCl_3$) δ 8.37 (2H, br s, NH), 8.10 (1H, br s, NH), 7.34-7.23 (5H, m, ArH, H-5,6,7), 5.73 (1H, ddd, *J* 24.0, 12.0, 2.6, CH, H-9), 5.15 (1H, d, *J* 16.0, CH_2, H-10), 5.05 (1H, d, *J* 16.0, CH_2, H-10), 4.59 (2H, s, CH_2, H-4), 4.46 (1H, br s, CH), 4.24-4.21 (1H, m, CH), 3.88-3.68 (2H, m, CH_2, H-8), 1.34 (3H, d, *J* 4.0, CH_3, H-3); **^{13}C NMR** (100 MHz; $CDCl_3$) δ 166.9 (C=O), 133.5 (C), 133.3 (CH), 128.5 (CH), 128.1 (CH), 127.9 (CH), 116.8 (CH_2), 73.7 (CH), 71.5 (CH_2), 57.0 (CH), 42.1 (CH_2), 16.1 (CH_3).

N-(*tert*-Butoxycarbonyl)-glutamic acid(*O*-benzyl)-threonine(*O*-benzyl)-*O*-allylamide, **78**



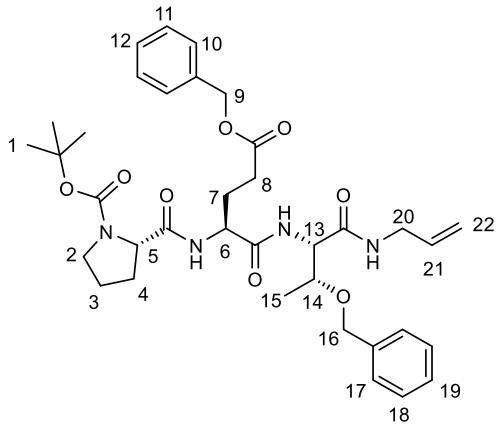
Threonine(*O*-benzyl)-*O*-allylamide hydrochloride, **77**, (1.97 g, 7.94 mmol) and *N*-(*tert*-butoxycarbonyl-*L*-glutamic acid 5-benzyl ester (2.68 g, 7.94 mmol) were dissolved in anhydrous DMF (20 ml). *N*,*N*-Diisopropylethylamine (9.67 ml, 55.6 mmol) was added, followed by HATU (6.04 g, 15.9 mmol) and the mixture was stirred at room temperature for 36 h. Ethyl acetate (200 ml) and water (200 ml) were added, the layers were separated and the organic phase was washed with water (2 x 200 ml), hydrochloric acid (1 M, 200 ml), a saturated solution of $NaHCO_3$ (200 ml), and aqueous LiCl (5 %, 200 ml), dried using $MgSO_4$ and concentrated under reduced pressure to give a brown solid. The crude product was purified by column chromatography eluting with 50% ethyl acetate in light petroleum to give the *title compound*, **78**, as a pale yellow solid (3.87 g, 6.83 mmol, 86%). **mp** 104-105 °C; **$[\alpha]_D^{25}$** +7.20 (*c* 1, CH_3OH); **MS** (ESI^+) calcd for $C_{31}H_{41}N_3O_7$ [M+H] 568.2945, found 568.3021; **υ_{max} (ATR)/cm^{-1}** 3297 (C-H), 3064, 1959, 1719 (C=O), 1686 (C=O), 1640 (C=C), 1523; **^{1}H NMR** (400 MHz; $CDCl_3$) δ 7.38-7.28 (10H, m, ArH, H-6,7,8,13,14,15), 7.06-7.02 (2H, br s, NH), 5.82 (1H, ddd, *J* 8.0, 12.0, 16.0, CH, H-17), 5.64 (1H, br s, NH), 5.20-5.08 (4H, m, CH_2, H-5,17), 4.61 (1H, d, *J* 12.0, CH_2, H-12), 4.52 (1H, d, *J* 12.0, CH_2, H-12), 4.47 (1H, d, *J* 8.0, CH), 4.37 (1H, br s, CH), 4.14-4.09 (1H, m, CH), 3.90 (2H, t, *J* 4.0, CH_2, H-16), 2.61-2.48 (2H, m, CH_2, H-4), 2.21 (1H, sex., *J* 8.0, CH_2, H-3), 2.06 (1H, sex., *J* 8.0, CH_2, H-3), 1.38 (9H, s, CH_3, H-1), 1.18 (3H, d, *J* 8.0, CH_3, H-11); **^{13}C NMR** (100 MHz; $CDCl_3$) δ 173.5 (C=O), 171.6 (C=O), 169.4 (C=O), 156.3 (C=O), 138.0 (C), 135.5 (C), 133.8 (CH), 128.6 (CH), 128.42 (CH), 128.40 (CH), 128.3 (CH), 127.8 (CH), 127.7 (CH), 116.3 (CH_2), 80.8 (C), 74.0 (CH), 71.7 (CH_2), 66.9 (CH_2), 57.2 (CH), 55.4 (CH), 42.1 (CH_2), 30.8 (CH_2), 28.2 (CH_3), 26.7 (CH_2), 16.4 (CH_3).

Glutamic acid(*O*-benzyl)-threonine(*O*-benzyl)-*O*-allylamide hydrochloride, **79**



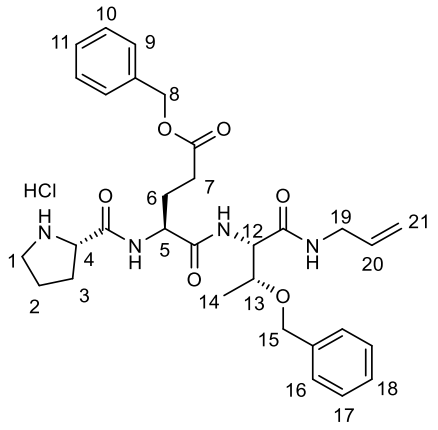
N-(*tert*-Butoxycarbonyl)-glutamic acid(*O*-benzyl)-threonine(*O*-benzyl)-*O*-allylamide, **78**, (3.87 g, 6.87 mmol) was dissolved in HCl in dioxane (4 M, 10.0 ml) and the solution was stirred at room temperature for 30 min. The reaction mixture was concentrated under reduced pressure to give the *title compound*, **79**, as a red gum (3.10 g, 6.64 mmol, quantitative yield). **$[\alpha]_D^{25}$** +17.8 (*c* 1, CH_3OH); **MS** (ESI^+) calcd for $C_{26}H_{33}N_3O_5$ [M+H] 468.2420, found 468.2511; **υ_{max} (ATR)/cm^{-1}** 3233 (C-H), 3032, 1968, 1729 (C=O), 1656 (C=C), 1528; **^{1}H NMR** (400 MHz; $CDCl_3$) δ 8.49 (2H, br s, NH), 8.20 (1H, d, *J* 8.0, NH), 7.41 (1H, br s, NH), 7.32-7.21 (10H, m, ArH, H-5,6,7,12,13,14), 5.73 (1H, ddd, *J* 12.0, 8.0, 4.0, CH, H-16), 5.11 (1H, dd, *J* 20.0, 4.0, CH_2), 5.06-4.98 (3H, m, CH_2), 4.77 (1H, dd, *J* 8.0, 4.0, CH), 4.56 (1H, d, *J* 12.0, CH_2, H-11), 4.50 (1H, d, *J* 12.0, CH_2, H-11), 4.37 (1H, br s, CH), 4.07-4.05 (1H, m, CH), 3.88-3.71 (2H, m, CH_2, H-15), 2.66 (2H, t, *J* 8.0, CH_2, H-3), 2.34-2.18 (2H, m, CH_2, H-2), 1.21 (3H, d, *J* 4.0, CH_3, H-10); **^{13}C NMR** (100 MHz; $CDCl_3$) δ 173.3 (C=O), 169.4 (C=O), 168.8 (C=O), 138.0 (C), 135.5 (C), 133.8 (CH), 128.5 (CH), 128.4 (CH), 128.3 (CH), 128.2 (CH), 127.9 (CH), 127.8 (CH), 116.4 (CH_2), 74.9 (CH), 71.4 (CH_2), 66.9 (CH_2), 57.5 (CH), 53.0 (CH), 42.0 (CH_2), 30.0 (CH_2), 26.6 (CH_2), 16.4 (CH_3).

N-(*tert*-Butoxycarbonyl)-proline-glutamic acid(*O*-benzyl)-threonine(*O*-benzyl)-*O*-allylamide, **80**



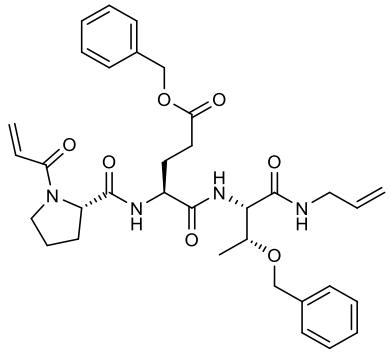
Glutamic acid(*O*-benzyl)-threonine(*O*-benzyl)-*O*-allylamide hydrochloride, **79**, (3.10 g, 6.44 mmol) and *N*-(*tert*-butoxycarbonyl)-L-proline (1.43 mg, 6.44 mmol) were dissolved in anhydrous DMF (30 ml). *N*,*N*-Diisopropylethylamine (8.10 ml, 46.5 mmol) was added, followed by HATU (5.01 g, 13.3 mmol) and the mixture was stirred at room temperature for 16 h. Ethyl acetate (300 ml) and water (300 ml) were added, the layers were separated and the organic phase was washed with water (2 x 300 ml), hydrochloric acid (1 M, 300 ml), a saturated solution of $NaHCO_3$ (300 ml), and aqueous LiCl (5 %, 300 ml), dried using $MgSO_4$ and concentrated under reduced pressure to give a brown solid. The crude product was purified by column chromatography eluting with 60% ethyl acetate in light petroleum to give the *title compound*, **80**, as a pale yellow solid (2.00 g, 3.01 mmol, 45%). **mp** 150-151 °C; $\mathbf{[\alpha]_D^{25}}$ -1.87 (*c* 1, CH_3OH); **MS** (ESI^+) calcd for $C_{36}H_{48}N_4O_8$ [M+H] 665.3472, found 665.3545; $\mathbf{\upsilon_{max}}$ **(ATR)/cm^{-1}** 3270 (C-H), 3086, 2103, 1737 (C=O), 1697 (C=O), 1633 (C=C), 1540, 1497; **^{1}H NMR** (400 MHz; $CDCl_3$) δ 7.90 (1H, br s, NH), 7.40-7.28 (10H, m, ArH, H-10,11,12,17,18,19), 7.14 (1H, br s, NH), 6.98 (1H, br s, NH), 5.84 (1H, ddd, *J* 16.0, 12.0, 8.0, CH, H-21), 5.19 (1H, d, *J* 16.0, CH_2, H-22), 5.14 (2H, s, CH_2, H-9), 5.09 (1H, d, *J* 16.0, CH_2, H-22), 4.62 (1H, d, *J* 12.0, CH_2, H-16), 4.53 (1H, d, *J* 12.0, CH_2, H-16), 4.50 (1H, d, *J* 8.0, CH), 4.32 (2H, br s, CH_2), 4.16 (1H, br s, CH), 3.97-3.88 (2H, m, CH_2), 3.44-3.33 (2H, m, CH_2), 2.61-2.50 (2H, m, CH_2), 2.24 (1H, br s, CH), 2.09-2.03 (2H, m, CH_2), 1.83 (2H, br s, CH_2), 1.44 (9H, s, CH_3, H-1), 1.16 (3H, d, *J* 8.0, CH_3, H-15); **^{13}C NMR** (100 MHz; $CDCl_3$) δ 173.6 (C=O), 173.5 (C=O), 171.2 (C=O), 169.5 (C=O), 155.7 (C=O), 138.3 (C), 135.6 (C), 134.0 (CH), 128.6 (CH), 128.5 (CH), 128.4 (CH), 128.2 (CH), 127.7 (CH), 127.6 (CH), 115.8 (CH_2), 80.6 (C), 73.9 (CH), 71.5 (CH_2), 66.7 (CH_2), 60.1 (CH), 57.4 (CH), 54.6 (CH), 47.1 (CH_2), 41.9 (CH_2), 30.7 (CH_2), 28.5 (CH_2), 28.3 (CH_3), 26.4 (CH_2), 24.6 (CH_2), 16.5 (CH_3).

Proline-glutamic acid(*O*-benzyl)-threonine(*O*-benzyl)-*O*-allylamide hydrochloride, **81**



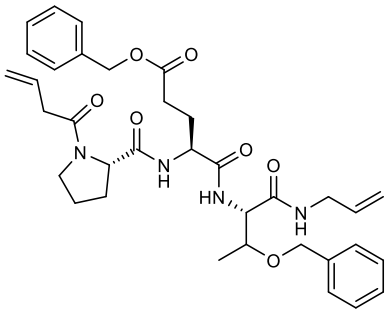
N-(*tert*-Butoxycarbonyl)-proline-glutamic acid(*O*-benzyl)-threonine(*O*-benzyl)-*O*-allylamide, **80**, (120 mg, 0.18 mmol) was dissolved HCl in dioxane (4 M, 1.00 ml) and the solution was stirred at room temperature for 1 h. The reaction mixture was concentrated under reduced pressure to give the *title compound*, **81**, as a colourless solid (100 mg, 0.18 mmol, quantitative yield). **mp** 120-121 °C; $[\alpha]_D^{25}$ +6.93 (*c* 1, CH_3OH); **MS** (ESI^+) calcd for $C_{31}H_{40}N_4O_6$ [M+H] 565.2948, found 565.3021; υ_{max} **(ATR)/cm^{-1}** 3061, 1961, 1729 (C=O), 1681 (C=O), 1657 (C=C), 1632; **^{1}H NMR** (400 MHz; CH_3OD) δ 7.38-7.29 (10H, m, ArH, H-9,10,11,16,17,18), 5.83 (1H, ddd, *J* 16.0, 12.0, 8.0, CH, H-20), 5.20 (1H, d, *J* 16.0, CH_2, H-21), 5.14 (2H, s, CH_2, H-8), 5.09 (1H, d, *J* 16.0, CH_2, H-21), 4.62 (1H, d, *J* 12.0, CH_2, H-15), 4.55-4.51 (2H, m, CH_2 and CH, H-15), 4.47-4.46 (1H, m, CH), 4.31-4.27 (1H, m, CH), 4.09-4.06 (1H, m, CH), 3.85-3.82 (2H, m, CH_2, H-19), 3.31-3.28 (2H, m, CH_2), 2.55-2.53 (2H, m, CH_2), 2.40-2.20 (2H, m, CH_2), 2.06-1.93 (4H, m, CH_2), 1.22 (3H, d, *J* 8.0, CH_3, H-14); **^{13}C NMR** (100 MHz; CH_3OD) δ 172.7 (C=O), 171.9 (C=O), 170.3 (C=O), 168.7 (C=O), 138.1 (C), 136.1 (C), 133.8 (CH), 128.2 (CH), 128.0 (CH), 127.9 (CH), 127.8 (CH), 127.7 (CH), 127.4 (CH), 115.1 (CH_2), 74.6 (CH), 70.9 (CH_2), 66.1 (CH_2), 59.5 (CH), 57.5 (CH), 53.1 (CH), 46.0 (CH_2), 41.5 (CH_2), 29.9 (CH_2), 29.6 (CH_2), 26.5 (CH_2), 23.6 (CH_2), 15.3 (CH_3).

N-Acryloyl-proline-glutamic acid(*O*-benzyl)-threonine(*O*-benzyl)-*O*-allylamide, **82**



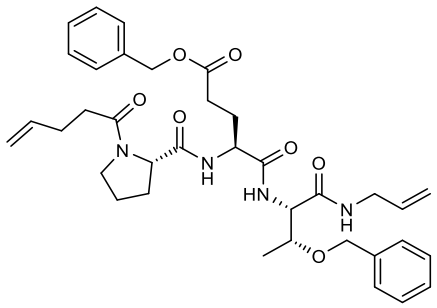
Proline-glutamic acid(*O*-benzyl)-threonine(*O*-benzyl)-*O*-allylamide hydrochloride, **81**, (100 mg, 0.18 mmol) was dissolved in anhydrous DMF (1.00 ml) and cooled to 0 °C. *N*,*N*-Diisopropylethylamine (31 µl, 0.53 mmol) was added followed by acryloyl chloride (16 µl, 0.18 mmol) and stirred at 0 °C for 2 h. Ethyl acetate (10 ml) and water (10 ml) were added, the layers were separated and the aqueous phase was re-extracted using ethyl acetate (2 x 10 ml). The organic extracts were combined, washed with a saturated solution of brine (10 ml), dried using $MgSO_4$ and concentrated under reduced pressure to give a pale orange solid. The crude product was purified by column chromatography eluting with 5% methanol in dichloromethane to give the *title compound*, **82**, as a colourless solid (42 mg, 0.07 mmol, 38%). **mp** 114-115 °C; **$[\alpha]_D^{25}$** +10.1 (*c* 1, CH_3OH); **MS** (ESI^+) calcd for $C_{34}H_{42}N_4O_7$ [M+H] 619.3053, found 619.3133; **υ_{max} (ATR)/cm^{-1}** 3084, 2106, 1736 (C=O), 1688 (C=O), 1632 (C=C), 1539, 1497; **^{1}H NMR** (400 MHz; $CDCl_3$) δ 8.07 (1H, d, *J* 8.0, NH), 7.39-7.25 (10H, m, ArH), 7.19 (1H, d, *J* 8.0, NH), 7.02 (1H, t, *J* 4.0, NH), 6.45 (1H, dd, *J* 20.0, 12.0, CH_2), 6.33 (1H, dd, *J* 20.0, 4.0, CH_2), 5.84 (1H, ddd, *J* 16.0, 12.0, 8.0, CH), 5.67 (1H, dd, *J* 16.0, 4.0, CH), 5.20 (1H, d, *J* 12.0, CH_2), 5.10 (2H, s, CH_2), 5.08 (1H, d, *J* 12.0, CH_2), 4.62-4.48 (4H, m, CH and CH_2), 4.39-4.28 (2H, m, CH_2), 4.00-3.81 (2H, m, CH_2), 3.71-3.66 (1H, m, CH), 3.58-3.52 (1H, m, CH), 2.58-2.49 (2H, m, CH_2), 2.23-1.88 (6H, m, CH_2), 1.18 (3H, d, *J* 4.0, CH_3); **^{13}C NMR** (100 MHz; $CDCl_3$) δ 173.8 (C=O), 172.7 (C=O), 171.1 (C=O), 169.5 (C=O), 165.8 (C=O), 138.4 (C), 135.5 (C), 134.1 (CH), 129.3 (CH_2), 128.6 (CH), 128.4 (CH), 128.3 (CH), 128.2 (CH), 127.8 (CH), 127.7 (CH), 127.6 (CH), 115.9 (CH_2), 74.1 (CH), 71.6 (CH_2), 66.8 (CH_2), 60.3 (CH), 57.3 (CH), 54.6 (CH), 47.4 (CH_2), 42.0 (CH_2), 30.7 (CH_2), 27.8 (CH_2), 26.1 (CH_2), 25.1 (CH_2), 16.6 (CH_3).

N-But-3-enoyl-proline-glutamic acid(*O*-benzyl)-threonine(*O*-benzyl)-*O*-allylamide, **83**



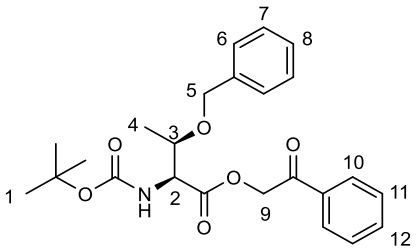
Proline-glutamic acid(*O*-benzyl)-threonine(*O*-benzyl)-*O*-allylamide hydrochloride, **81**, (250 mg, 0.44 mmol) and vinylacetic acid (38 µl, 0.44 mmol) were dissolved in DMF (2.5 ml). *N,N*-Diisopropylethylamine (0.46 ml, 2.66 mmol) was added, followed by HATU (337 mg, 0.89 mmol) and stirred at room temperature for 16 h. Ethyl acetate (30 ml) and water (30 ml) were added, the layers were separated and the organic phase was washed with water (2 x 30 ml), hydrochloric acid (1 M, 30 ml), a saturated solution of $NaHCO_3$ (30 ml), and aqueous LiCl (5 %, 30 ml), dried using $MgSO_4$ and concentrated under reduced pressure to give a yellow gum. The crude product was purified by column chromatography eluting with 10% methanol in dichloromethane to give the *title compound*, **83**, as a pale-yellow glass (180 mg, 0.28 mmol, 64%). $\mathbf{[\alpha]_D^{25}}$ -23.1 (*c* 1, CH_3OH); **MS** (ESI^+) calcd for $C_{35}H_{44}N_4O_7$ [M+H] 633.3283, found 633.3288; $\mathbf{\upsilon_{max}}$ **(ATR)/cm^{-1}** 3270 (C-H), 3082, 2975, 2930, 2873, 1736 (C=O), 1688 (C=O), 1632 (C=C), 1538; **^{1}H NMR** (400 MHz; $CDCl_3$) δ 7.91 (1H, d, *J* 8.0, NH), 7.37-7.27 (10H, m, ArH), 7.12 (1H, d, *J* 8.0, NH), 6.98 (1H, t, *J* 8.0, NH), 5.97-5.79 (2H, m, CH_2), 5.21-5.06 (5H, m, CH_2 and CH), 4.61 (1H, d, *J* 12.0, CH_2), 4.53 (1H, d, *J* 12.0, CH_2), 4.49 (1H, dd, *J* 8.0, 4.0, CH), 4.43-4.40 (1H, m, CH), 4.36-4.27 (2H, m, CH_2), 3.98-3.82 (2H, m, CH_2), 3.59-3.53 (1H, m, CH), 3.45-3.32 (1H, m, CH), 3.11-3.09 (2H, m, CH_2), 2.57-2.52 (2H, m, CH_2), 2.23-2.19 (1H, m, CH), 2.12-1.84 (6H, m, CH_2), 1.17 (3H, d, *J* 8.0, CH_3); **^{13}C NMR** (100 MHz; $CDCl_3$) δ 173.8 (C=O), 172.9 (C=O), 171.2 (C=O), 171.1 (C=O), 169.5 (C=O), 138.3 (C), 135.5 (C), 134.0 (CH), 130.6 (CH), 128.6 (CH), 128.4 (CH), 128.3 (CH), 128.2 (CH), 127.7 (CH), 127.6 (CH), 118.3 (CH_2), 115.9 (CH_2), 74.1 (CH), 71.6 (CH_2), 66.8 (CH_2), 60.1 (CH), 57.3 (CH), 54.6 (CH), 47.5 (CH_2), 42.0 (CH_2), 39.7 (CH_2), 30.8 (CH_2), 27.9 (CH_2), 26.2 (CH_2), 25.0 (CH_2), 16.5 (CH_3).

N-Pent-4-enoyl-proline-glutamic acid(*O*-benzyl)-threonine(*O*-benzyl)-*O*-allylamide, **84**



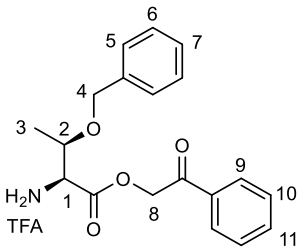
4-Pentenoic acid (51 µl, 0.50 mmol) and triethylamine (0.16 ml, 1.15 mmol) were dissolved in anhydrous dichloromethane (1.00 ml) and cooled to 0 °C. Isobutyl chloroformate (23 µl, 0.18 mmol) was added and stirred vigorously for 2 min. Proline-glutamic acid(*O*-benzyl)-threonine(*O*-benzyl)-*O*-allylamide hydrochloride, **81**, (250 mg, 0.45 mmol) and triethylamine (0.15 ml, 1.10 mmol) in anhydrous dichloromethane (1.00 ml) were added. The reaction mixture was then warmed to room temperature and stirred for 17 h. Dichloromethane (20 ml) and water (20 ml) were added, the layers were separated and the organic phase was washed with a saturated solution of $NaHCO_3$ (20 ml) and a saturated solution of brine (20 ml), dried using sodium sulfate and concentrated under reduced pressure to give a pale yellow gum. The crude product was purified by column chromatography eluting with 2% methanol in dichloromethane to give the *title compound*, **84**, as a pale-yellow glass (200 mg, 0.31 mmol, 70%). $\mathbf{[\alpha]_D^{25}}$ +3.88 (*c* 1, CH_3OH); **MS** (ESI^+) calcd for $C_{36}H_{46}N_4O_7$ [M+H] 647.3366, found 647.3453; $\mathbf{\upsilon_{max}}$ **(ATR)/cm^{-1}** 3271, 3081, 1735 (C=O), 1689 (C=O), 1632 (C=C), 1542, 1496; **^{1}H NMR** (400 MHz; $CDCl_3$) δ 7.95 (1H, d, *J* 8.0, NH), 7.40-7.25 (10H, m, ArH), 7.15 (1H, d, *J* 8.0, NH), 7.00 (1H, t, *J* 8.0, NH), 5.88-5.78 (1H, m, CH), 5.18 (1H, d, *J* 16.0, CH_2), 5.13 (2H, s, CH_2), 5.07-4.97 (3H, m, CH and CH_2), 4.61 (1H, d, *J* 12.0, CH_2), 4.55-4.49 (2H, m, CH and CH_2), 4.44-4.41 (1H, m, CH), 4.36-4.27 (2H, m, CH), 3.98-3.82 (2H, m, CH_2), 3.58-3.53 (1H, m, CH_2), 3.47-3.40 (1H, m, CH_2), 2.57-2.52 (2H, m, CH_2), 2.41-2.36 (4H, m, CH_2), 2.13-1.85 (6H, m, CH_2), 1.18 (3H, d, *J* 4.0, CH_3); **^{13}C NMR** (100 MHz; $CDCl_3$) δ 173.8 (C=O), 173.0 (C=O), 172.7 (C=O), 171.1 (C=O), 169.5 (C=O), 138.3 (C), 137.2 (CH), 135.5 (C), 134.0 (CH), 128.6 (CH), 128.4 (CH), 128.3 (CH), 128.2 (CH), 127.7 (CH), 127.6 (CH), 115.9 (CH_2), 115.4 (CH_2), 74.1 (CH), 71.5 (CH_2), 66.8 (CH_2), 60.1 (CH_2), 57.3 (CH), 54.6 (CH), 47.5 (CH_2), 42.0 (CH_2), 33.8 (CH_2), 30.8 (CH_2), 28.5 (CH_2), 27.9 (CH_2), 26.2 (CH_2), 25.0 (CH_2), 16.5 (CH_3).

N-(*tert*-Butoxycarbonyl)-threonine(*O*-benzyl)-*O*-phenacyl, **87**



N-(*tert*-Butoxycarbonyl)-*O*-benzyl-L-threonine, **74**, (3.0 g, 9.71 mmol) was dissolved in ethyl acetate (30 ml). Triethylamine (1.49 ml, 10.7 mmol) was added, followed by phenacyl bromide, **86**, (2.13 g, 10.7 mmol) and the reaction mixture was stirred at room temperature for 1.5 h. Ethyl acetate (100 ml) and saturated brine (100 ml) were added and the layers were separated. The organic phase was washed with a saturated solution of $NaHCO_3$ (100 ml), saturated brine (2 x 100 ml), dried using $MgSO_4$ and concentrated under reduced pressure to give a yellow gum. The crude product was purified by column chromatography eluting with 20 % ethyl acetate in light petroleum to give the *title compound*, **87**, as a yellow gum (3.0 g, 7.03 mmol, 72%) $\mathbf{[\alpha]_D^{25}}$ +8.66 (*c* 1, CH_3OH); **MS** (ESI^+) calcd for $C_{24}H_{29}NO_6$ [M+ $C_3H_5N_2$] 496.1995, found 496.2436; $\mathbf{\upsilon_{max}}$ **(ATR)/cm^{-1}** 3438, 1757 (C=O), 1703 (C=O), 1158 (C-O); **^{1}H NMR** (400 MHz; $CDCl_3$) δ 7.92 (2H, d, *J* 8.0, ArH), 7.64 (1H, t, *J* 8.0, ArH), 7.51 (2H, t, *J* 8.0, ArH), 7.37-7.32 (4H, m, ArH), 7.30-7.26 (1H, m, ArH), 5.44-5.40 (1H, m, CH_2, H-9), 5.29 (1H, d, *J* 16.4, CH_2, H-9), 4.64 (1H, d, *J* 11.4, CH_2, H-5), 4.60 (1H, d, *J* 11.5, CH_2, H-5), 4.48 (1H, dd, *J* 9.5, 2.1, CH), 4.36 (1H, qd, *J* 6.2, 2.1, CH), 1.48 (9H, s, CH_3, H-1), 1.35 (3H, d, *J* 6.3, CH_3, H-4); **^{13}C NMR** (100 MHz; $CDCl_3$) δ 191.5 (C=O), 170.8 (C=O), 156.2 (C=O), 138.3 (C), 134.2 (C), 133.9 (CH), 128.9 (CH), 128.3 (CH), 128.0 (CH), 127.8 (CH), 127.7 (CH), 79.9 (C), 74.7 (CH_2), 71.3 (CH_2), 66.4 (CH), 58.2 (CH), 28.3 (CH_3), 16.8 (CH_3).

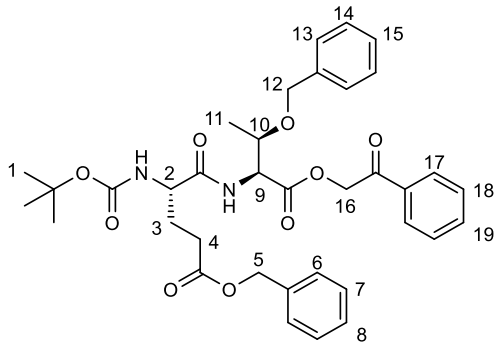
Threonine(*O*-benzyl)-*O*-phenacyl trifluoroacetate, **88**



N-(*tert*-Butoxycarbonyl)-threonine(*O*-benzyl)-*O*-phenacyl, **87**, (3.0 g, 7.03 mmol) was dissolved in anisole (2 ml) and cooled to 0 °C. Trifluoroacetic acid (8.0 ml) was added and the reaction mixture was stirred at 0 °C for 1 h then warmed to room temperature and

concentrated under reduced pressure. Diethyl ether (10 ml) was added to the residue and a colourless solid formed. The solid was filtered and washed with diethyl ether to give the *title compound*, **88**, as a colourless solid (2.27 g, 6.94 mmol, 98%). **mp** 106-107 °C; **[α]$_D^{25}$** +13.96 (*c* 1, CH_3OH); **MS** (ESI^+) calcd for $C_{19}H_{21}NO_4$ [M+H] 328.1471, found 328.1543; **υ_{max} (ATR)/cm^{-1}** 3270, 1756 (C=O), 1673 (C=O), 1201 (C-O); **^{1}H NMR** (400 MHz; CH_3OD) δ 7.99 (2H, d, *J* 8.0, ArH), 7.70 (1H, t, *J* 8.0, ArH), 7.57 (2H, t, *J* 8.0, ArH), 7.43-7.29 (5H, m, ArH), 5.61 (1H, d, *J* 16.0, CH_2, H-8), 5.55 (1H, d, *J* 16.0, CH_2, H-8), 4.75 (1H, d, *J* 12.0, CH_2, H-4), 4.64 (1H, d, *J* 11.5, CH_2, H-4), 4.40-4.34 (1H, m, CH), 4.28 (1H, d, *J* 3.8, CH), 1.48 (3H, d, *J* 6.5, CH_3, H-3); **^{13}C NMR** (100 MHz; CH_3OD) δ 191.6 (C=O), 167.3 (C=O), 138.0 (C), 134.0 (CH), 133.8 (C), 128.7 (CH), 128.1 (CH), 128.0 (CH), 127.6 (CH), 127.5 (CH), 72. 1 (CH), 71.0 (CH_2), 67.5 (CH_2), 57.5 (CH), 15.3 (CH_3).

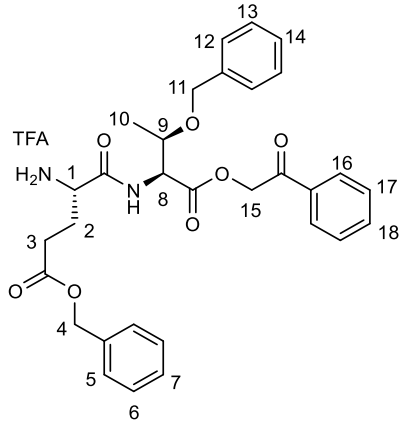
<u>*N*-(*tert*-Butoxycarbonyl)-glutamic acid(*O*-benzyl)-threonine(*O*-benzyl)-*O*-phenacyl, **89**</u>



Threonine(*O*-benzyl)-*O*-phenacyl trifluoroacetate, **88**, (2.27 g, 6.94 mmol) was dissolved in anhydrous DMF (30 ml) and *N*-(*tert*-butoxycarbonyl)-L-glutamic acid 5-benzyl ester (2.34 g, 6.94 mmol) was added, followed by HATU (5.27 g, 13.9 mmol) and anhydrous *N,N*-diisopropylethylamine (7.2 ml, 41.6 mmol) and the reaction mixture was stirred at room temperature for 18 h. Ethyl acetate (300 ml) was added followed by saturated brine (300 ml). The layers were separated and the organic phase was washed with saturated brine (3 x 300 ml), hydrochloric acid (1 M, 300 ml), a saturated solution of $NaHCO_3$ (300 ml) and aqueous LiCl (5%, 300 ml), dried using $MgSO_4$ and concentrated under reduced pressure to give a dark orange gum. The crude product was purified by column chromatography eluting with 20 % ethyl acetate in light petroleum to give *title compound*, **89**, as a yellow gum (2.82 g, 4.37 mmol, 63%). **[α]$_D^{25}$** +4.27 (*c* 1, CH_3OH); **MS** (ESI^+) calcd for $C_{36}H_{42}N_2O_9$ [M+H] 647.2890, found 647.2963; **υ_{max} (ATR)/cm^{-1}** 3352, 1702 (C=O), 1671 (C=O), 1597, 1158 (C-O); **^{1}H NMR** (400 MHz; $CDCl_3$) δ 7.88 (2H, d, *J* 8.0, ArH), 7.62 (1H, t, *J* 7.4, ArH), 7.49 (2H, t, *J* 7.4, ArH), 7.37-7.27 (10H, m, ArH), 6.95 (1H, br s, NH), 5.36 (1H, d, *J* 16.4, CH_2, H-16), 5.27 (1H, d, *J* 16.4, CH_2, H-

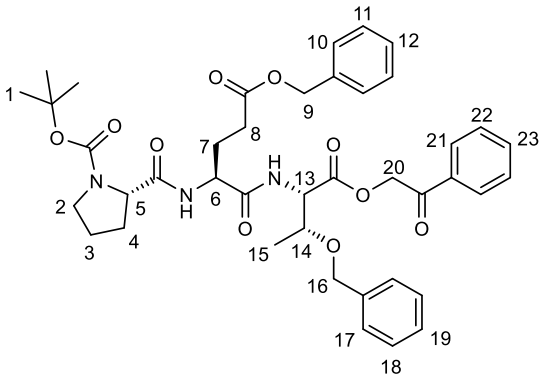
16), 5.09 (2H, s, CH_2, H-5), 4.78 (1H, dd, *J* 8.9, 2.2, CH), 4.66 (1H, d, *J* 11.6, CH_2, H-12), 4.59 (1H, d, *J* 11.6, CH_2, H-12), 4.38-4.34 (2H, m, CH), 2.57-2.52 (2H, m, CH_2, H-4), 2.23-2.18 (1H, m, CH_2, H-3), 2.02-1.94 (1H, m, CH_2, H-3), 1.44 (9H, s, CH_3, H-1), 1.30 (3H, d, *J* 6.3, CH_3, H-11); **^{13}C NMR** (100 MHz; $CDCl_3$) δ 191.4 (C=O), 173.1 (C=O), 172.2 (C=O), 171.3 (C=O), 170.0 (C=O), 138.2 (C), 135.9 (C), 134.2 (CH), 134.1 (C), 134.0 (CH), 129.0 (CH), 128.6 (CH), 128.4 (CH), 128.3 (CH), 128.1 (CH), 127.9 (CH), 127.8 (CH), 80.0 (C), 74.3 (CH), 71.3 (CH_2), 66.6 (CH_2), 66.5 (CH_2), 60.5 (CH_2), 56.8 (CH), 53.6 (CH), 30.4 (CH_2), 28.4 (CH_3), 14.3 (CH_3).

Glutamic acid(*O*-benzyl)-threonine(*O*-benzyl)-*O*-phenacyl trifluoroacetate, **90**



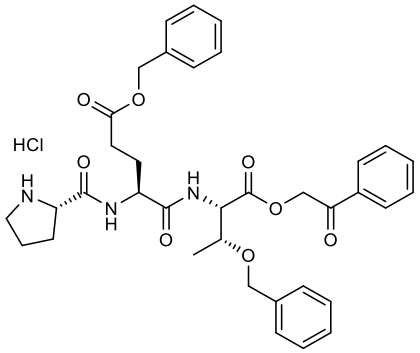
N-(*tert*-Butoxycarbonyl)-glutamic acid(*O*-benzyl)-threonine(*O*-benzyl)-*O*-phenacyl, **89**, (2.82 g, 4.37 mmol) was dissolved in anisole (1.5 ml) and cooled to 0 °C. Trifluoroacetic acid (6.0 ml) was added and the reaction mixture was stirred at 0 °C for 1 h then warmed to room temperature and concentrated under reduced pressure. Diethyl ether (10 ml) was added to the residue and removed under reduced pressure to give a red gum. The crude product was purified by column chromatography eluting using 50 % ethyl acetate in light petroleum to remove anisole and then flushing with 10 % MeOH in CH_2Cl_2 to give the *title compound*, **90**, as a red solid (2.19 g, 4.01 mmol, 92%). **mp** 74-75 °C; **$[\alpha]_D^{25}$** +8.89 (*c* 1, CH_3OH); **MS** (ESI^+) calcd for $C_{31}H_{34}N_2O_7$ [M+H] 547.2366, found 547.2439; **υ_{max} (ATR)/cm^{-1}** 2934, 1673 (C=O), 1200 (C-O); **^{1}H NMR** (400 MHz; CH_3OD) δ 7.95 (2H, d, *J* 8.0, ArH), 7.68 (1H, t, *J* 8.0, ArH), 7.54 (2H, t, *J* 8.0 ArH), 7.40-7.25 (10H, m, ArH), 5.45 (2H, s, CH_2, H-15), 5.07 (2H, s, CH_2, H-4), 4.85 (1H, d, *J* 2.7, CH), 4.68 (1H, d, *J* 11.4, CH_2, H-11), 4.59 (1H, d, *J* 11.4, CH_2, H-11), 4.41 (1H, qd, *J* 6.3, 2.7, CH), 4.15 (1H, t, *J* 6.6, CH), 2.73-2.60 (2H, m, CH_2, H-3), 2.29-2.16 (2H, m, CH_2, H-2), 1.34 (3H, d, *J* 6.3, CH_3, H-10). **^{13}C NMR** (100 MHz; CH_3OD) δ 192.2 (C=O), 172.4 (C=O), 169.6 (C=O), 169.0 (C=O), 138.2 (C), 135.9 (C), 134.0 (C), 133.8 (CH), 128.7 (CH), 128.1 (CH), 127.92 (CH), 127.90 (CH), 127.8 (CH), 127.7 (CH), 127.5 (CH), 127.4 (CH), 74.0 (CH), 71.1 (CH_2), 66.7 (CH_2), 66.2 (CH_2), 57.2 (CH), 52.0 (CH), 28.7 (CH_2), 26.4 (CH_2), 15.4 (CH_3).

N-(*tert*-Butoxycarbonyl)-proline-glutamic acid(*O*-benzyl)-threonine(*O*-benzyl)-*O*-phenacyl, **91**



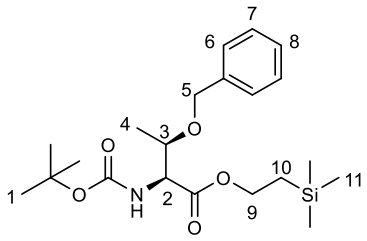
Glutamic acid(*O*-benzyl)-threonine(*O*-benzyl)-*O*-phenacyl trifluoroacetate, **90**, (2.19 g, 4.07 mmol) and *N*-(*tert*-butoxycarbonyl)-proline (862 mg, 4.01 mmol) were dissolved in anhydrous DMF (20 ml). HATU (3.04 g, 8.02 mmol) was added, followed by anhydrous *N,N*-diisopropylamine (3.5 ml, 20.1 mmol) and the reaction mixture was stirred at room temperature for 40 h. Ethyl acetate (200 ml) and saturated brine (200 ml) were added. The layers were separated and the organic phase was washed with saturated brine (3 x 200 ml), hydrochloric acid (1 M, 300 ml), a saturated solution of $NaHCO_3$ (300 ml) and aqueous LiCl (5%, 300ml), dried using $MgSO_4$ and concentrated under reduced pressure to give a dark orange gum. The crude product was purified by column chromatography eluting with 50 % ethyl acetate in light petroleum to give the *title compound*, **91**, as a yellow gum (1.0 g, 1.35 mmol, 34%). **$[\alpha]_D^{25}$** -7.11 (*c* 1, CH_3OH); **MS** (ESI^+) calcd for $C_{41}H_{49}N_3O_{10}$ [M+H] 744.3418, found 744.3491; **υ_{max} (ATR)/cm^{-1}** 3294, 1734 (C=O), 1658 (C=O), 1598, 1159 (C-O); **^{1}H NMR** (400 MHz; $CDCl_3$) δ 7.88 (2H, d, *J* 8.0, ArH), 7.63 (1H, t, *J* 7.4, ArH), 7.50 (2H, t, *J* 7.7, ArH), 7.42 (1H, br s, NH), 7.38-7.25 (10H, m, ArH), 6.96 (1H, br s, NH), 5.36 (1H, d, *J* 16.4, CH_2, H-20), 5.28 (1H, d, *J* 16.4, CH_2, H-20), 5.09 (2H, s, CH_2, H-9), 4.77 (1H, dd, *J* 8.9, 2.3, CH), 4.67-4.57 (3H, m, CH and CH_2), 4.36 (1H, br s, CH), 4.26 (1H, br s, CH), 3.48 (2H, br s, CH_2), 2.56-2.50 (2H, m, CH_2), 2.22 (2H, br s, CH_2), 2.04-1.97 (2H, m, CH_2), 1.90-1.85 (2H, m, CH_2), 1.44 (9H, s, CH_3), 1.29 (3H, d, *J* 6.4, CH_3, H-15); **^{13}C NMR** (100 MHz; $CDCl_3$) δ 191.3 (C=O), 173.0 (C=O), 172.3 (C=O), 171.5 (C=O), 171.0 (C=O), 169.9 (C=O), 138.2 (C), 135.8 (C), 134.2 (CH), 134.1 (C), 128.9 (CH), 128.5 (CH), 128.3 (CH), 128.2 (CH), 128.1 (CH), 128.0 (CH), 127.8 (CH), 127.7 (CH), 80.4 (C), 74.1 (CH), 71.2 (CH_2), 66.5 (CH_2), 60.4 (CH), 56.8 (CH), 52.3 (CH), 47.0 (CH_2), 30.2 (CH_2), 28.6 (CH_2), 28.3 (CH_3), 28.2 (CH_2), 21.1 (CH_2), 16.9 (CH_3).

Proline-glutamic acid(*O*-benzyl)-threonine(*O*-benzyl)-*O*-phenacyl hydrochloride, **92**



N-(*tert*-Butoxycarbonyl)-proline-glutamic acid(*O*-benzyl)-threonine(*O*-benzyl)-*O*-phenacyl, **91**, (500 mg, 0.27 mmol) was dissolved in HCl in dioxane (4 M, 2.5 ml). The mixture was stirred at room temperature for 1 h and then concentrated under reduced pressure to give the *title compound*, **92**, as a pale-yellow gum (161 mg, 0.25 mmol, 93%). $\mathbf{[\alpha]_D^{25}}$ +2.77 (*c* 1, CH_3OH); **MS** (ESI^+) calcd for $C_{36}H_{41}N_3O_8$ [M+H] 644.2894, found 644.2977; $\mathbf{\upsilon_{max}}$ **(ATR)/cm^{-1}** 3303, 1665 (C=O), 1199 (C-O); **^{1}H NMR** (400 MHz; CH_3OD) δ 8.66 (1H, d, *J* 7.2, NH), 8.19 (1H, d, *J* 9.0, NH), 7.94 (2H, dd, *J* 8.4, 1.2, ArH), 7.66 (1H, t, *J* 8.0, ArH), 7.52 (2H, t, *J* 7.7, ArH), 7.38-7.25 (10 H, m, ArH), 5.43 (2H, s, CH_2), 5.06 (2H, s, CH_2), 4.77 (1H, dd, *J* 9.0, 2.6, CH), 4.65 (3H, m, CH_2 and CH), 4.36-4.28 (2H, m, CH_2), 3.33-3.27 (2H, m, CH_2), 2.55 (2H, t, *J* 7.8, CH_2), 2.37 (1H, sex., *J* 8.0, CH), 2.18 (1H, sex., *J* 8.0, CH), 2.07-1.94 (4H, m, CH_2), 1.28 (3H, d, *J* 6.3, CH_3); **^{13}C NMR** (100 MHz; CH_3OD) δ 192.3 (C=O), 172.8 (C=O), 172.3 (C=O), 169.8 (C=O), 168.3 (C=O), 138.3 (C), 136.1 (C), 134.1 (C), 133.8 (CH), 128.7 (CH), 128.1 (CH), 127.93 (CH), 127.90 (CH), 127.79 (CH), 127.77 (CH), 127.5 (CH), 127.3 (CH), 74.3 (CH), 71.0 (CH_2), 66.7 (CH_2), 66.6 (CH_2), 66.0 (CH_2), 59.6 (CH), 56.9 (CH), 52.9 (CH), 46.1 (CH_2), 29.7 (CH_2), 26.8 (CH_2), 23.6 (CH_2), 15.5 (CH_3).

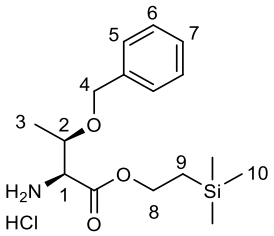
N-(*tert*-Butoxycarbonyl)-threonine(*O*-benzyl)-*O*-(trimethylsilyl)ethyl ester, **96**



N-(*tert*-Butoxycarbonyl)-*O*-benzyl-L-threonine, **74**, (2.5 g, 8.09 mmol) was dissolved in a 1 : 1 solution of DMF : dichloromethane (12.5 ml : 12.5 ml). Trimethylsilylethanol, **95**, (1.38 ml, 9.71 mmol) was added followed by HBTU (4.0 g, 10.5 mmol), triethylamine (1.5 ml, 10.5 mmol) and 4-(dimethylamino)pyridine (99 mg, 0.81 mmol) and stirred at room temperature

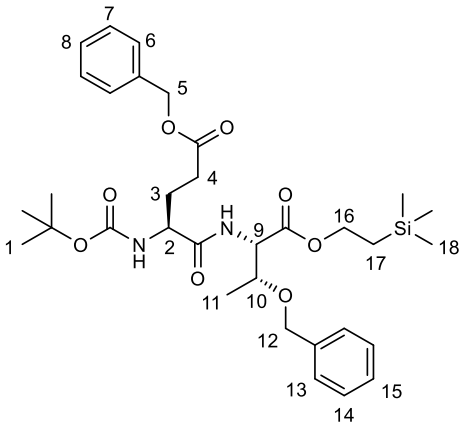
for 24 h. Water (100ml) and diethyl ether (100 ml) were added, the layers were separated and the organic phase was washed with water (2 x 100 ml) and brine (3 x 100 ml), before drying with $MgSO_4$ and concentrating under reduced pressure to give a colourless oil. The crude product was purified by column chromatography eluting with 25% ethyl acetate in light petroleum to give the *title compound*, **96**, as a colourless oil (2.35 g, 5.75 mmol, 71%). **$[\alpha]_D^{25}$** +17.1 (*c* 1, CH_3OH); **MS** (ESI^+): calcd for $C_{21}H_{35}N_1O_5Si$ $[M+H]^+$ 410.2357, found 410.2361; **υ_{max} (ATR)/cm^{-1}** 3064, 2976, 2326, 1715 (C=O), 1619 (C=O); **^{1}H NMR** (400 MHz; $CDCl_3$) δ 7.33-7.25 (5H, m, ArH, H-6,7,8), 5.30 (1H, d, *J* 9.7, CH), 4.57 (1H, d, *J* 11.8, CH_2, H-5), 4.38 (1H, d, *J* 11.8, CH_2, H-5), 4.28 (1H, dd, *J* 9.8, 2.1, CH), 4.20-4.10 (2H, m, CH_2, H-9), 1.46 (9H, s, CH_3, H-1), 1.27 (3H, d, *J* 6.3, CH_3, H-4), 0.96-0.86 (2H, m, CH_2, H-10), 0.04 (9H, s, CH_3, H-11); **^{13}C NMR** (100 MHz; $CDCl_3$) δ 171.2 (C=O), 156.2 (C=O), 138.0 (C), 128.3 (CH), 127.7 (CH), 127.7 (CH), 79.6 (C), 74.5 (CH), 70.8 (CH_2), 63.6 (CH_2), 58.4 (CH), 28.3 (CH_3), 17.3 (CH_2), 16.2 (CH_3), -1.55 (CH_3).

Threonine(*O*-benzyl)-*O*-(trimethylsilyl)ethyl ester hydrochloride, **97**



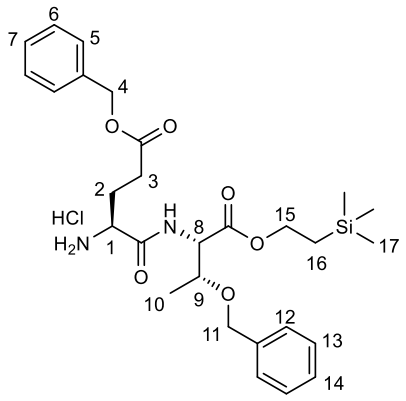
N-(*tert*-Butoxycarbonyl)-threonine(*O*-benzyl)-*O*-(trimethylsilyl)ethyl ester, **96**, (2.35 g, 5.75 mmol) was dissolved in HCl in dioxane (4 M, 5.0 ml) and stirred at room temperature for 1 h. The reaction mixture was then concentrated under reduced pressure to give the *title compound*, **97**, as a colourless gum (1.77 g, 5.73 mmol, quantitative yield). **$[\alpha]_D^{25}$** -35.8 (*c* 1, CH_3OH); **MS** (ESI^+): calcd for $C_{16}H_{27}N_1O_3Si$ $[M+H]^+$ 310.1833, found 310.1831; **υ_{max} (ATR)/cm^{-1}** 2952, 2895, 1739 (C=O); **^{1}H NMR** (400 MHz; CH_3OD) δ 7.40-7.30 (5H, m, ArH, H-5,6,7), 4.72 (1H, d, *J* 11.9, CH_2, H-4), 4.48 (1H, d, *J* 12.0, CH_2, H-4), 4.30-4.25 (1H, m, CH), 4.23-4.19 (2H, m, CH_2, H-8), 4.09 (1H, d, *J* 4.0, CH), 1.42 (3H, d, *J* 6.3, CH_3, H-3), 1.00-0.94 (2H, m, CH_2, H-9), -0.06 (9H, s, CH_3, H-10); **^{13}C NMR** (100 MHz; $CDCl_3$) δ 167.5 (C=O), 137.5 (C), 128.3 (CH), 128.0 (CH), 127.7 (CH), 72.0 (CH), 70.7 (CH_2), 65.1 (CH_2), 57.7 (CH), 17.3 (CH_2), 16.8 (CH_3), -1.58 (CH_3).

N-(*tert*-Butoxycarbonyl)-glutamic acid(*O*-benzyl)-threonine(*O*-benzyl)-*O*-(trimethylsilyl)ethyl ester, **98**



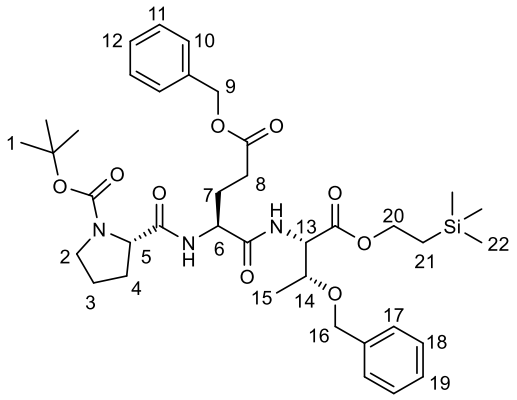
Threonine(*O*-benzyl)-*O*-(trimethylsilyl)ethyl ester hydrochloride, **97**, (1.77 g, 5.73 mmol) was dissolved in anhydrous DMF (17 ml). *N*-(*tert*-butoxycarbonyl)-L-glutamic acid 5-benzyl ester (1.93 g, 5.73 mmol) was added, followed by *N,N*-diisopropylethylamine (6.0 ml, 34.4 mmol) and HATU (4.35 g, 11.5 mmol) and stirred at room temperature for 16 h. The reaction mixture was diluted with ethyl acetate (100 ml) and water (100 ml). The layers were separated, and the organic phase was washed with water (2 x 100 ml), hydrochloric acid (1 M, 100 ml), a saturated solution of $NaHCO_3$ (100 ml) and saturated brine (100 ml), then dried using $MgSO_4$ and concentrated under reduced pressure to give a pale pink gum. The crude product was purified by column chromatography eluting with 25% ethyl acetate in light petroleum to give the *title compound*, **98**, as a pale-yellow gum (3.3 g, 5.25 mmol, 92%). **$[\alpha]_D^{25}$** +1.87 (*c* 1, CH_3OH); **MS** (ESI^+): calcd for $C_{33}H_{48}N_2O_8Si$ $[M+H]^+$ 629.3253, found 629.3273; **υ_{max} (ATR)/cm^{-1}** 3328, 3023, 2952, 1731 (C=O), 1717 (C=O), 1668 (C=O); **^{1}H NMR** (400 MHz; $CDCl_3$) δ 7.37-7.28 (10H, m, ArH, H-6,7,8, 13,14,15), 5.32 (1H, s, CH), 5.14 (2H, s, CH_2, H-5), 4.62 (1H, s, CH), 4.59 (1H, d, *J* 12.0, CH_2, H-12), 4.41 (1H, d, *J* 12.0, CH_2, H-12), 4.21-4.17 (1H, m, CH), 4.14-4.10 (2H, m, CH_2, H-16), 2.58 (2H, td, *J* 7.3, 2.4, CH_2, H-4), 2.23 (1H, sex., *J* 8.0, CH_2, H-3), 1.99 (1H, sex., *J* 8.0, CH_2, H-3), 1.45 (9H, s, CH_3, H-1), 1.24 (3H, d, *J* 6.3, CH_3, H-11), 0.98-0.88 (2H, m, CH_2, H-17), 0.04 (9H, s, CH_3, H-18); **^{13}C NMR** (100 MHz; $CDCl_3$) δ 173.0 (C=O), 171.9 (C=O), 171.2 (C=O), 170.3 (C=O), 137.9 (C), 135.8 (C), 128.6 (CH), 128.4 (CH), 128.34 (CH), 128.30 (CH), 128.2 (CH), 127.8 (CH), 80.0 (C), 74.0 (CH), 70.7 (CH_2), 66.5 (CH_2), 63.9 (CH_2), 56.9 (CH), 53.6 (CH), 30.4 (CH_2), 28.3 (CH_3), 28.0 (CH_2), 17.4 (CH_2), 16.3 (CH_3), -1.55 (CH_3).

Glutamic acid(*O*-benzyl)-threonine(*O*-benzyl)-*O*-(trimethylsilyl)ethyl ester hydrochloride, **99**



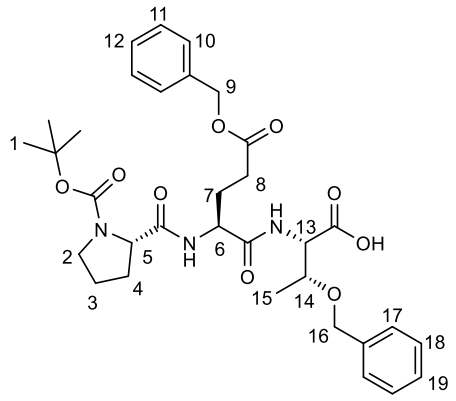
N-(*tert*-Butoxycarbonyl)-glutamic acid(*O*-benzyl)-threonine(*O*-benzyl)-*O*-(trimethylsilyl)ethyl ester, **98**, (3.3 g, 5.25 mmol) was dissolved in HCl in dioxane (4 M, 7.0 ml) and stirred at room temperature for 1 h. The reaction mixture was concentrated under reduced pressure to give the *title compound*, **99**, as a pale orange gum (2.7 g, 5.25 mmol, quantitative yield). **[α]$_D^{25}$** +31.1 (*c* 1, CH_3OH); **MS** (ESI^+): calcd for $C_{28}H_{40}N_2O_6Si$ $[M+H]^+$ 529.2718, found 529.2736; **υ_{max} (ATR)/cm^{-1}** 3031, 2951, 1731 (C=O), 1684 (C=O); **^{1}H NMR** (400 MHz; $CDCl_3$) δ 7.31-7.27 (10H, m, ArH, H-5, 6,7,12,13,14), 5.11-5.03 (2H, m, CH_2, H-4), 4.67 (1H, d, *J* 11.9, CH), 4.60-4.56 (2H, m, CH and CH_2, H-11), 4.41 (1H, d, *J* 11.9, CH_2, H-11), 4.21-4.18 (1H, m, CH), 4.15-4.08 (2H, m, CH_2, H-15), 2.79-2.74 (2H, m, CH_2, H-3), 2.36 (1H, br s, CH_2, H-2), 2.16 (1H, br s, CH_2, H-2), 1.31 (3H, d, *J* 6.3, CH_3, H-10), 0.92-0.89 (2H, m, CH_2, H-16), 0.00 (9H, s, CH_3, H-17); **^{13}C NMR** (100 MHz; $CDCl_3$) δ 173.3 (C=O), 170.1 (C=O), 169.0 (C=O), 137.8 (C), 135.7 (C), 128.5 (CH), 128.4 (CH), 128.3 (CH), 128.1 (CH), 127.8 (CH), 127.7 (CH), 74.5 (CH), 70.9 (CH_2), 66.7 (CH_2), 64.0 (CH_2), 57.0 (CH), 52.4 (CH), 29.8 (CH_2), 26.5 (CH_2), 17.3 (CH_2), 16.7 (CH_3), -1.58 (CH_3).

N-(*tert*-Butoxycarbonyl)-proline-glutamic acid(*O*-benzyl)-threonine(*O*-benzyl)-*O*-(trimethyl silyl)ethyl ester, **100**



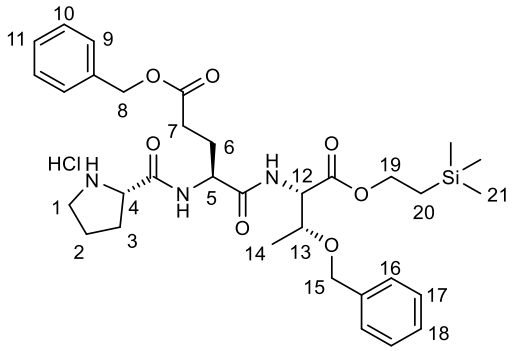
Glutamic acid(*O*-benzyl)-threonine(*O*-benzyl)-*O*-(trimethylsilyl)ethyl ester hydrochloride, **99**, (2.7 g, 5.11 mmol) was dissolved in anhydrous DMF (20 ml). *N*-(*tert*-Butoxycarbonyl)proline (1.10 g, 5.11 mmol) was added, followed by *N,N*-diisopropylethylamine (5.3 ml, 30.7 mmol) and HATU (3.88 g, 10.2 mmol) and the reaction mixture was stirred at room temperature for 16 h. The reaction mixture was diluted with ethyl acetate (100 ml) and water (100 ml). The layers were separated, and the organic phase was washed with water (2 x 100 ml), hydrochloric acid (1 M, 100 ml), a saturated solution of $NaHCO_3$ (100 ml) and saturated brine (100 ml), then dried using $MgSO_4$ and concentrated under reduced pressure to give a pale pink gum. The crude product was purified by column chromatography eluting with 25% ethyl acetate in light petroleum to give the *title compound*, **100**, as a pale-yellow oil (2.35 g, 3.24 mmol, 63%). **$[\alpha]_D^{25}$** -12.9 (*c* 1, CH_3OH); **MS** (ESI^+): calcd for $C_{38}H_{55}N_3O_9Si$ $[M+H]^+$ 726.3780, found 726.3777; **υ_{max} (ATR)/cm^{-1}** 3304, 3066, 3033, 2892, 1734 (C=O), 1692 (C=O), 1655, 1604, 1519; **^{1}H NMR** (400 MHz; $CDCl_3$) δ 7.34-7.27 (10H, m, ArH, H-10,11,12,17,18,19), 5.12 (2H, s, CH_2, H-9), 4.61-4.55 (3H, m, CH x 2, CH_2, H-16), 4.40 (1H, d, *J* 11.9, CH_2, H-16), 4.24 (1H, br s, CH), 4.23-4.17 (1H, m, CH), 4.16-4.07 (2H, m, CH_2, H-20), 3.48 (2H, br s, CH_2), 2.58-2.53 (2H, m, CH_2), 2.22 (2H, br s, CH_2), 2.00 (2H, br s, CH_2), 1.86 (2H, br s, CH_2), 1.44 (9H, s, CH_3, H-1), 1.22 (3H, d, *J* 6.3, CH_3, H-15), 0.95-0.89 (2H, m, CH_2, H-21), 0.03 (9H, s, CH_3, H-22); **^{13}C NMR** (100 MHz; $CDCl_3$) δ 173.0 (C=O), 172.4 (C=O), 171.4 (C=O), 170.3 (C=O), 151.3 (C=O), 137.9 (C), 135.8 (C), 129.3 (CH), 128.5 (CH), 128.3 (CH), 128.2 (CH), 128.1 (CH), 127.7 (CH), 80.4 (C), 73.9 (CH), 70.7 (CH_2), 66.4 (CH_2), 63.9 (CH_2), 60.0 (CH), 56.9 (CH), 52.4 (CH), 47.0 (CH_2), 30.2 (CH_2), 28.2 (CH_3), 27.9 (CH_2), 24.6 (CH_2), 23.7 (CH_2), 17.3 (CH_2), 16.3 (CH_3), -1.56 (CH_3).

N-(*tert*-Butoxycarbonyl)-proline-glutamic acid(*O*-benzyl)-threonine(*O*-benzyl)-OH, **93**



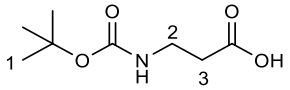
N-(*tert*-Butoxycarbonyl)-proline-glutamic acid(*O*-benzyl)-threonine(*O*-benzyl)-*O*-(trimethyl silyl)ethyl ester, **100**, (200 mg, 0.28 mmol) was dissolved in anhydrous DMF (1.5 ml) and tris(dimethylamino)sulfonium difluorotrimethylsilicate (152 mg, 0.55 mmol) was added and the reaction mixture was stirred at room temperature for 16 h. The reaction mixture was then diluted with ethyl acetate (20 ml) and washed with a saturated solution of NH_4Cl (3 x 20 ml), dried using $MgSO_4$ and concentrated under reduced pressure to give the *title compound*, **93**, as a yellow oil (180 mg, 0.28 mmol, 98%). **$[\alpha]_D^{25}$** +3.12 (*c* 1, CH_3OH); **MS** (ESI^+) calcd for $C_{33}H_{43}N_3O_9$ [M+H] 626.3072, found 626.3072; **υ_{max} (ATR)/cm^{-1}** 3307, 3033, 2975, 2931, 1734 (C=O), 1655 (C=O), 1524; **^{1}H NMR** (400 MHz; $CDCl_3$) δ 7.29-7.23 (10H, m, ArH, H-10,11,12,17,18,19), 5.08 (2H, s, CH_2, H-9), 4.64 (1H, d, *J* 8.8, CH), 4.58-4.55 (2H, m, CH and CH_2, H-16), 4.45 (1H, d, *J* 11.8, CH_2, H-16), 4.22 (2H, br s, CH), 3.44 (2H, br s, CH_2), 2.50 (2H, br s, CH_2), 2.22-2.12 (2H, m, CH_2), 2.01-1.93 (2H, m, CH_2), 1.80 (2H, br s, CH_2), 1.41 (9H, s, CH_3, H-1), 1.19 (3H, d, *J* 6.3, CH_3, H-15); **^{13}C NMR** (100 MHz; $CDCl_3$) δ 173.2 (C=O), 173.0 (C=O), 171.3 (C=O), 170.3 (C=O), 163.3 (C=O), 137.8 (C), 135.8 (C), 129.3 (CH), 128.5 (CH), 128.3 (CH), 128.2 (CH), 128.1 (CH), 127.7 (CH), 80.3 (C), 74.2 (CH), 71.0 (CH_2), 66.4 (CH_2), 60.5 (CH), 56.7 (CH), 52.5 (CH), 46.9 (CH_2), 30.2 (CH_2), 28.7 (CH_2), 28.3 (CH_3), 24.5 (CH_2), 23.6 (CH_2), 16.3 (CH_3).

Proline-glutamic acid(*O*-benzyl)-threonine(*O*-benzyl)-*O*-(trimethylsilyl)ethyl ester hydrochloride, **105**



N-(*tert*-Butoxycarbonyl)-proline-glutamic acid(*O*-benzyl)-threonine(*O*-benzyl)-*O*-(trimethyl silyl)ethyl ester, **100**, (250 mg, 0.34 mmol) was dissolved in HCl in dioxane (4 M, 1.0 ml) and the reaction mixture was stirred at room temperature for 1 h. The reaction mixture was concentrated under reduced pressure to give the *title compound*, **105**, as a pale-yellow gum (215 mg, 0.34 mmol, quantitative yield). $\mathbf{[\alpha]_D^{25}}$ -11.0 (*c* 1, CH_3OH); **MS** (ESI^+): calcd for $C_{33}H_{47}N_3O_9Si$ $[M+H]^+$ 626.3072, found 626.3089; $\mathbf{\upsilon_{max}}$ **(ATR)/cm^{-1}** 3195, 3032, 2951, 1733 (C=O), 1659 (C=O), 1539, 1453; **^{1}H NMR** (400 MHz; CH_3OD) δ 7.37-7.30 (10H, m, ArH, H-9,10,11,16,17,18), 5.13 (2H, d, *J* 12.0, CH_2, H-8), 4.61 (1H, d, *J* 8.0, CH_2, H-15), 4.60-4.54 (2H, m, CH_2, CH, H-15), 4.41 (1H, d, *J* 12.0, CH), 4.37 (1H, br s, CH), 4.26-4.13 (3H, m, CH_2, CH, H-19), 3.36-3.34 (2H, m, CH_2), 2.56 (2H, dt, *J* 8.0, 12.0, CH_2), 2.40 (2H, br s, CH_2), 2.07-2.00 (4H, m, CH_2), 1.24 (3H, d, *J* 6.3, CH_3, H-14), 1.03-0.92 (2H, m, CH_2, H-20), 0.04 (9H, s, CH_3, H-21); **^{13}C NMR** (100 MHz; CH_3OD) δ 172.8 (C=O), 172.3 (C=O), 170.3 (C=O), 168.4 (C=O), 138.1 (C), 136.2 (C), 128.2 (CH), 128.0 (CH), 127.9 (CH), 127.6 (CH), 127.5 (CH), 127.4 (CH), 74.2 (CH), 70.6 (CH_2), 66.7 (CH_2), 63.4 (CH_2), 59.6 (CH), 57.2 (CH), 52.9 (CH), 46.1 (CH_2), 29.7 (CH_2), 26.9 (CH_2), 23.6 (CH_2), 17.0 (CH_2), 15.1 (CH_3), -2.84 (CH_3).

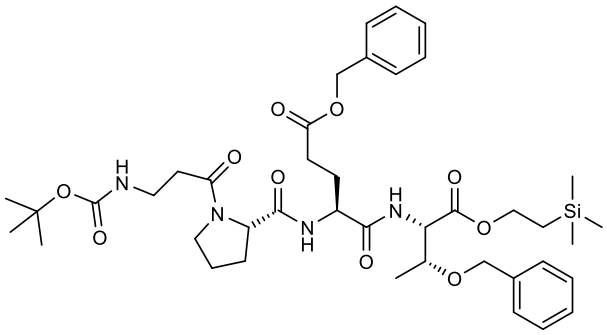
N-(*tert*-Butoxycarbonyl)-3-aminopropanoic acid, **104a**



β-Alanine, **103a**, (300 mg, 3.37 mmol) was dissolved in 1,4-dioxane (5.0 ml) and water (2.5 ml) and sodium hydroxide (135 mg, 3.37 mmol) was added then cooled to 0 °C. Di-*tert*-butyl dicarbonate (808 g, 3.71 mmol) was added in three equal portions then warmed to room temperature and stirred for 4 h. The reaction mixture was concentrated under reduced pressure, the residue was dissolved in water (30 ml) and ethyl acetate (30 ml). The layers

were separated, and the aqueous phase was extracted with ethyl acetate (30 ml). The aqueous phase was acidified to pH 1 using hydrochloric acid (1 M) and extracted with ethyl acetate (3 x 30 ml), dried using Na_2SO_4 and concentrated under reduced pressure to give the *title compound*, **104a**, as a colourless solid (517 mg, 2.74 mmol, 81%). **mp** 78-79 °C; **MS** (ESI^+): calcd for $C_8H_{15}N_1O_4$ $[M-H]^-$ 188.0928, found 188.0921; **υ_{max} (ATR)/cm^{-1}** 3438, 2965, 2910, 1698 (C=O); **^{1}H NMR** (400 MHz; $CDCl_3$) δ 5.11 (1H, br s, NH), 3.41 (2H, br s, CH_2, H-2), 2.59 (2H, br s, CH_2, H-3), 1.46 (9H, s, CH_3, H-1); **^{13}C NMR** (100 MHz; $CDCl_3$) δ 177.6 (C=O), 155.9 (C=O), 79.7 (C), 35.9 (CH_2), 34.5 (CH_2), 28.4 (CH_3). Data match literature values.[214]

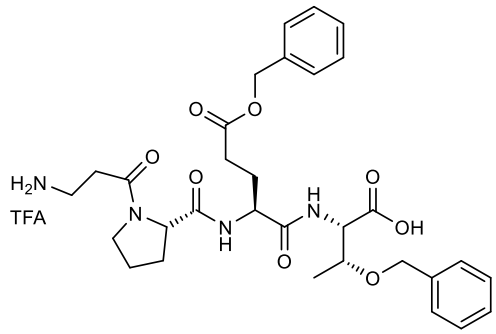
<u>*N*-(*tert*-Butoxycarbonyl)-β-alanine-proline-glutamic acid (*O*-benzyl)-threonine (*O*-benzyl)-*O*-(trimethylsilyl)ethyl ester, **106a**</u>



Proline-glutamic acid (*O*-benzyl)-threonine (*O*-benzyl)-*O*-(trimethylsilyl)ethyl ester hydrochloride, **105**, (340 mg, 0.54 mmol) and 3-(*tert*-butoxycarbonyl)-3-aminopropanoic acid, **104a**, (103 mg, 0.54 mmol) were dissolved in anhydrous DMF (3.0 ml). *N,N*-Diisopropylethylamine (0.6 ml, 3.26 mmol) and HATU (413 mg, 1.09 mmol) were added and the reaction mixture was stirred at room temperature for 16 h. The reaction mixture was diluted with ethyl acetate (30 ml) and water (30 ml). The layers were separated, and the organic phase was washed with water (2 x 30 ml), hydrochloric acid (1 M, 30 ml), a saturated solution of $NaHCO_3$ (30 ml) and saturated brine (30 ml), then dried using $MgSO_4$ and concentrated under reduced pressure to give an orange gum. The crude product was purified by column chromatography eluting with 80 % ethyl acetate in light petroleum to give the *title compound*, **106a**, as a yellow gum (400 mg, 0.50 mmol, 92%). **$[\alpha]_D^{25}$** -75.6 (*c* 1, CH_3OH); **MS** (ESI^+): calcd for $C_{41}H_{60}N_4O_{10}Si$ $[M+H]^+$ 797.4151, found 797.4126; **υ_{max} (ATR)/cm^{-1}** 3303, 3031, 2951, 2249, 2073, 1733 (C=O), 1709 (C=O), 1653; **^{1}H NMR** (400 MHz; $CDCl_3$) δ 7.31 (1H, d, *J* 8.0, NH), 7.27-7.19 (10H, m, ArH), 6.99 (1H, d, *J* 12.0, NH), 5.49 (1H, br s, NH), 5.04 (2H, d, *J* 4.0, CH_2), 4.54-4.49 (2H, m, CH and CH_2), 4.46-4.43 (1H, m, CH), 4.42-4.40 (1H, m, CH), 4.33 (1H, d, *J* 12.0, CH_2), 4.12-4.08 (2H, m, CH_2), 4.05-4.01 (1H, m, CH), 3.47-3.22 (4H, m, CH_2), 2.49-2.45 (2H, m, CH_2), 2.16-2.10 (2H, m, CH_2), 1.98-1.85 (6H, m, CH_2), 1.33 (9H, s, CH_3), 1.14

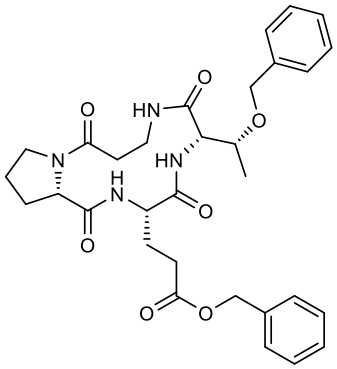
(3H, d, *J* 8.0, CH_3), 0.87-0.81 (2H, m, CH_2), -0.06 (9H, s, CH_3); **^{13}C NMR** (100 MHz; $CDCl_3$) δ 173.5 (C=O), 171.9 (C=O), 171.5 (C=O), 171.4 (C=O), 170.2 (C=O), 156.2 (C=O), 137.9 (C), 135.8 (C), 128.6 (CH), 128.3 (CH), 128.2 (CH), 128.1 (CH), 127.77 (CH), 127.72 (CH), 79.0 (C), 74.2 (CH), 70.8 (CH_2), 66.6 (CH_2), 63.9 (CH_2), 60.2 (CH), 56.9 (CH), 52.8 (CH), 47.4 (CH_2), 36.2 (CH_2), 34.7 (CH_2), 30.4 (CH_2), 28.5 (CH_3), 28.3 (CH_2), 27.7 (CH_2), 24.9 (CH_2), 17.3 (CH_2), 16.4 (CH_3), -1.54 (CH_3).

<u>β-alanine-proline-glutamic acid (*O*-benzyl)-threonine (*O*-benzyl)-OH trifluoroacetate, **107a**</u>



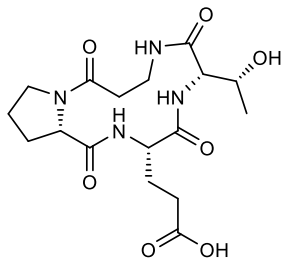
N-(*tert*-Butoxycarbonyl)-β-alanine-proline-glutamic acid (*O*-benzyl)-threonine (*O*-benzyl)-*O*-(trimethylsilyl)ethyl ester, **106a**, (114 mg, 0.14 mmol) was dissolved in dichloromethane (1.0 ml) and trifluoroacetic acid (1.5 ml) was added. The reaction mixture was stirred at room temperature for 15 h, then concentrated under reduced pressure to give the *title compound*, **107a**, as an orange gum (82 mg, 0.14 mmol, quantitative yield). **$[\alpha]_D^{25}$** +11.3 (*c* 1, CH_3OH); **MS** (ESI^+): calcd for $C_{31}H_{40}N_4O_8$ $[M+H]^+$ 597.2919, found 597.2921; **υ_{max} (ATR)/cm^{-1}** 3033, 2931, 1729 (C=O), 1640, 1524, 1452; **^{1}H NMR** (400 MHz; $CDCl_3$) δ 8.23 (1H, br s, NH), 7.62 (1H, d, *J* 8.0, NH), 7.34-7.30 (10H, m, ArH), 5.09 (2H, s, CH_2), 4.60-4.54 (2H, m, CH and CH_2), 4.49 (1H, br s, CH), 4.39 (1H, d, *J* 8.0, CH_2), 4.35 (1H, br s, CH), 4.20 (1H, br s, CH), 3.74-3.70 (1H, m, CH_2), 3.51 (1H, br s, CH_2), 3.34 (1H, br s, CH_2), 3.16-3.11 (2H, m, CH_2), 2.93 (1H, br s, CH_2), 2.68 (1H, br s, CH_2), 2.47-2.44 (3H, m, CH_2), 2.27-2.13 (4H, m, CH_2), 1.16 (3H, d, *J* 4.0, CH_3); **^{13}C NMR** (100 MHz; $CDCl_3$) δ 173.6 (C=O), 173.4 (C=O), 172.9 (C=O), 172.8 (C=O), 170.6 (C=O), 137.9 (C), 135.7 (C), 128.6 (CH), 128.5 (CH), 128.34 (CH), 128.31 (CH), 128.2 (CH), 128.1 (CH), 74.2 (CH), 71.2 (CH_2), 66.6 (CH_2), 61.1 (CH), 57.1 (CH), 54.2 (CH), 47.3 (CH_2), 42.4 (CH_2), 35.8 (CH_2), 30.6 (CH_2), 29.7 (CH_2), 26.6 (CH_2), 24.7 (CH_2), 15.8 (CH_3).

Cyclo-β-alanine-proline-glutamic acid(*O*-benzyl)-threonine(*O*-benzyl), **108a**



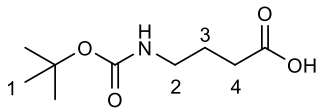
β-alanine-proline-glutamic acid (*O*-benzyl)-threonine (*O*-benzyl)-OH trifluoroacetate, **107a**, (150 mg, 0.25 mmol) was dissolved in anhydrous DMF (5.0 ml). *N,N*-Diisopropylethylamine (0.3 ml, 1.51 mmol) and HATU (191 mg, 0.50 mmol) were added and the reaction mixture was stirred at room temperature for 16 h. The reaction mixture was diluted with ethyl acetate (50 ml) and water (50 ml). The layers were separated, and the organic phase was washed with water (2 x 50 ml), hydrochloric acid (1 M, 50 ml), a saturated solution of $NaHCO_3$ (50 ml) and saturated brine (50 ml), then dried using $MgSO_4$ and concentrated under reduced pressure to give a yellow gum. The crude product was purified by column chromatography eluting with 10 % propan-2-ol in chloroform to give the *title compound*, **108a**, as a 3:1 mixture of rotamers and a pale orange gum (10 mg, 0.02 mmol, 7%). Data for major compound: $\mathbf{[\alpha]_D^{25}}$ +1.66 (*c* 1, CH_3OH); **MS** (ESI^+): calcd for $C_{31}H_{38}N_4O_7$ $[M+H]^+$ 579.2813, found 579.2825; $\mathbf{\upsilon_{max}}$ **(ATR)/cm^{-1}** 3838, 3767, 3748, 3286, 3063, 2924, 2872, 2325, 2236, 2218, 2187, 2175, 2144, 2083, 2052, 2005, 1993, 1981, 1948, 1906, 1731 (C=O), 1644 (C=O), 1522, 1443; **^{1}H NMR** (400 MHz; $CDCl_3$) δ 7.37-7.21 (10H, m, ArH), 5.09 (2H, s, CH_2), 4.54 (2H, dd, *J* 47.8, 11.2, CH_2), 4.44-4.34 (2H, m, CH), 4.09 (1H, br s, CH), 3.85-3.84 (1H, m, CH), 3.28-3.19 (2H, m, CH_2), 2.52-2.39 (4H, m, CH_2), 2.32-2.22 (4H, m, CH_2), 2.08-1.74 (4H, m, CH_2), 1.25 (3H, d, *J* 6.3, CH_3); **^{13}C NMR** (100 MHz; $CDCl_3$) δ 173.0 (C=O), 172.6 (C=O), 171.8 (C=O), 171.3 (C=O), 169.8 (C=O), 138.8 (C), 135.9 (C), 128.7 (CH), 128.5 (CH), 128.4 (CH), 128.3 (CH), 128.1 (CH), 128.0 (CH), 77.4 (CH), 74.1 (CH), 72.6 (CH), 71.9 (CH_2), 66.6 (CH_2), 58.3 (CH), 47.1 (CH_2), 35.1 (CH_2), 33.7 (CH_2), 31.0 (CH_2), 27.3 (CH_2), 26.2 (CH_2), 25.2 (CH_2), 17.8 (CH_3).

Cyclo-β-alanine-proline-glutamic acid-threonine, **109a**



Cyclo-β-alanine-proline-glutamic acid(*O*-benzyl)-threonine(*O*-benzyl), **108a**, (10 mg, 0.02 mmol) was dissolved in methanol (1 ml). $Pd(OH)_2/C$ (1.0 mg, 0.006 mmol) was added and the reaction mixture was evacuated under reduced pressure and back-filled with Ar. This was repeated three times. After the final evacuation, the reaction flask was charged with H_2 and the mixture was stirred vigorously at room temperature for 72 h. The reaction mixture was filtered through celite and washed with methanol. The filtrate was then concentrated under reduced pressure to give the *title compound*, **109a**, as a 3:1 mixture of rotamers and as a pale orange solid (2 mg, 0.005 mmol, 25%). **MS** (ESI^+) calcd for $C_{17}H_{26}N_4O_7$ $[M+H]^+$ 399.1874, found 399.1870; Major compound: **^{1}H NMR** (400 MHz, CH_3OD) δ 4.28 (1H, dd, *J* 8.3, 6.8, CH), 4.22 (1H d, *J* 4.4, CH), 4.14 (1H, qd, *J* 6.4, 4.2, CH), 4.00-3.94 (1H, m, CH), 3.61–3.46 (4H, m, CH_2), 2.37-2.16 (6H, m, CH_2), 2.12–1.90 (4H, m, CH_2), 1.19 (3H, d, *J* 6.4, CH_3). Minor compound: **^{1}H NMR** (400 MHz, CH_3OD) δ 4.55 (1H, dd, *J* 10.0, 5.8, CH), 4.17 (1H, d, *J* 1.7, CH), 3.92-3.89 (1H, m, CH), 3.77-3.70 (1H, m, CH), 3.24 (2H, ddd, *J* 13.1, 4.1, 2.7, CH_2), 2.96 (2H, ddd, *J* 16.6, 12.6, 4.1, CH_2), 2.43 (2H, dt, *J* 16.5, 3.2, CH_2), 1.90–1.77 (8H, m, CH_2), 1.22 (3H, d, *J* 6.3, CH_3).

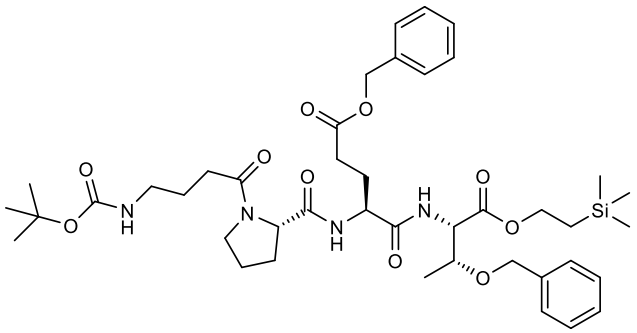
4-((*tert*-Butoxycarbonyl)amino)butanoic acid, **104b**



4-Aminobutyric acid, **103b**, (250 mg, 2.43 mmol) was dissolved in 1,4-dioxane (5.0 ml) and water (2.5 ml) and sodium hydroxide (97 mg, 2.43 mmol) was added then cooled to 0 °C. Di-*tert*-butyl dicarbonate (582 g, 2.67 mmol) was added in three equal portions then warmed to room temperature and stirred for 18 h. The reaction mixture was concentrated under reduced pressure then the residue was dissolved in water (10 ml) and ethyl acetate (10 ml). The layers were separated, and the aqueous phase was extracted with ethyl acetate (10 ml). The aqueous phase was acidified to pH 1 using hydrochloric acid (1 M) and extracted with ethyl acetate (3 x 10 ml), dried using Na_2SO_4 and concentrated under reduced pressure to give the *title compound*, **104b**, as a colourless gum (369 mg, 1.82 mmol, 75%). **MS** (ESI^+): calcd

for $C_9H_{17}N_1O_4$ $[M-H]^-$ 202.1085, found 202.1078; **υ_{max} (ATR)/cm^{-1}** 3272, 3082, 2976, 2933, 1687 (C=O), 1633; **^{1}H NMR** (400 MHz; $CDCl_3$) δ 3.18 (2H, br s, CH_2, H-2), 2.39 (2H, t, *J* 7.2, CH_2, H-4), 1.82 (2H, quint., *J* 7.2, CH_2, H-3), 1.44 (9H, s, CH_3, H-1); **^{13}C NMR** (100 MHz; $CDCl_3$) δ 178.1 (C=O), 156.2 (C=O), 79.5 (C), 39.7 (CH_2), 31.3 (CH_2), 28.4 (CH_3), 25.2 (CH_2). Data match literature values.[215]

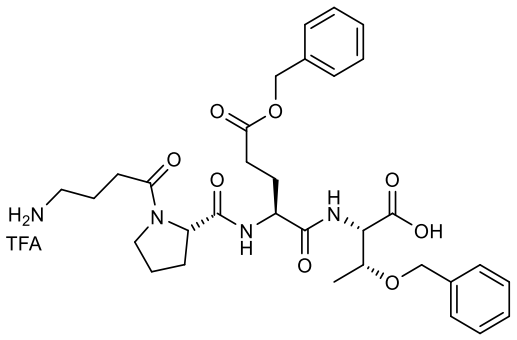
N-(*tert*-Butoxycarbonyl)-γ-aminobutyric acid-proline-glutamic acid(*O*-benzyl)-threonine (*O*-benzyl)-*O*-(trimethylsilyl)ethyl ester, **106b**



Proline-glutamic acid (*O*-benzyl)-threonine (*O*-benzyl)-*O*-(trimethylsilyl)ethyl ester hydrochloride, **105**, (170 mg, 0.27 mmol) and 4-((*tert*-butoxycarbonyl)amino)butanoic acid, **104b**, (55 mg, 0.27 mmol) were dissolved in anhydrous DMF (2.0 ml). *N,N*-Diisopropylethylamine (0.3 ml, 1.63 mmol) and HATU (207 mg, 0.54 mmol) were added and the reaction mixture was stirred at room temperature for 16 h. The reaction mixture was diluted with ethyl acetate (10 ml) and water (10 ml). The layers were separated and the organic phase was washed with water (2 x 10 ml), hydrochloric acid (1 M, 10 ml), a saturated solution of $NaHCO_3$ (10 ml) and saturated brine (10 ml), then dried using $MgSO_4$ and concentrated under reduced pressure to give a yellow gum. The crude product was purified by column chromatography eluting with 50 % ethyl acetate in light petroleum to give the *title compound*, **106b**, as a yellow gum (111 mg, 0.14 mmol, 50%). **$[\alpha]_D^{25}$** -10.6 (*c* 1, CH_3OH); **MS** (ESI^+): calcd for $C_{42}H_{62}N_4O_{10}$ $[M+H]^+$ 811.4308, found 811.4303; **υ_{max} (ATR)/cm^{-1}** 3307, 3032, 2952, 1734 (C=O), 1709 (C=O), 1655 (C=O), 1516, 1450; **^{1}H NMR** (400 MHz; $CDCl_3$) δ 7.52 (1H, d, *J* 7.1, NH), 7.37-7.28 (10H, m, ArH), 6.99 (1H, d, *J* 8.7, NH), 6.76 (1H, d, *J* 9.2, NH), 5.12 (2H, s, CH_2), 4.80 (1H, br s, CH), 4.63-4.60 (2H, m, CH_2), 4.58 (1H, br s, CH), 4.54-4.50 (2H, m, CH_2), 4.43 (1H, d, *J* 12.0, CH_2), 4.24-4.08 (3H, m, CH_2 and CH), 3.57-3.38 (2H, m, CH_2), 3.21-3.06 (2H, m, CH_2), 2.57-2.53 (2H, m, CH_2), 2.28-1.94 (6H, m, CH_2), 1.82 (2H, br s, CH_2), 1.44 (9H, s, CH_3), 1.23 (3H, d, *J* 6.3, CH_3), 1.00-0.89 (2H, m, CH_2), 0.03 (9H, s, CH_3); **^{13}C NMR** (100 MHz; $CDCl_3$) δ 173.1 (C=O), 172.4 (C=O), 171.8 (C=O), 171.5 (C=O), 170.3 (C=O), 156.4 (C=O), 138.1 (C), 135.9 (C), 128.5 (CH), 128.4 (CH), 128.3 (CH), 128.2 (CH), 127.7 (CH), 127.6 (CH), 79.1 (C), 74.2 (CH),

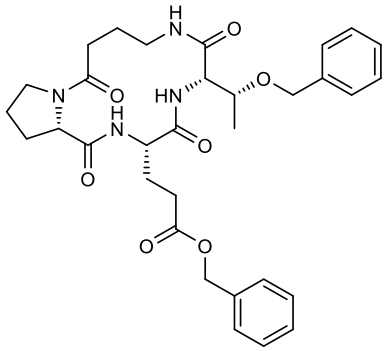
70.7 (CH_2), 66.4 (CH_2), 63.8 (CH_2), 60.1 (CH), 56.8 (CH), 52.8 (CH), 47.4 (CH_2), 39.6 (CH_2), 31.1 (CH_2), 30.5 (CH_2), 28.4 (CH_3), 28.3 (CH_2), 27.2 (CH_2), 24.9 (CH_2), 22.7 (CH_2), 17.3 (CH_2), 16.3 (CH_3), -1.55 (CH_3).

<u>γ-Aminobutyric acid-proline-glutamic acid(*O*-benzyl)-threonine (*O*-benzyl)-OH trifluoroacetate, **107b**</u>



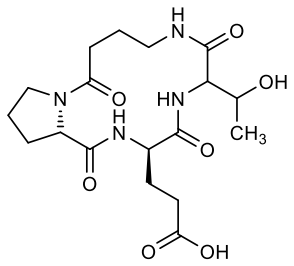
N-(*tert*-Butoxycarbonyl)-γ-aminobutyric acid-proline-glutamic acid(*O*-benzyl)-threonine (*O*-benzyl)-*O*-(trimethylsilyl)ethyl ester, **106b**, (114 mg, 0.14 mmol) was dissolved in dichloromethane (1.0 ml) and trifluoroacetic acid (1.5 ml) was added. The reaction mixture was stirred at room temperature for 15 h, then concentrated under reduced pressure to give the *title compound*, **107b**, as an orange gum (65 mg, 0.14 mmol, quantitative yield). $\mathbf{[\alpha]_D^{25}}$ +17.3 (*c* 1, CH_3OH); **MS** (ESI^+): calcd for $C_{32}H_{42}N_4O_8$ $[M+H]^+$ 611.3075, found 611.3082; $\mathbf{\upsilon_{max}}$ **(ATR)/cm^{-1}** 3271, 3065, 2928, 1649 (C=O), 1528, 1452; 1 **^{1}H NMR** (400 MHz; $CDCl_3$) δ 12.0 (1H, br s, OH), 8.49 (1H, br s, NH), 7.55 (1H, br s, NH), 7.35-7.32 (10H, m, ArH), 7.05 (1H, br s, NH), 5.08 (2H, s, CH_2), 4.96 (1H, br s, CH), 4.58-4.55 (2H, m, CH and CH_2), 4.42 (1H, br s, CH), 4.39-4.35 (2H, m, CH and CH_2), 3.63 (1H, br s, CH_2), 3.40 (1H, br s, CH_2), 2.68 (2H, br s, CH_2), 2.50 (4H, br s, CH_2), 2.20-1.82 (8H, m, CH_2), 1.25 (3H, d, *J* 4.0, CH_3); **^{13}C NMR** (100 MHz; $CDCl_3$) δ 175.3 (C=O), 174.4 (C=O), 174.3 (C=O), 160.7 (C=O), 160.2 (C=O), 137.2 (C), 135.4 (C), 128.8 (CH), 128.6 (CH), 128.4 (CH), 128.3 (CH), 128.2 (CH), 128.0 (CH), 74.6 (CH), 71.7 (CH_2), 67.1 (CH_2), 63.9 (CH_2), 61.4 (CH), 57.6 (CH), 54.4 (CH), 48.0 (CH_2), 42.7 (CH_2), 40.3 (CH_2), 30.4 (CH_2), 29.6 (CH_2), 26.1 (CH_2), 24.5 (CH_2), 17.3 (CH_3).

Cyclo-γ-aminobutyric acid-proline-glutamic acid(*O*-benzyl)-threonine(*O*-benzyl), **108b**



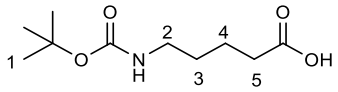
N-((*S*)-2-((*S*)-1-(4-Aminobutanoyl)pyrrolidine-2-carboxamido)-5-benzyloxy-5-oxopentanoyl)-*O*-benzyl-*L*-threonine, **107b**, (280 mg, 0.46 mmol) was dissolved in anhydrous DMF (5.0 ml). *N,N*-Diisopropylethylamine (0.5 ml, 0.50 mmol) and HATU (349 mg, 0.92 mmol) were added and the reaction mixture was stirred at room temperature for 16 h. The reaction mixture was diluted with ethyl acetate (100 ml) and water (100 ml). The layers were separated, and the organic phase was washed with water (2 x 100 ml), hydrochloric acid (1 M, 100 ml), a saturated solution of $NaHCO_3$ (100 ml) and saturated brine (100 ml), then dried using $MgSO_4$ and concentrated under reduced pressure to give a yellow gum. The crude product was purified by column chromatography eluting with 10 % propan-2-ol in chloroform to give the *title compound*, **108b**, as a 3:1 mixture of rotamers and an orange gum (75 mg, 0.13 mmol, 28%). Data for the major compound: $\mathbf{[\alpha]_D^{25}}$ -5.61 (*c* 1, CH_3OH); **MS** (ESI^+): calcd for $C_{32}H_{40}N_4O_7$ $[M+H]^+$ 593.2970, found 593.2961; $\mathbf{\upsilon_{max}}$ **(ATR)/cm^{-1}** 3327, 3064, 2921, 2851, 2086, 1732 (C=O), 1639, 1525; **^{1}H NMR** (400 MHz; $CDCl_3$) δ 7.68 (1H, br s, NH), 7.46 (1H, br s, NH), 7.25-7.14 (10H, m, ArH), 6.65 (1H, br s, NH), 5.03 (2H, s, CH_2), 4.49-4.45 (2H, m, CH), 4.36-4.30 (2H, m, CH_2), 4.20 (1H, dd, *J* 7.9, 3.6, CH), 3.76-3.73 (1H, m, CH), 3.25-3.17 (2H, m, CH_2), 3.13-2.95 (2H, m, CH_2), 2.39-2.33 (4H, m, CH_2), 2.10-2.01 (4H, m, CH_2), 1.76-1.48 (4H, m, CH_2), 1.08 (3H, d, *J* 6.3, CH_3); **^{13}C NMR** (100 MHz; $CDCl_3$) δ 174.2 (C=O), 173.8 (C=O), 173.3 (C=O), 172.4 (C=O), 170.7 (C=O), 139.2 (C), 135.9 (C), 128.7 (CH), 128.4 (CH), 128.3 (CH), 128.2 (CH), 127.8 (CH), 127.4 (CH), 74.8 (CH), 71.7 (CH_2), 66.6 (CH_2), 60.9 (CH), 59.7 (CH), 57.6 (CH), 47.0 (CH_2), 40.9 (CH_2), 32.9 (CH_2), 31.2 (CH_2), 29.8 (CH_2), 27.6 (CH_2), 25.6 (CH_2), 21.4 (CH_2), 16.8 (CH_3).

Cyclo-γ-aminobutyric acid-proline-glutamic acid-threonine, **109b**



Cyclo-γ-aminobutyric acid-proline-glutamic acid(*O*-benzyl)-threonine(*O*-benzyl), **108b**, (75 mg, 0.13 mmol) was dissolved in methanol (1 ml). $Pd(OH)_2/C$ (4.0 mg, 0.02 mmol) was added and the reaction mixture was evacuated under reduced pressure and back-filled with Ar. This was repeated three times. After the final evacuation, the reaction flask was charged with H_2 and the mixture was stirred vigorously at room temperature for 72 h. The reaction mixture was filtered through celite and washed with methanol. The filtrate was then concentrated under reduced pressure to give the *title compound*, **109b**, as a 3:1 mixture of rotamers and as a pale orange solid (8 mg, 0.02 mmol, 15%). **MS** (ESI^+) calcd for $C_{18}H_{28}N_4O_7$ $[M+H]^+$ 413.2031, found 413.2048; Major compound: **^{1}H NMR** (400 MHz, CH_3OD) δ 4.44 (1H, dd, *J* 8.7, 3.6, CH), 4.33 (1H, qd, *J* 6.5, 2.6, CH), 4.27–4.22 (1H, m, CH), 4.08 (1H, d, *J* 2.6, CH), 3.72 – 3.55 (4H, m, CH_2), 2.65 – 2.48 (2H, m, CH_2), 2.30 – 1.81 (10H, m, CH_2), 1.25 (3H, d, *J* 6.5, CH_3). Minor compound: **^{1}H NMR** (400 MHz, CH_3OD) δ 4.52 (1H, qd, *J* 6.5, 2.5, CH), 4.27–4.22 (2H, m, CH), 3.87–3.79 (1H, m, CH), 3.54–3.45 (2H, m, CH_2), 3.41 (2H, dt, *J* 13.8, 3.9, CH_2), 3.20–3.10 (2H, m, CH_2), 2.82 (2H, t, *J* 12.8, CH_2), 2.49 (2H, m, CH_2), 1.82–1.67 (4H, m, CH_2), 1.59 (2H, td, *J* 13.4, 12.9, 3.5, CH_2), 1.12 (3H, d, *J* 6.5, CH_3).

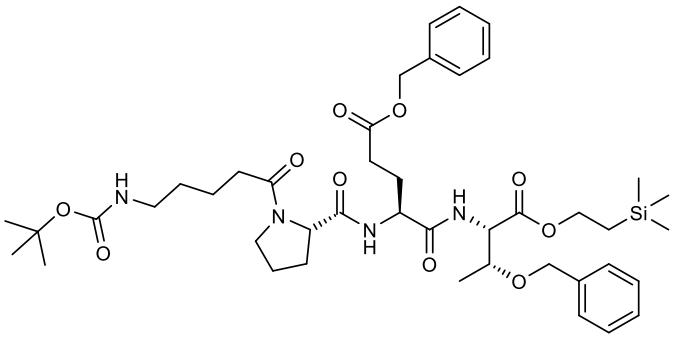
5-((*tert*-Butoxycarbonyl)amino)pentanoic acid, **104c**



5-Aminovalaric acid, **103c**, (500 mg, 4.27 mmol) was dissolved in 1,4-dioxane (10 ml) and water (5.0 ml) and sodium hydroxide (171 mg, 4.17 mmol) was added then cooled to 0 °C. Di-*tert*-butyl dicarbonate (1.02 g, 4.70 mmol) was added in three equal portions then warmed to room temperature and stirred for 18 h. The reaction mixture was concentrated under reduced pressure then the residue was dissolved in water (15 ml) and ethyl acetate (15 ml). The layers were separated, and the aqueous phase was extracted with ethyl acetate (15 ml). The aqueous phase was acidified to pH 1 using hydrochloric acid (1 M) and extracted with ethyl acetate (3 x 15 ml), dried using Na_2SO_4 and concentrated under reduced pressure

to give the *title compound*, **104c**, as a colourless gum (800 mg, 3.69 mmol, 86%). **MS** (ESI^+): calcd for $C_{10}H_{19}N_1O_4$ $[M-H]^-$ 216.1241, found 216.1242; **υ_{max} (ATR)/cm^{-1}** 3370, 2950, 2876, 1705 (C=O), 1682 (C=O), 1519; **^{1}H NMR** (400 MHz; $CDCl_3$) δ 3.10 (2H, br s, CH_2, H-2), 2.33 (2H, t, *J* 7.3, CH_2, H-5), 1.63 (2H, quint., *J* 7.3, CH_2), 1.50 (2H, quint., *J* 7.2, CH_2), 1.41 (9H, s, CH_3, H-1); **^{13}C NMR** (100 MHz; $CDCl_3$) δ 178.7 (C=O), 156.1 (C=O), 79.3 (C), 40.1 (CH_2), 33.6 (CH_2), 29.4 (CH_2), 28.4 (CH_3), 21.9 (CH_2). Data match literature values.[216]

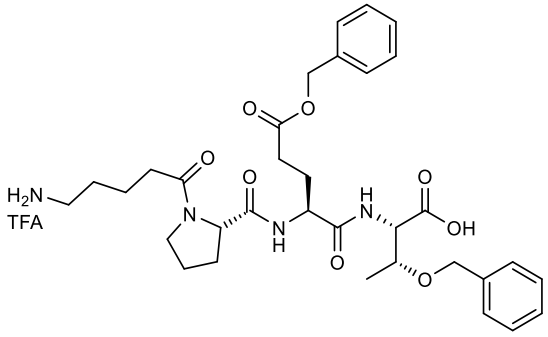
<u>*N*-(*tert*-Butoxycarbonyl)-aminovaleric acid-proline-glutamic acid(*O*-benzyl)-threonine(*O*-benzyl)-*O*-(trimethylsilyl)ethyl ester, **106c**</u>



Proline-glutamic acid (*O*-benzyl)-threonine (*O*-benzyl)-*O*-(trimethylsilyl)ethyl ester hydrochloride, **105**, (215 mg, 0.34 mmol) and 5-((*tert*-butoxycarbonyl) amino)pentanoic acid, **104c**, (75 mg, 0.34 mmol) were dissolved in anhydrous DMF (2.0 ml). *N,N*-Diisopropylethylamine (0.4 ml, 2.06 mmol) and HATU (261 mg, 0.69 mmol) were added and the reaction mixture was stirred at room temperature for 16 h. The reaction mixture was diluted with ethyl acetate (10 ml) and water (10 ml). The layers were separated and the organic phase was washed with water (2 x 10 ml), hydrochloric acid (1 M, 10 ml), a saturated solution of $NaHCO_3$ (10 ml) and saturated brine (10 ml), then dried using $MgSO_4$ and concentrated under reduced pressure to give a yellow gum. The crude product was purified by column chromatography eluting with 50 % ethyl acetate in light petroleum to give the *title compound*, **106c**, as a yellow gum (250 mg, 0.30 mmol, 88%). **$[\alpha]_D^{25}$** -10.5 (*c* 1, CH_3OH); **MS** (ESI^+): calcd for $C_{43}H_{64}N_4O_{10}Si$ $[M+H]^+$ 825.4464, found 825.4486; **υ_{max} (ATR)/cm^{-1}** 3304, 3033, 2952, 1734 (C=O), 1709 (C=O), 1655, 1516; **^{1}H NMR** (400 MHz; $CDCl_3$) δ 7.34-7.27 (10H, m, ArH), 5.12 (2H, s, CH_2), 4.61 (1H, br s, CH), 4.58 (2H, br s, CH and CH_2), 4.53 (1H, br s, CH), 4.51 (1H, br s, CH), 4.41 (1H, d, *J* 11.9, CH_2), 4.20-4.17 (2H, m, CH_2), 3.53-3.42 (2H, m, CH_2), 3.10 (2H, br s, CH_2), 2.57-2.53 (2H, m, CH_2), 2.35-2.22 (4H, m, CH_2), 2.02-1.85 (4H, m, CH_2), 1.71-1.62 (2H, m, CH_2), 1.55-1.50 (2H, m, CH_2), 1.44 (9H, s, CH_3), 1.22 (3H, d, *J* 6.3, CH_3), 0.92-0.87 (2H, m, CH_2), 0.03 (9H, s, CH_3); **^{13}C NMR** (100 MHz; $CDCl_3$) δ 173.2 (C=O), 172.9 (C=O), 171.6 (C=O), 171.4 (C=O), 170.3 (C=O), 156.1 (C=O), 138.0 (C), 135.9 (C), 128.6 (CH), 128.5 (CH),

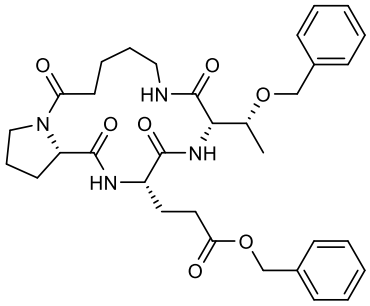
128.3 (CH), 128.2 (CH), 127.7 (CH), 127.6 (CH), 79.0 (C), 74.1 (CH), 70.7 (CH_2), 66.5 (CH_2), 63.9 (CH_2), 59.9 (CH), 56.9 (CH), 52.6 (CH), 47.5 (CH_2), 40.2 (CH_2), 33.9 (CH_2), 30.4 (CH_2), 29.5 (CH_2), 28.5 (CH_3), 27.9 (CH_2), 27.7 (CH_2), 25.0 (CH_2), 21.8 (CH_2), 17.3 (CH_2), 16.3 (CH_3), -1.56 (CH_3).

Aminovaleric acid-proline-glutamic acid(*O*-benzyl)-threonine(*O*-benzyl)-OH trifluoroacetate, **107c**



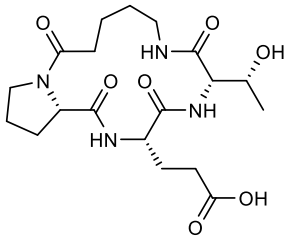
N-(*tert*-Butoxycarbonyl)-aminovaleric acid-proline-glutamic acid(*O*-benzyl)-threonine(*O*-benzyl)-*O*-(trimethylsilyl)ethyl ester, **106c**, (250 mg, 0.30 mmol) was dissolved in dichloromethane (1.0 ml) and trifluoroacetic acid (1.5 ml) was added and stirred at room temperature for 6 h. The reaction mixture was concentrated under reduced pressure to give the *title compound*, **107c**, as a pale orange gum (189 mg, 0.30 mmol, quantitative yield). **$[\alpha]_D^{25}$** +3.50 (*c* 1, CH_3OH); **MS** (ESI^+): calcd for $C_{33}H_{44}N_4O_8$ $[M+H]^+$ 625.3232, found 625.3230; **υ_{max} (ATR)/cm^{-1}** 2942, 1719 (C=O), 1654 (C=O), 1625, 1526, 1452; **^{1}H NMR** (400 MHz; CH_3OD) δ 7.37-7.26 (10H, m, ArH), 5.12 (2H, s, CH_2), 4.84-4.81 (1H, m, CH), 4.60 (1H, d, *J* 8.0, CH), 4.55-4.53 (2H, m, CH_2), 4.48 (1H, br s, CH), 4.43-4.40 (1H, m, CH), 3.64-3.56 (2H, m, CH_2), 2.92 (2H, br s, CH_2), 2.55-2.43 (4H, m, CH_2), 2.21-2.14 (2H, m, CH_2), 2.03-1.97 (4H, m, CH_2), 1.70 (4H, br s, CH_2), 1.25 (3H, d, *J* 4.0, CH_3); **^{13}C NMR** (100 MHz; CH_3OD) δ 173.5 (C=O), 173.1 (C=O), 172.7 (C=O), 172.0 (C=O), 171.6 (C=O), 138.2 (C), 136.2 (C), 128.2 (CH), 127.9 (CH), 127.8 (CH), 127.7 (CH), 127.5 (CH), 127.2 (CH), 74.5 (CH), 70.6 (CH_2), 66.0 (CH_2), 60.1 (CH), 55.1 (CH), 52.3 (CH), 47.3 (CH_2), 38.9 (CH_2), 32.9 (CH_2), 29.8 (CH_2), 29.4 (CH_2), 26.9 (CH_2), 26.6 (CH_2), 24.4 (CH_2), 20.6 (CH_2), 15.0 (CH_3).

Cyclo-aminovaleric acid-proline-glutamic acid(*O*-benzyl)-threonine(*O*-benzyl), **108c**



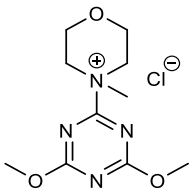
Aminovaleric acid-proline-glutamic acid(*O*-benzyl)-threonine(*O*-benzyl)-OH trifluoroacetate, **107c**, (240 mg, 0.38 mmol) was dissolved in anhydrous DMF (5.0 ml). *N,N*-Diisopropylethylamine (0.4 ml, 2.31 mmol) and HATU (292 mg, 0.77 mmol) were added and the reaction mixture was stirred at room temperature for 16 h. The reaction mixture was diluted with ethyl acetate (100 ml) and water (100 ml). The layers were separated, and the organic phase was washed with water (2 x 100 ml), hydrochloric acid (1 M, 100 ml), a saturated solution of $NaHCO_3$ (100 ml) and saturated brine (100 ml), then dried using $MgSO_4$ and concentrated under reduced pressure to give a yellow gum. The crude product was purified by column chromatography eluting with 10% propan-2-ol in chloroform to give the *title compound*, **108c**, as a 3:1 mixture of rotamers and an orange gum (130 mg, 0.21 mmol, 55%). Data for major compound: $\mathbf{[\alpha]_D^{25}}$ +6.71 (*c* 1, CH_3OH); **MS** (ESI^+): calcd for $C_{33}H_{42}N_4O_7$ $[M+H]^+$ 607.3126, found 607.3133; $\mathbf{\upsilon_{max}}$ **(ATR)/cm^{-1}** 3293, 3064, 3033, 2932, 2874, 1732 (C=O), 1648, 1515, 1452; **^{1}H NMR** (400 MHz; $CDCl_3$) δ 7.87 (1H, br s, NH), 7.37-7.26 (10H, m, ArH), 7.13 (1H, br s, NH), 6.93 (1H, br s, NH), 5.13-5.10 (2H, m, CH_2), 4.57 (1H, d, *J* 8.0, CH_2), 4.53 (2H, m, CH), 4.40 (1H, d, *J* 8.0, CH_2), 4.33-4.30 (1H, m, CH), 3.89-3.85 (1H, m, CH), 3.62-3.55 (2H, m, CH_2), 3.28 (2H, br s, CH_2), 3.20 (2H, br s, CH_2), 2.66-2.62 (1H, m, CH_2), 2.51-2.48 (2H, m, CH_2), 2.43-2.39 (1H, m, CH_2), 2.24-2.16 (4H, m, CH_2), 1.94-1.86 (2H, m, CH_2), 1.62-1.58 (2H, m, CH_2), 1.23 (3H, d, *J* 6.3, CH_3); **^{13}C NMR** (100 MHz; $CDCl_3$) δ 174.7 (C=O), 174.1 (C=O), 172.8 (C=O), 172.5 (C=O), 170.3 (C=O), 138.6 (C), 135.8 (C), 128.6 (CH), 128.3 (CH), 128.2 (CH), 128.1 (CH), 127.8 (CH), 127.4 (CH), 74.7 (CH), 71.6 (CH_2), 66.5 (CH_2), 60.4 (CH), 58.3 (CH), 57.6 (CH), 47.5 (CH_2), 38.7 (CH_2), 32.9 (CH_2), 31.0 (CH_2), 28.4 (CH_2), 27.6 (CH_2), 25.4 (CH_2), 24.9 (CH_2), 21.8 (CH_2), 16.9 (CH_3).

Cyclo-aminovaleric acid-proline-glutamic acid-threonine, **109c**



Cyclo-aminovaleric acid-proline-glutamic acid(*O*-benzyl)-threonine(*O*-benzyl), **108c**, (130 mg, 0.21 mmol) was dissolved in methanol (2 ml). $Pd(OH)_2/C$ (6.0 mg, 0.04 mmol) was added and the reaction mixture was evacuated under reduced pressure and back-filled with Ar. This was repeated three times. After the final evacuation, the reaction flask was charged with H_2 and the mixture was stirred vigorously at room temperature for 72 h. The reaction mixture was filtered through celite and washed with methanol. The filtrate was then concentrated under reduced pressure to give the *title compound*, **109c**, as a 1:1 mixture of rotamers and as a pale orange solid (26 mg, 0.06 mmol, 29%). **MS** (ESI^+) calcd for $C_{19}H_{30}N_4O_7$ $[M+H]^+$ 427.2187, found 427.2198; Major and minor: **^{1}H NMR** (400 MHz, CH_3OD) δ 4.54 (1H, dd, *J* 8.7, 2.5, CH), 4.48 (1H, qd, *J* 6.5, 3.1, CH), 4.40–4.30 (2H, m, CH), 4.27 (1H, dd, *J* 9.3, 6.5, CH), 4.16 (1H, d, *J* 3.1, CH), 4.04 (1H, d, *J* 4.6, CH), 4.00 (1H, dd, *J* 9.4, 5.7, CH), 3.76–3.65 (2H, m, CH_2), 3.65–3.54 (2H, m, CH_2), 3.42 (2H, ddd, *J* 13.5, 6.1, 2.9, CH_2), 3.27 (2H, ddd, *J* 13.1, 9.5, 2.7, CH_2), 3.17–3.08 (2H, m, CH_2), 2.60 (2H, ddd, *J* 14.8, 9.1, 3.7, CH_2), 2.36–2.11 (10H, m, CH_2), 2.07–1.90 (8H, m, CH_2), 1.74–1.54 (5H, m, CH_2), 1.21 (3H, d, *J* 6.4, CH_3), 1.18 (3H, d, *J* 6.3, CH_3). Unable to distinguish the two isomers as 1:1 ratio.

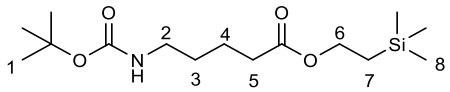
DMTMM, **40**



2-Chloro-4,6-dimethoxy-1,3,5-triazine, **39**, (200 mg, 1.14 mmol) was dissolved in THF (10 ml). 4-methylmorpholine (0.125 ml, 1.14 mmol) was added slowly to the reaction mixture and stirred at room temperature for 30 mins. The reaction mixture was then filtered and the solid was washed with diethyl ether to give the *title compound*, **40**, as a colourless solid (247 mg, 1.02 mmol, 90%). **mp** 116-117 °C; **υ_{max} (ATR)/cm^{-1}** 3448, 1618, 1540, 1482, 1366, 1191, 1130; **^{1}H NMR** (400 MHz; CH_3OD) δ 4.56-4.53 (2H, m, CH_2), 4.18 (6H, s, CH_3), 4.09-4.05 (2H, m, CH_2),

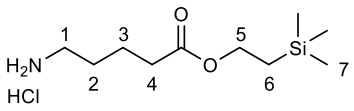
3.93-3.81 (4H, m, CH_2), 3.54 (3H, s, CH_3); **^{13}C NMR** (100 MHz; $CDCl_3$) δ 175.5 (C), 172.0 (C), 63.2 (CH_2), 61.4 (CH_2), 57.6 (CH_3), 56.5 (CH_3). Data match literature values.[89]

2-(Trimethylsilyl)ethyl 5-((*tert*-butoxycarbonyl)amino)pentanoate, **111**



5-((*tert*-Butoxycarbonyl)amino)pentanoic acid, **104c**, (280 mg, 1.29 mmol) was dissolved in a 1 : 1 mixture of dichloromethane (1.50 ml) and DMF (1.50 ml). Trimethylsilyl ethanol, **95**, (0.22 ml, 1.55 mmol) was added, followed by HBTU (636 mg, 1.68 mmol), triethylamine (0.23 ml, 1.68 mmol) and 4-(dimethylamino)pyridine (16 mg, 0.13 mmol) and stirred at room temperature for 16 h. Water (20 ml) and diethyl ether (20 ml) were added to the reaction mixture, the layers were separated and the organic phase was washed with water (2 x 20 ml) and brine (3 x 20 ml). The combined organic extracts were dried using $MgSO_4$ and concentrated under reduced pressure to give a yellow oil. The crude product was purified using column chromatography eluting with 25% ethyl acetate in pentane to give the *title compound*, **111**, as a colourless oil (169 mg, 0.53 mmol, 41%); **MS** (ESI^+) calcd for $C_{15}H_{31}NO_4Si$ [M+H] 318.2095, found 318.2092; **υ_{max} (ATR)/cm^{-1}** 3367, 2955, 1691 (C=O); **^{1}H NMR** (400 MHz; $CDCl_3$) δ 4.61 (1H, br s, NH), 4.15-4.10 (2H, m, CH_2, H-6), 3.09 (2H, dd, *J* 12.6, 6.3, CH_2, H-2), 2.27 (2H, t, *J* 7.3, CH_2, H-5), 1.65-1.58 (2H, m, CH_2), 1.50-1.46 (2H, m, CH_2), 1.40 (9H, s, CH_3, H-1), 0.97-0.92 (2H, m, CH_2, H-7), 0.01 (9H, s, CH_3, H-8); **^{13}C NMR** (100 MHz; $CDCl_3$) δ 173.7 (C=O), 156.1 (C=O), 79.1 (C), 62.6 (CH_2), 40.2 (CH_2), 34.1 (CH_2), 29.6 (CH_2), 28.5 (CH_3), 22.2 (CH_2), 17.4 (CH_2), -1.41 (CH_3).

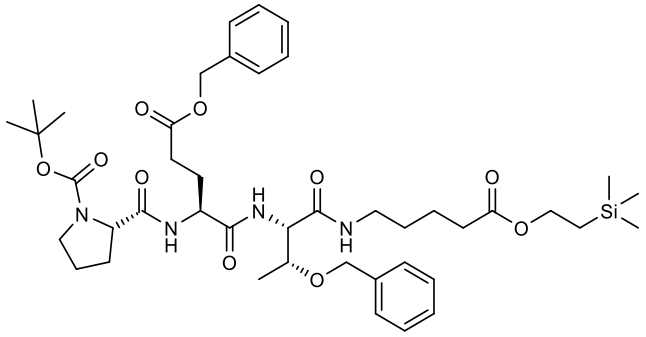
2-(Trimethylsilyl)ethyl 5-aminopentanoate, **112**



2-(Trimethylsilyl)ethyl 5-((*tert*-butoxycarbonyl)amino)pentanoate, **111**, (169 mg, 0.53 mmol) was dissolved in HCl in dioxane (4 M, 2 ml) and stirred at room temperature for 3 h. The reaction mixture was concentrated under reduced pressure to give the *title compound*, **112**, as a colourless solid (115 mg, 0.53 mmol, quantitative yield); **MS** (ESI^+) calcd for $C_{10}H_{23}NO_2Si$ [M+H] 218.1571, found 218.1574; **υ_{max} (ATR)/cm^{-1}** 3367, 2950, 2223, 1728 (C=O); **^{1}H NMR** (400 MHz; $CDCl_3$) δ 8.23 (2H, br s, NH), 4.15 (2H, dd, *J* 10.6, 6.3, CH_2, H-5), 3.04 (2H, br s, CH_2, H-1), 2.34 (2H, t, *J* 6.3, CH_2, H-4), 1.83 (2H, br s, CH_2), 1.74 (2H, br s, CH_2), 1.00-0.95 (2H, m,

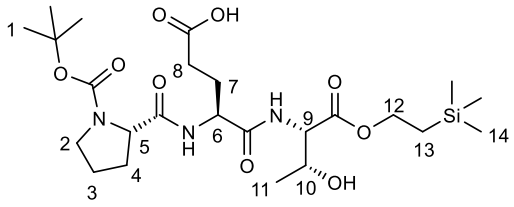
CH_2, H-6), 0.04 (9H, s, CH_3, H-7); **^{13}C NMR** (100 MHz; CH_3OD) δ 174.9 (C=O), 63.7 (CH_2), 40.4 (CH_2), 34.4 (CH_2), 27.9 (CH_2), 22.7 (CH_2), 18.2 (CH_2), -1.49 (CH_3).

N-(*tert*-Butoxycarbonyl)-proline-glutamic acid(*O*-benzyl)-threonine(*O*-benzyl)-aminovaleric acid-*O*-(trimethylsilyl)ethyl ester, **113**



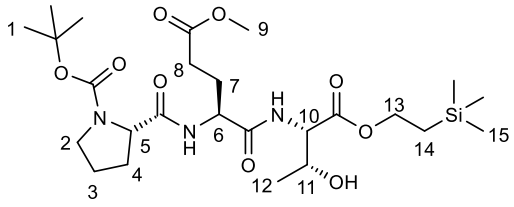
N-(*tert*-Butoxycarbonyl)-proline-glutamic acid(*O*-benzyl)-threonine(*O*-benzyl)-OH, **93**, (351 mg, 0.56 mmol) and 2-(trimethylsilyl)ethyl 5-aminopentanoate, **112**, (122 mg, 0.56 mmol) were dissolved in anhydrous DMF (5.0 ml). *N*,*N*-Diisopropylethylamine (0.59 ml, 3.37 mmol) was added, followed by HATU (427 mg, 1.12 mmol) and the mixture was stirred at room temperature for 16 h. Ethyl acetate (50 ml) and water (50 ml) were added, the layers were separated and the organic phase was washed with water (2 x 50 ml), hydrochloric acid (1 M, 50 ml), a saturated solution of $NaHCO_3$ (50 ml), and saturated brine (50 ml), dried using $MgSO_4$ and concentrated under reduced pressure to give a brown solid. The crude product was purified by column chromatography eluting with 75% ethyl acetate in light petroleum to give the *title compound*, **113**, as a pale-yellow gum (290 mg, 0.35 mmol, 63%). **$[\alpha]_D^{25}$** +37.35 (*c* 1, CH_3OH); **MS** (ESI^+) calcd for $C_{43}H_{64}N_4O_{10}Si$ [M+H] 825.4464, found 825.4488; **υ_{max} (ATR)/cm^{-1}** 3279, 2953, 1726 (C=O), 1690 (C=O), 1635, 1542, 1497; **^{1}H NMR** (400 MHz; $CDCl_3$) δ 7.87 (1H, s, NH), 7.36-7.32 (10H, ArH), 7.12 (1H, s, NH), 6.87 (1H, s, NH), 5.11 (2H, s, CH_2), 4.52 (2H, dd, *J* 31.4, 11.6, CH_2), 4.43 (1H, d, *J* 7.9, CH), 4.27, (1H, br s, CH), 4.14-4.09 (2H, m, CH), 3.41-3.23 (4H, m, CH_2), 2.57-2.51 (2H, m, CH_2), 2.25-2.22 (2H, m, CH_2), 2.07-2.00 (4H, m, CH_2), 1.80 (2H, br s, CH_2), 1.62-1.51 (4H, m, CH_2), 1.40 (9H, s, CH_3), 1.25-1.22 (2H, m, CH_2), 1.11 (3H, d, *J* 6.1, CH_3), 0.95 (2H, t, *J* 8.3, CH_2), 0.02 (9H, s, CH_3); **^{13}C NMR** (100 MHz; $CDCl_3$) δ 173.7 (C=O), 173.6 (C=O), 171.2 (C=O), 169.6 (C=O), 155.8 (C=O), 151.8 (C=O), 139.4 (C), 135.7 (C), 128.7 (CH), 128.5 (CH), 128.4 (CH), 127.9 (CH), 127.8 (CH), 127.7 (CH), 80.7 (C), 74.0 (CH), 71.6 (CH_2), 66.9 (CH_2), 62.6 (CH_2), 60.5 (CH_2), 60.2 (CH), 57.4 (CH), 54.7 (CH), 47.2 (CH_2), 39.4 (CH_2), 34.1 (CH_2), 30.4 (CH_2), 29.8 (CH_2), 28.9 (CH_2), 28.4 (CH_3), 24.8 (CH_2), 22.3 (CH_2), 17.4 (CH_2), 14.3 (CH_3).

N-(*tert*-Butoxycarbonyl)-proline-glutamic acid-threonine-*O*-(trimethylsilyl)ethyl ester, **116**



tert-Butyl 2-((7-(1-benzyloxyethyl)-2,2-dimethyl-6,9,13-trioxo-15-phenyl-5,14-dioxa-8-aza-2-sila pentadecan-10-yl)carbamoyl)pyrrolidine-1-carboxylate, **100**, (50 mg, 0.07 mmol) was dissolved in DMF (1 ml). $PdCl_2$ (4.0 mg, 0.02 mmol) was added and the reaction mixture was evacuated under reduced pressure and back-filled with Ar. This was repeated three times. After the final evacuation, the reaction flask was charged with H_2 and the mixture was stirred vigorously at room temperature for 3 h. The reaction mixture was filtered through celite and washed with methanol. The filtrate was then concentrated under reduced pressure to give the *title compound*, **116**, as a colourless solid (35 mg, 0.06 mmol, 93%). **mp** 56-57 °C; **$[\alpha]_D^{25}$** -5.75 (*c* 1, CH_3OH); **MS** (ESI^+) calcd for $C_{24}H_{43}N_3O_9Si$ [M+H] 546.2841, found 546.2842; **υ_{max} (ATR)/cm^{-1}** 3297, 3068, 2974, 2954, 1649 (C=O), 1529, 1477; **^{1}H NMR** (400 MHz; CH_3OD) δ 4.49-4.39 (2H, m, CH_2, H-12), 4.30-4.24 (4H, m, CH), 3.51-3.41 (2H, m, CH_2), 2.47 (2H, br s, CH_2), 2.47 (2H, br s, CH_2), 1.98-1.87 (4H, m, CH_2), 1.43 (9H, s, CH_3, H-1), 1.19 (3H, d, *J* 6.3, CH_3, H-11), 1.05 (2H, br s, CH_2, H-13), 0.06 (9H, s, CH_3, H-14); **^{13}C NMR** (100 MHz; CH_3OD) δ 175.6 (C=O), 174.0 (C=O), 172.0 (C=O), 156.4 (C=O), 156.0 (C=O), 81.5 (C), 68.3 (CH), 64.8 (CH_2), 61.4 (CH), 59.4 (CH), 54.1 (CH), 47.9 (CH_2), 32.4 (CH_2), 31.3 (CH_2), 28.7 (CH_3), 2.54 (CH_2), 24.6 (CH_2), 20.4 (CH_2), 18.2 (CH_3), -1.55 (CH_3).

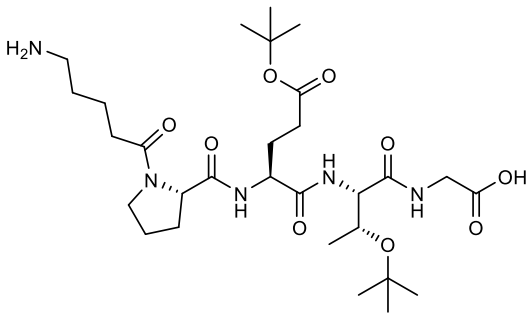
N-(*tert*-Butoxycarbonyl)-proline-glutamic acid-(*O*-methyl)-threonine-*O*-(trimethylsilyl)ethyl ester, **117**



tert-Butyl 2-((7-(1-benzyloxyethyl)-2,2-dimethyl-6,9,13-trioxo-15-phenyl-5,14-dioxa-8-aza-2-sila pentadecan-10-yl)carbamoyl)pyrrolidine-1-carboxylate, **100**, (75 mg, 0.10 mmol) was dissolved in methanol (1 ml). $PdCl_2$ (5.0 mg, 0.03 mmol) was added and the reaction mixture was evacuated under reduced pressure and back-filled with Ar. This was repeated three times. After the final evacuation, the reaction flask was charged with H_2 and the mixture was

stirred vigorously at room temperature for 1 h. The reaction mixture was filtered through celite and washed with methanol. The filtrate was then concentrated under reduced pressure to give the *title compound*, **117**, as a colourless gum (54 mg, 0.09 mmol, 94%). **$[\alpha]_D^{25}$** -2.29 (*c* 1, CH_3OH); **MS** (ESI^+) calcd for $C_{25}H_{45}N_3O_9Si$ [M+H] 560.2998, found 560.3005; **υ_{max} (ATR)/cm^{-1}** 3306, 2953, 1733 (C=O), 1653 (C=O), 1526, 1478, 1249, 1164; **^{1}H NMR** (400 MHz; CH_3OD) δ 4.55-4.48 (1H, m, CH), 4.38 (1H, d, *J* 2.9, CH), 4.32-4.30 (1H, m, CH), 4.27-4.22 (3H, m, CH and CH_2, H-13), 3.67 (3H, s, CH_3, H-9), 3.51-3.38 (2H, m, CH_2), 2.53-2.46 (2H, m, CH_2), 2.22-2.14 (2H, m, CH_2), 2.06-1.85 (4H, m, CH_2), 1.42 (9H, s, CH_3, H-1), 1.18 (3H, d, *J* 6.4, CH_3, H-12), 1.07-1.02 (2H, m, CH_2, H-14), 0.06 (9H, s, CH_3, H-15); **^{13}C NMR** (100 MHz; CH_3OD) δ 175.6 (C=O), 174.8 (C=O), 173.9 (C=O), 173.6 (C=O), 171.9 (C=O), 81.5 (C), 68.2 (CH), 64.8 (CH_2), 61.3 (CH), 59.5 (CH_3), 53.9 (CH), 52.2 (CH), 32.4 (CH_2), 31.0 (CH_2), 28.7 (CH_3), 28.4 (CH_2), 28.2 (CH_2), 24.6 (CH_2), 20.4 (CH_2), 18.2 (CH_3), -1.53 (CH_3).

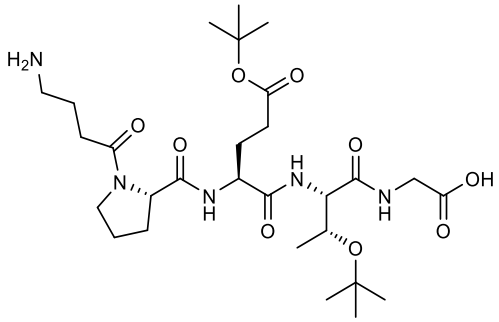
Aminovaleric acid-proline-glutamic acid(*O-tert*-butyl)-threonine(*O-tert*-butyl)-glycine-OH, **146**



2-Chlorotrityl chloride resin (600 mg, 1.00 mmol/g loading) was swelled in dichloromethane for 30 mins, then coupled to Fmoc-glycine, **143**, (1 equiv., 178 mg), *N*,*N*-diisopropylethylamine (5 equiv., 522 µl) in dichloromethane (4.0 ml). The reaction mixture was shaken at room temperature for 18 h. The solvent was then removed, and the resin washed with dichloromethane (3 x 4 ml). The unreacted resin was then capped using methanol (1 ml) and *N*,*N*-diisopropylethylamine (1 ml) in dichloromethane (5 ml) and shaken at room temperature for 1 h. The solvent was removed, and the resin was washed with dichloromethane (3 x 4 ml). The resin was then dried and the remaining peptide synthesis was carried out on a Biotage Initiator+ Alstra Peptide Synthesiser using Fmoc-Pro, Fmoc-Glu(O^tBu)-OH, Fmoc-Thr(O^tBu)-OH, (4 equiv.), Fmoc-aminovaleric acid (1 equiv.), *N,N'*-diisopropylcarbodiimide (4 equiv.), ethyl cyanohydroxyiminoacetate (4.5 M in *N*-methyl-2-pyrrolidone, 4 equiv.). Fmoc deprotection was achieved using 20% piperidine in DMF and capping was done using acetic anhydride (5 M in DMF) and pyridine. The peptide

was then cleaved from the resin using 20% hexafluoroisopropanol in dichloromethane (3 x 5 ml) and then concentrated under reduced pressure to give the *title compound*, **146**, as a colourless solid (169 mg, 0.28 mmol, 47%). **mp** decomposed at 150 °C; **$[\alpha]_D^{25}$** -5.12 (*c* 1, CH_3OH); **MS** (ESI^+) calcd for $C_{29}H_{51}N_5O_9$ [M+H] 614.3760, found 614.3787; **υ_{max} (ATR)/cm^{-1}** 3263, 3085, 2976, 2929, 1727 (C=O), 1634, 1549, 1451; **^{1}H NMR** (400 MHz; CH_3OD) δ 4.66 (2H, sept., *J* 6.5, CH_2), 4.49-4.44 (1H, m, CH), 4.40 (1H, dd, *J* 9.2, 5.1, CH), 4.33 (1H, d, *J* 2.9, CH), 4.18 (1H, qd, *J* 6.3, 3.0, CH), 3.84-3.69 (2H, m, CH_2), 3.67-3.49 (2H, m, CH_2), 3.00-2.86 (2H, m, CH_2), 2.55-2.32 (4H, m, CH_2), 2.26-2.14 (2H, m, CH_2), 2.09-1.91 (4H, m, CH_2), 1.73-1.70 (2H, m, CH_2), 1.46 (9H, s, CH_3), 1.22 (9H, s, CH_3), 1.11 (3H, d, *J* 6.4, CH_3); **^{13}C NMR** (100 MHz; CH_3OD) δ 175.4 (C=O), 175.0 (C=O), 174.4 (C=O), 174.1 (C=O), 173.5 (C=O), 171.1 (C=O), 81.9 (C), 75.8 (C), 68.1 (CH), 61.4 (CH), 59.7 (CH), 54.4 (CH), 48.8 (CH_2), 44.5 (CH_2), 40.2 (CH_2), 34.2 (CH_2), 32.8 (CH_2), 31.0 (CH_2), 28.7 (CH_3), 28.4 (CH_3), 28.1 (CH_2), 27.9 (CH_2), 25.9 (CH_2), 22.0 (CH_2), 19.7 (CH_3).

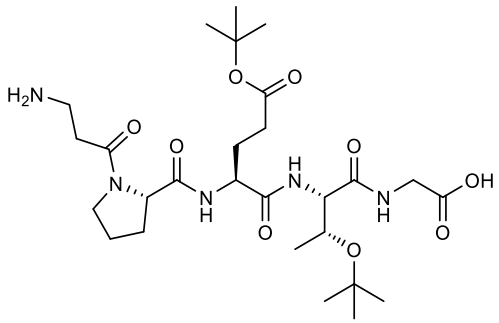
<u>γ-Aminobutyric acid-proline-glutamic acid(*O-tert*-butyl)-threonine(*O-tert*-butyl)-glycine-OH, **151b**</u>



2-Chlorotrityl chloride resin (600 mg, 1.00 mmol/g loading) was swelled in dichloromethane for 30 mins, then coupled to Fmoc-glycine, **143**, (1 equiv., 178 mg), *N*,*N*-diisopropylethylamine (5 equiv., 522 µl) in dichloromethane (4.0 ml). The reaction mixture was shaken at room temperature for 16 h. The solvent was then removed, and the resin washed with dichloromethane (3 x 4 ml). The unreacted resin was then capped using methanol (1 ml) and *N*,*N*-diisopropylethylamine (1 ml) in dichloromethane (5 ml) and shaken at room temperature for 1 h. The solvent was removed, and the resin was washed with dichloromethane (3 x 4 ml). The resin was then dried and the remaining peptide synthesis was carried out on a Biotage Initiator+ Alstra Peptide Synthesiser using Fmoc-Pro, Fmoc-Glu(O^tBu)-OH, Fmoc-Thr(O^tBu)-OH, (4 equiv.), 4-(Fmoc-amino)butyric acid (1 equiv.), *N,N'*-diisopropylcarbodiimide (4 equiv.), ethyl cyanohydroxyiminoacetate (4.5 M in *N*-Methyl-2-pyrrolidone, 4 equiv.). Fmoc deprotection was achieved using 20% piperidine in

DMF and capping was done using acetic anhydride (5 M in DMF) and pyridine. The peptide was then cleaved from the resin using 20% hexafluoroisopropanol in dichloromethane (3 x 5 ml) and then concentrated under reduced pressure to give the *title compound*, **151b**, as a colourless solid (249 mg, 0.42 mmol, 69%). **mp** 106-107 °C; **$[\alpha]_D^{25}$** +14.36 (*c* 1, CH_3OH); **MS** (ESI^+) calcd for $C_{28}H_{49}N_5O_9$ [M-H] 598.3458, found 598.3433; **υ_{max} (ATR)/cm^{-1}** 3262, 3089, 2874, 2924, 1725 (C=O), 1691 (C=O), 1632, 1552; **^{1}H NMR** (400 MHz; CH_3OD) δ 4.66 (1H, sept., *J* 6.5, CH), 4.47-4.35 (2H, m, CH), 4.17 (1H, qd, *J* 6.3, 3.1, CH), 3.83-3.71 (2H, m, CH_2), 3.69-3.51 (2H, m, CH_2), 3.02-2.98 (2H, m, CH_2), 2.65-2.33 (4H, m, CH_2), 2.28-1.89 (8H, m, CH_2), 1.46 (9H, s, CH_3), 1.22 (9H, s, CH_3), 1.11 (3H, d, *J* 6.4, CH_3); **^{13}C NMR** (100 MHz; CH_3OD) δ 175.3 (C=O), 175.1 (C=O), 174.0 (C=O), 173.4 (C=O), 173.3 (C=O), 171.2 (C=O), 81.8 (C), 75.9 (C), 68.1 (CH), 61.4 (CH), 59.6 (CH), 54.5 (CH), 48.7 (CH_2), 44.5 (CH_2), 40.4 (CH_2), 32.8 (CH_2), 32.6 (CH_2), 31.0 (CH_2), 28.7 (CH_3), 28.4 (CH_3), 28.0 (CH_2), 25.9 (CH_2), 23.4 (CH_2), 19.6 (CH_3).

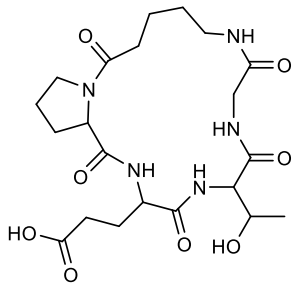
β-Alanine-proline-glutamic acid(*O-tert*-butyl)-threonine(*O-tert*-butyl)-glycine-OH, **151a**



2-Chlorotrityl chloride resin (600 mg, 1.00 mmol/g loading) was swelled in dichloromethane for 30 mins, then coupled to Fmoc-glycine, **143**, (1 equiv., 178 mg), *N*,*N*-diisopropylethylamine (5 equiv., 522 µl) in dichloromethane (4.0 ml). The reaction mixture was shaken at room temperature for 16 h. The solvent was then removed, and the resin washed with dichloromethane (3 x 4 ml). The unreacted resin was then capped using methanol (1 ml) and *N*,*N*-diisopropylethylamine (1 ml) in dichloromethane (5 ml) and shaken at room temperature for 1 h. The solvent was removed, and the resin was washed with dichloromethane (3 x 4 ml). The resin was then dried and the remaining peptide synthesis was carried out on a Biotage Initiator+ Alstra Peptide Synthesiser using Fmoc-Pro, Fmoc-Glu(O^{t}Bu)-OH, Fmoc-Thr(O^{t}Bu)-OH, (4 equiv.), Fmoc-β-alanine (1 equiv.), *N,N'*-diisopropylcarbodiimide (4 equiv.), ethyl cyanohydroxyiminoacetate (4.5 M in *N*-Methyl-2-pyrrolidone, 4 equiv.). Fmoc deprotection was achieved using 20% piperidine in DMF and capping was done using acetic anhydride (5 M in DMF) and pyridine. The peptide was then cleaved from the resin using 20% hexafluoroisopropanol in dichloromethane (3 x 5

ml) and then concentrated under reduced pressure to give the *title compound*, **151a**, as a colourless solid (146 mg, 0.25 mmol, 42%). **mp** decomposed at 150 °C; **$[\alpha]_D^{25}$** +5.37 (*c* 1, CH_3OH); **MS** (ESI^+) calcd for $C_{27}H_{47}N_5O_9$ [M-H] 584.3301, found 584.3299; **υ_{max} (ATR)/cm^{-1}** 3264, 3090, 2977, 2935, 1734 (C=O), 1692 (C=O), 1633, 1552; **^{1}H NMR** (400 MHz; CH_3OD) δ 4.66 (1H, sept., *J* 6.6, CH), 4.48-4.35 (2H, m, CH), 4.17 (1H, qd, *J* 6.2, 3.2, CH), 3.83-3.68 (2H, m, CH_2), 3.67-3.54 (2H, m, CH_2), 3.27-3.15 (2H, m, CH_2), 2.84-2.64 (2H, m, CH_2), 2.47-2.32 (2H, m, CH_2), 2.29-2.13 (2H, m, CH_2), 2.10-1.90 (4H, m, CH_2), 1.46 (9H, s, CH_3), 1.23 (9H, s, CH_3), 1.10 (3H, d, *J* 6.3, CH_3); **^{13}C NMR** (100 MHz; CH_3OD) δ 175.4 (C=O), 175.0 (C=O), 174.0 (C=O), 173.5 (C=O), 171.09 (C=O), 171.06 (C=O), 81.9 (C), 75.9 (C), 68.1 (CH), 61.4 (CH), 59.6 (CH), 54.5 (CH), 48.6 (CH_2), 44.5 (CH_2), 36.7 (CH_2), 32.8 (CH_2), 32.0 (CH_2), 31.0 (CH_2), 28.6 (CH_3), 28.4 (CH_3), 28.0 (CH_2), 25.8 (CH_2), 19.5 (CH_3).

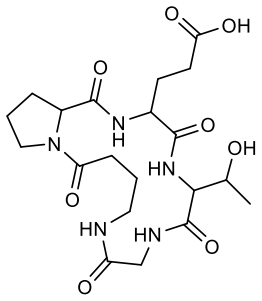
Cyclic-proline-glutamic acid-threonine-glycine-aminovaleric acid, **148**



Aminovaleric acid-proline-glutamic acid(*O-tert*-butyl)-threonine(*O-tert*-butyl)-glycine-OH, **146**, (81 mg, 0.13 mmol) was dissolved in anhydrous THF (50 ml). 4-Methylmorpholine (58 µl, 0.53 mmol) was added, followed by 4-(4,6-dimethoxy-1,3,5-triazin-2-yl)-4-methyl-morpholinium chloride (36 mg, 0.13 mmol) and stirred at room temperature for 64 h. The reaction mixture was then concentrated under reduced pressure and re-dissolved in ethyl acetate (20 ml). The organic phase was washed with water (20 ml) and hydrochloric acid (1 M, 20 ml), then dried using Na_2SO_4 and concentrated under reduced pressure to give a colourless gum. Trifluoroacetic acid was then added, and the reaction mixture was stirred at room temperature for 2 h. Diethyl ether was added to the reaction mixture before the mixture was centrifuged at 3000 rpm for 5 min and the supernatant was removed. The crude product was purified by preparative HPLC on a gradient on 2-40% over 30 min to give the *title compound*, **148**, as a colourless solid (3 mg, 6.21x10^{-3} mmol, 5%). **mp** decomposed at 180 °C; **$[\alpha]_D^{25}$** -16.75 (*c* 1, CH_3OH); **MS** (ESI^+) calcd for $C_{21}H_{33}N_5O_8$ [M-H] 482.2256, found 482.2254; **υ_{max} (ATR)/cm^{-1}** 3381, 3310, 3248, 2973, 2929, 1711 (C=O), 1665 (C=O), 1650, 1638, 1614, 1543; **^{1}H NMR** data presented in Chapter 3, p98; **^{13}C NMR** (200 MHz; 2% DMSO-

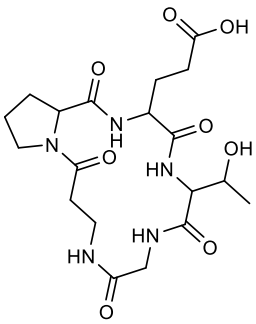
*d*6, 10% D_2O in H_2O) δ 66.7 (CH), 61.8 (CH), 61.4 (CH), 53.4 (CH), 47.8 (CH_2), 43.2 (CH_2), 38.6 (CH_2), 31.8 (CH_2), 30.1 (CH_2), 25.8 (CH_2), 25.0 (CH_2), 23.5 (CH_2), 22.8 (CH_2), 22.6 (CH_2), 18.6 (CH_3). ^{13}C assigned from HSQC data.

Cyclic-proline-glutamic acid-threonine-glycine-γ-aminobutyric acid, **149b**



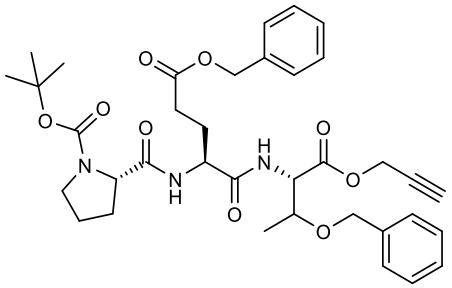
γ-Aminobutyric acid-proline-glutamic acid(*O-tert*-butyl)-threonine(*O-tert*-butyl)-glycine-OH, **151b**, (74 mg, 0.12 mmol) was dissolved in anhydrous THF (50 ml). 4-Methylmorpholine (54 µl, 0.49 mmol) was added, followed by 4-(4,6-dimethoxy-1,3,5-triazin-2-yl)-4-methyl-morpholinium chloride (34 mg, 0.12 mmol) and stirred at room temperature for 18 h. The reaction mixture was then concentrated under reduced pressure and re-dissolved in ethyl acetate (20 ml). The organic phase was washed with water (20 ml) and hydrochloric acid (1 M, 20 ml), then dried using Na_2SO_4 and concentrated under reduced pressure to give a colourless gum. Trifluoroacetic acid was then added, and the reaction mixture was stirred at room temperature for 2 h. Diethyl ether was added to the reaction mixture before the mixture was centrifuged at 3000 rpm for 5 min and the supernatant was removed. The crude product was purified by preparative HPLC on a gradient on 2-40% over 30 min to give the *title compound*, **149b**, as a colourless solid (3 mg, $6.40x10^{-3}$ mmol, 5%). **mp** decomposed at 160 °C; **$[\alpha]_D^{25}$** +16.19 (*c* 1, CH_3OH); **MS** (ESI^+) calcd for $C_{20}H_{31}N_5O_8$ [M-H] 468.2100, found 468.2093; **υ_{max} (ATR)/cm^{-1}** 3379, 3314, 2973, 2929, 1711 (C=O), 1666 (C=O), 1638; **^{1}H NMR** data presented in Chapter 3, p99; **^{13}C NMR** (200 MHz; 2% DMSO-*d*6, 10% D_2O in H_2O) δ 66.3 (CH), 62.8 (CH), 61.0 (CH), 53.7 (CH), 47.4 (CH_2), 42.8 (CH_2), 34.9 (CH_2), 33.6 (CH_2), 30.9 (CH_2), 29.0 (CH_2), 26.2 (CH_2), 24.4 (CH_2), 22.9 (CH_2), 18.9 (CH_3).^{13}C assigned from HSQC data.

Cyclic-proline-glutamic acid-threonine-glycine-β-alanine, **149a**



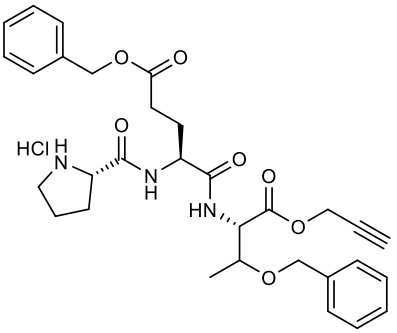
β-Alanine-proline-glutamic acid(*O-tert*-butyl)-threonine(*O-tert*-butyl)-glycine-OH, **151a**, (100 mg, 0.17 mmol) was dissolved in anhydrous THF (50 ml). 4-Methylmorpholine (75 µl, 0.68 mmol) was added, followed by 4-(4,6-dimethoxy-1,3,5-triazin-2-yl)-4-methyl-morpholinium chloride (47 mg, 0.17 mmol) and stirred at room temperature for 18 h. The reaction mixture was then concentrated under reduced pressure and re-dissolved in ethyl acetate (20 ml). The organic phase was washed with water (20 ml) and hydrochloric acid (1 M, 20 ml), then dried using Na_2SO_4 and concentrated under reduced pressure to give a colourless gum. Trifluoroacetic acid was then added, and the reaction mixture was stirred at room temperature for 2 h. Diethyl ether was added to the reaction mixture before the mixture was centrifuged at 3000 rpm for 5 min and the supernatant was removed. The crude product was purified by preparative HPLC on a gradient on 2-40% over 30 min to give the *title compound*, **149a**, as a colourless solid (2 mg, 4.39×10^{-3} mmol, 3%). **mp** decomposed at 160 °C; **$[\alpha]_D^{25}$** -13.58 (*c* 1, CH_3OH); **MS** (ESI^+) calcd for $C_{19}H_{29}N_5O_8$ [M-H] 454.1943, found 454.1940; **υ_{max} (ATR)/cm^{-1}** 3462, 3307, 2954, 2923, 2853, 1743 (C=O), 1666 (C=O), 1562; **^{1}H NMR** data presented in Chapter 3, p100; **^{13}C NMR** (200 MHz; 2% DMSO-*d*6, 10% D_2O in H_2O) δ 66.2 (CH), 62.1 (CH), 61.2 (CH), 52.2 (CH), 48.0 (CH_2), 43.0 (CH_2), 39.3 (CH_2), 33.4 (CH_2), 29.6 (CH_2), 26.9 (CH_2), 24.5 (CH_2), 21.1 (CH_2), 18.9 (CH_3).^{13}C assigned from HSQC data.

N-(*tert*-Butoxycarbonyl)-proline-glutamic acid(*O*-benzyl)-threonine(*O*-benzyl)-*O*-prop-2-yn-1-yl, **156**



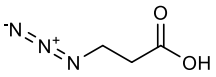
N-(*tert*-Butoxycarbonyl)-proline-glutamic acid(*O*-benzyl)-threonine(*O*-benzyl)-OH, **93**, (170 mg, 0.27 mmol) was dissolved in anhydrous THF (1.0 ml) and cooled to 0 °C. 1,1'-Carbonyldiimidazole (53 mg, 0.33 mmol) was added and stirred at 0 °C for 1 h. Propargyl alcohol (20 µl, 0.33 mmol) was added, then warmed to room temperature and stirred for 16 h. The reaction mixture was concentrated under reduced pressure and the residue was dissolved in ethyl acetate (10 ml), then washed with a saturated solution of $NaHCO_3$ (2 x 10 ml), hydrochloric acid (1 M, 2 x 10 ml), water (10 ml) and saturated brine (10 ml), dried using $MgSO_4$ and concentrated under reduced pressure to give a pale yellow gum. The crude product was purified by column chromatography eluting with 50% ethyl acetate in light petroleum to give the *title compound*, **156**, as a colourless gum (114 mg, 0.17 mmol, 63%). **$[\alpha]_D^{25}$** +2.15 (*c* 1, CH_3OH); **MS** (ESI^+) calcd for $C_{36}H_{45}N_3O_9$ [M+H] 664.3229, found 664.3233; **υ_{max} (ATR)/cm^{-1}** 3294 (C-H), 3003, 2976, 2931, 2125 (C≡C), 1760 (C=O), 1653 (C=O), 1516; **^{1}H NMR** (400 MHz; $CDCl_3$) δ 7.36-7.28 (10H, m, ArH), 5.12 (2H, s, CH_2), 4.79 (2H, d, *J* 2.5, CH_2), 4.67-4.66 (1H, m, CH), 4.65-4.64 (1H, m, CH), 4.61-4.56 (2H, m, CH and CH_2), 4.43 (1H, d, *J* 12.0, CH_2), 4.25 (1H, br s, CH), 4.21 (1H, br s, CH), 3.49 (2H, br s, CH_2), 2.57-2.53 (2H, m, CH_2), 2.42 (1H, t, *J* 2.5, CH), 2.25 (2H, br s, CH_2), 2.04-1.97 (2H, m, CH_2), 1.86 (2H, br s, CH_2), 1.44 (9H, s, CH_3), 1.23 (3H, d, *J* 4.0, CH_3); **^{13}C NMR** (100 MHz; $CDCl_3$) δ 173.0 (C=O), 172.4 (C=O), 171.5 (C=O), 171.5 (C=O), 169.5 (C=O), 137.8 (C), 135.8 (C), 128.6 (CH), 128.5 (CH), 128.3 (CH), 128.2 (CH), 127.8 (CH), 127.7 (CH), 80.5 (C), 80.3 (C), 73.5 (CH), 70.8 (CH_2), 68.3 (CH), 66.6 (CH_2), 60.4 (CH_2), 56.8 (CH), 52.8 (CH_2), 52.3 (CH), 51.4 (CH), 47.0 (CH_2), 30.2 (CH_2), 28.5 (CH_2), 28.3 (CH_3), 24.6 (CH_2), 16.3 (CH_3).

Proline-glutamic acid(*O*-benzyl)-threonine(*O*-benzyl)-*O*-prop-2-yn-1-yl hydrochloride, **157**



N-(*tert*-Butoxycarbonyl)-proline-glutamic acid(*O*-benzyl)-threonine(*O*-benzyl)-*O*-prop-2-yn-1-yl, **156**, (100 mg, 0.15 mmol) was dissolved in HCl in dioxane (4 M, 1 ml) and stirred at room temperature for 1 h. The reaction mixture was then concentrated under reduced pressure to give the *title compound*, **157**, as a colourless gum (85 mg, 0.15 mmol, quantitative yield). **$[\alpha]_D^{25}$** +5.20 (*c* 1, CH_3OH); **MS** (ESI^+) calcd for $C_{31}H_{47}N_3O_7$ [M+H] 564.2704, found 564.2719; **υ_{max} (ATR)/cm^{-1}** 3206 (C-H), 3032, 2931, 2763, 2124 (C≡C), 1732 (C=O), 1660 (C=O), 1535; **^{1}H NMR** (400 MHz; CH_3OD) δ 7.38-7.32 (10H, m, ArH), 5.15 (2H, s, CH_2), 4.72 (2H, d, *J* 2.5, CH_2), 4.65-4.56 (4H, m, CH x3 and CH_2), 4.46 (1H, d, *J* 12.0, CH_2), 4.33-4.30 (1H, m, CH), 4.25 (1H, dd, *J* 6.3, 2.6, CH), 3.68 (2H, s, CH_2), 2.94 (1H, t, *J* 2.5, CH), 2.58 (2H, t, *J* 8.0, CH_2), 2.45-2.38 (2H, m, CH_2), 2.23-2.17 (2H, m, CH_2), 2.01-1.99 (2H, br s, CH_2), 1.25 (3H, d, *J* 8.0, CH_3); **^{13}C NMR** (100 MHz; CH_3OD) δ 172.8 (C=O), 172.4 (C=O), 169.5 (C=O), 168.4 (C=O), 138.0 (C), 136.1 (C), 128.2 (CH), 128.0 (CH), 127.9 (CH), 127.8 (CH), 127.7 (CH), 127.4 (CH), 77.0 (CH), 75.6 (C), 74.1 (CH), 70.9 (CH_2), 66.1 (CH_2), 59.6 (CH), 57.9 (CH), 52.9 (CH), 52.3 (CH_2), 46.2 (CH_2), 29.9 (CH_2), 29.7 (CH_2), 26.9 (CH_2), 23.6 (CH_2), 15.2 (CH_3).

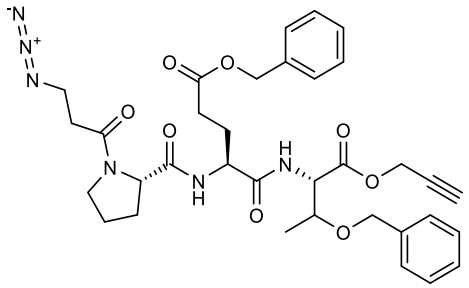
3-Azidopropanoic acid, **159**



3-Chloropropanoic acid, **158**, (150 mg, 1.39 mmol) was dissolved in anhydrous DMF (1.0 ml). Sodium azide (181 mg, 2.78 mmol) was added and then heated to 50 °C and stirred for 20 h. The reaction mixture was cooled to room temperature, and then diluted with water (10 ml) and ethyl acetate (10 ml). The layers were separated, and the organic phase was washed with water (2 x 10 ml), dried using $MgSO_4$ and concentrated under reduced pressure to give the *title compound*, **159**, as a colourless oil (50 mg, 0.43 mmol, 31%). **MS** (ESI^+) calcd for $C_3H_5N_3O_2$ [M-H] 114.0382, found 114.0309; **υ_{max} (ATR)/cm^{-1}** 2931, 2662, 2097 (N=N=N), 1711 (C=O),

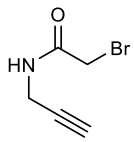
1402 (O-H); **^{1}H NMR** (400 MHz; $CDCl_3$) δ 3.60 (2H, t, *J* 8.0, CH_2), 2.65 (2H, t, *J* 8.0, CH_2); **^{13}C NMR** (100 MHz; $CDCl_3$) δ 176.5 (C=O), 46.5 (CH_2), 33.7 (CH_2). Data match literature values.[217]

N-3-Azidopropanyl-proline-glutamic acid(*O*-benzyl)-threonine(*O*-benzyl)-*O*-prop-2-yn-1-yl, **160**



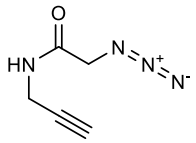
3-Azidopropanoic acid, **159**, (15 mg, 0.13 mmol) was dissolved in anhydrous dichloromethane (1 ml) and cooled to 0 °C. EDC hydrochloride (29 mg, 0.15 mmol) and HOBt hydrate (20 mg, 0.15 mmol) were added and the reaction mixture was stirred at 0 °C for 30 mins. Proline-glutamic acid(*O*-benzyl)-threonine(*O*-benzyl)-*O*-prop-2-yn-1-yl hydrochloride, **157**, (85 mg, 0.15 mmol) and *N,N*-diisopropylethylamine (80 µl, 0.45 mmol) were added, warmed to room temperature and the mixture was stirred for 16 h. The reaction mixture was concentrated under reduced pressure and the residue was diluted with ethyl acetate (10 ml) and washed with a saturated solution of $NaHCO_3$ (10 ml), hydrochloric acid (1 M, 10 ml), water (10 ml), brine (10 ml), dried using Na_2SO_4 and concentrated under reduced pressure to give the *title compound*, **160**, as a colourless gum (48 mg, 0.07 mmol, 48%). **$[\alpha]_D^{25}$** +6.37 (*c* 1, CH_3OH); **MS** (ESI^+) calcd for $C_{34}H_{40}N_6O_8$ [M+H] 661.2980, found 661.2985; **υ_{max} (ATR)/cm^{-1}** 3295, 3064, 2960, 2926, 2101 (N=N=N), 1729 (C=O), 1643 (C=O), 1527; **^{1}H NMR** (400 MHz; $CDCl_3$) δ 7.37-7.28 (10H, m, ArH), 5.12 (2H, s, CH_2), 4.71-4.65 (3H, m, CH), 4.59 (1H, d, *J* 12.0, CH_2), 4.55-4.50 (2H, m, CH_2), 4.44 (1H, d, *J* 12.0, CH_2), 4.23-4.18 (1H, m, CH), 3.62-3.53 (4H, m, CH_2), 3.46-3.40 (1H, m, CH), 2.58-2.52 (4H, m, CH_2), 2.27-2.21 (2H, m, CH_2), 2.10-1.90 (4H, m, CH_2), 1.23 (3H, d, *J* 4.0, CH_3); **^{13}C NMR** (100 MHz; $CDCl_3$) δ 175.4 (C=O), 173.1 (C=O), 172.8 (C=O), 169.3 (C=O), 169.0 (C=O), 137.5 (C), 135.6 (C), 128.6 (CH), 128.4 (CH), 128.3 (CH), 128.2 (CH), 127.9 (CH), 127.8 (CH), 75.6 (C), 73.9 (CH), 71.0 (CH_2), 70.6 (CH_2), 67.3 (CH), 66.7 (CH_2), 57.0 (CH), 56.8 (CH), 54.5 (CH_2), 52.9 (CH_2), 52.1 (CH), 40.2 (CH_2), 30.9 (CH_2), 29.7 (CH_2), 27.9 (CH_2), 24.4 (CH_2), 16.1 (CH_3).

2-Bromo-*N*-(prop-2-yn-1-yl)acetamide, **164**



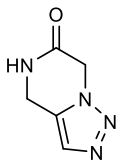
Bromoacetyl chloride, **162**, (1.1 ml, 13.5 mmol) in anhydrous dichloromethane (45 ml) was cooled to -15 °C. A solution of propargylamine, **163**, (0.86 ml, 13.5 mmol) and *N,N*-diisopropylethylamine (2.3 ml, 13.5 mmol) in anhydrous dichloromethane (20 ml) was added over 40 min, and the resulting solution was stirred at -15 °C for 1 h. The reaction mixture was warmed to room temperature and concentrated under reduced pressure then resuspended in ethyl acetate (10 ml) and filtered through a silica plug. The crude product was recrystallised from ethyl acetate and light petroleum to give the *title compound*, **164**, as a beige solid (1.5 g, 8.57 mmol, 63%) **mp** 60-62 °C; **MS** (ESI^+) calcd for $C_5H_6{}^{79}Br_1N_1O_1$ [M+H] 175.9706, found 175.9708; **υ_{max} (ATR)/cm^{-1}** 3284 (C-H), 3226, 3048, 3006, 2955, 2918, 2861, 1671 (C=O), 1634, 1584; **^{1}H NMR** (400 MHz; $CDCl_3$) δ 6.74 (1H, br s, NH), 4.08 (2H, dd, *J* 5.9, 3.1 Hz, CH_2), 3.90 (2H, s, CH_2), 2.27 (1H, t, *J* 2.6, CH); **^{13}C NMR** (100 MHz; $CDCl_3$) δ 165.3 (C=O), 78.7 (C), 72.3 (CH), 30.1 (CH_2), 28.8 (CH_2). Data match literature values.[160]

2-Azido-*N*-(prop-2-yn-1-yl)acetamide, **165**



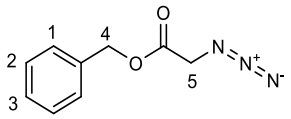
2-Bromo-*N*-(prop-2-yn-1-yl)acetamide, **164**, (200mg, 1.14 mmol) was dissolved in anhydrous DMF (2.0 ml) and sodium azide (297 mg, 4.57 mmol) was added. The reaction mixture was stirred at room temperature for 18 h before diluting with water (20 ml) and extracting with diethyl ether (3 x 20 ml). The organic extracts were combined, dried using Na_2SO_4 and concentrated under reduced pressure to give the crude azide, **165**, as a pale-yellow solid that was reacted on without purification (90 mg, 0.65 mmol, 57%). **mp** decomposed at 230 °C; **MS** (ESI^+) calcd for $C_5H_6N_4O_1$ [M+H] 139.0614, found 139.0604; **υ_{max} (ATR)/cm^{-1}** 3282 (C-H), 3078, 2994, 2950, 2106 (N=N=N), 1654 (C=O), 1555; **^{1}H NMR** (400 MHz; $CDCl_3$) δ 7.03 (1H, br s, NH), 4.02 (2H, dd, *J* 2.6, 5.4 Hz, CH_2), 3.92 (2H, s, CH_2), 2.21 (1H, t, *J* 2.6, CH); **^{13}C NMR** (100 MHz; $CDCl_3$) δ 166.9 (C=O), 79.0 (C), 71.7 (CH), 52.2 (CH_2), 29.0 (CH_2). Data match literature values.[160]

4,5-Dihydro-[1,2,3]triazolo[1,5-a]pyrazin-6(7*H*)-one, **166**



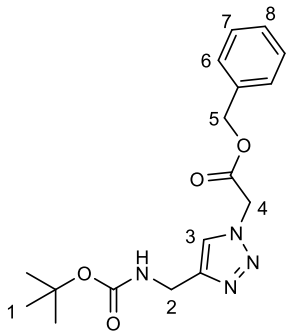
2-Azido-*N*-(prop-2-yn-1-yl)acetamide, **165**, (90 mg, 0.65 mmol) was dissolved in toluene (5.0 ml) and heated to reflux for 20 h. The reaction was then allowed to cool to room temperature and concentrated under reduced pressure to give the *title compound*, **166**, as a colourless solid and was reacted without purification (80 mg, 0.58 mmol, 89%). **mp** decomposed at 200 ^{o}C; **MS** (ESI^{+}) calcd for $C_5H_6N_4O_1$ [M+H] 139.0602, found 139.0604; **υ_{max} (ATR)/cm^{-1}** 3282, 3208, 3076, 2977, 2940, 1667 (C=O); **^{1}H NMR** (400 MHz; $(CD_3)_2SO$) δ 8.55 (1H, br s, NH), 7.66 (1H, s, ArH), 4.98 (2H, s, CH_2), 4.55-4.54 (2H, m, CH_2); **^{13}C NMR** (100 MHz; $(CD_3)_2SO$) δ 164.2 (C=O), 128.8 (C), 124.6 (CH), 48.2 (CH_2), 36.1 (CH_2). Data match literature values.[160]

Benzyl 2-azidoacetate, **169**



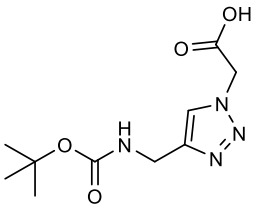
Benzyl bromoacetate, **168**, (200 mg, 0.87 mmol) was dissolved in DMF (2.0 ml) and sodium azide (114 mg, 1.75 mmol) was added. The reaction mixture was stirred at room temperature for 16 h before diluting with saturated brine (20 ml) and extracting with ethyl acetate (3 x 20 ml). The organic extracts were combined, dried using Na_2SO_4 and concentrated under reduced pressure to give the *title compound*, **169**, as a colourless oil (140 mg, 0.73 mmol, 84%). **MS** (ESI^{+}): calcd for $C_9H_9N_3O_2$ [M+Na]$^{+}$ 214.0587, found 214.0587; **υ_{max} (ATR)/cm^{-1}** 3033 2921, 2187, 2102 (N=N=N), 1742 (C=O); **^{1}H NMR** (400 MHz; $CDCl_3$) δ 7.39-7.37 (5H, m, ArH, H-1,2,3), 5.23 (2H, s, CH_2, H-4), 3.91 (2H, s, CH_2, H-5); **^{13}C NMR** (100 MHz; $CDCl_3$) δ 168.3 (C=O), 135.0 (C), 128.82 (CH), 128.79 (CH), 128.68 (CH), 67.7 (CH_2), 50.5 (CH_2). Data match literature values.[160]

Benzyl 2-(4-((*tert*-butoxycarbonylamino)methyl)-1*H*-1,2,3-triazol-1-yl)acetate, **171**



Benzyl 2-azidoacetate, **169**, (100 mg, 0.52 mmol) and *N*-boc-propargylamine, **170**, (81 mg, 0.52 mmol) were dissolved in a 1 : 1 : 1 solution of dichloromethane (0.6 ml), water (0.6 ml) and *tert*-butanol (0.6 ml). Sodium ascorbate (10 mg, 0.05 mmol) and copper(II) sulfate (13 mg, 0.05 mmol) were added and the reaction mixture was stirred at room temperature for 18 h. The reaction mixture was diluted with dichloromethane (10 ml) and water (10 ml), the layers were separated, and the aqueous phase was re-extracted using dichloromethane (2 x 10 ml). The combined organics were then washed with brine (3 x 10 ml), dried using $MgSO_4$ and concentrated under reduced pressure to give a yellow solid. The crude product was purified by column chromatography eluting with 1% methanol in dichloromethane to give the *title compound*, **171**, as a colourless solid (174 mg, 0.50 mmol, 96%). **mp** 118-120 ^{o}C**; MS** (ESI^+): calcd for $C_{17}H_{22}N_4O_4$ $[M+H]^+$ 347.1714, found 347.1717; **υ_{max} (ATR)/cm^{-1}** 3389 2975, 2963, 1741 (C=O), 1706 (C=O), 1518, ; **^{1}H NMR** (400 MHz; $CDCl_3$) δ 7.64 (1H, s, ArH, H-3), 7.39-7.32 (5H, m, ArH, H-6,7,8), 5.22 (2H, s, CH_2), 5.17 (2H, s, CH_2), 4.42 (2H, d, *J* 4.0, CH_2), 1.44 (9H, s, CH_3, H-1); **^{13}C NMR** (100 MHz; $CDCl_3$) δ 166.3 (C=O), 155.9 (C=O), 146.0 (C), 134.6 (C), 128.9 (CH), 128.8 (CH), 128.6 (CH), 123.4 (CH), 79.7 (C), 68.1 (CH_2), 50.9 (CH_2), 36.2 (CH_2), 28.4 (CH_3).

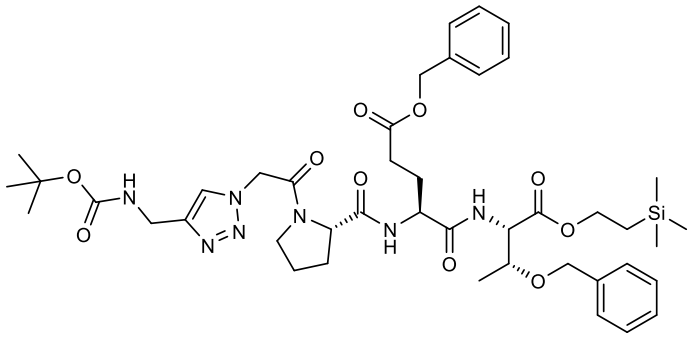
2-(4-((*tert*-Butoxycarbonylamino)methyl)-1*H*-1,2,3-triazol-1-yl)acetic acid, **172**



Benzyl 2-(4-((*tert*-butoxycarbonylamino)methyl)-1*H*-1,2,3-triazol-1-yl)acetate, **171**, (79 mg, 0.23 mmol) was dissolved in a 1 : 1 solution of methanol (1 ml) and dichloromethane (1 ml). Pd/C (12 mg, 0.11 mmol) was added and the reaction mixture was evacuated under reduced

pressure and back-filled with Ar. This was repeated three times. After the final evacuation, the reaction flask was charged with H_2 and the reaction mixture was stirred vigorously at room temperature for 18 h. The reaction mixture was filtered through Celite and washed with methanol. The filtrate was then concentrated under reduced pressure to give the *title compound*, **172**, as a colourless solid (50 mg, 0.20 mmol, 86%). **mp** 105-106 °C; **MS** (ESI^+): calcd for $C_{10}H_{16}N_4O_4$ $[M-H]^-$ 255.1099, found 255.1097; **υ_{max} (ATR)/cm^{-1}** 3338, 2977 (O-H), 2930, 1687 (C=O), 1628, 1512; **^{1}H NMR** (400 MHz; CH_3OD) δ 7.84 (1H, s, ArH), 5.13 (2H, s, CH_2), 4.32 (2H, s, CH_2), 1.44 (9H, s, CH_3); **^{13}C NMR** (100 MHz; CH_3OD) δ 171.1 (C=O), 158.2 (C=O), 147.0 (C), 125.4 (CH), 80.4 (C), 52.8 (CH_2), 36.7 (CH_2), 28.7 (CH_3).

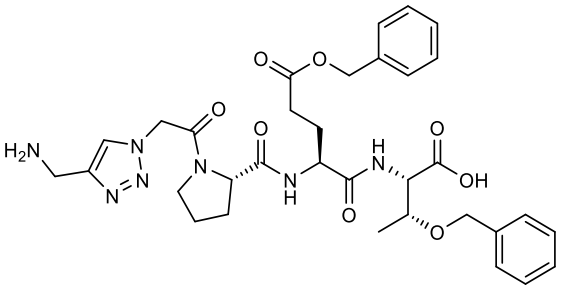
2-(4-((*tert*-butoxycarbonylamino)methyl)-1*H*-1,2,3-triazol-1-yl)acetic amide-proline-glutamic acid(*O*-benzyl)-threonine(*O*-benzyl)-*O*-(trimethylsilyl)ethyl ester, **173**



Proline-glutamic acid(*O*-benzyl)-threonine(*O*-benzyl)-*O*-(trimethylsilyl)ethyl ester hydrochloride, **105**, (146 mg, 0.23 mmol) and 2-(4-((*tert*-butoxycarbonylamino)methyl)-1*H*-1,2,3-triazol-1-yl)acetic acid, **172**, (60 mg, 0.23 mmol) were dissolved in anhydrous DMF (1.5 ml). *N,N*-Diisopropylethylamine (0.25 ml, 1.41 mmol) and HATU (178 mg, 0.47 mmol) and the mixture was stirred at room temperature for 16 h. The reaction mixture was diluted with ethyl acetate (20 ml) and water (20 ml). The layers were separated, and the organic phase was washed with water (2 x 20 ml), hydrochloric acid (1 M, 20 ml), a saturated solution of $NaHCO_3$ (20 ml) and saturated brine (20 ml), then dried using $MgSO_4$ and concentrated under reduced pressure to give an orange gum. The crude product was purified by column chromatography eluting with 5% propan-2-ol in chloroform to give the *title compound*, **173**, as a pale-yellow gum (111 mg, 0.13 mmol, 55%). **$[\alpha]_D^{25}$** -5.80 (*c* 1, CH_3OH); **MS** (ESI^+): calcd for $C_{43}H_{61}N_7O_{10}Si$ $[M+H]^+$ 864.4322, found 864.4313; **υ_{max} (ATR)/cm^{-1}** 3315, 2953, 1713 (C=O), 1655 (C=O), 1517, 1451; **^{1}H NMR** (400 MHz; $CDCl_3$) δ 7.64 (1H, s, ArH), 7.34-7.26 (11H, m, ArH and NH), 7.13 (1H, d, *J* 7.6, NH), 6.86 (1H, d, *J* 9.1, NH), 5.21-5.10 (4H, m, CH_2), 4.98 (1H, d, *J* 16.1, CH), 4.56 (2H, dd, *J* 9.2, 2.4, CH_2), 4.53-4.49 (1H, m, CH), 4.46-4.44 (1H, m, CH), 4.38-

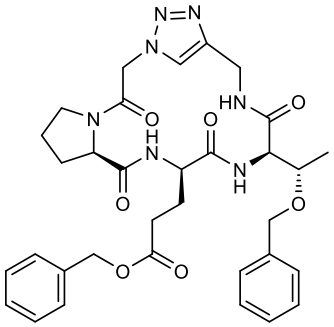
4.35 (4H, m, CH_2), 4.21-4.08 (3H, m, CH and CH_2), 3.62-3.52 (2H, m, CH_2), 2.57-2.48 (2H, m, CH_2), 2.23-2.17 (2H, m, CH_2), 2.04-1.96 (2H, m, CH_2), 1.43 (9H, s, CH_3), 1.19 (3H, d, *J* 6.3, CH_3), 0.93-0.88 (2H, m, CH_2), 0.01 (9H, s, CH_3); **^{13}C NMR** (100 MHz; $CDCl_3$) δ 173.6 (C=O), 171.6 (C=O), 171.4 (C=O), 170.9 (C=O), 170.4 (C=O), 164.6 (C=O), 145.7 (C), 138.0 (C), 135.9 (C), 128.7 (CH), 128.51 (CH), 128.47 (CH), 128.43 (CH), 128.40 (CH), 127.9 (CH), 123.6 (CH), 79.7 (C), 74.2 (CH), 70.9 (CH_2), 66.7 (CH_2), 64.1 (CH_2), 60.7 (CH), 57.0 (CH), 52.8 (CH), 51.7 (CH_2), 47.1 (CH_2), 36.4 (CH_2), 30.4 (CH_2), 28.5 (CH_3), 28.4 (CH_2), 27.7 (CH_2), 25.2 (CH_2), 17.5 (CH_2), 16.5 (CH_3) -1.42 (CH_3).

2-(4-Aminomethyl)-1*H*-1,2,3-triazol-1-yl)acetic amide-proline-glutamic acid(*O*-benzyl)-threonine(*O*-benzyl)-OH, **174**



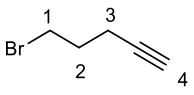
2-(4-((*tert*-butoxycarbonylamino)methyl)-1*H*-1,2,3-triazol-1-yl)acetic amide-proline-glutamic acid(*O*-benzyl)-threonine(*O*-benzyl)-*O*-(trimethylsilyl)ethyl ester, **173**, (111 mg, 0.13 mmol) was dissolved in dichloromethane (0.5 ml) and trifluoroacetic acid (0.5 ml) was added. The reaction mixture was stirred at room temperature for 5 h, before concentrating under reduced pressure to give the *title compound*, **174**, as a pale orange gum (85 mg, 0.13 mmol, quantitative yield). **$[\alpha]_D^{25}$** +4.53 (*c* 1, CH_3OH); **MS** (ESI^+): calcd for $C_{33}H_{41}N_7O_8$ $[M-H]^-$ 662.2944, found 662.2919; **υ_{max} (ATR)/cm^{-1}** 2934, 1776, 1726 (C=O), 1650 (C=O), 1531, 1451, 1412; **^{1}H NMR** (400 MHz; CH_3OD) δ 8.01 (1H, s, ArH), 7.91 (1H, d, *J* 9.1, NH), 7.35-7.24 (10H, m, ArH), 5.44 (2H, dd, *J* 32.4, 16.9 CH_2), 5.10 (2H, s, CH_2), 4.62-4.59 (1H, m, CH), 4.55-4.52 (1H, m, CH), 4.49-4.44 (3H, m, CH and CH_2), 4.25-4.22 (3H, m, CH and CH_2), 3.70-3.66 (2H, m, CH_2), 2.58-2.47 (2H, m, CH_2), 2.21-2.14 (2H, m, CH_2), 2.06-1.94 (4H, m, CH_2), 1.22 (3H, d, *J* 6.3, CH_3); **^{13}C NMR** (100 MHz; CH_3OD) δ 174.7 (C=O), 174.3 (C=O), 174.0 (C=O), 173.3 (C=O), 166.5 (C=O), 141.0 (C), 139.6 (C), 138.0 (C), 129.6 (CH), 129.3 (CH), 129.2 (CH), 129.1 (CH), 128.9 (CH), 128.7 (CH), 127.2 (CH), 76.0 (CH), 72.4 (CH_2), 67.4 (CH_2), 61.6 (CH), 58.1 (CH), 54.0 (CH), 52.7 (CH_2), 48.0 (CH_2), 35.4 (CH_2), 31.4 (CH_2), 30.7 (CH_2), 28.0 (CH_2), 25.8 (CH_2), 16.7 (CH_3).

Cyclo-2-(4-aminomethyl)-1*H*-1,2,3-triazol-1-yl)acetic amide-proline-glutamic acid(*O*-benzyl)-threonine(*O*-benzyl), **175**



2-(4-Aminomethyl)-1*H*-1,2,3-triazol-1-yl)acetic amide-proline-glutamic acid(*O*-benzyl)-threonine(*O*-benzyl)-OH, **174**, (85 mg, 0.13 mmol) was dissolved in anhydrous DMF (5.0 ml). *N*,*N*-Diisopropylethylamine (0.15 ml, 0.77 mmol) was added, followed by HATU (97 mg, 0.26 mmol) and the mixture was stirred at room temperature for 16 h. Ethyl acetate (10 ml) and water (10 ml) were added, the layers were separated and the organic phase was washed with water (2 x 10 ml), hydrochloric acid (1 M, 10 ml), a saturated solution of $NaHCO_3$ (10 ml), and saturated brine (10 ml), dried using $MgSO_4$ and concentrated under reduced pressure to give the crude *title compound*, **175**, as a pale brown solid (22 mg, 0.03 mmol, 27%). **MS** (ESI^+): calcd for $C_{33}H_{39}N_7O_7$ $[M+H]^+$ 668.2803, found 668.2801; **^{1}H NMR** (400 MHz; $CDCl_3$) δ 8.08 (1H, s, ArH), 7.39-7.20 (10H, m, ArH), 5.30 (2H, s, CH_2), 5.09 (2H, s, CH_2), 4.78-4.66 (1H, m, CH), 4.61-4.55 (1H, m, CH), 4.52-4.40 (3H, m, CH and CH_2), 4.38-4.19 (3H, m, CH and CH_2), 3.68-3.66 (2H, m, CH_2), 2.63-2.42 (2H, m, CH_2), 2.25-2.19 (2H, m, CH_2), 2.07-1.88 (4H, m, CH_2), 1.28 (3H, d, *J* 6.3, CH_3).

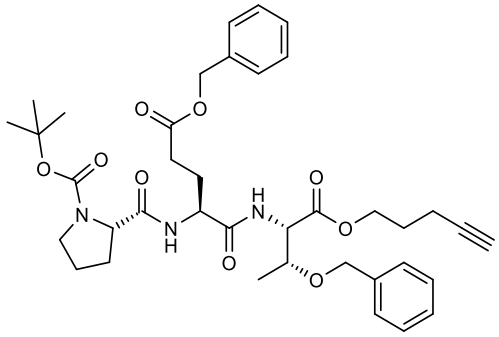
5-Bromopent-1-yne, **183**



4-Pentyn-1-ol, **180**, (0.8 ml, 8.60 mmol) was dissolved in anhydrous dichloromethane (12.0 ml) and cooled to 0 °C. Carbon tetrabromide (4.2 g, 12.9 mmol) was added, followed by triphenylphosphine (3.2 g, 12.9 mmol) allowed to warm to room temperature and the reaction mixture was stirred for 1 h. The reaction mixture was directly distilled to give the *title compound*, **183**, as a pale orange liquid (0.1 ml, 0.70 mmol, 9%). **bp** 121-122 °C; **υ_{max} (ATR)/cm^{-1}** 3303 (alkyne C-H), 3062, 2976, 2933, 1708, 1642, 1513, 1451; **^{1}H NMR** (400 MHz; $CDCl_3$) δ 3.53 (2H, t, *J* 6.8, CH_2, H-1), 2.39 (2H, td, *J* 6.8, 2.7, CH_2, H-3), 2.05 (2H, quint, *J*

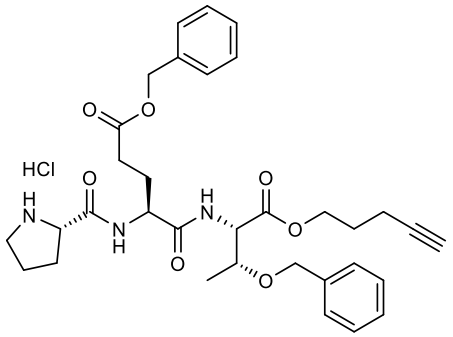
6.8, CH_2, H-2), 1.99 (1H, t, *J* 2.7, CH, H-4); **^{13}C NMR** (100 MHz; $CDCl_3$) δ 82.6 (C), 69.5 (CH), 32.3 (CH_2), 31.3 (CH_2), 17.3 (CH_2). Data match literature values.[218]

N-(*tert*-Butoxycarbonyl)-proline-glutamic acid(*O*-benzyl)-threonine(*O*-benzyl)-4-pentyn-1-yl ester, **181**



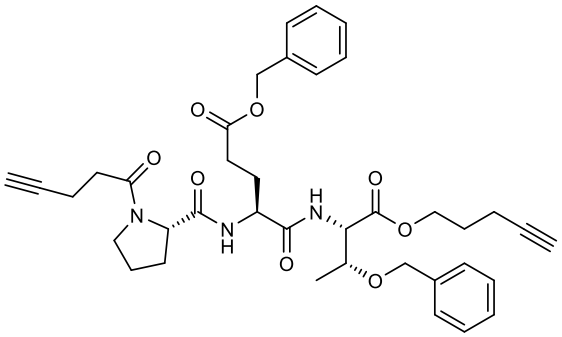
N-(*tert*-Butoxycarbonyl)-proline-glutamic acid(*O*-benzyl)-threonine(*O*-benzyl)-OH, **93**, (100 mg, 0.16 mmol) was dissolved in anhydrous DMF (1.0 ml) and cooled to 0 °C. 5-Bromopent-1-yne, **183**, (25 µl, 0.24 mmol) was added, followed by sodium carbonate (67 mg, 0.64 mmol) and the reaction mixture was stirred at room temperature for 18 h. Water (10 ml) and ethyl acetate (10 ml) were added, the layers were separated, and the organic phase was washed with water (10 ml) and brine (2 x 10 ml). The organic extracts were combined, dried using $MgSO_4$ and concentrated under reduced pressure to give a pale-yellow gum. The crude product was purified by column chromatography eluting with 50% ethyl acetate in light petroleum to give the *title compound*, **181**, as a pale-yellow gum (43 mg, 0.06 mmol, 39%). **$[\alpha]_D^{25}$** +3.39 (*c* 1, CH_3OH); **MS** (ESI^+): calcd for $C_{38}H_{49}N_3O_9$ $[M+H]^+$ 692.3542, found 692.3568; **υ_{max} (ATR)/cm^{-1}** 3295 (alkyne C-H), 3033, 2975, 2932, 2119 (C≡C), 1734 (C=O), 1652 (C=O), 1516, 1453; **^{1}H NMR** (400 MHz; $CDCl_3$) δ 7.35-7.25 (10H, m, ArH), 6.85 (1H, br s, NH), 5.10 (2H, s, CH_2), 4.62-4.52 (3H, m, CH and CH_2), 4.39-4.36 (1H, m, CH), 4.24-4.09 (5H, m, CH and 2 x CH_2), 3.47-3.33 (2H, m, CH_2), 2.55-2.51 (2H, m, CH_2), 2.23-2.17 (2H, m, CH_2), 1.93 (1H, t, *J* 2.6, CH), 1.87-1.83 (2H, m, CH_2), 1.78-1.72 (4H, m, CH_2), 1.42 (9H, s, CH_3), 1.20 (3H, d, *J* 6.3, CH_3); **^{13}C NMR** (100 MHz; $CDCl_3$) δ 173.2 (C=O), 173.0 (C=O), 171.3 (C=O), 170.3 (C=O), 156.8 (C=O), 137.5 (C), 135.7 (C), 128.8 (CH), 128.7 (CH), 128.5 (CH), 128.4 (CH), 128.3 (CH), 127.9 (CH), 80.9 (C), 80.3 (C), 77.4 (CH), 70.9 (CH_2), 69.3 (CH_2), 67.6 (CH), 64.2 (CH_2), 61.2 (CH), 57.0 (CH), 49.3 (CH), 47.0 (CH_2), 34.1 (CH_2), 30.4 (CH_2), 28.5 (CH_3), 28.0 (CH_2), 27.4 (CH_2), 25.8 (CH_2), 25.1 (CH_2), 16.4 (CH_3).

Proline-glutamic acid(*O*-benzyl)-threonine(*O*-benzyl)-4-pentyn-1-yl ester hydrochloride, **184**



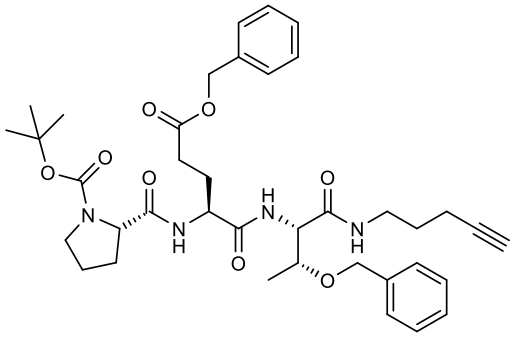
N-(*tert*-Butoxycarbonyl)-proline-glutamic acid(*O*-benzyl)-threonine(*O*-benzyl)-4-pentyn-1-yl ester, **181**, (200 mg, 0.29 mmol) was dissolved in HCl in dioxane (4 M, 2 ml) and stirred at room temperature for 2 h. The reaction mixture was concentrated under reduced pressure to give the *title compound*, **184**, as a pale-yellow gum (170 mg, 0.29 mmol, quantitative yield); **[*α*]$_D^{25}$** +4.69 (*c* 1, CH_3OH); **MS** (ESI^+) calcd for $C_{33}H_{41}N_3O_7$ [M+H] 592.3017, found 592.3027; **υ_{max} (ATR)/cm^{-1}** 3194 (C-H), 3031, 2958, 2117 (C≡C), 1732 (C=O), 1665 (C=O), 1536; **^{1}H NMR** (400 MHz; CH_3OD) δ 8.71 (1H, d, *J* 7.3, NH), 8.09 (1H, d, *J* 8.7, NH), 7.37-7.25 (10H, m, ArH), 5.12 (2H, s, CH_2), 4.62-4.55 (3H, m, CH and CH_2), 4.41-4.38 (1H, m, CH), 4.37-4.35 (1H, m, CH), 4.23-4.08 (3H, m, CH and CH_2), 3.39-3.30 (2H, m, CH_2), 2.59-2.55 (2H, m, CH_2), 2.45-2.36 (2H, m, CH_2), 2.26 (1H, t, *J* 2.6, CH), 2.22-2.17 (2H, m, CH_2), 2.08-1.93 (4H, m, CH_2), 1.83-1.72 (2H, m, CH_2), 1.23 (3H, d, *J* 6.3, CH_3); **^{13}C NMR** (100 MHz; CH_3OD) δ 174.1 (C=O), 173.6 (C=O), 171.5 (C=O), 169.8 (C=O), 139.4 (C), 137.4 (C), 129.5 (CH), 129.4 (CH), 129.2 (CH), 129.0 (CH), 128.9 (CH), 128.8 (CH), 83.7 (C), 75.5 (CH), 72.0 (CH_2), 70.5 (CH), 67.4 (CH_2), 65.1 (CH), 60.83 (CH), 58.3 (CH), 54.2 (CH_2), 47.4 (CH_2), 31.2 (CH_2), 31.0 (CH_2), 28.5 (CH_2), 28.2 (CH_2), 24.9 (CH_2), 16.4 (CH_3), 15.7 (CH_2).

N-Pent-4-ynamide-proline-glutamic acid(*O*-benzyl)-threonine(*O*-benzyl)-4-pentyn-1-yl ester, **186**



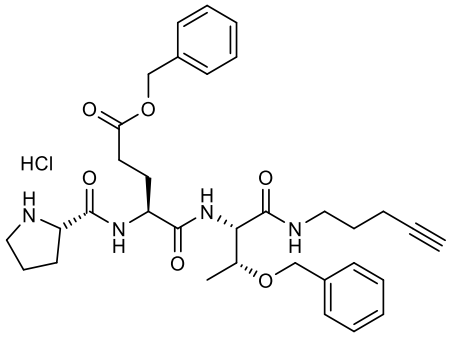
Proline-glutamic acid(*O*-benzyl)-threonine(*O*-benzyl)-4-pentyn-1-yl ester hydrochloride, **184**, (171 mg, 0.29 mmol) was dissolved in anhydrous DMF (2.0 ml) and 4-pentynoic acid, **185**, (28 mg, 0.29 mmol) was added. *N*,*N*-Diisopropylethylamine (0.30 ml, 1.74 mmol) was added, followed by HATU (220 mg, 0.58 mmol) and the mixture was stirred at room temperature for 17 h. Ethyl acetate (20 ml) and water (20 ml) were added, the layers were separated and the organic phase was washed with water (2 x 20 ml), hydrochloric acid (1 M, 20 ml), a saturated solution of $NaHCO_3$ (20 ml), and saturated brine (20 ml), dried using $MgSO_4$ and concentrated under reduced pressure to give a brown solid. The crude product was purified by column chromatography eluting with 1% methanol in dichloromethane to give the *title compound*, **186**, as a pale-yellow gum (121 mg, 0.18 mmol, 62%). **$[\alpha]_D^{25}$** -3.56 (*c* 1, CH_3OH); **MS** (ESI^+) calcd for $C_{38}H_{45}N_3O_8$ [M+H] 672.3279, found 672.3292; **υ_{max} (ATR)/cm^{-1}** 3292 (C-H), 3064, 3033, 2934, 2117 (C≡C), 1732 (C=O), 1648 (C=O), 1521; **^{1}H NMR** (400 MHz; $CDCl_3$) δ 7.44 (1H, d, *J* 7.5, NH), 7.35-7.28 (10H, m, ArH), 6.96 (1H, d, *J* 9.0, NH), 5.10 (2H, s, CH_2), 4.62 (1H, dd, *J* 9.1, 2.4, CH), 4.60-4.55 (1H, m, CH), 4.53-4.46 (2H, m, CH_2), 4.41-4.38 (1H, m, CH), 4.24-4.18 (1H, m, CH), 4.17-4.09 (2H, m, CH_2), 3.60-3.37 (2H, m, CH_2), 2.57-2.45 (6H, m, CH_2), 2.30-2.23 (2H, m, CH_2), 2.22-2.18 (2H, m, CH), 2.07-1.87 (6H, m, CH_2), 1.80-1.73 (2H, m, CH_2), 1.21 (3H, d, *J* 6.3, CH_3); **^{13}C NMR** (100 MHz; $CDCl_3$) δ 173.4 (C=O), 171.6 (C=O), 171.5 (C=O), 171.2 (C=O), 170.3 (C=O), 138.0 (C), 135.9 (C), 128.7 (CH), 128.5 (CH), 128.4 (CH), 128.3 (CH), 127.9 (CH), 127.8 (CH), 83.4 (C), 83.0 (C), 74.3 (CH), 70.9 (CH_2), 69.3 (CH), 69.0 (CH), 66.6 (CH_2), 64.1 (CH_2), 60.1 (CH), 56.9 (CH), 52.9 (CH), 47.5 (CH_2), 33.6 (CH_2), 30.5 (CH_2), 28.0 (CH_2), 27.5 (CH_2), 27.4 (CH_2), 25.1 (CH_2), 16.4 (CH_3), 15.2 (CH_2), 14.3 (CH_2).

N-(*tert*-Butoxycarbonyl)-proline-glutamic acid(*O*-benzyl)-threonine(*O*-benzyl)-4-pentyn-1-ylamide, **189**



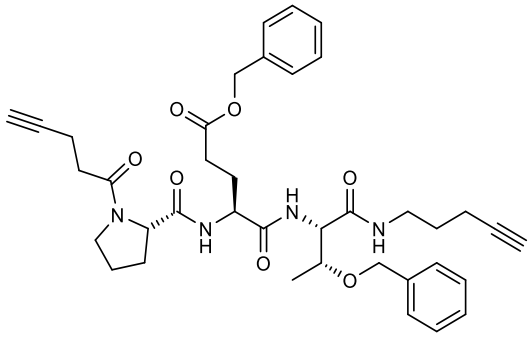
N-(*tert*-Butoxycarbonyl)-proline-glutamic acid(*O*-benzyl)-threonine(*O*-benzyl)-OH, **93**, (200 mg, 0.32 mmol) and 4-pentyne-1-amine hydrochloride, **188**, (38 mg, 0.32 mmol) were dissolved in anhydrous DMF (2.0 ml). *N*,*N*-Diisopropylethylamine (0.33 ml, 1.92 mmol) was added, followed by HATU (243 mg, 0.64 mmol) and the mixture was stirred at room temperature for 16 h. Ethyl acetate (20 ml) and water (20 ml) were added, the layers were separated and the organic phase was washed with water (2 x 20 ml), hydrochloric acid (1 M, 20 ml), a saturated solution of $NaHCO_3$ (20 ml), and saturated brine (20 ml), dried using $MgSO_4$ and concentrated under reduced pressure to give a brown solid. The crude product was purified by column chromatography eluting with 75% ethyl acetate in light petroleum to give the *title compound*, **189**, as a pale yellow solid (134 mg, 0.19 mmol, 61%). **mp** 122-123 °C **$[\alpha]_D^{25}$** +13.75 (*c* 1, CH_3OH); **MS** (ESI^+) calcd for $C_{38}H_{50}N_4O_8$ [M+H] 691.3701, found 691.3718; **υ_{max} (ATR)/cm^{-1}** 3274 (C-H), 2973, 2930, 2873, 2118 (C≡C), 1735 (C=O), 1695 (C=O), 1663 (C=O), 1535, 1497; **^{1}H NMR** (400 MHz; $CDCl_3$) δ 7.90 (1H, br s, NH), 7.38-7.28 (10H, m, ArH), 7.11 (1H, br s, NH), 6.91 (1H, br s, NH), 5.12 (2H, s, CH_2), 4.53 (2H, dd, *J* 20.3, 11.6, CH_2), 4.44 (1H, dd, *J* 8.1, 2.3, CH), 4.32 (1H, br s, CH), 4.26 (1H, br s, CH), 4.16 (1H, br s, CH), 3.44-3.30 (4H, m, CH_2), 2.61-2.48 (2H, m, CH_2), 2.22-2.18 (4H, m, CH_2), 2.09-2.02 (2H, m, CH_2), 1.93 (1H, t, *J* 2.6), 1.81-1.77 (2H, m, CH_2), 1.76-1.72 (2H, m, CH_2), 1.41 (9H, s, CH_3), 1.12 (3H, d, *J* 6.4, CH_3); **^{13}C NMR** (100 MHz; $CDCl_3$) δ 173.8 (C=O), 173.7 (C=O), 171.3 (C=O), 169.8 (C=O), 155.8 (C=O), 138.5 (C), 135.6 (C), 128.7 (CH), 128.5 (CH), 128.4 (CH), 128.3 (CH), 127.8 (CH), 127.7 (CH), 83.9 (C), 80.8 (C), 74.0 (CH), 71.6 (CH), 68.9 (CH_2), 66.9 (CH_2), 60.3 (CH), 58.0 (CH), 54.9 (CH), 47.2 (CH_2), 38.8 (CH_2), 30.9 (CH_2), 28.4 (CH_2), 28.2 (CH_3), 26.4 (CH_2), 24.8 (CH_2), 21.2 (CH_2), 16.3 (CH_2), 16.1 (CH_3).

Proline-glutamic acid(*O*-benzyl)-threonine(*O*-benzyl)-4-pentyn-1-ylamide hydrochloride, **190**



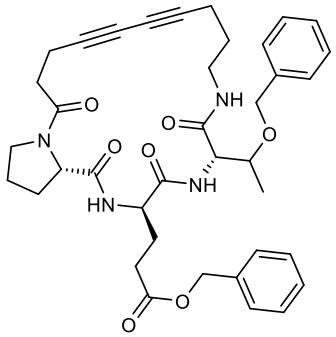
N-(*tert*-Butoxycarbonyl)-proline-glutamic acid(*O*-benzyl)-threonine(*O*-benzyl)-4-pentyn-1-ylamide, **189**, (200 mg, 0.29 mmol) was dissolved HCl in dioxane (4 M, 2.00 ml) and the solution was stirred at room temperature for 3 h. The reaction mixture was concentrated under reduced pressure to give the *title compound*, **190**, as a colourless solid (171 mg, 0.29 mmol, quantitative yield). **mp** 116-117 ^{o}C $\mathbf{[\alpha]_D^{25}}$ +0.83 (*c* 1, CH_3OH); **MS** (ESI^+) calcd for $C_{33}H_{42}N_4O_6$ [M+H] 591.3177, found 591.3205; $\mathbf{\upsilon_{max}}$ **(ATR)/cm^{-1}** 3293 (C-H), 3062, 2927, 2435, 2360 (C≡C), 1990, 1733 (C=O), 1681 (C=O), 1630, 1543, 1494; **^{1}H NMR** (400 MHz; CH_3OD) δ 7.35-7.26 (10H, m, ArH), 5.11 (2H, s, CH_2), 4.60-4.52 (2H, m, CH_2), 4.46-4.44 (1H, m, CH), 4.44-4.42 (1H, m, CH), 4.36-4.32 (1H, m, CH), 4.07-4.02 (1H, m, CH), 3.33-3.26 (4H, m, CH_2), 2.58-2.43 (2H, m, CH_2), 2.25 (1H, t, *J* 2.6, CH), 2.19-2.14 (4H, m, CH_2), 2.05-1.89 (4H, m, CH_2), 1.71-1.64 (2H, m, CH_2), 1.19 (3H, d, *J* 6.3, CH_3); **^{13}C NMR** (100 MHz; CH_3OD) δ 174.1 (C=O), 173.2 (C=O), 171.8 (C=O), 170.1 (C=O), 139.5 (C), 137.4 (C), 129.5 (CH), 129.4 (CH), 129.3 (CH), 129.2 (CH), 129.0 (CH), 128.8 (CH), 84.1 (C), 76.0 (CH), 72.2 (CH_2), 70.2 (CH_2), 68.1 (CH), 67.5 (CH_2), 60.9 (CH), 58.8 (CH), 54.4 (CH), 47.5 (CH_2), 39.6 (CH_2), 31.3 (CH_2), 31.1 (CH_2), 29.3 (CH_2), 27.8 (CH_2), 25.0 (CH_2), 16.6 (CH_3).

N-Pent-4-ynamide-proline-glutamic acid(*O*-benzyl)-threonine(*O*-benzyl)-4-pentyn-1-ylamide, **191**



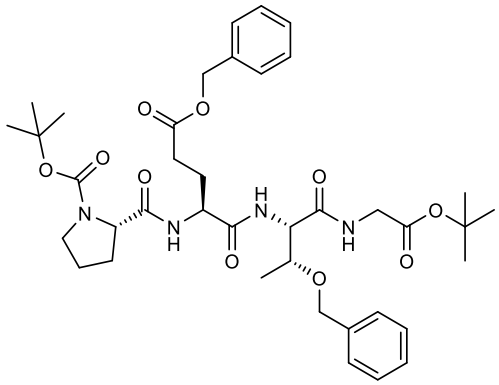
Proline-glutamic acid(*O*-benzyl)-threonine(*O*-benzyl)-4-pentyn-1-ylamide hydrochloride, **190**, (150 mg, 0.25 mmol) and 4-pentynoic acid, **185**, (25 mg, 0.25 mmol) were dissolved in anhydrous DMF (1.5 ml). *N*,*N*-Diisopropylethylamine (0.27 ml, 1.53 mmol) was added, followed by HATU (193 mg, 0.50 mmol) and the mixture was stirred at room temperature for 16 h. Ethyl acetate (20 ml) and water (20 ml) were added, the layers were separated and the organic phase was washed with water (2 x 20 ml), hydrochloric acid (1 M, 20 ml), a saturated solution of $NaHCO_3$ (20 ml), and saturated brine (20 ml), dried using $MgSO_4$ and concentrated under reduced pressure to give a brown solid. The crude product was purified by column chromatography eluting with 3% methanol in dichloromethane to give the *title compound*, **191**, as a pale-yellow solid (75 mg, 0.11 mmol, 45%). **mp** 145-146 ^{o}C **$[\alpha]_D^{25}$** -0.28 (*c* 1, CH_3OH); **MS** (ESI^+) calcd for $C_{38}H_{46}N_4O_7$ [M+H] 671.3439, found 671.3457; **υ_{max} (ATR)/cm^{-1}** 3281 (C-H), 3066, 3032, 2931, 2873, 2115 (C≡C), 1725 (C=O), 1678 (C=O), 1542, 1497; **^{1}H NMR** (400 MHz; $CDCl_3$) δ 7.85 (1H, d, *J* 5.6, NH), 7.38-7.28 (10H, m, ArH), 7.12 (1H, d, *J* 8.4, NH), 6.90 (1H, t, *J* 5.5, NH), 5.12 (2H, s, CH_2), 4.59-4.49 (2H, m, CH_2), 4.47-4.45 (1H, m, CH), 4.41-4.39 (1H, m, CH), 4.37-4.32 (1H, m, CH), 4.28-4.23 (1H, m, CH), 3.61-3.56 (1H, m, CH), 3.48-3.38 (2H, m, CH_2), 3.33-3.25 (1H, m, CH), 2.58-2.37 (6H, m, CH_2), 2.23-2.17 (4H, m, CH_2), 2.12-2.04 (2H, m, CH_2), 1.99-1.89 (4H, m, CH_2), 1.78-1.73 (2H, m, CH_2), 1.14 (3H, d, *J* 6.4, CH_3); **^{13}C NMR** (100 MHz; $CDCl_3$) δ 174.1 (C=O), 172.9 (C=O), 171.5 (C=O), 171.1 (C=O), 169.8 (C=O), 138.6 (C), 135.6 (C), 128.8 (CH), 128.6 (CH), 128.4 (CH), 128.3 (CH), 127.8 (CH), 127.7 (CH), 83.9 (C), 83.5 (C), 74.1 (CH), 71.7 (CH_2), 69.2 (CH), 68.8 (CH), 67.0 (CH_2), 60.5 (CH), 57.5 (CH), 54.9 (CH), 47.6 (CH_2), 38.8 (CH_2), 33.5 (CH_2), 31.0 (CH_2), 28.3 (CH_2), 28.2 (CH_2), 26.2 (CH_2), 25.2 (CH_2), 16.8 (CH_3), 16.1 (CH_2), 14.2 (CH_2).

Cyclic-*N*-pent-4-ynamide-proline-glutamic acid(*O*-benzyl)-threonine(*O*-benzyl)-4-pentyn-1-ylamide, **192**



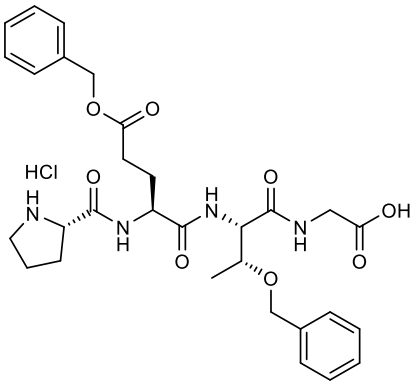
N-Pent-4-ynamide-proline-glutamic acid(*O*-benzyl)-threonine(*O*-benzyl)-4-pentyn-1-ylamide, **191**, (75 mg, 0.11 mmol) was dissolved in anhydrous DMF (0.5 ml). Copper(II) acetate monohydrate (22 mg, 0.11 mmol) and nickel chloride (14 mg, 0.11 mmol) were added, followed by triethylamine (47 µl, 0.34 mmol) and pyridine (45 µl, 0.56 mmol) and the reaction mixture was placed under oxygen. The reaction mixture was then heated to 60 °C and stirred for 16 h. The reaction mixture was then concentrated under reduced pressure to give a green oil. The crude product was first purified by column chromatography eluting with 1% methanol in dichloromethane to give the crude *title compound*, **192**, as a pale-green gum (8 mg, 0.01 mmol, 11%). **MS** (ESI^+) calcd for $C_{38}H_{44}N_4O_7$ [M+H] 669.3283, found 669.3280; **^{1}H NMR** (400 MHz; $CDCl_3$) δ 7.35-7.28 (10H, m, ArH), 5.12 (2H, s, CH_2), 4.57-4.54 (3H, m, CH_2 and CH), 4.49-4.42 (1H, m, CH), 4.40-4.31 (1H, m, CH), 4.31-4.24 (1H, m, CH), 3.57-3.44 (2H, m, CH_2), 2.54-2.36 (6H, m, CH_2), 2.25-2.17 (4H, m, CH_2), 2.12-2.02 (2H, m, CH_2), 1.98-1.88 (2H, m, CH_2), 1.75-1.62 (4H, m, CH_2), 1.14 (3H, d, *J* 6.4, CH_3); **^{13}C NMR** (100 MHz; $CDCl_3$) δ 174.5 (C=O), 173.9 (C=O), 171.2 (C=O), 171.1 (C=O), 170.4 (C=O), 138.2 (C), 135.5 (C), 128.6 (CH), 128.4 (CH), 128.3 (CH), 128.2 (CH), 128.0 (CH), 127.7 (CH), 83.9 (C), 83.5 (C), 75.6 (C), 72.0 (C), 74.0 (CH), 60.4 (CH_2), 59.8 (CH), 58.3 (CH), 55.9 (CH), 47.8 (CH_2), 43.0 (CH_2), 38.1 (CH_2), 32.6 (CH_2), 31.2 (CH_2), 29.0 (CH_2), 26.3 (CH_2), 24.6 (CH_2), 21.1 (CH_2), 17.4 (CH_3), 16.4 (CH_2), 14.2 (CH_2).

N-(*tert*-Butoxycarbonyl)-proline-glutamic acid(*O*-benzyl)-threonine(*O*-benzyl)-glycine *tert*-butyl ester, **212**



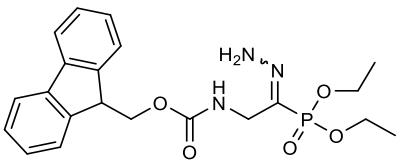
N-(*tert*-Butoxycarbonyl)-proline-glutamic acid(*O*-benzyl)-threonine(*O*-benzyl)-OH, **93**, (215 mg, 0.34 mmol) and glycine *tert*-butyl ester hydrochloride (75 mg, 0.34 mmol) were dissolved in anhydrous DMF (2.0 ml). *N,N*-Diisopropylethylamine (0.4 ml, 2.06 mmol) and HATU (261 mg, 0.69 mmol) and the mixture was stirred at room temperature for 16 h. The reaction mixture was diluted with ethyl acetate (10 ml) and water (10 ml). The layers were separated and the organic phase was washed with water (2 x 10 ml), hydrochloric acid (1 M, 10 ml), a saturated solution of $NaHCO_3$ (10 ml) and saturated brine (10 ml), then dried using $MgSO_4$ and concentrated under reduced pressure to give a yellow gum. The crude product was purified by column chromatography eluting with 50 % ethyl acetate in light petroleum to give the *title compound*, **212**, as a colourless gum (250 mg, 0.30 mmol, 88%). $\mathbf{[\alpha]_D^{25}}$ +27.7 (*c* 1, CH_3OH); **MS** (ESI^+) calcd for $C_{39}H_{54}N_4O_{10}$ [M+H] 739.3913, found 739.3912; $\mathbf{\upsilon_{max}}$ **(ATR)/cm^{-1}** 3275, 3088, 2975, 2933, 2875, 1737 (C=O), 1697 (C=O), 1635, 1536, 1478, 1452; **^{1}H NMR** (400 MHz; $CDCl_3$) **^{1}H NMR** (400 MHz; $CDCl_3$) δ 7.75 (1H, br s, NH), 7.35-7.28 (10H, m, ArH), 7.17 (1H, br s, NH), 7.06 (1H, br s, NH), 5.13 (2H, s, CH_2), 4.62 (2H, br s, CH_2), 4.55 (1H, d, *J* 8.0, CH), 4.39 (1H, br s, CH), 4.25 (2H, br s, CH), 3.95-3.92 (2H, m, CH_2), 3.44 (2H, br s, CH_2), 2.54-2.51 (2H, m, CH_2), 2.23 (2H, br s, CH_2), 2.07-2.01 (2H, m, CH_2), 1.83 (2H, br s, CH_2), 1.47 (9H, s, CH_3), 1.43 (9H, br s, CH_3), 1.17 (3H, d, *J* 6.3, CH_3); **^{13}C NMR** (100 MHz; $CDCl_3$) δ 173.2 (C=O), 171.2 (C=O), 169.7 (C=O), 169.4 (C=O), 168.4 (C=O), 155.7 (C=O), 138.2 (C), 135.7 (C), 128.6 (CH), 128.4 (CH), 128.3 (CH), 128.2 (CH), 127.8 (CH), 127.6 (CH), 81.8 (C), 80.5 (C), 73.8 (CH), 71.5 (CH_2), 66.6 (CH_2), 59.9 (CH), 56.7 (CH), 53.8 (CH), 47.1 (CH_2), 42.1 (CH_2), 30.5 (CH_2), 27.9 (CH_2), 28.3 (CH_3), 28.0 (CH_3), 26.9 (CH_2), 24.7 (CH_2), 16.2 (CH_3).

Proline-glutamic acid(*O*-benzyl)-threonine(*O*-benzyl)-glycine-OH hydrochloride, **213**



N-(*tert*-Butoxycarbonyl)-proline-glutamic acid(*O*-benzyl)-threonine(*O*-benzyl)-glycine *tert*-butyl ester, **212**, (263 mg, 0.36 mmol) was dissolved in HCl in dioxane (4 M, 1 ml) and stirred at room temperature for 16 h. The reaction mixture was concentrated under reduced pressure to give the *title compound*, **213**, as a colourless solid (200 mg, 0.36 mmol, quantitative yield). $[\alpha]_D^{25}$ +19.1 (*c* 1, CH_3OH); **MS** (ESI^+) calcd for $C_{30}H_{37}N_4O_8$ [M+H] 583.2762, found 583.2755; υ_{max} **(ATR)/cm^{-1}** 3298, 3062, 2932, 2687, 2438, 2166, 2088, 1730 (C=O), 1634, 1543, 1496; **^{1}H NMR** (400 MHz; CH_3OD) δ 8.23-8.21 (1H, m, NH), 8.12 (1H, br s, NH), 7.88-7.86 (1H, m, NH), 7.37-7.32 (10H, m, ArH), 7.28 (1H, br s, NH), 5.14 (2H, s, CH_2), 4.61-4.60 (1H, m, CH_2), 4.56-4.52 (3H, m, CH and CH_2), 4.32-4.28 (1H, m, CH), 4.12-4.10 (1H, m, CH), 4.00-3.97 (2H, m, CH_2), 3.73 (2H, s, CH_2), 2.58-2.49 (2H, m, CH_2), 2.42-2.35 (1H, m, CH_2), 2.24-2.21 (1H, m, CH_2), 2.08-1.84 (4H, m, CH_2), 1.24 (3H, d, *J* 6.3, CH_3); **^{13}C NMR** (100 MHz; CH_3OD) δ 174.5 (C=O), 173.6 (C=O), 172.7 (C=O), 171.8 (C=O), 170.3 (C=O), 139.9 (C), 137.8 (C), 129.8 (CH), 129.6 (CH), 129.5 (CH), 129.44 (CH), 129.40 (CH), 129.0 (CH), 76.4 (CH), 72.8 (CH_2), 67.8 (CH_2), 61.2 (CH), 58.8 (CH), 54.8 (CH), 52.9 (CH), 47.7 (CH_2), 42.2 (CH_2), 31.6 (CH_2), 31.3 (CH_2), 28.1 (CH_2), 25.3 (CH_2), 17.2 (CH_3).

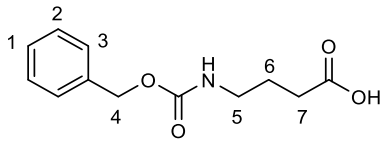
(9*H*-Fluoren-9-yl)methyl (2-(diethoxyphosphoryl)-2-hydrazonoethyl)carbamate, **218**



Oxalyl chloride (56 µl, 0.67 mmol) was added to a solution of DMF (52 µl, 0.67 mmol) in dichloromethane (2.0 ml) at 0 °C. After 20 min pyridine (54 µl, 0.67 mmol) was added, and after a further 2 min, *N*-(*tert*-Butoxycarbonyl)-glycine, **143**, (200 mg, 0.67 mmol) was added to the resulting solution. The mixture was stirred at 0 °C for 3 h, then concentrated under

reduced pressure to give an orange oil. The residue was re-dissolved in dichloromethane (0.3 ml) and triethyl phosphite (115 µl, 0.67 mmol) was added. After stirring at room temperature for 4 h, ethanol (1.0 ml) was added, and the mixture was added to a solution of hydrazine hydrate (21 µl, 0.67 mmol) in ethanol and acetic acid (10 : 1, 1.1 ml). The reaction mixture was stirred at room temperature for 16 h, diluted with water (10 ml) and the aqueous phase was extracted with dichloromethane (2 x 10 ml). The combined organic phases were dried using Na_2SO_4 and concentrated under reduced pressure. The crude product was purified by column chromatography eluting with ethyl acetate in light petroleum (3 : 1) to give the *title compound*, **218**, as a colourless solid (187 mg, 0.43 mmol, 64%). **mp** 169-170 °C; **MS** (ESI^+) calcd for $C_{21}H_{26}N_3O_5P_1$ [M+Na] 440.1233, found 440.1227; **υ_{max} (ATR)/cm^{-1}** 3302, 2983, 2936, 1719 (C=O), 1525, 1447, 1075; **^{1}H NMR** (400 MHz; $CDCl_3$) δ 7.75 (2H, d, *J* 7.5, ArH), 7.59 (2H, d, *J* 7.4, ArH), 7.38 (2H, t, *J* 7.3, ArH), 7.30 (2H, td, *J* 7.4, 1.1, ArH), 4.39 (2H, d, *J* 7.2, CH_2), 4.24-4.19 (2H, m, CH_2), 4.17-4.08 (4H, m, CH_2), 4.01 (1H, d, *J* 5.4, CH), 1.36 (6H, t, *J* 7.1, CH_3); **^{13}C NMR** (100 MHz; $CDCl_3$) δ 172.5 (C=O), 156.5 (C), 143.9 (C), 141.4 (C), 127.8 (CH), 127.2 (CH), 125.2 (CH), 120.1 (CH), 64.1 (d, *J*, 5.8, CH_2), 62.3 (d, *J*, 5.7, CH_2), 47.2 (CH), 42.7 (CH_2), 16.4 (d, *J* 6.2, CH_3).

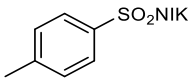
<u>*N*-Carbobenzoxy-4-aminobutyric acid, **220**</u>



γ-Aminobutyric acid, **103b**, (1.03 g, 10 mmol) was dissolved in water (5.0 ml) and sodium hydrogen carbonate (924 mg, 11 mmol) was added. Benzyl chloroformate (1.35 ml, 9.5 mmol) was dissolved in 1,4-dioxane (5.0 ml) and added to the reaction mixture, which was then stirred at room temperature for 16 h. The reaction mixture was concentrated under reduced pressure, then re-dissolved in ethyl acetate (50 ml) and aqueous hydrochloric acid was added (1 M, 50 ml). The layers were separated, and the aqueous phase was re-extracted using ethyl acetate (2 x 50 ml). The organic extracts were combined, dried using $MgSO_4$ and concentrated under reduced pressure to give a colourless solid. The crude product was purified by column chromatography eluting with ethyl acetate in light petroleum (1 : 1) to give the *title compound*, **220**, as a colourless solid (732 mg, 3.09 mmol, 31%). **m.p.** 64-65 °C; **MS** (ESI^+) calcd for $C_{12}H_{16}N_1O_4$ [M+H] 238.1074, found 238.1084; **υ_{max} (ATR)/cm^{-1}** 3324 (O-H), 2941, 1743 (C=O), 1568, 1475; **^{1}H NMR** (400 MHz; CH_3OD) δ 7.34-7.27 (5H, m, ArH, H1,2,3), 5.06 (2H, s, CH_2, H4), 3.15 (2H, t, *J* 6.9, CH_2, H5), 2.32 (2H, t, *J* 7.4, CH_2, H7), 1.78 (2H, pent., *J*

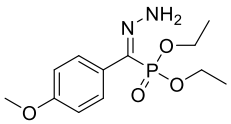
7.2, CH_2, H6); **^{13}C NMR** (100 MHz; CH_3OD) δ 177.0 (C=O), 158.9 (C=O), 138.4 (C), 129.4 (CH), 128.9 (CH), 128.8 (CH), 67.4 (CH_2), 41.1 (CH_2), 32.0 (CH_2), 26.3 (CH_2). Data match literature values.[219]

Potassium *N*-iodo *p*-toluenesulfonamide (TsNIK), **276**



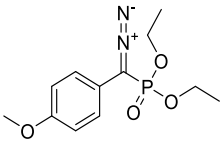
A solution of *p*-toluenesulfonamide, **275**, (5.14 g, 30.0 mmol) in aqueous potassium hydroxide (50%; 12 mL) was added to a solution of potassium iodide (19.92 g, 120 mmol) and iodine (10.15 g, 40 mmol) in water (20 mL). Aqueous potassium hydroxide (50%; 6 mL) was then added resulting a yellow precipitate. The solid was filtered and washed with diethyl ether to give the *title compound*, **276**, as a yellow solid (9.40 g, 94%); **mp** 222-223 °C; **MS** (ESI$^+$): calcd for $C_7H_9KNO_2S$ $[M+H]^+$ 209.9982, found 209.9986; **ν_{max} (ATR)/cm^{-1}** 3055, 2977, 2954, 2916, 2088, 1933, 1669, 1600, 1497; **^{1}H NMR** (400 MHz, DMSO-d_6) δ 7.49 (2H, d, *J* 8.1, ArH), 7.14 (2H, d, *J* 7.9, ArH), 2.31 (3H, s, CH_3); **^{13}C NMR** (100 MHz, DMSO-d_6) δ 144.0 (C), 138.1 (C), 128.0 (CH), 126.7 (CH), 20.8 (CH_3); Data match literature values.[177]

Diethyl (hydrazono(4-methoxyphenyl)methyl)phosphonate, **309**



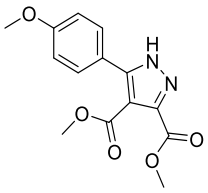
Triethyl phosphite (0.86 ml, 5.00 mmol) was added to 4-methoxybenzoyl chloride, **308**, (1.70 g, 10.0 mmol) and stirred at room temperature for 1 h. The solution was diluted with ethanol (10 ml) and was then added to hydrazine hydrate (0.62 ml, 10.0 mmol) in ethanol : acetic acid (10 : 1; 10 ml : 1.0 ml) and stirred at room temperature for 18 h. The reaction mixture was diluted with water (40 ml) and dichloromethane was added (40 ml). The layers were separated, and the aqueous phase was washed with dichloromethane (2 x 40 ml). The combined organic extracts were dried using Na_2SO_4 and concentrated under reduced pressure to give a pale-yellow oil. Column chromatography eluting with 1 : 1 ethyl acetate : light petroleum gave the *title compound*, **309**, as a pale yellow oil (390 mg, 1.36 mmol, 14 %). **MS** (ESI$^+$): calcd for $C_{12}H_{19}N_2O_4P$ $[M+H]^+$ 287.1155, found 287.1154; **ν_{max} (ATR)/cm^{-1}** 3391, 3257, 3196, 2981, 2934, 2907, 2837, 2332, 2114, 1606, 1574, 1508, 1463, 1226 (C-O), 1096 (C-O); **^{1}H NMR** (400 MHz, $CDCl_3$) δ 8.06 (2H, br s, NH), 7.54-7.51 (2H, m, ArH), 6.86-6.83 (2H, m, ArH), 4.18-3.97 (4H, m, CH_2), 3.79 (3H, s, CH_3), 1.26 (6H, t, *J* 7.1, CH_3); **^{13}C NMR** (100 MHz, $CDCl_3$) δ 159.3 (C), 130.0 (d, *J* 27.6, C), 127.9 (d, *J* 3.2, CH), 113.6 (CH), 62.4 (d, *J* 4.6, CH_2), 55.3 (CH_3), 16.2 (d, *J* 6.4, CH_3), signal due to CN not observed.

Diethyl (diazo(4-methoxyphenyl)methyl)phosphonate, **310**



Diethyl (hydrazono(4-methoxyphenyl)methyl)phosphonate, **309**, (350 mg, 1.22 mmol) was dissolved in THF (8.0 ml) and TsNIK, **276**, (450 mg, 1.35 mmol) was added, followed by potassium hydroxide solution (1 M, 2.4 ml) and stirred at room temperature for 1 h. The reaction mixture was diluted with potassium hydroxide solution (1 M, 20 ml) and diethyl ether (20 ml) was added. The layers were separated, and the aqueous phase was re-extracted using diethyl ether (2 x 20 ml). The combined organic extracts were dried using Na_2SO_4 and concentrated under reduced pressure to give a red oil. Column chromatography eluting with 1 : 1 ethyl acetate : light petroleum gave the *title compound*, **310**, as a dark orange oil (257 mg, 0.90 mmol, 74%); **MS** (ESI^+): calcd for $C_{12}H_{17}N_2O_4P$ $[M+H]^+$ 285.0999, found 285.0990; **ν_{max} (ATR)/cm^{-1}** 2982, 2935, 2907, 2837, 2069, 1607, 1573, 1510, 1461, 1443, 1249 (C-O), 1096 (C-O); **^{1}H NMR** (400 MHz, $CDCl_3$) δ 7.13-7.09 (2H, m, ArH), 6.93-6.89 (2H, m, ArH), 4.25-4.06 (4H, m, CH_2), 3.79 (3H, s, CH_3), 1.32 (6H, t, *J* 7.1, CH_3); **^{13}C NMR** (100 MHz, $CDCl_3$) δ 157.7 (C), 124.5 (d, *J* 4.4, CH), 118.0 (d, *J* 9.7, C), 115.1 (CH), 63.0 (d, *J* 5.0, CH_2), 55.5 (CH_3), 16.3 (d, *J* 6.9, CH_3), signal due to $\underline{C}N_2$ not observed.

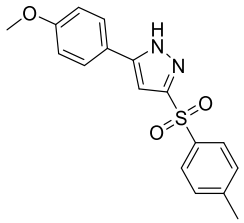
Dimethyl 5-(4-methoxyphenyl)-1*H*-pyrazole-3,4-dicarboxylate, **313**



Diethyl (diazo(4-methoxyphenyl)methyl)phosphonate, **310**, (100 mg, 0.35 mmol) was dissolved in dichloromethane (2.0 ml) and dimethyl acetylenedicarboxylate, **311**, (48 µl, 0.39 mmol) was added. The reaction was stirred at reflux for 2 h, before concentrating under reduced pressure to give a yellow oil. Methanol (2.0 ml) was then added, followed by sodium hydroxide (14 mg, 0.35 mmol) in water (0.40 ml) and stirred at room temperature for 1 h. The mixture was then diluted with water (20 ml) and extracted using ethyl acetate (3 x 20 ml). The combined organic extracts were dried using $MgSO_4$ and concentrated under reduced pressure to give a yellow oil. Column chromatography eluting with ethyl acetate and light petroleum (1:1) gave the *title compound*, **313**, as a colourless oil (73 mg, 0.25 mmol, 71%); **MS** (ESI^+): calcd for $C_{14}H_{14}N_2O_5$ $[M+H]^+$ 291.0974, found, 291.0975; **ν_{max} (ATR)/cm^{-1}** 3116, 2953, 2839, 1720 (C=O), 1613, 1581, 1509, 1226 (C-O), 1181 (C-O), 1069 (C-O); **^{1}H NMR** (400

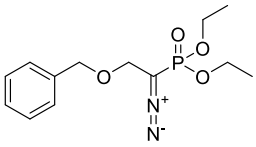
MHz, $CDCl_3$) δ 12.6 (1H, br s, NH), 7.50-7.45 (2H, m, ArH), 6.98-6.86 (2H, m, ArH), 3.81 (3H, s, CH_3), 3.79 (3H, s, CH_3), 3.70 (3H, s, CH_3); **^{13}C NMR** (100 MHz, $CDCl_3$) δ 164.5 (C=O), 161.6 (C=O), 160.7 (C), 146.0 (C), 141.8 (C), 129.6 (CH), 120.4 (C), 114.2 (CH), 112.3 (C), 55.4 (CH_3), 52.4 (CH_3), 52.3 (CH_3).

5-(4-Methoxyphenyl)-3-tosyl-1*H*-pyrazole, **314**



Diethyl (diazo(4-methoxyphenyl)methyl)phosphonate, **310**, (100 mg, 0.35 mmol) was dissolved in toluene (1.0 ml) and 1-(ethynylsulfonyl)-4-methylbenzene, **312**, (70 mg, 0.39 mmol) was added. The reaction was stirred at reflux for 2 h, before concentrating under reduced pressure to give a yellow oil. Methanol (2.0 ml) was then added, followed by sodium hydroxide (14 mg, 0.35 mmol) in water (0.40 ml) and stirred at room temperature for 2 h. The mixture was then diluted with water (30 ml) and extracted using ethyl acetate (3 x 30 ml). The combined organic extracts were dried using $MgSO_4$ and concentrated under reduced pressure to give a yellow oil. Column chromatography eluting with ethyl acetate and light petroleum (1:1) gave a colourless solid, which was then recrystallised from dichloromethane to give the *title compound*, **314**, as a colourless crystalline solid (58 mg, 0.18 mmol, 50%); **mp** 184-186 °C; **MS** (ESI^+): calcd for $C_{17}H_{16}N_2O_3S$ $[M-H]^-$ 327.0809, found, 327.0826; **ν_{max} (ATR)/cm^{-1}** 3271, 3147, 3071, 2959, 2923, 2837, 1617, 1253 (C-O), 1054 (C-O); **^{1}H NMR** (400 MHz, $(CH_3)_2SO$) δ 14.1 (1H, br s, NH), 7.85 (2H, d, *J* 8.3, ArH), 7.76-7.73 (2H, m, ArH), 7.43 (2H, d, *J* 8.3, ArH), 7.20 (1H, s, ArH), 7.03 (2H, d, *J* 8.8, ArH), 3.79 (3H, s, CH_3), 2.37 (3H, s, CH_3); **^{13}C NMR** (100 MHz, $(CH_3)_2SO$) δ 159.8 (C), 152.7 (C), 144.3 (C), 138.2 (C), 130.0 (CH), 127.3 (CH), 127.1 (CH), 120.3 (C), 114.5 (CH), 102.5 (CH), 55.3 (CH_3), 21.1 (CH_3), signal due to NCS not observed.

Diethyl (2-benzyloxy-1-diazoethyl)phosphonate, **319**

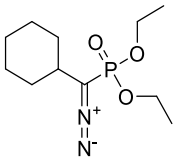


Triethyl phosphite (0.855 ml, 5.00 mmol) was added to benzyloxyacetyl chloride, **315**, (0.789 ml, 5.00 mmol) at 0 °C, then stirred at room temperature for 2 h. The reaction mixture was then diluted with ethanol (5.0 ml) and added to a solution of hydrazine hydrate (0.31 ml, 5.0

mmol) in ethanol and acetic acid (10 : 1; 5.5 ml). The mixture was stirred at room temperature for 16 h, diluted with water (30 ml) and extracted with dichloromethane (3 x 20 ml). The combined organic phases were dried using Na_2SO_4 and concentrated under reduced pressure to give the crude hydrazone.

The mixture was dissolved in THF (20 ml), and TsNIK, **276**, (1.84 g, 5.50 mmol) was added. Potassium hydroxide solution (1 M, 5.0 mL, 5.00 mmol) was added, and the mixture was stirred at RT for 1.5 h, diluted with potassium hydroxide solution (1 M, 20 ml, 20.0 mmol) and extracted with ether (3 x 30 ml). The combined organic phases were dried using Na_2SO_4 and concentrated under reduced pressure. Column chromatography eluting with ethyl acetate and light petroleum (1:1) gave the *title compound*, **319**, as a yellow oil (504 mg, 1.69 mmol, 34%); **MS** (ESI^+): calcd for $C_{13}H_{19}N_2O_4P$ $[M+H]^+$ 299.1155, found 299.1151; **ν_{max} (ATR)/cm^{-1}** 3423, 3031, 2981, 2930, 2905, 2861, 2083, 1994, 1724, 1625; **^{1}H NMR** (400 MHz, $CDCl_3$) δ 7.38-7.28 (5H, m, ArH), 4.56 (2H, s, CH_2), 4.27 (2H, d, *J* 11.9, CH_2), 4.19-4.09 (4H, m, CH_2), 1.34 (6H, td, *J* 7.1, 0.6, CH_3); **^{13}C NMR** (100 MHz, $CDCl_3$) δ 137.7 (C), 128.6 (CH), 128.0 (CH), 127.9 (CH), 71.7 (CH_2), 65.8 (d, *J* 9.5, CH_2), 62.8 (d, *J* 5.3, CH_2), 16.4 (d, *J* 6.9, CH_3), signal due to $\underline{C}N_2$ not observed.

Diethyl (cyclohexyl(diazo)methyl)phosphonate, **320**

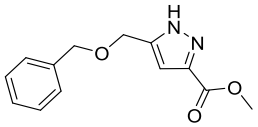


Triethyl phosphite (0.855 ml, 5.00 mmol) was added to cyclohexanecarbonyl chloride, **316**, (0.669 ml, 5.00 mmol) at 0 °C, then stirred at room temperature for 2 h. The reaction mixture was then diluted with ethanol (5.0 ml) and added to a solution of hydrazine hydrate (0.31 ml, 5.00 mmol) in ethanol and acetic acid (10 : 1; 5.5 ml). The mixture was stirred at room temperature for 16 h, diluted with water (30 ml) and extracted with dichloromethane (3 x 20 ml). The combined organic phases were dried using Na_2SO_4 and concentrated under reduced pressure to give the crude hydrazone.

The mixture was dissolved in THF (20 ml), and TsNIK, **276**, (1.84 g, 5.50 mmol) was added. Potassium hydroxide solution (1 M, 5.0 mL, 5.00 mmol) was added, and the mixture was stirred at room temperature for 1.5 h, diluted with potassium hydroxide solution (1 M, 20 ml, 20.0 mmol) and extracted with ether (3 x 30 ml). The combined organic phases were dried using Na_2SO_4 and concentrated under reduced pressure. Column chromatography eluting with ethyl acetate and light petroleum (1:1) gave the *title compound*, **320**, as a yellow oil (524 mg, 2.02 mmol, 40%); **MS** (ESI^+): calcd for $C_{11}H_{21}N_2O_3P$ $[M+H]^+$ 261.1363, found 261.1374;

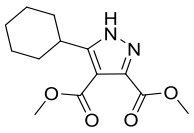
ν_{max} (ATR)/cm^{-1} 3391, 2981, 2927, 2852, 2064, 1632; **^{1}H NMR** (400 MHz, $CDCl_3$) δ 4.16-4.01 (4H, m, CH_2), 2.03-1.95 (1H, m, CH), 1.90-1.86 (2H, m, CH_2), 1.79-1.75 (3H, m, CH_2), 1.67-1.62 (1H, m, CH_2), 1.35-1.31 (6H, m, CH_3), 1.27-1.11 (4H, m, CH_2); **^{13}C NMR** (100 MHz, $CDCl_3$) δ 62.4 (d, *J* 5.4, CH_2), 33.1 (d, *J* 8.4, CH), 31.7 (d, *J* 3.2, CH_2), 26.7 (CH_2), 25.7 (CH_2), 16.3 (d, *J* 6.9, CH_3) signal due to $\underline{C}N_2$ not observed.

Methyl 5-((benzyloxy)methyl)-1*H*-pyrazole-3-carboxylate, **322**



Diethyl (2-benzyloxy-1-diazoethyl)phosphonate, **319**, (148 mg, 0.50 mmol) was dissolved in toluene (1.0 ml) and methyl propiolate, **321**, (49 µl, 0.55 mmol) was added. The reaction was stirred at reflux for 2 h, before concentrating under reduced pressure to give a yellow oil. Methanol (2 ml) was then added, followed by sodium hydroxide (20 mg, 0.50 mmol) in water (0.50 ml) and stirred at room temperature for 4 h. The mixture was then diluted with water (20 ml) and extracted using ethyl acetate (3 x 20 ml). The combined organic extracts were dried using $MgSO_4$ and concentrated under reduced pressure to give a yellow oil. Column chromatography eluting with ethyl acetate and light petroleum (1:3) gave the *title compound*, **322**, as a colourless oil (11 mg, 0.04 mmol, 9%); **MS** (ESI$^+$): calcd for $C_{13}H_{14}N_2O_3$ $[M-H]^-$ 245.0932, found 245.0940; **ν_{max} (ATR)/cm^{-1}** 3140, 2997, 2952, 2859, 1721 (C=O), 1166 (C-O); **^{1}H NMR** (400 MHz, $CDCl_3$) δ 7.36-7.27 (5H, m, ArH), 6.81 (1H, s, ArH), 4.62 (2H, s, CH_2), 4.55 (2H, s, CH_2), 3.90 (3H, s CH_3); **^{13}C NMR** (100 MHz, $CDCl_3$) δ 161.7 (C=O), 145.7 (C), 139.9 (C), 137.5 (C), 128.6 (CH), 128.1 (CH), 128.0 (CH), 107.8 (CH), 72.5 (CH_2), 63.9 (CH_2), 52.2 (CH_3).

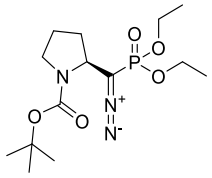
Dimethyl 5-cyclohexyl-1*H*-pyrazole-3,4-dicarboxylate, **323**



Diethyl (cyclohexyl(diazo)methyl)phosphonate, **320**, (420 mg, 1.61 mmol) was dissolved in toluene (5.0 ml) and dimethyl acetylenedicarboxylate, **311**, (0.2 ml, 1.78 mmol) was added. The reaction was stirred at reflux for 4 h, before concentrating under reduced pressure to give a yellow oil. Methanol (2 ml) was then added, followed by sodium hydroxide (65 mg, 1.61 mmol) in water (0.50 ml) and stirred at room temperature for 3 h. The mixture was then diluted with water (40 ml) and extracted using ethyl acetate (3 x 40 ml). The combined organic extracts were dried using $MgSO_4$ and concentrated under reduced pressure to give a yellow oil. Column chromatography eluting with ethyl acetate and light petroleum (1:1) gave

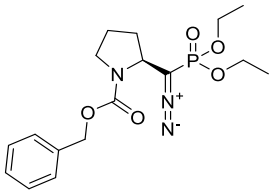
the *title compound*, **323**, as a colourless solid (244 mg, 0.92 mmol, 57%); **mp** 118-120 °C; **MS** (ESI^+): calcd for $C_{13}H_{18}N_2O_4$ $[M-H]^-$ 265.1194, found 265.1207; **ν_{max} (ATR)/cm^{-1}** 3144, 3085, 3007, 2928, 2851, 1736 (C=O), 1716 (C=O), 1216 (C-O), 1149 (C-O); **^{1}H NMR** (400 MHz, $CDCl_3$) δ 3.89 (3H, s, CH_3), 3.84 (3H, s, CH_3), 3.18-3.14 (1H, m, CH), 1.95-1.93 (2H, m, CH_2), 1.82-1.80 (2H, m, CH_2), 1.74 (2H, d, *J* 14.2, CH_2), 1.45-1.33 (4H, m, CH_2); **^{13}C NMR** (100 MHz, $CDCl_3$) δ 163.8 (C=O), 162.6 (C=O), 153.5 (C), 143.3 (C), 110.4 (C), 52.3 (CH_3), 51.9 (CH_3), 35.2 (CH), 31.8 (CH_2), 26.3 (CH_2), 25.7 (CH_2).

tert-Butyl (*S*)-2-(diazo(diethoxyphosphoryl)methyl)pyrrolidine-1-carboxylate, **327**



Oxalyl chloride (84 µl, 1.00 mmol) was added to a solution of DMF (77 µl, 1.00 mmol) in dichloromethane (10 ml) at 0 °C. After 20 min pyridine (81 µl, 1.00 mmol) was added, followed by Boc-proline, **324**, (215 mg, 1.00 mmol). The mixture was stirred at 0 °C for 1 h, then triethyl phosphite (0.17 ml, 1.00 mmol) was added. After stirring at room temperature for 4 h, ethanol (1 ml) was added, and the mixture was added to a solution of hydrazine hydrate (62 µl, 1.00 mmol) in ethanol and acetic acid (10 : 1, 1.1 ml). The mixture was stirred at room temperature for 16 h, diluted with water (20 ml) and the aqueous phase was extracted with dichloromethane (2 x 20 ml). The combined organic phases were dried using Na_2SO_4 and concentrated under reduced pressure to give the hydrazine as a yellow oil. The mixture was dissolved in THF (4.0 ml), and TsNIK (368 g, 1.10 mmol) was added. Potassium hydroxide solution (1 M; 1.0 ml, 1.00 mmol) was added, and the mixture was stirred at room temperature for 1 h, diluted with potassium hydroxide solution (1 M; 10 ml, 10 mmol) and extracted with ether (3 x 10 ml). The combined organic phases were dried using Na_2SO_4 and concentrated under reduced pressure. Column chromatography eluting with ethyl acetate and light petroleum (1 : 1) gave the *title compound*, **327**, as a yellow oil (17 mg, 0.05 mmol, 5%); **MS** (ESI^+): calcd for $C_{14}H_{26}N_3O_5P$ $[M+H]^+$ 348.1683, found 348.1687; **ν_{max} (ATR)/cm^{-1}** 2977, 2932, 2332, 2079, 1692 (C=O), 1630; **^{1}H NMR** (400 MHz, $CDCl_3$) δ 4.48 (1H, q, *J* 4.0, CH), 4.15-4.06 (4H, m, CH_2), 3.34 (2H, br s, CH_2), 2.10 (2H, br s, CH_2), 1.97-1.79 (2H, m, CH_2), 1.44 (9H, s, CH_3), 1.31 (6H, tdd, *J* 7.1, 2.8, 0.5, CH_3); **^{13}C NMR** (100 MHz, $CDCl_3$) δ 154.3 (C=O), 80.1 (d, *J* 82.5, C), 63.5 (CH_2), 54.9 (d, *J* 11.1, CH), 46.6 (CH_2), 32.4 (d, *J* 100, CH_2), 28.5 (CH_3), 23.7 (d, *J* 88.2, CH_2), 16.3 (d, *J* 6.9, CH_3), signal due to CN not observed.

(*S*)-2-(diazo(diethoxyphosphoryl)methyl)pyrrolidine-1-carboxylate, **334**

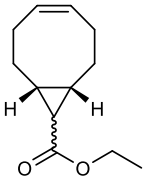


L-Proline, **330**, (575 mg, 5.00 mmol) was dissolved in aqueous NaOH (1 M, 10 ml) and cooled to 0 °C. Benzyl chloroformate (0.71 ml, 5.00 mmol) was added, then the reaction mixture was allowed to warm to room temperature and stirred for 16 h. The reaction mixture was acidified using hydrochloric acid (1 M, 20 ml), then extracted using ethyl acetate (3 x 20 ml). The organic extracts were combined, dried using $MgSO_4$ and concentrated under reduced pressure to give a colourless oil before reacting on without purification.

Oxalyl chloride (0.42 ml, 5.00 mmol) was added to a solution of DMF (0.38 ml, 5.00 mmol) in dichloromethane (50 ml) at 0 °C. After 20 min a white precipitate had formed; pyridine (0.40 ml, 5.00 mmol) was added, and after a further 3 min, Cbz-proline (1.20 g, 4.80 mmol) was added to the resulting solution. The mixture was stirred at 0 °C for 1 h, then triethyl phosphite (1.30 ml, 5.00 mmol) was added. After stirring at RT for 4 h, ethanol (5.0 ml) was added, and the mixture was added to a solution of hydrazine hydrate (0.32 ml, 5.00 mmol) in ethanol and acetic acid (10 : 1, 5.50 ml).

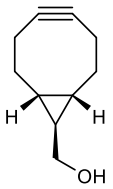
The mixture was stirred at room temperature for 17 h, diluted with water (20 ml) and the aqueous phase was extracted with dichloromethane (2 x 20 ml). The combined organic phases were dried using Na_2SO_4 and concentrated under reduced pressure to give the crude hydrazone. The mixture was dissolved in THF (4 ml), and TsNIK (201 mg, 0.60 mmol) was added. Potassium hydroxide solution (1 M; 1 ml, 1 mmol) was added, and the mixture was stirred at room temperature for 1 h, diluted with potassium hydroxide solution (1 M; 3 ml, 3 mmol) and extracted with ether (3 x 10 ml). The combined organic phases were dried using Na_2SO_4 and concentrated under reduced pressure. Column chromatography eluting with ethyl acetate and light petroleum (1 : 1) gave the *title compound*, **334**, as a yellow oil (77 mg, 0.20 mmol, 37%); **MS** (ESI^+): calcd for $C_{17}H_{24}N_3O_5P$ $[M+H]^+$ 382.1526, found 382.1513; **ν_{max} (ATR)/cm^{-1}** 2977, 2932, 2332, 2079, 1692, 1630; **^{1}H NMR** (400 MHz, $CDCl_3$) δ 7.36-7.27 (5H, m, ArH), 5.15 (2H, s, CH_2), 4.54 (1H, s, CH), 4.10-3.89 (4H, m, CH_2), 3.47-3.41 (2H, m, CH_2), 2.18-2.13 (2H, m, CH_2), 1.98-1.82 (2H, m, CH_2), 1.31-1.23 (6H, m, CH_3); **^{13}C NMR** (100 MHz, $CDCl_3$) δ 154.9 (d, *J* 22.1, C), 136.6 (d, *J* 35.4, C), 128.7 (CH), 128.6 (CH), 128.4 (CH), 128.2 (CH), 127.9 (CH), 67.3 (d, *J* 63.3, CH_2), 62.6 (CH_2), 55.4 (d, *J* 77.9, CH), 46.9 (d, *J* 45.2, CH_2), 32.4 (d, *J* 111, CH_2), 23.8 (d, *J* 85.6 CH_2), 16.3 (d, *J* 7.1. CH_3).

Ethyl (1*R*,8*S*,*Z*)-bicyclo[6.1.0]non-4-ene-9-carboxylate, **341**



$Rh_2(OAc)_4$ (17 mg, 0.04 mmol) was dissolved in anhydrous dichloromethane under Ar (1.0 ml) and cyclooctadiene, **339**, (0.9 ml, 7.61 mmol) was added. Ethyl diazoacetate, **340**, (0.1 ml, 0.95 mmol) was also dissolved in anhydrous dichloromethane (1.0 ml) and placed under Ar and added slowly to the cyclooctadiene solution, with evolution of N_2 gas. The reaction mixture was stirred at room temperature for 42 h, then the solvent was evaporated. Column chromatography eluting with 1% diethyl ether in light petroleum gave the *title compound*, **341**, as a colourless oil (*endo* 69 mg, 0.36 mmol, 37%; *exo* 111 mg, 0.57 mmol, 60%). **394-4 (*endo*): MS** (ESI^+): calcd for $C_{12}H_{18}O_2$ $[M+Na]^+$ 217.1199, found 217.1191; **ν_{max} (ATR)/cm^{-1}** 2979, 2935, 2877, 2325, 2101, 1989, 1719 (C=O), 1655, 1486, 1149 (C-O); **^{1}H NMR** (400 MHz, $CDCl_3$) δ 5.64-5.56 (2H, m, CH), 4.11 (2H, q, *J* 7.1, CH_2), 2.54-2.46 (2H, m, CH_2), 2.22-2.15 (2H, m, CH_2), 2.08-2.02 (2H, m, CH_2), 1.85-1.80 (2H, m, CH_2), 1.70 (t, *J* 8.8, CH), 1.43-1.34 (2H, m, CH), 1.26 (t, *J* 7.1, CH_3); **^{13}C NMR** (100 MHz, $CDCl_3$) δ 172.5 (C=O), 129.6 (CH), 59.9 (CH_2), 27.2 (CH_2), 24.3 (CH), 22.8 (CH_2), 21.4 (CH), 14.5 (CH_3). **394-5 (*exo*): MS** (ESI^+): calcd for $C_{12}H_{18}O_2$ $[M+H]^+$ 195.1380, found 195.1380; **ν_{max} (ATR)/cm^{-1}** 2979, 2933, 1719 (C=O), 1478, 1442 1182 (C-O); **^{1}H NMR** (400 MHz, $CDCl_3$) δ 5.64-5.56 (2H, m, CH), 4.06 (2H, q, *J* 7.1, CH_2), 2.31-2.23 (2H, m, CH_2), 2.20-2.12 (2H, m, CH_2), 2.09-2.01 (2H, m, CH_2), 1.56-1.50 (2H, m, CH_2), 1.49-1.40 (2H, m, CH_2), 1.22 (3H, t, *J* 7.1, CH_3), 1.15 (1H, t, *J* 4.5, CH); **^{13}C NMR** (100 MHz, $CDCl_3$) δ 174.4 (C=O), 130.0 (CH), 60.3 (CH_2), 28.3 (CH_2), 27.9 (CH), 27.8 (CH), 26.7 (CH_2), 14.4 (CH_3). Data match literature values.[210]

((1*R*,8*S*,9r)-Bicyclo[6.1.0]non-4-yn-9-yl)methanol (*exo*), **344**



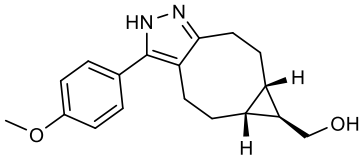
Lithium aluminium hydride (20 mg, 0.53 mmol) was suspended in anhydrous diethyl ether (2.0 ml) and cooled to 0 °C. Ethyl (1*R*,8*S*,*Z*)-bicyclo[6.1.0]non-4-ene-9-carboxylate, **341**, (111 mg, 0.58 mmol) was dissolved in anhydrous diethyl ether (2.0 ml) and added to the $LiAlH_4$ suspension at 0 °C, then warmed to room temperature and stirred for 15 min. The

reaction mixture was then cooled to 0 °C and water was added slowly until the solid turned white. Na_2SO_4 was added to the reaction mixture then filtered through celite, washing with diethyl ether. The filtrate was concentrated under reduced pressure before reacting on without purification.

The alcohol, **342**, was dissolved in dichloromethane (4.0 ml) and cooled to 0 °C. A solution of bromine (24 µl) in dichloromethane (2.0 ml) was added until the light orange colour persisted. The reaction mixture was quenched with 10% sodium thiosulfate solution and extracted using dichloromethane (3 x 10 ml). The organic extracts were combined, dried using Na_2SO_4, concentrated under reduced pressure to give the dibromide, **343**, and reacted on without purification.

The dibromide, **343**, was dissolved in anhydrous THF (5.0 ml) and cooled to 0 °C. Potassium *tert*-butoxide (1 M, 1.50 ml) was added slowly, then the reaction mixture was stirred at reflux for 2 h. The reaction mixture was cooled to room temperature, quenched with saturated ammonium chloride solution and extracted using dichloromethane (3 x 10 ml), dried using $MgSO_4$ and concentrated under reduced pressure to give a pale-yellow oil. Column chromatography eluting with 25% diethyl ether in light petroleum gave the *title compound*, **344**, as a colourless solid (12 mg, 0.08 mmol, 14%); **ν_{max} (ATR)/cm^{-1}** 3339 (O-H), 2921 (O-H), 2846, 2325, 2117, 1991, 1646; **^{1}H NMR** (400 MHz, $CDCl_3$) δ 3.55 (2H, d, *J* 6.3, CH_2), 2.44-2.40 (2H, m, CH_2), 2.32-2.35 (2H, m, CH_2), 2.18-2.14 (2H, m, CH_2), 1.58 (1H, br s, OH), 1.41-1.32 (2H, m, CH_2), 0.74-0.64 (3H, m, CH); **^{13}C NMR** (100 MHz, $CDCl_3$) δ 99.0 (C), 67.3 (CH_2), 33.6 (CH_2), 27.5 (CH), 22.7 (CH), 21.6 (CH_2). Data match literature values.[210]

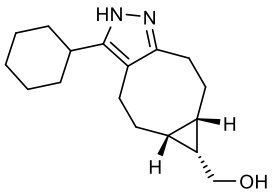
((5a*R*,6*S*,6a*R*)-3-(4-Methoxyphenyl)-2,4,5,5a,6,6a,7,8-octahydrocyclopropa[5,6]cycloocta[1,2-c]pyrazol-6-yl)methanol, **345**



Diethyl (diazo(4-methoxyphenyl)methyl)phosphonate, **310**, (20 mg, 0.07 mmol) was dissolved in dichloromethane (1.0 ml) and ((1*R*,8*S*,9r)-bicyclo[6.1.0]non-4-yn-9-yl)methanol, **344**, (12 mg, 0.08 mmol) was added. The reaction was stirred at room temperature for 5 h, before concentrating under reduced pressure to give a yellow oil. Methanol (1.0 ml) was then added, followed by sodium hydroxide (3 mg, 0.07 mmol) in water (0.20 ml) and stirred at room temperature for 2 h. The mixture was then diluted with water (10 ml) and extracted

using ethyl acetate (3 x 10 ml). The combined organic extracts were dried using $MgSO_4$ and concentrated under reduced pressure to give a yellow oil. Column chromatography eluting with ethyl acetate and light petroleum (3:1) gave the *title compound*, **345**, as a colourless solid (14 mg, 0.05 mmol, 59%); **MS** (ESI^+): calcd for $C_{18}H_{22}N_2O_2$ $[M+H]^+$ 299.1756, found, 299.1754; **ν_{max} (ATR)/cm^{-1}** 3196 (C-O), 3060, 2928, 2855, 1653, 1615, 1569, 1529, 1512, 1248 (C-O), 1092 (C-O); **^{1}H NMR** (400 MHz, $CDCl_3$) δ 7.38-7.35 (2H, m, ArH), 6.99-6.95 (2H, m, ArH), 4.56 (1H, br s, OH), 3.86 (3H, s, CH_3), 3.50 (2H, d, *J* 6.9, CH_2), 2.89 (2H, dddd, *J* 15.2, 11.5, 8.0, 3.1, CH_2), 2.71 (1H, ddd, *J* 15.2, 9.2, 3.1, CH_2), 2.51 (1H, ddd, *J* 15.2, 8.0, 3.1, CH_2), 2.45-2.39 (2H, m, CH_2), 1.36-1.23 (2H, m, CH_2), 0.92-0.85 (2H, m, CH), 0.77-0.72 (1H, m, CH); **^{13}C NMR** (100 MHz, $CDCl_3$) δ 159.5 (C), 149.1 (C), 145.7 (C), 129.6 (CH), 124.8 (C), 116.0 (C), 114.2 (CH), 66.8 (CH_2), 55.5 (CH_3), 29.8 (CH_2), 29.0 (CH), 28.4 (CH_2), 26.5 (CH_2), 23.4 (CH), 23.2 (CH), 22.4 (CH_2).

((5a*R*,6*R*,6a*S*)-3-Cyclohexyl-2,4,5,5a,6,6a,7,8-octahydrocyclopropa[5,6]cycloocta[1,2-c]pyrazol-6-yl)methanol, **346**



Diethyl (cyclohexyl(diazo)methyl)phosphonate, **320**, (39 mg, 0.15 mmol) was dissolved in dichloromethane (1.0 ml) and ((1*R*,8*S*,9r)-bicyclo[6.1.0]non-4-yn-9-yl)methanol, **344**, (25 mg, 0.17 mmol) was added. The reaction was stirred at room temperature for 3.5 h, before concentrating under reduced pressure to give a colourless oil. Methanol (1.0 ml) was then added, followed by sodium hydroxide (7 mg, 0.17 mmol) in water (0.20 ml) and stirred at room temperature for 18 h. The mixture was then diluted with water (10 ml) and extracted using ethyl acetate (3 x 10 ml). The combined organic extracts were dried using $MgSO_4$ and concentrated under reduced pressure to give a pale-yellow oil. Column chromatography eluting with ethyl acetate and light petroleum (3:1) gave the *title compound*, **346**, as a colourless solid (30 mg, 0.11 mmol, 66%); **mp** 109-110 °C; **MS** (ESI^+): calcd for $C_{17}H_{26}N_2O_1$ $[M+H]^+$ 275.2118, found, 275.2120; **ν_{max} (ATR)/cm^{-1}** 3193 (O-H), 2922, 2849, 1447, 1061; **^{1}H NMR** (400 MHz, $CDCl_3$) δ 3.69 (2H, d, *J* 7.5, CH_2), 2.94 (1H, ddd, *J* 15.0, 7.8, 2.8, CH), 2.73-2.62 (2H, m, CH_2), 2.62-2.55 (1H, m, CH), 2.41 (1H, ddd, *J* 15.0, 8.1, 2.8, CH), 2.32-2.17 (2H, m, CH_2), 1.84 (4H, t, *J* 11.8, CH_2), 1.74 (1H, d, *J* 12.6, CH), 1.50-1.23 (8H, m, CH_2), 1.11-1.04 (2H, m, CH_2); **^{13}C NMR** (100 MHz, $CDCl_3$) δ 149.9 (C), 148.5 (C), 114.6 (C), 59.9 (CH_2), 35.5 (CH), 32.8

(CH_2), 32.7 (CH_2), 26.8 (CH_2), 26.2 (CH_2), 25.0 (CH_2), 23.7 (CH_2), 22.3 (CH_2), 21.8 (CH), 21.0 (CH), 20.8 (CH).

8. PIPS Reflective Statement

Note to examiners:

This statement is included as an appendix to the thesis in order that the thesis accurately captures the PhD training experienced by the candidate as a BBSRC Doctoral Training Partnership student.

The Professional Internship for PhD Students is a compulsory 3-month placement which must be undertaken by DTP students. It is usually centred on a specific project and must not be related to the PhD project. This reflective statement is designed to capture the skills development which has taken place during the student's placement and the impact on their career plans it has had.

PIPS Reflective Statement

For my three-month placement I worked at a company called Sygnature Discovery in their DMPK department. Taking a break from chemistry and going into a completely different area, to which I had no background knowledge was challenging, but a challenge I very much enjoyed.

On my first day I met my line manager Jamie, and we had a good conversation about what I wanted to achieve within my placement. One thing I enjoyed about working at Sygnature is that they were always keen for me to meet my own goals and help in any way they could. My goal was simply to learn as much as possible while I was there as I was interested in going into DMPK after I finish my PhD. One of the first key assays I was taught was microsomal stability for the measurement of phase one metabolism and therefore a half-life of a compound. I was completely trained in this assay and testing client compounds within a couple of weeks of me starting my placement. As well as this assay, I was trained to run logD assays, PAMPA, plasma protein binding, hepatocyte stability, as well as being trained in cell culture, and I had the opportunity to get involved in metabolite identification. I got to experience the different sides of DMPK, including the more physical chemistry, as well as ADME and discovery toxicology, though my real interest lay with Met ID.

While I was at Sygnature I was also put in charge of developing an assay for studying mitochondrial toxicity using an Extracellular Flux Analyser, or Seahorse, from Agilent. This assay would be used to test if any client compounds had any potential for causing mitochondrial toxicity and consequently drug induced liver injury. Through this I was not only able to improve my cell culture techniques but also learn how to manage a project and train others in the technique. I gave a presentation at a company meeting about the progress I had achieved, which involved me thoroughly researching the background not only in mitochondrial toxicity but also in the assay itself. This vastly improved my confidence in my work as I received very good feedback and had lots if suggestions and ideas of where I could go with it next.

My placement felt like it went extremely fast though I guess that is a sign of how much I enjoyed it. I had the chance to work with a genuinely lovely team of people, who were always friendly and never got tired of my endless questions. The only thing I regret about the

placement was due to the short timeframe, not being able to spend more time doing metabolite identification as I that was where I felt my strengths lay. I hope in the future I get to experience this more. I can say I really enjoyed the challenge of this placement, of going into a completely new area and broadening my skills set. They kept me very busy, which is just how I like it to be.

9. References

(1) Cafarelli, T.; Desbuleux, A.; Wang, Y.; Choi, S.; De Ridder, D.; Vidal, M. *Curr. Opin. Struct. Biol.* **2017**, *44*, 201–210.

(2) Villoutreix, B. O.; Kuenemann, M. A.; Poyet, J.-L.; Bruzzoni-Giovanelli, H.; Labbé, C.; Lagorce, D.; Sperandio, O.; Miteva, M. A. *Mol. Inform.* **2014**, *33*, 414–437.

(3) *Protein-Protein Interactions*; Wendt, M. D., Ed.; Topics in Medicinal Chemistry; Springer-Verlag: Berlin Heidelberg, 2012.

(4) Nooren, I. M. A.; Thornton, J. M. *EMBO J.* **2003**, *22*, 3486–3492.

(5) Jones, S.; Thornton, J. M. *Proc. Natl. Acad. Sci.* **1996**, *93*, 13–20.

(6) Keskin, O.; Ma, B.; Nussinov, R. *J. Mol. Biol.* **2005**, *345*, 1281–1294.

(7) Clackson, T.; Wells, J. A. *Science* **1995**, *267*, 383–386.

(8) Bogan, A. A.; Thorn, K. S. *J. Mol. Biol.* **1998**, *280*, 1–9.

(9) Tsai, C.-J.; Lin, S. L.; Wolfson, H. J.; Nussinov, R. *Protein Sci.* **1997**, *6*, 53–64.

(10) Lee, K. H.; Xie, D.; Freire, E.; Amzel, L. M. *Proteins Struct. Funct. Bioinforma.* **1994**, *20*, 68–84.

(11) Ryan, D. P.; Matthews, J. M. *Curr. Opin. Struct. Biol.* **2005**, *15*, 441–446.

(12) Sarvagalla, S.; Cheung, C. H. A.; Tsai, J.-Y.; Hsieh, H. P.; Coumar, M. S. *RSC Adv.* **2016**, *6*, 31947–31959.

(13) Hopkins, A. L.; Groom, C. R. *Nat. Rev. Drug Discov.* **2002**, *1*, 727–730.

(14) Stelzl, U.; Worm, U.; Lalowski, M.; Haenig, C.; Brembeck, F. H.; Goehler, H.; Stroedicke, M.; Zenkner, M.; Schoenherr, A.; Koeppen, S.; et al. *Cell* **2005**, *122*, 957–968.

(15) Wells, J. A.; McClendon, C. L. *Nature* **2007**, *450*, 1001–1009.

(16) Guo, W.; Wisniewski, J. A.; Ji, H. *Bioorg. Med. Chem. Lett.* **2014**, *24*, 2546–2554.

(17) Patel, S.; Player, M. R. *Expert Opin. Investig. Drugs* **2008**, *17*, 1865–1882.

(18) Gonzalez-Lopez de Turiso, F.; Sun, D.; Rew, Y.; Bartberger, M. D.; Beck, H. P.; Canon, J.; Chen, A.; Chow, D.; Correll, T. L.; Huang, X.; et al. *J. Med. Chem.* **2013**, *56*, 4053–4070.

(19) Arkin, M. R.; Tang, Y.; Wells, J. A. *Chem. Biol.* **2014**, *21*, 1102–1114.

(20) Lipinski, C. A.; Lombardo, F.; Dominy, B. W.; Feeney, P. J. *Adv. Drug Deliv. Rev.* **2001**, *46*, 3–26.

(21) Fischer, G.; Rossmann, M.; Hyvönen, M. *Curr. Opin. Biotechnol.* **2015**, *35*, 78–85.

(22) Vassilev, L. T.; Vu, B. T.; Graves, B.; Carvajal, D.; Podlaski, F.; Filipovic, Z.; Kong, N.; Kammlott, U.; Lukacs, C.; Klein, C.; et al. *Science* **2004**, *303*, 844–848.

(23) Tovar, C.; Graves, B.; Packman, K.; Filipovic, Z.; Xia, B. H. M.; Tardell, C.; Garrido, R.; Lee, E.; Kolinsky, K.; To, K.-H.; et al. *Cancer Res.* **2013**, *73*, 2587–2597.

(24) Vu, B.; Wovkulich, P.; Pizzolato, G.; Lovey, A.; Ding, Q.; Jiang, N.; Liu, J.-J.; Zhao, C.; Glenn, K.; Wen, Y.; et al. *ACS Med. Chem. Lett.* **2013**, *4*, 466–469.

(25) Majmudar, C. Y.; Højfeldt, J. W.; Arevang, C. J.; Pomerantz, W. C.; Gagnon, J. K.; Schultz, P. J.; Cesa, L. C.; Doss, C. H.; Rowe, S. P.; Vásquez, V.; et al. *Angew. Chem. Int. Ed.* **2012**, *51*, 11258–11262.

(26) Turnbull, A. P.; Boyd, S. M.; Walse, B. Fragment-based drug discovery and protein–protein interactions https://www.dovepress.com/fragment-based-drug-discovery-and-proteinndashprotein-interactions-peer-reviewed-article-RRBC (accessed Jan 3, 2019).

(27) Ciulli, A.; Williams, G.; Smith, A. G.; Blundell, T. L.; Abell, C. *J. Med. Chem.* **2006**, *49*, 4992–5000.

(28) Hann, M. M.; Leach, A. R.; Harper, G. *J. Chem. Inf. Comput. Sci.* **2001**, *41*, 856–864.

(29) Lepre, C. A.; Moore, J. M.; Peng, J. W. *Chem. Rev.* **2004**, *104*, 3641–3676.

(30) Swayze, E. E.; Jefferson, E. A.; Sannes-Lowery, K. A.; Blyn, L. B.; Risen, L. M.; Arakawa, S.; Osgood, S. A.; Hofstadler, S. A.; Griffey, R. H. *J. Med. Chem.* **2002**, *45*, 3816–3819.
(31) Hartshorn, M. J.; Murray, C. W.; Cleasby, A.; Frederickson, M.; Tickle, I. J.; Jhoti, H. *J. Med. Chem.* **2005**, *48*, 403–413.
(32) Fragment library screening and lead characterization using SPR biosensors - Beactica AB http://www.beactica.com/news/publications/fragment-library-screening-and-lead-characterization-using-spr-biosensors (accessed Jan 3, 2019).
(33) Sheng, C.; Dong, G.; Miao, Z.; Zhang, W.; Wang, W. *Chem. Soc. Rev.* **2015**, *44*, 8238–8259.
(34) Murray, C. W.; Verdonk, M. L.; Rees, D. C. *Trends Pharmacol. Sci.* **2012**, *33*, 224–232.
(35) Babaoglu, K.; Shoichet, B. K. *Nat. Chem. Biol.* **2006**, *2*, 720–723.
(36) Oltersdorf, T.; Elmore, S. W.; Shoemaker, A. R.; Armstrong, R. C.; Augeri, D. J.; Belli, B. A.; Bruncko, M.; Deckwerth, T. L.; Dinges, J.; Hajduk, P. J.; et al. *Nature* **2005**, *435*, 677–681.
(37) *The Practice of Medicinal Chemistry*; Elsevier, 2015.
(38) Vega, M. J. P. de; Gonzalez-Muniz, M. M.-M. and R. Modulation of Protein-Protein Interactions by Stabilizing/Mimicking Protein Secondary Structure Elements http://www.eurekaselect.com/77548/article (accessed Jan 3, 2019).
(39) Henchey, L. K.; Jochim, A. L.; Arora, P. S. *Curr. Opin. Chem. Biol.* **2008**, *12*, 692–697.
(40) Klingler, T. M.; Brutlag, D. L. *Protein Sci.* **1994**, *3*, 1847–1857.
(41) Balaram, P. *Curr. Opin. Struct. Biol.* **1992**, *2*, 845–851.
(42) Phelan, J. C.; Skelton, N. J.; Braisted, A. C.; McDowell, R. S. *J. Am. Chem. Soc.* **1997**, *119*, 455–460.
(43) Jackson, D. Y.; King, D. S.; Chmielewski, J.; Singh, S.; Schultz, P. G. *J. Am. Chem. Soc.* **1991**, *113*, 9391–9392.
(44) Blackwell, H. E.; Grubbs, R. H. *Angew. Chem. Int. Ed.* **1998**, *37*, 3281–3284.
(45) Schafmeister, C. E.; Po, J.; Verdine, G. L. *J. Am. Chem. Soc.* **2000**, *122*, 5891–5892.
(46) Chu, Q.; Moellering, R. E.; Hilinski, G. J.; Kim, Y.-W.; Grossmann, T. N.; Yeh, J. T.-H.; Verdine, G. L. *MedChemComm* **2015**, *6*, 111–119.
(47) Hayes, J. D.; McMahon, M. *Trends Biochem. Sci.* **2008**, *34*, 176–188.
(48) Gorrini, C.; Harris, I. S.; Mak, T. W. *Nat. Rev. Drug Discov.* **2013**, *12*, 931–947.
(49) Cullinan, S. B.; Gordan, J. D.; Jin, J.; Harper, J. W.; Diehl, J. A. *Mol. Cell. Biol.* **2004**, *24*, 8477–8486.
(50) Kobayashi, A.; Kang, M.-I.; Okawa, H.; Ohtsuji, M.; Zenke, Y.; Chiba, T.; Igarashi, K.; Yamamoto, M. *Mol. Cell. Biol.* **2004**, *24*, 7130–7139.
(51) Wilson, A. J.; Kerns, J. K.; Callahan, J. F.; Moody, C. J. *J. Med. Chem.* **2013**, *56*, 7463–7476.
(52) Zipper, L. M.; Mulcahy, R. T. *J. Biol. Chem.* **2002**, *277*, 36544–36552.
(53) Lu, M.-C.; Ji, J.-A.; Jiang, Z.-Y.; You, Q.-D. *Med. Res. Rev.* **2016**.
(54) Davis, T. G.; Wixted, W. E.; Coyle, J. E.; Griffiths-Jones, C.; Hearn, K.; McMenamin, R.; Norton, D.; Rich, S. J.; Richardson, C.; Saxty, G.; et al. *J. Med. Chem.* **2016**, *59*, 3991–4006.
(55) Zhang, D. D.; Lo, S.-C.; Cross, J. V.; Templeton, D. J.; Hannink, M. *Mol. Cell. Biol.* **2004**, *24*, 10941–10953.
(56) Tong, K. I.; Katoh, Y.; Kusunoki, H.; Itoh, K.; Tanaka, T.; Yamamoto, M. *Mol. Cell. Biol.* **2006**, *26*, 2887–2900.
(57) Padmanabhan, B.; Tong, K. I.; Ohta, T.; Nakamura, Y.; Scharlock, M.; Ohtsuji, M.; Kang, M.-I.; Kobayashi, A.; Yokoyama, S.; Yamamoto, M. *Mol. Cell* **2006**, *21*, 689–700.
(58) Li, X.; Zhang, D.; Hannick, M.; Beamer, L. J. *J. Biol. Chem.* **2004**, *279*, 54750–54758.

(59) Tong, K. I.; Padmanabhan, B.; Kobayashi, A.; Shang, C.; Hirotsu, Y.; Yokoyama, S.; Yamamoto, M. *Mol. Cell. Biol.* **2007**, *27*, 7511–7521.
(60) Hancock, R.; Bertrand, H. C.; Tsujita, T.; Naz, S.; El-Bakry, A.; Laoruchupong, J.; Hayes, J. D.; Wells, G. *Free Radic. Biol. Med.* **2012**, *52*, 444–451.
(61) Wells, G. *Biochem. Soc. Trans.* **2015**, *43*, 674–679.
(62) Zhuang, C.; Narayanapillai, S.; Zhang, W.; Sham, Y. Y.; Xing, C. *J. Med. Chem.* **2014**, *57*, 1121–1126.
(63) Hu, L.; Magesh, S.; Chen, L.; Wang, L.; Lewis, T. A.; Chen, Y.; Khodier, C.; Inoyama, D.; Beamer, L. J.; Emge, T. J.; et al. *Bioorg. Med. Chem. Lett.* **2013**, *23*, 3039–3043.
(64) Marcotte, D.; Zeng, W.; Hus, J.-C.; McKenzie, A.; Hession, C.; Jin, P.; Bergeron, C.; Lugovskoy, A.; Enyedy, I.; Cuervo, H.; et al. *Bioorg. Med. Chem.* **2013**, *21*, 4011–4019.
(65) Sun, H.-P.; Jiang, Z.-Y.; Zhang, M.-Y.; Lu, M.-C.; Yang, T.-T.; Pan, Y.; Huang, H.-Z.; Zhang, X.-J.; You, Q.-D. *Med. Chem. Commun.* **2014**, *5*, 93–98.
(66) Hancock, R.; Schaap, M.; Pfister, H.; Wells, G. *Org. Biomol. Chem.* **2013**, *11*, 3553–3557.
(67) Lu, M.-C.; Jiao, Q.; Liu, T.; Tan, S.-J.; Zhou, H.-S.; You, Q.-D.; Jiang, Z.-Y. *Eur. J. Med. Chem.* **2018**, *143*, 1578–1589.
(68) Sheehan, J. C.; Hess, G. P. *J. Am. Chem. Soc.* **1955**, *77*, 1067–1068.
(69) König, W.; Geiger, R. *Chem. Ber.* **1970**, *103*, 788–798.
(70) Gibson, F. S.; Park, M. S.; Rapoport, H. *J. Org. Chem.* **1994**, *59*, 7503–7507.
(71) Carpino, L. A.; Imazumi, H.; Foxman, B. M.; Vela, M. J.; Henklein, P.; El-Faham, A.; Klose, J.; Bienert, M. *Org. Lett.* **2000**, *2*, 2253–2256.
(72) SubirÃ³s-Funosas, R.; Prohens, R.; Barbas, R.; El-Faham, A.; Albericio, F. *Chem. - Eur. J.* **2009**, *15*, 9394–9403.
(73) Carpino, L. A.; Imazumi, H.; El-Faham, A.; Ferrer, F. J.; Zhang, C.; Lee, Y.; Foxman, B. M.; Henklein, P.; Hanay, C.; Mügge, C.; et al. *Angew. Chem. Int. Ed.* **2002**, *41*, 441–445.
(74) Gawne, G.; Kenner, G. W.; Sheppard, R. C. *J. Am. Chem. Soc.* **1969**, *91*, 5669–5671.
(75) Castro, B.; Dormoy, J. R.; Evin, G.; Selve, C. *Tetrahedron Lett.* **1975**, *14*, 1219–1222.
(76) Coste, J.; Le-Nguyen, D.; Castro, B. *Tetrahedron Lett.* **1990**, *31*, 205–208.
(77) Kim, M. H.; Patel, D. V. *Tetrahedron Lett.* **1994**, *35*, 5603.
(78) Coste, J.; Campagne, J. M. *Tetrahedron Lett.* **1995**, *36*, 4253–4256.
(79) Shioiri, T.; Ninomiya, K.; Yamada, S. *J. Am. Chem. Soc.* **1972**, *94*, 6203–6205.
(80) Shioiri, T. No. 134, 18.
(81) Brady, S. F.; Varga, S. L.; Freidinger, R. M.; Schwenk, D. A.; Mendlowski, M.; Holly, F. W.; Veber, D. F. *J. Org. Chem.* **1979**, *44*, 3101–3105.
(82) Brady, S. F.; Freidinger, R. M.; Paleveda, W. J.; Colton, C. D.; Homnick, C. F.; Whitter, W. L.; Curley, P.; Nutt, R. F.; Veber, D. F. *J. Org. Chem.* **1987**, *52*, 764–769.
(83) Lee, K.-C.; Loh, T.-P. *Chem. Commun.* **2006**, No. 40, 4209–4211.
(84) Cai, Q.; He, G.; Ma, D. *J. Org. Chem.* **2006**, *71*, 5268–5273.
(85) Yamada, S.; Kasai, Y.; Shioiri, T. *Tetrahedron Lett.* **1973**, *14*, 1595–1598.
(86) Kiso, Y.; Miyazaki, T.; Satomi, M.; Hiraiwa, H.; Akita, T. *J Chem Soc Chem Commun* **1980**, No. 21, 1029–1030.
(87) Kamiński, Z. J. *Tetrahedron Lett.* **1985**, *26*, 2901–2904.
(88) Kamiński, Z. J. *Synthesis* **1987**, *10*, 917–920.
(89) Kunishima, M.; Kawachi, C.; Monta, J.; Terao, K.; Iwasaki, F.; Tani, S. *Tetrahedron* **1999**, *55*, 13159–13170.
(90) Kunishima, M.; Kitao, A.; Kawachi, C.; Watanabe, Y.; Iguchi, S.; Hioki, K.; Tani, S. *Chem. Pharm. Bull. (Tokyo)* **2002**, *50*, 549–550.
(91) Shieh, W.-C.; Chen, Z.; Xue, S.; McKenna, J.; Wang, R.-M.; Prasad, K.; Repič, O. *Tetrahedron Lett.* **2008**, *49*, 5359–5362.

(92) Merrifield, R. B. *J. Am. Chem. Soc.* **1963**, *85*, 2149–2154.
(93) Merrifield, B. *Br. Polym. J.* **1984**, *16*, 173–178.
(94) Kenner, G. W.; McDermott, J. R.; Sheppard, R. C. *J. Chem. Soc. Chem. Commun.* **1971**, No. 12, 636.
(95) Wang, J.-X.; Fang, G.-M.; He, Y.; Qu, D.-L.; Yu, M.; Hong, Z.-Y.; Liu, L. *Angew. Chem. Int. Ed.* **2015**, *54*, 2194–2198.
(96) Elashal, H. E.; Cohen, R. D.; Raj, M. *Chem. Commun.* **2016**, *52*, 9699–9702.
(97) Kohler, A. *Justus Liebigs Ann. Chem.* **1865**, *134*, 367–372.
(98) Borthwick, A. D. *Chem. Rev.* **2012**, *112*, 3641–3716.
(99) Tullberg, M.; Grøtli, M.; Luthman, K. *Tetrahedron* **2006**, *62*, 7484–7491.
(100) Golebiowski, A.; Klopfenstein, S. R.; Chen, J. J.; Shao, X. 4.
(101) Golebiowski, A.; Klopfenstein, S. R.; Shao, X.; Chen, J. J.; Colson, A.-O.; Grieb, A. L.; Russell, A. F. *Org. Lett.* **2000**, *2*, 2615–2617.
(102) El Tayar, N.; Mark, A. E.; Vallat, P.; Brunne, R. M.; Testa, B.; van Gunsteren, W. F. *J. Med. Chem.* **1993**, *36*, 3757–3764.
(103) Thakkar, A.; Trinh, T. B.; Pei, D. *ACS Comb. Sci.* **2013**, *15*, 120–129.
(104) Song, K. H.; Kang, S. O.; Ko, J. *Chem. – Eur. J.* **2007**, *13*, 5129–5134.
(105) Miller, S. J.; Grubbs, R. H. *J. Am. Chem. Soc.* **1995**, *117*, 5855–5856.
(106) Kingsbury, J. S.; Harrity, J. P. A.; Bonitatebus, P. J.; Hoveyda, A. H. *J. Am. Chem. Soc.* **1999**, *121*, 791–799.
(107) Garber, S. B.; Kingsbury, J. S.; Gray, B. L.; Hoveyda, A. H. *J. Am. Chem. Soc.* **2000**, *122*, 8168–8179.
(108) Jean-Louis Hérisson, P.; Chauvin, Y. *Makromol. Chem.* **1971**, *141*, 161–176.
(109) Stewart, I. C.; Ung, T.; Pletnev, A. A.; Berlin, J. M.; Grubbs, R. H.; Schrodi, Y. *Org. Lett.* **2007**, *9*, 1589–1592.
(110) Hong, S. H.; Day, M. W.; Grubbs, R. H. *J. Am. Chem. Soc.* **2004**, *126*, 7414–7415.
(111) Hong, S. H.; Sanders, D. P.; Lee, C. W.; Grubbs, R. H. *J. Am. Chem. Soc.* **2005**, *127*, 17160–17161.
(112) Kolb, H. C.; Finn, M. G.; Sharpless, K. B. *Angew. Chem. Int. Ed.* **2001**, *40*, 2004–2021.
(113) Huisgen, R. *Proc. Chem. Soc.* **1961**, 357–390.
(114) Oh, K.; Guan, Z. *Chem Commun* **2006**, No. 29, 3069–3071.
(115) Bock, V. D.; Perciaccante, R.; Jansen, T. P.; Hiemstra, H.; van Maarseveen, J. H. *Org. Lett.* **2006**, *8*, 919–922.
(116) Turner, R. A.; Oliver, A. G.; Lokey, R. S. *Org. Lett.* **2007**, *9*, 5011–5014.
(117) Gray, N.; Choi, H. G.; Tan, L. WO 2015/006492 (A1), July 9, 2014.
(118) Stach, M.; Weidkamp, A. J.; Yang, S.-H.; Hung, K.; Furkert, D. P.; Harris, P. W. R.; Smaill, J. B.; Patterson, A. V.; Brimble, M. A. *Eur. J. Org. Chem.* **2015**, *2015*, 6341–6350.
(119) Sastry, T. V. R. S.; Banerji, B.; Kiran Kumar, S.; Kunwar, A. C.; Das, J.; Nandy, J. P.; Iqbal, J. *Tetrahedron Lett.* **2002**, *43*, 7621–7625.
(120) Reichwein, J. F.; Versluis, C.; Liskamp, R. M. J. *J. Org. Chem.* **2000**, *65*, 6187–6195.
(121) Hong, S. H.; Sanders, D. P.; Lee, C. W.; Grubbs, R. H. *J. Am. Chem. Soc.* **2005**, *127*, 17160–17161.
(122) Bergmann, M.; Zervas, L. *Berichte Dtsch. Chem. Ges. B Ser.* **1932**, *65*, 1192–1201.
(123) Barany, G.; Merrifield, R. B. *J. Am. Chem. Soc.* **1977**, *99*, 7363–7365.
(124) Kaiser, E.; Picart, F.; Kubiak, T.; Tam, J. P.; Merrifield, R. B. *J. Org. Chem.* **1993**, *58*, 5167–5175.
(125) Stewart, J. M.; Young, J. D. *Solid Phase Peptide Synthesis*, 2nd ed.; Pierce Chemical Co: Rockford, Ill, 1984.
(126) Wuts, P. G. M.; Greene, T. W. *Greene's Protective Groups in Organic Synthesis*; John Wiley & Sons, Inc.: Hoboken, NJ, USA, 2006.
(127) Speckmeier, E.; Zeitler, K. *ACS Catal.* **2017**, *7*, 6821–6826.

(128) SHIN, S. Y.; KABURAKI, Y.; WATANABE, M.; MUNEKATA, E. *Biosci. Biotechnol. Biochem.* **1992**, *56*, 108–112.
(129) Hendrickson, J. B.; Kandall, C. *Tetrahedron Lett.* **1970**, *11*, 343–344.
(130) Inman, M.; Carvalho, C.; Lewis, W.; Moody, C. J. *J. Org. Chem.* **2016**, *81*, 7924–7930.
(131) Fábián, A.; Ruff, F.; Farkas, Ö. *J. Phys. Org. Chem.* **2008**, *21*, 988–996.
(132) Sheehan, J. C.; Daves, G. D. *J. Org. Chem.* **1964**, *29*, 2006–2008.
(133) Namikoshi, M.; Kundu, B.; Rinehart, K. L. *J. Org. Chem.* **1991**, *56*, 5464–5466.
(134) Sieber, P. *Helv. Chim. Acta* **1977**, *60*, 2711–2716.
(135) Marlowe, C. K. *Bioorg. Med. Chem. Lett.* **1993**, *3*, 437–440.
(136) Scheidt, K. A.; Chen, H.; Follows, B. C.; Chemler, S. R.; Coffey, D. S.; Roush, W. R. *J. Org. Chem.* **1998**, *63*, 6436–6437.
(137) Inman, M.; Dexter, H. L.; Moody, C. J. *Org. Lett.* **2017**, *19*, 3454–3457.
(138) Gowda, D. C.; Mahesh, B.; Gowda, S. *Indian J. Chem.* **2001**, *40B*, 75–77.
(139) Channe Gowda, D. *Tetrahedron Lett.* **2002**, *43*, 311–313.
(140) Ben-Ishai, D.; Berger, A. *J. Org. Chem.* **1952**, *17*, 1564–1570.
(141) Boeckman, R. K.; Potenza, J. C. *Tetrahedron Lett.* **1985**, *26*, 1411–1414.
(142) Congreve, M. S.; Davison, E. C.; Fuhry, M. A. M.; Holmes, A. B.; Payne, A. N.; Robinson, R. A.; Ward, S. E. *Synlett* **1993**, *1993*, 663–664.
(143) Selvaraj, A.; Chen, H.-T.; Ya-Ting Huang, A.; Kao, C.-L. *Chem. Sci.* **2017**, *9*, 345–349.
(144) Bellamy, F. D.; Ou, K. *Tetrahedron Lett.* **1984**, *25*, 839–842.
(145) Albericio, F.; El-Faham, A. *Org. Process Res. Dev.* **2018**, *22*, 760–772.
(146) Hanwell, M. D.; Curtis, D. E.; Lonie, D. C.; Vandermeersch, T.; Zurek, E.; Hutchison, G. R. *J. Cheminformatics* **2012**, *4*.
(147) Ichimura, Y.; Waguri, S.; Sou, Y.; Kageyama, S.; Hasegawa, J.; Ishimura, R.; Saito, T.; Yang, Y.; Kouno, T.; Fukutomi, T.; et al. *Mol. Cell* **2013**, *51*, 618–631.
(148) Wang, J.; Wolf, R. M.; Caldwell, J. W.; Kollman, P. A.; Case, D. A. *J. Comput. Chem.* **2004**, *25*, 1157–1174.
(149) *The PyMOL Molecular Graphics System*; Schrodinger LLC.
(150) Gustafson, C. L.; Parsley, N. C.; Asimgil, H.; Lee, H.-W.; Ahlbach, C.; Michael, A. K.; Xu, H.; Williams, O. L.; Davis, T. L.; Liu, A. C.; et al. *Mol. Cell* **2017**, *66*, 447-457.e7.
(151) Scholz, R.; Molohon, K. J.; Nachtigall, J.; Vater, J.; Markley, A. L.; Sussmuth, R. D.; Mitchell, D. A.; Borriss, R. *J. Bacteriol.* **2011**, *193*, 215–224.
(152) Kaldas, S. J.; Yudin, A. K. *Chem. - Eur. J.* **2018**, *24*, 7074–7082.
(153) Hamdan, F.; Tahoori, F.; Balalaie, S. *RSC Adv.* **2018**, *8*, 33893–33926.
(154) Zhang, L.; Chen, X.; Xue, P.; Sun, H. H. Y.; Williams, I. D.; Sharpless, K. B.; Fokin, V. V.; Jia, G. *J. Am. Chem. Soc.* **2005**, *127*, 15998–15999.
(155) Bock, V. D.; Speijer, D.; Hiemstra, H.; van Maarseveen, J. H. *Org. Biomol. Chem.* **2007**, *5*, 971.
(156) Paul, R.; Anderson, G. W. *J. Am. Chem. Soc.* **1960**, *82*, 4596–4600.
(157) Meldal, M.; Tornøe, C. W. *Chem. Rev.* **2008**, *108*, 2952–3015.
(158) Moorman, R. M.; Collier, M. B.; Frohock, B. H.; Womble, M. D.; Chalker, J. M. *Org. Biomol. Chem.* **2015**, *13*, 1974–1978.
(159) Aneja, B.; Irfan, M.; Kapil, C.; Jairajpuri, M. A.; Maguire, R.; Kavanagh, K.; Rizvi, M. M. A.; Manzoor, N.; Azam, A.; Abid, M. *Org. Biomol. Chem.* **2016**, *14*, 10599–10619.
(160) Pokorski, J. K.; Miller Jenkins, L. M.; Feng, H.; Durell, S. R.; Bai, Y.; Appella, D. H. *Org. Lett.* **2007**, *9*, 2381–2383.
(161) Glaser, C. *Ann. Chem. Pharm.* **1870**, *154*, 137–171.
(162) Eglinton, G.; Galbraith, A. R. *J. Chem. Soc. Resumed* **1959**, No. 0, 889–896.
(163) Hay, A. S. *J. Org. Chem.* **1962**, *27*, 3320–3321.
(164) Auberger, N.; Pisa, M. D.; Larregola, M.; Chassaing, G.; Peroni, E.; Lavielle, S.; Papini, A.-M.; Lequin, O.; Mallet, J.-M. *Bioorg. Med. Chem.* **2014**, *22*, 6924–6932.

(165) Verlinden, S.; Geudens, N.; Martins, J. C.; Tourwé, D.; Ballet, S.; Verniest, G. *Org. Biomol. Chem.* **2015**, *13*, 9398–9404.
(166) Verlinden, S.; Ballet, S.; Verniest, G. *Eur. J. Org. Chem.* **2016**, *2016*, 5807–5812.
(167) Neises, B.; Steglich, W. *Angew. Chem. Int. Ed. Engl.* **1978**, *17*, 522–524.
(168) Appel, R. *Angew. Chem. Int. Ed. Engl.* **1975**, *14*, 801–811.
(169) Jain, N.; Pathak, D. P.; Mishra, P.; Jain, S. *J. Iran. Chem. Soc.* **2009**, *6*, 77–81.
(170) Hutt, M. P.; Elslager, E. F.; Werbel, L. M. *J. Heterocycl. Chem.* **1970**, *7*, 511–518.
(171) Silvestrini, B.; Pozzatti, C. *Br. J. Pharmacol.* **1961**, *16*, 209–217.
(172) Wang, L.; Cao, J.; Chen, Q.; He, M. *J. Org. Chem.* **2015**, *80*, 4743–4748.
(173) Wong, M. Y.; Krotkus, S.; Copley, G.; Li, W.; Murawski, C.; Hall, D.; Hedley, G. J.; Jaricot, M.; Cordes, D. B.; Slawin, A. M. Z.; et al. *ACS Appl. Mater. Interfaces* **2018**, *10*, 33360–33372.
(174) Ramazani, A.; Rezaei, A. *Org. Lett.* **2010**, *12*, 2852–2855.
(175) Frost, J. R.; Scully, C. C. G.; Yudin, A. K. *Nat. Chem.* **2016**, *8*, 1105–1111.
(176) Faria, J. V.; Vegi, P. F.; Miguita, A. G. C.; dos Santos, M. S.; Boechat, N.; Bernardino, A. M. R. *Bioorg. Med. Chem.* **2017**, *25*, 5891–5903.
(177) Nicolle, S. M.; Moody, C. J. *Chem. - Eur. J.* **2014**, *20*, 4420–4425.
(178) Zheng, J.; Lin, J.-H.; Yu, L.-Y.; Wei, Y.; Zheng, X.; Xiao, J.-C. *Org. Lett.* **2015**, *17*, 6150–6153.
(179) Griffiths, D. V.; Hughes, J. M. *Tetrahedron* **1997**, *53*, 17815–17822.
(180) Cai, Y.; Lu, Y.; Yu, C.; Lyu, H.; Miao, Z. *Org. Biomol. Chem.* **2013**, *11*, 5491.
(181) Knorr, L. *Chem. Ber.* **1883**, *16*, 2597–2599.
(182) Bekhit, A. A.; Ashour, H. M. A.; Abdel Ghany, Y. S.; Bekhit, A. E.-D. A.; Baraka, A. *Eur. J. Med. Chem.* **2008**, *43*, 456–463.
(183) Perry, B.; Beevers, R.; Bennett, G.; Buckley, G.; Crabbe, T.; Gowers, L.; James, L.; Jenkins, K.; Lock, C.; Sabin, V.; et al. *Bioorg. Med. Chem. Lett.* **2008**, *18*, 5299–5302.
(184) Liu, X.-H.; Cui, P.; Song, B.-A.; Bhadury, P. S.; Zhu, H.-L.; Wang, S.-F. *Bioorg. Med. Chem.* **2008**, *16*, 4075–4082.
(185) Vijesh, A. M.; Isloor, A. M.; Shetty, P.; Sundershan, S.; Fun, H. K. *Eur. J. Med. Chem.* **2013**, *62*, 410–415.
(186) Shetty, S. C.; Bhagat, V. C. *Asian J. Chem.* **2008**, *20*, 5037–5045.
(187) Velcicky, J.; Feifel, R.; Hawtin, S.; Heng, R.; Huppertz, C.; Koch, G.; Kroemer, M.; Moebitz, H.; Revesz, L.; Scheufler, C.; et al. *Bioorg. Med. Chem. Lett.* **2010**, *20*, 1293–1297.
(188) Singh, S. K.; Srinivasa Reddy, M.; Shivaramakrishna, S.; Kavitha, D.; Vasudev, R.; Babu, J. M.; Sivalakshmidevi, A.; Rao, Y. K. *Tetrahedron Lett.* **2004**, *45*, 7679–7682.
(189) Gosselin, F.; O'Shea, P. D.; Webster, R. A.; Reamer, R. A.; Tillyer, R. D.; Grabowski, E. J. J. *Synlett* **2006**, *19*, 3267–3270.
(190) Ko, Y. O.; Chun, Y. S.; Park, C.-L.; Kim, Y.; Shin, H.; Ahn, S.; Hong, J.; Lee, S. *Org. Biomol. Chem.* **2009**, *7*, 1132.
(191) Harigae, R.; Moriyama, K.; Togo, H. *J. Org. Chem.* **2014**, *79*, 2049–2058.
(192) Safaei, S.; Mohammadpoor-Baltork, I.; Khosropour, A.; Moghadam, M.; Tangestaninejad, S.; Mirkhani, V. *Synlett* **2011**, *2011*, 2214–2222.
(193) Huisgen, R. *Angew. Chem. Int. Ed. Engl.* **1963**, *2*, 565–598.
(194) Huisgen, R. *Angew. Chem. Int. Ed. Engl.* **1963**, *2*, 633–645.
(195) He, S.; Chen, L.; Niu, Y.-N.; Wu, L.-Y.; Liang, Y.-M. *Tetrahedron Lett.* **2009**, *50*, 2443–2445.
(196) Qi, X.; Ready, J. M. *Angew. Chem. Int. Ed.* **2007**, *46*, 3242–3244.
(197) Pechmann, H. V. *Berichte Dtsch. Chem. Ges.* **1894**, *27*, 1888–1891.
(198) Curtius, T. *Berichte Dtsch. Chem. Ges.* **1883**, *16*, 2230–2231.
(199) Regitz, M. *Angew. Chem. Int. Ed.* **1967**, *6*, 733–749.

(200) Maas, G. New Syntheses of Diazo Compounds https://onlinelibrary.wiley.com/doi/abs/10.1002/anie.200902785 (accessed Aug 30, 2019).
(201) Regitz, M.; Maas, G. *Diazo Compounds: Properties and Synthesis*; Academic Press Inc: Orlando, 1986.
(202) Javed, M. I.; Brewer, M. *Org. Lett.* **2007**, *9*, 1789–1792.
(203) Nicolle, S. M.; Moody, C. J. *Chem. - Eur. J.* **2014**, *20*, 4420–4425.
(204) Barton, D. H. R.; O'Brien, R. E.; Sternhell, S. *J. Chem. Soc.* **1962**, 470.
(205) Bamford, W. R.; Stevens, T. S. *J. Chem. Soc.* **1952**, 4735.
(206) House, H. O.; Blankley, C. J. *J. Org. Chem.* **1968**, *33*, 53–60.
(207) Archibald, T. G.; Huang, D. S.; Pratton, M. H.; Barnard, J. C. *US5817778* **1998**.
(208) Michaelis, A.; Kaehne, R. *Berichte Dtsch. Chem. Ges.* **1898**, *31*, 1048–1055.
(209) Wittig, G.; Krebs, A. *Chem. Ber.* **1961**, *94*, 3260–3275.
(210) Dommerholt, J.; Schmidt, S.; Temming, R.; Hendriks, L. J. A.; Rutjes, F. P. J. T.; van Hest, J. C. M.; Lefeber, D. J.; Friedl, P.; van Delft, F. L. *Angew. Chem. Int. Ed.* **2010**, *49*, 9422–9425.
(211) Nielsen, B. V. *Eur. Pharm. Rev.* **2013**, *18*, 18–22.
(212) Ben-Nissan, G.; Sharon, M. *Curr. Opin. Chem. Biol.* **2018**, *42*, 25–33.
(213) Castelhano, A. L.; Krantz, A.; Pliura, D. H.; Venuti, M. C.; De, Y. L. M. EP0237082 (A2).
(214) Gavande, N.; Kim, H.-L.; Doddareddy, M. R.; Johnston, G. A. R.; Chebib, M.; Hanrahan, J. R. *ACS Med. Chem. Lett.* **2013**, *4*, 402–407.
(215) Zhao, L.-X.; Park, J. G.; Moon, Y.-S.; Basnet, A.; Choi, J.; Kim, E.; Jeong, T. C.; Jahng, Y.; Lee, E.-S. *Il Farm.* **2004**, *59*, 381–388.
(216) Perrone, M. G.; Vitale, P.; Panella, A.; Ferorelli, S.; Contino, M.; Lavecchia, A.; Scilimati, A. *ChemMedChem* **2016**, *11*, 1172–1187.
(217) Yang, C.; Mi, J.; Feng, Y.; Ngo, L.; Gao, T.; Yan, L.; Zheng, Y. G. *J. Am. Chem. Soc.* **2013**, *135*, 7791–7794.
(218) Ortiz-Soto, M. E.; Ertl, J.; Mut, J.; Adelmann, J.; Le, T. A.; Shan, J.; Teßmar, J.; Schlosser, A.; Engels, B.; Seibel, J. *Chem. Sci.* **2018**, *9*, 5312–5321.
(219) Ansorge, S.; Bank, U.; Heimburg, A.; Julius, H.; Nordhoff, K.; Taeger, M. US2012028995 (A1).

10. Appendix

Table 1 Crystal data and structure refinement for FRSCMA.

Identification code	FRSCMA
Empirical formula	$C_{17}H_{16}N_2O_3S$
Formula weight	328.38
Temperature/K	120(2)
Crystal system	monoclinic
Space group	$P2_1/c$
a/Å	17.8692(2)
b/Å	7.26321(8)
c/Å	11.99541(16)
α/°	90
β/°	99.4692(13)
γ/°	90
Volume/Å^3	1535.64(3)
Z	4
ρ_{calc}g/cm^3	1.420
μ/mm^{-1}	2.023
F(000)	688.0
Crystal size/mm^3	0.215 × 0.195 × 0.046
Radiation	CuKα (λ = 1.54184)
2Θ range for data collection/°	5.014 to 147.702
Index ranges	-22 ≤ h ≤ 22, -8 ≤ k ≤ 8, -12 ≤ l ≤ 14
Reflections collected	21598
Independent reflections	3077 [R_{int} = 0.0309, R_{sigma} = 0.0145]
Data/restraints/parameters	3077/0/213
Goodness-of-fit on F^2	1.050
Final R indexes [I>=2σ (I)]	R_1 = 0.0339, wR_2 = 0.0948
Final R indexes [all data]	R_1 = 0.0351, wR_2 = 0.0962
Largest diff. peak/hole / e Å^{-3}	0.60/-0.36

Table 2 Fractional Atomic Coordinates (×10^4) and Equivalent Isotropic Displacement Parameters (Å^2×10^3) for FRSCMA. U_{eq} is defined as 1/3 of of the trace of the orthogonalised U_{IJ} tensor.

Atom	*x*	*y*	*z*	U(eq)
S1	2027.3(2)	-2412.6(4)	578.9(3)	17.11(12)
O2	2532.9(5)	-3867.3(13)	1067.2(8)	23.0(2)
O3	1966.4(6)	-2021.4(15)	-605.5(8)	24.0(2)

C4	2338.9(7)	-439.2(18)	1349.7(11)	17.4(3)
N5	2158.4(6)	1217.8(15)	910.7(9)	19.5(2)
N6	2500.1(7)	2367.9(16)	1716.3(10)	18.8(2)
C7	2890.1(7)	1492.5(18)	2635.7(11)	17.8(3)
C8	2786.6(7)	-363.5(19)	2427.1(11)	19.0(3)
C9	3318.8(7)	2475.0(18)	3607.3(11)	18.4(3)
C10	3464.0(8)	4354(2)	3582.6(12)	23.4(3)
C11	3851.2(8)	5268(2)	4523.7(12)	23.9(3)
C12	4103.2(7)	4291(2)	5509.4(11)	22.1(3)
C13	3979.3(8)	2399(2)	5537.2(12)	24.2(3)
C14	3588.9(8)	1502(2)	4599.5(11)	23.1(3)
O15	4471.0(6)	5055.0(15)	6489.6(8)	27.2(2)
C16	4532.7(9)	7017(2)	6524.9(13)	30.2(3)
C17	1116.9(7)	-2889.5(18)	881.6(11)	17.7(3)
C18	487.5(8)	-2279.8(19)	138.7(12)	20.9(3)
C19	-233.5(8)	-2608.9(19)	385.0(12)	22.5(3)
C20	-330.8(8)	-3563.4(19)	1358.3(12)	22.2(3)
C21	311.7(8)	-4198.0(19)	2079.0(11)	22.6(3)
C22	1037.2(8)	-3863.6(19)	1857.4(11)	20.9(3)
C23	-1110.4(8)	-3877(2)	1642.2(14)	30.0(3)

Table 3 Anisotropic Displacement Parameters ($Å^2×10^3$) for FRSCMA. The Anisotropic displacement factor exponent takes the form: $-2π^2[h^2a^{*2}U_{11}+2hka^*b^*U_{12}+…]$.

Atom	U_{11}	U_{22}	U_{33}	U_{23}	U_{13}	U_{12}
S1	19.13(19)	14.52(19)	17.33(18)	-1.32(10)	1.95(13)	-1.35(10)
O2	22.6(5)	16.4(5)	29.0(5)	-2.1(4)	1.5(4)	1.5(4)
O3	28.2(5)	26.5(5)	17.5(5)	-1.4(4)	4.3(4)	-4.7(4)
C4	17.5(6)	16.4(6)	18.1(6)	-0.9(5)	2.7(5)	-1.5(5)
N5	21.0(5)	15.7(6)	20.7(5)	-1.4(4)	0.2(4)	-2.1(4)
N6	21.2(6)	13.0(6)	21.1(6)	-0.9(4)	0.2(4)	-1.3(4)
C7	16.8(6)	18.7(6)	18.1(6)	-0.6(5)	3.5(5)	-0.6(5)
C8	20.1(6)	17.5(6)	19.2(6)	0.8(5)	2.0(5)	0.2(5)
C9	17.2(6)	19.6(7)	18.3(6)	-2.3(5)	2.8(5)	-0.4(4)
C10	25.9(7)	21.4(7)	21.3(6)	-0.9(5)	-0.6(5)	0.2(5)
C11	25.3(7)	19.4(7)	25.6(7)	-3.7(5)	0.0(5)	-1.1(5)
C12	17.4(6)	28.3(7)	20.3(6)	-6.2(5)	2.2(5)	-0.7(5)
C13	24.4(7)	27.6(8)	19.4(7)	1.9(5)	0.1(6)	-1.4(5)
C14	25.2(7)	21.1(7)	22.6(7)	0.6(5)	3.1(5)	-3.3(5)
O15	25.8(5)	31.6(6)	21.7(5)	-6.8(4)	-2.9(4)	-2.2(4)
C16	25.6(7)	32.8(8)	30.1(8)	-12.6(7)	-1.4(6)	-2.0(6)

C17	19.6(6)	15.6(6)	17.4(6)	-1.8(5)	1.6(5)	-2.7(5)
C18	24.7(7)	18.5(6)	18.8(6)	1.7(5)	1.8(5)	-0.5(5)
C19	22.0(7)	21.1(7)	23.1(7)	-1.2(5)	-0.4(5)	0.8(5)
C20	25.0(7)	18.6(7)	23.6(6)	-6.6(5)	5.9(5)	-4.2(5)
C21	31.3(7)	19.8(7)	16.9(6)	-0.6(5)	5.0(5)	-4.5(5)
C22	26.0(7)	18.7(7)	16.8(6)	-0.5(5)	-0.6(5)	-1.5(5)
C23	27.2(7)	31.5(8)	32.9(8)	-6.9(6)	9.5(6)	-6.6(6)

Table 4 Bond Lengths for FRSCMA.

Atom	Atom	Length/Å	Atom	Atom	Length/Å
S1	O2	1.4496(10)	C11	C12	1.389(2)
S1	O3	1.4354(10)	C12	C13	1.393(2)
S1	C4	1.7463(13)	C12	O15	1.3666(16)
S1	C17	1.7586(13)	C13	C14	1.385(2)
C4	N5	1.3319(17)	O15	C16	1.430(2)
C4	C8	1.4047(18)	C17	C18	1.3877(19)
N5	N6	1.3455(15)	C17	C22	1.3950(19)
N6	C7	1.3614(17)	C18	C19	1.389(2)
C7	C8	1.3779(19)	C19	C20	1.393(2)
C7	C9	1.4699(18)	C20	C21	1.397(2)
C9	C10	1.3906(19)	C20	C23	1.5048(19)
C9	C14	1.4001(19)	C21	C22	1.387(2)
C10	C11	1.3915(19)			

Table 5 Bond Angles for FRSCMA.

Atom	Atom	Atom	Angle/˚	Atom	Atom	Atom	Angle/˚
O2	S1	C4	105.14(6)	C9	C10	C11	121.35(13)
O2	S1	C17	108.01(6)	C12	C11	C10	119.72(14)
O3	S1	O2	119.01(6)	C11	C12	C13	119.57(13)
O3	S1	C4	109.10(6)	O15	C12	C11	124.61(13)
O3	S1	C17	108.74(6)	O15	C12	C13	115.82(13)
C4	S1	C17	106.11(6)	C14	C13	C12	120.36(14)
N5	C4	S1	119.80(9)	C13	C14	C9	120.66(14)
N5	C4	C8	113.11(11)	C12	O15	C16	116.99(12)
C8	C4	S1	127.08(10)	C18	C17	S1	118.96(10)
C4	N5	N6	103.02(10)	C18	C17	C22	121.12(13)
N5	N6	C7	113.78(11)	C22	C17	S1	119.92(10)
N6	C7	C8	105.92(11)	C17	C18	C19	119.39(13)
N6	C7	C9	123.10(12)	C18	C19	C20	120.79(13)

C8	C7	C9	130.98(12)	C19	C20	C21	118.66(13)
C7	C8	C4	104.15(12)	C19	C20	C23	120.85(13)
C10	C9	C7	122.30(12)	C21	C20	C23	120.48(13)
C10	C9	C14	118.31(13)	C22	C21	C20	121.51(12)
C14	C9	C7	119.39(12)	C21	C22	C17	118.51(12)

Table 6 Hydrogen Bonds for FRSCMA.

D	H	A	d(D-H)/Å	d(H-A)/Å	d(D-A)/Å	D-H-A/°
N6	H6	O2[1]	0.843(19)	2.012(19)	2.8464(15)	170.2(17)

[1]+X,1+Y,+Z

Table 7 Torsion Angles for FRSCMA.

A	B	C	D	Angle/˚	A	B	C	D	Angle/˚
S1	C4	N5	N6	-178.93(9)	C8	C7	C9	C10	168.76(14)
S1	C4	C8	C7	178.24(10)	C8	C7	C9	C14	-11.7(2)
S1	C17	C18	C19	-178.37(10)	C9	C7	C8	C4	-178.61(13)
S1	C17	C22	C21	179.23(10)	C9	C10	C11	C12	0.3(2)
O2	S1	C4	N5	159.16(10)	C10	C9	C14	C13	1.1(2)
O2	S1	C4	C8	-20.07(13)	C10	C11	C12	C13	1.3(2)
O2	S1	C17	C18	-151.00(11)	C10	C11	C12	O15	-178.25(13)
O2	S1	C17	C22	29.12(13)	C11	C12	C13	C14	-1.8(2)
O3	S1	C4	N5	30.46(12)	C11	C12	O15	C16	6.2(2)
O3	S1	C4	C8	-148.77(12)	C12	C13	C14	C9	0.6(2)
O3	S1	C17	C18	-20.55(13)	C13	C12	O15	C16	-173.37(13)
O3	S1	C17	C22	159.57(11)	C14	C9	C10	C11	-1.5(2)
C4	S1	C17	C18	96.68(12)	O15	C12	C13	C14	177.84(12)
C4	S1	C17	C22	-83.19(12)	C17	S1	C4	N5	-86.53(11)
C4	N5	N6	C7	0.41(14)	C17	S1	C4	C8	94.24(12)
N5	C4	C8	C7	-1.03(15)	C17	C18	C19	C20	-0.9(2)
N5	N6	C7	C8	-1.06(15)	C18	C17	C22	C21	-0.6(2)
N5	N6	C7	C9	178.76(11)	C18	C19	C20	C21	-0.5(2)
N6	C7	C8	C4	1.18(14)	C18	C19	C20	C23	178.35(13)
N6	C7	C9	C10	-11.0(2)	C19	C20	C21	C22	1.4(2)
N6	C7	C9	C14	168.56(13)	C20	C21	C22	C17	-0.8(2)
C7	C9	C10	C11	178.03(13)	C22	C17	C18	C19	1.5(2)
C7	C9	C14	C13	-178.49(13)	C23	C20	C21	C22	-177.48(13)
C8	C4	N5	N6	0.40(14)					

Table 8 Hydrogen Atom Coordinates (Å×10^4) and Isotropic Displacement Parameters (Å^2×10^3) for FRSCMA.

Atom	*x*	*y*	*z*	U(eq)
H6	2480(10)	3510(30)	1587(15)	23
H8	2974.83	-1362.74	2902.88	23
H10	3295.34	5028.23	2909.37	28
H11	3942.68	6553.44	4492.05	29
H13	4163.49	1720.95	6203.06	29
H14	3503.65	213.17	4629.96	28
H16A	4846.14	7428.01	5974.48	45
H16B	4768.12	7405.14	7284.48	45
H16C	4026.01	7563.95	6339.98	45
H18	549.03	-1643.18	-532.11	25
H19	-665.41	-2177.82	-116.24	27
H21	250.3	-4873.97	2735.87	27
H22	1470.16	-4288.52	2358.94	25
H23A	-1136.29	-3357.84	2388.93	45
H23B	-1213.91	-5201.68	1648.49	45
H23C	-1488.59	-3275.86	1073.99	45

Experimental

Single crystals of $C_{17}H_{16}N_2O_3S$ **[FRSCMA]** were **[]**. A suitable crystal was selected and **[]** on a **SuperNova, Titan S2** diffractometer. The crystal was kept at 120(2) K during data collection. Using Olex2 [1], the structure was solved with the olex2.solve [2] structure solution program using Charge Flipping and refined with the ShelXL [3] refinement package using Least Squares minimisation.

1. Dolomanov, O.V., Bourhis, L.J., Gildea, R.J, Howard, J.A.K. & Puschmann, H. (2009), J. Appl. Cryst. 42, 339-341.
2. Bourhis, L.J., Dolomanov, O.V., Gildea, R.J., Howard, J.A.K., Puschmann, H. (2015). Acta Cryst. A71, 59-75.
3. Sheldrick, G.M. (2015). Acta Cryst. C71, 3-8.

Crystal structure determination of [FRSCMA]

Crystal Data for $C_{17}H_{16}N_2O_3S$ (*M* =328.38 g/mol): monoclinic, space group $P2_1/c$ (no. 14), *a* = 17.8692(2) Å, *b* = 7.26321(8) Å, *c* = 11.99541(16) Å, *β* = 99.4692(13)°, *V* = 1535.64(3) Å^3, *Z* = 4, *T* = 120(2) K, μ(CuKα) = 2.023 mm^{-1}, *Dcalc* = 1.420 g/cm^3, 21598 reflections measured (5.014° ≤ 2Θ ≤ 147.702°), 3077 unique (R_{int} = 0.0309, R_{sigma} = 0.0145) which were used in all calculations. The final R_1 was 0.0339 (I > 2σ(I)) and wR_2 was 0.0962 (all data).

Refinement model description

Number of restraints - 0, number of constraints - unknown.

Details:

1. Fixed Uiso
 At 1.2 times of:
  All C(H) groups, All N(H) groups
 At 1.5 times of:
  All C(H,H,H) groups
2.a Aromatic/amide H refined with riding coordinates:
 C8(H8), C10(H10), C11(H11), C13(H13), C14(H14), C18(H18), C19(H19), C21(H21), C22(H22)
2.b Idealised Me refined as rotating group:
 C16(H16A,H16B,H16C), C23(H23A,H23B,H23C)